STANFORD GEOTHERMAL PROGRAM
STANFORD UNIVERSITY

STANFORD, CALIFORNIA 94305

SGP-TR-55

PROCEEDINGS OF THE SEVENTH WORKSHOP
ON
GEOTHERMAL RESERVOIR ENGINEERING

Editors

Paul Kruger
Henry J. Ramey, Jr.
Frank G. Miller
Roland N. Horne
William E. Brigham
Tan G. Donaldson
Jon S. Gudmundsson

December 15-17, 1981

SPONSORED BY
THE GEOTHERMAL AND HYDROPOWER TECHNOLOGIES DIVISION
OF THE DEPARTMENT OF ENERGY
STANFORD-DOE CONTRACT NO. DE-AT03-80SF11459

TABLE OF CONTENTS

PREFACE

The Seventh Workshop on Geothermal Reservoir Engineering convened at Stanford University on December 15, 1981. Attendance at this workshop remained constant at 104. The continued growth of foreign participation was evident with 16 visitors from 5 countries.

The Seventh Workshop was noteworthy in both looking backward with the first session on Overviews of the Developments in Geothermal Reservoir Engineering over the past six workshops and in looking forward with the theme of the panel session on Future Directions of Geothermal Reservoir Engineering Development.

The excellent results of the workshop clearly confirm the major objectives of the Stanford Geothermal Reservoir Engineering Workshop in bringing together the active researchers and engineers in the development of geothermal energy as a viable electrical energy source and in providing a forum for prompt reporting of progress and exchange of ideas. This latter is especially important in this era of government retrenchment and continuous pressure to find alternate energy sources for the anticipated declines in fossil fuel resources.

The overviews on past developments outlined the efforts of many sectors of the geothermal community: academic, national laboratory, government agency, resource developers, and utilities. The growing role of cooperative research with many foreign countries was clearly visible as an important "resource" for future geothermal development in the United States.

The expanding list of geothermal fields was noted in the growth of the program sessions dedicated to Field Development. The two sessions included reviews of Cerro Prieto and Los Azufres in Mexico; Reykjanes and Krafla in Iceland, and technical developments at Baca, New Mexico and Larderello, in Italy.

Other noteworthy areas were the reports on tracer studies in fractured reservoirs and the developments in the role of geochemistry in geothermal reservoir engineering. The session on Modeling showed the continued advances being made to understand the physical and chemical processes occurring in geothermal reservoirs.

In summary, the year 1981 showed a continuous record of advances in geothermal reservoir engineering and the prospects for future development appear bright.

One of the main reasons that the Seventh Workshop was well organized and ran smoothly and successfully was the careful planning of our Program Managers and SGP staff. This year in particular, Professors Ramey, Horne, Brigham, Miller and I are extremely grateful for the great organizational efforts of Dr. Ian G. Donaldson, who unfortunately (for us) returned to New Zealand before the workshop and of Dr. Jon S. Gudmundsson who fortunately (for us) is visiting from Iceland. We also are grateful to our competent staff Jean Cook, Joanne Hartford, and Marilyn King for running the Workshop so efficiently, and to Terri Ramey and Amy Osugi for helping prepare the Proceedings.

We express our appreciation to the Department of Energy for supporting the workshop, and we are underway in planning Workshop Eight for December 14–16, 1982.

Paul Kruger
Stanford University
March 15, 1982

Proceedings Seventh Workshop Geothermal Reservoir Engineering
Stanford, December 1981. SGP-TR-55.

STANFORD GEOTHERMAL WORKSHOPS: THE FIRST SIX YEARS

Ian G. Donaldson* and Paul Kruger

Stanford Geothermal Program
Stanford University
Stanford, CA 94305

Introduction The First Stanford Geothermal Reservoir Engineering Workshop was convened in December, 1975. Its success in compiling the scattered information on geothermal reservoir engineering resulted in its establishment as an annual event of the Stanford Geothermal Program. In this seventh Workshop, it is appropriate to look back over the efforts of the past *six* years and to evaluate the overall results. Three questions may be raised: (1) Are the Workshops achieving the same aims and objectives of the initial meeting?; (2) What progress in geothermal reservoir engineering has been achieved over these six years?; and (3) Have the Workshops developed any special values of their own that distinguish them from other geothermal meetings?.

The development of the Stanford Geothermal Engineering Workshops is well recorded in its Proceedings. At the first Workshop, some 50 papers were presented over a three-day period. These papers, including two overviews, covered the following general areas of geothermal engineering:

(1) Reservoir Physics - studies to evaluate the physical processes occurring in geothermal reservoirs
(2) Well Testing - techniques used in specific and generic fields to determine volumetric and extractive characteristics of a reservoir
(3) Field Development - methods for optimum commercialization of producing fields
(4) Well Stimulation - techniques for improving energy and fluid recovery from geothermal resources
(5) Modeling - mathematical methods to study geothermal reservoirs.

During the ensuing five Workshops, the weighting given to these general areas have changed; different areas were introduced at various times, for example the area of well testing was expanded to include reservoir testing and formation evaluation; and special sessions were added for topics such as production engineering, geopressured systems, and risk analysis. The three-day format of the Workshop has been retained; and in 1977, a major change in program content occurred with the introduction of a panel session. The panel session is now an integral part of the workshop program; the specific theme for each workshop is chosen to reflect a topic most appropriate to the state of geothermal reservoir engineering at that time. The topics discussed at the four prior annual workshops are listed in Table I.

The development of geothermal reservoir engineering is also reflected in the changes in sponsorship of the Stanford Geothermal Program, indicating the general change in government support of geothermal energy research and. development over this time period. The sponsorship of the workshop program is listed in Table 11.

Aims and Objectives During the past *six* years of the Workshop, the aims and objectives have been kept rather constant. In the Introduction to the Proceedings of the First Workshop, they were clearly defined:

"The purpose of the Workshop convened here at Stanford this December, 1975, is two-fold. First, the Workshop was designed to bring together researchers active in the various physical and mathematical branches of this newly-emerging field so that the participants could learn about the very many studies underway and share experiences through an exchange of research results. The second purpose was to prepare these Proceedings of the Workshop so that the integrated information could be disseminated to the geothermal community responsible for the development, utilization, and regulation aspects of the industry."

These purposes may be contrasted to the objectives as stated in the Introduction to the Proceedings of the Sixth Workshop in 1980:

"The objectives of the Workshop, the bringing together of researchers, engineers, and managers involved in geothermal reservoir study and development and the provision of a forum for the prompt and open reporting of progress and for the exchange of ideas, continue to be met."

In retrospect, the stated objectives of the Workshop have been constant, but have they indeed been met? This can best be answered by looking at three aspects of the Workshop:

* current address: DSIR, New Zealand

Table I

SGP Workshop Panel Discussion Topics

Workshop	Year	Topic Theme
Third	1977	Definitions of Geothermal Reserves
Fourth	1978	Geochemistry
Fifth	1979	Reservoir Models--Simulation vs. Reality
Sixth	1980	Numerical Model Intercomparison Study

Table II

Sponsors of the SGP Geothermal Workshops

Workshop	Year	Sponsor
First	1975	National Science Foundation: RANN Program
Second	1976	{National Science Foundation: RA" Program Energy Res. and Dev. Adm.: Div. Geoth. En.
Third	1977	Dept. of Energy: Div. Geoth. En. (thru LBL)
Fourth	1978	Dept. of Energy: Div. Geoth. En. (thru LBL)
Fifth	1979	Dept. of Energy: Div. Geoth. En. (thru LBL)
Sixth	1980	Dept. of Energy: Div. Geoth. En. (thru SF00)

(1) the people who participate by presenting papers and attending the sessions, (2) the coverage of the papers offered, and (3) the status of the Proceedings.

Throughout the six years, Workshop participants have come from a wide spectrum of research and development groups--from government agencies (such as the Department of Energy and the U.S. Geological Survey), from the universities, from the National Laboratories, and from the many sectors of the industry (developers, utilities, and consultants). In addition, there has been considerable input and participation from abroad. For example, 21 attendees from 11 foreign countries participated in the 1979 Workshop; 18 attendees from 6 nations participated in the 1980 Workshop. This 20% attendance from abroad indicates a strong international nature of the Workshop. A significant feature is that these participants keep coming back.

Progress in Geothermal Reservoir Engineering

During the six annual Workshops, the distribution of general topics covered has become discernable. Table III shows the number of papers by the headings that have been used in the Proceedings' programs for the six Workshops. The totals for the last three also include panel discussion papers. The averages indicate a program of 2 overview papers, 9 reservoir science papers, 10 field evaluation papers, 9 field development papers, 3 stimulation papers, and 11 modeling papers. By decision, a feature of the Workshops is a balance between theoretical and practical papers; one that has been maintained through the six years.

One lasting feature of the Workshops has been the set of Proceedings that have become an important part of the literature on geothermal reservoir engineering. From the start, copies have been in demand to such an extent that reprintings have been required for some and increased first printings are now essential. Papers in the Proceedings are regularly cited in the professional literature as well as in review articles and in books. The Proceedings are often the only public source of information relating to some research and to some aspects of field development.

In reviewing the Proceedings, a major observation becomes readily apparent. In each of the topic areas, the context of the papers shows a marked transition from reports on "research intent" to reports of "significant achievements." This is especially true in the topics of field evaluation and field development, where successes (and problems) in bringing new fields on line have been shared among the participants. The sessions on modeling also show a rapid acceleration from "How to" papers to analysis of complex fields. A special part of the 1980 Workshop Proceedings (SGP-TR-42) was issued separately on the code intercomparison study sponsored by the Department of Energy in which it was noted that six independently constructed simulators could arrive at reasonable agreement of results given the same input information.

Table III

Distribution of Papers by Topics in the SGP Annual Workshop Proceedings

Topic	Workshop First	Second	Third	Fourth	Fifth	Sixth	Total	Average
Overviews	2	3	2	4	1	1	13	2.2
Reservoir Physics	9	8	8	7	4	12	48	8.1
Reservoir Chemistry						4	4	
Well Testing	10	5				3	18	
Well & Reservoir Testing			12				12	10.0
Well Test & Formation Eval.				15			15	
Pressure Transient Analysis					15		15	
Field Development	9	9		4	7	9	38	
Geopressured Systems						4	4	9.0
Production Engineering					6	6	12	
Well Stimulation	6	6		6			18	3.0
Modeling	14	13	11	9	10	9	66	11.0
Risk Analysis						2	2	0.3
Totals	50	44	33	45	43	50	265	44.2

The Special Values of the Workshops In contrast to the many overall meetings on geothermal research and development, the SGP Workshops might be classified as relatively small and specialized. The result has been a set of Workshops in which all participants are able to be involved over the whole meeting. With an average of about 100 attendees, the meetings are informal, with much cross-discussions of issues raised during the presentations. Over the three-day period, the participants can get to know or renew acquaintance with a large proportion of the attendees. A large amount of information transfer and exchange of ideas occurs through this open structure.

Although centered about the engineering aspects of the geothermal reservoir, the Workshop is still broad enough to attract papers from a wide spectrum of disciplines: social, economic, environmental. The balance between theoretical and practical aspects of geothermal reservoir developments allows a wide degree of perspective to each participant.

A second special value feature of the Workshops is the panel discussion. To date the panels have had excellent support from both the audience and the panelists. Fortunately, there has been little difficulty so far in finding topics appropriate to the research and development climate existing at the time of each Workshop. With the nation's energy picture still not in sharp focus, this situation is likely to remain yet for some time.

The third special value feature of the Workshops are the meeting preprints and the Workshop Proceedings. These have proved an excellent means of circulating recent research findings and field development information quickly to the many scientists, engineers, and managers responsible for the development of geothermal energy. This year, the advent of the "camera-ready" copy for preprints and Proceedings should result in even faster communication of results to the geothermal community.

A basic principle of the SGP Workshops is that all papers accepted for the Workshop be published in the Proceedings. This is now especially important today in that not all papers offered can be presented orally at the sessions. Although this principle could lead to publication of ideas that might not be accepted for publication in archival journals with full reviewing process, the publication in the Workshop Proceedings puts them on record. Like the Workshop itself, the Proceedings are a forum for discussion and hence new or alternative viewpoints should continue to be acceptable.

Achievements of the Workshops The Stanford Geothermal Reservoir Workshops have made "significant achievements" in their short lifetime. They certainly have brought together those interested in geothermal reservoir research and development and provided the participants with a forum for expression and exchange of ideas and results. Through the Proceedings, these ideas and results are maintained for later reference.

Another significant achievement results from the informality and openness of the meeting. The Workshop has become accepted as the medium for reporting new research ideas and development information--well in advance of more formal publication, if any. Several research themes have continued through several workshops, indicating a feedback mechanism from exposure and discussion of ideas to development into research programs and results. A major case in point was the panel discussion of the Fifth Workshop in 1979, "Geothermal Reservoir Models--Simulation vs. Reality," which in effect set the stage for the Department of Energy sponsored numerical modeling intercomparison study carried out over the next year and reviewed in the panel discussion of the Sixth Workshop in 1980.

Summary The Stanford Geothermal Reservoir Workshops are now firmly established as an international forum for those interested in the geothermal reservoir, its study, and its development. The industry is yet in its infancy with respect to its future potential in meeting the nation's energy requirements. Thus, the problems of geothermal reservoir engineering need to be investigated for some time yet. New appropriate topics for future workshops will not be in short supply. The Proceedings of the Workshops have become an important part of the baseline of current knowledge of geothermal reservoirs. However, the distribution to date has been rather limited. With wider references to them appearing in the general literature, their availability should be expanded. The avenues for wider circulation to technical libraries and other geothermal reference systems are being examined.

The Stanford Geothermal Reservoir Engineering Workshops have played a significant role in the current development of geothermal energy. The momentum is forward, and maintaining a perspective of the growth of geothermal exploitation will be an interesting part of future Stanford Geothermal Workshops.

Bibliography

SGP-TR-12 Geothermal Reservoir Engineering, December, 1975.

SGP-TR-20 Summaries, Second Workshop, Geothermal Reservoir Engineering, December, 1976.

SGP-TR-25 Proceedings, Third Workshop, Geothermal Reservoir Engineering, December, 1977.

SGP-TR-30 Proceedings, Fourth Workshop, Geothermal Reservoir Engineering, December, 1978.

SGP-TR-40 Proceedings, Fifth Workshop, Geothermal Reservoir Engineering, December, 1979.

SGP-TR-42 Proceedings, Special Panel on Geothermal Model Intercomparison Study, December, 1980.

SGP-TR-50 Proceedings, Sixth Workshop, Geothermal Reservoir Engineering, December, 1980.

Proceedings Seventh Workshop Geothermal Reservoir Engineering
Stanford. December 1981. SGP-TR-55.

OVERVIEW - UNIVERSITY RESEARCH IN GEOTHERMAL RESERVOIR ENGINEERING

Roland N. Horne

Stanford University

University research into reservoir engineering aspects of geothermal utilisation has undergone a long development since work first gathered speed in the early **1970's.** University research, appropriately enough, has remained somewhat academic throughout that time although with a constant watch over the philosophically troubling problems associated with industrial utilisation of the resource. Research in the university environment is charged with finding the answer "why?" as much as **"how?".**

The Past One of the earlier popular areas of university research was the behaviour of convection in porous media--a region of interest stimulated by fundamental questions of how geothermal reservoirs form and what mechanisms are important in their behaviour. Work in this area was done at the University of Hawaii by Prof. Ping Cheng, at University of Colorado by Prof. David Kassoy, at Stanford University by Profs. George Homsy and Roland Horne, and at UCLA by Prof. George Schubert and Dr. Joe Straus. Physical situations in which non-isothermal fluid flow through porous media **is** important also appear in other engineering fields and have been studied in other universities with frequent cross references to geothermal energy. Much productive work was generated in the area of convection, however most activity drew to a close with a subtle change of emphasis towards more practical problems, perhaps originating with ERDA's **1975** catch-phrase of "megawatts on-line".

Methods for reservoir modelling have been investigated continuously from the beginning and still are of current interest. The field can be split somewhat untidily into the regions of analytical modelling, physical modelling and numerical modelling. Full scale numerical modelling has been undertaken at the university level by Prof. George Pinder at Princeton University and Prof. Paul Witherspoon at U. C. Berkeley who have made major contributions in philosophical insights into aspects of the field. Nuts-and-bolts code development has remained principally outside the academic environment and has been tackled by commercial companies and the national laboratories.

Analytical modelling is somewhat inappropriately named since most examples use numerical methods, however the term has come to be used with reference to lumped parameter, linearised **or** otherwise simplified models. Some of these models such **as** University of Colorado's fault-charged **model** (Kassoy and Goyal, **1979)** grew out of earlier convection work, while others at Stanford University originated from petroleum engineering material balance techniques (Brigham and Neri, **1980,** and Westwood and Castanier--this conference). Prof. Gunnar Bodvarsson of Oregon State University **has** also contributed a wide range of conceptual models from his geophysical background. The arguments concerning the appropriateness of this type of model compared to full scale distributed parameter models have yet to be resolved, and **it is** likely that work in both areas will continue in research, as **it does** in industry.

Physical modelling of full scale systems **has** never been undertaken in university research (despite suggestions of sand box models at Colorado State University - Fort Collins), but laboratory studies of large scale heat transfer has been undertaken in the chimney model at Stanford.

With the change in the later **1970's** towards more immediate practical problems, greater attention was placed upon well testing and well test analysis. Research in this area had been in progress at Stanford under the direction of Prof. Ramey since considerably before that time, however Stanford was joined by the University of Hawaii and other non-university establishments in the renewed interest. Well testing is an area on which all sectors of the geothermal reservoir engineering area depend, including numerical simulation, economics, reservoir modelling, station design, pipeline design and even environmental impact investigation.

Interest in fundamental rock and fluid properties has been maintained because of the continued importance that physical and chemical behaviour have in exploration, well test analysis and simulation. Work in fluid flow has been followed at Stanford University

in the bench scale experiments investigating absolute permeability, steam/water relative permeability and adsorption. The impact of the adsorption experiments has been far reaching in the engineering of vapor dominated systems, but the determination of steam/water relative permeability (which is of major importance in reservoir simulation) continues to be elusive. The difficulty in measuring relative permeabilities may well arise philosophically in their definition, making their study an ideal candidate for academic research.

The chemical behaviour of geothermal fluid flow has also been investigated in university research, with the mineralogical and stable isotope studies performed at U. C. Riverside and the non condensable gas studies at Stanford.

The Present and Future The principal philosophical problem suffered by geothermal reservoir engineering is the application of techniques developed for porous media to systems which have substantial fracture permeability. A great deal of effort in university research is now being applied in this direction. Tracer testing has been perceived as one of the clearest means to define fracture systems and the design and interpretation of a major tracer field test has been undertaken by Stanford in cooperation with the Instituto de Investigaciones Electricas in Mexico. Well test analysis, and non condensable gas monitoring techniques are being developed for this use also, and the heat transfer behaviour of fractured systems is also in progress.

In September 1980, LBL drafted an updated plan (Howard, Goldstein and Graf, 1980) for the support of geothermal reservoir engineering research by the U.S. Department of Energy. Twenty top priority research needs were identified and presently 8 of these research topics are under investigation (either formally or informally) at universities.

References

Brigham, W. E., and Neri, G.: "A Depletion Model of the Gabbro Zone," Proc. Second DOE-ENEL Workshop Cooperative Research Geothermal Energy. LBL report 11555, January 1981.

Howard, J. H., Goldstein, N. E., and Graf, A. N.; "An Updated Plan for Support of Research Related to Geothermal Reservoir Engineering," LBL report 10807, September 1980.

Kassoy, D. R., and Goyal, K. P.; "Modelling Heat and Mass Transfer at the Mesa Anomaly, Imperial Valley, California," LBL, GREMP Series #3 (LBL-8784), 1979.

Westwood, J. D., and Castanier, L.M.; "Application of a Lumped Parameter Model to the Cerro Prieto Geothermal Field," Geothermal Resources Council, Transactions, 5 (1981) (also this meeting).

Proceedings Seventh Workshop Geothermal Reservoir Engineering
Stanford, December 1981. SGP-TR-55.

THE ROLE OF THE NATIONAL LABORATORIES IN GEOTHERMAL RESERVOIR ENGINEERING

P.A. Witherspoon and C.F. Tsang

Earth Sciences Division
Lawrence Berkeley Laboratory
Berkeley, California 94720

INTRODUCTION The national laboratories, since the beginning of the national geothermal energy development program, have played an important research role for the U. S. Department of Energy (DOE) and its predecessor agencies. These laboratories, specifically, Lawrence Berkeley Laboratory (LBL), Lawrence Livermore National Laboratory (LLNL), Los Alamos National Laboratory (LANL), Sandia National Laboratory (SNL), Brookhaven National Laboratory (BNL), Argonne National Laboratory (ANL), and the Idaho National Eng. Laboratory (INEL), have large, multidisciplined scientific, engineering and technical support staff, and excellent research facilities, enabling the laboratories to conduct and manage research projects beyond the abilities of university departments and many geothermal developers. LBL has the unique feature of being located adjacent to the Berkeley campus of the University of California. As a result, faculty, graduate students and staff augment the Laboratory staff and make significant contributions.

In general, the boundary relationship between the national laboratories and industry is defined by the laboratories' focus on long-term, high-risk generic research and their facilities and special capabilities, many of which are lacking in industrial laboratories and are nonexistent within the organizations of many private geothermal energy developers. At the same time, the national laboratories maintain close contact with industry, thus ensuring relevancy of the research and the transfer of technology.

Because we are most familiar with LBL and the research performed there, and because LBL has been the lead laboratory in geothermal reservoir engineering research, this paper will deal largely with LBL's role. From our perspective, however, we see the following basic strengths within most of the national laboratories:

1. Starting with initial strengths in computer technology and advanced engineering facilities, the laboratories are able to design, build, and test new or improved tools together with supporting methodologies and numerical analyses.

2. With their multidisciplinary staffs, the national laboratories have the proper mix of scientists, engineers, technicians and managers needed to conduct longer-term research, and to respond more quickly to the emergency needs of DOE and other government agencies.

3. Because public service and high-quality research are central to the functioning of national laboratories, they are capable of providing independent and unbiased assessments and solutions to problems brought to them. They are committed to the transfer of technology to the private sector.

RECENT ACCOMPLISHMENTS OF THE NATIONAL LABORATORIES The current work performed by the national laboratories addresses various aspects of geothermal energy developpent in nearly all important areas. These areas and the corresponding involvement of the various laboratories are reviewed below, with emphasis being placed on the laboratories most involved with the respective research area.

Reservoir Engineering The primary work in geothermal reservoir engineering is being done by Lawrence Berkeley Laboratory (LBL). LBL is also carrying out studies that correlate geophysics with reservoir engineering. Details on LBL's role in reservoir engineering follow in the next section.

Geochemistry Lawrence Livermore National Laboratory (LLNL) has carried out a comprehensive R&D program at the Salton Sea geothermal field in the Imperial Valley, California. The program included reservoir evaluation, scale control, corrosion, H_2S abatement, and brine injection studies. More recently LLNL assessed the injectability of brines and methane extraction from geopressured resources of the Gulf Coast.

High Temperature Drilling and Completion Technology and Tools The development of drilling completion and well testing technology has been considerably advanced by the work of the national laboratories. New drilling hardware and fluids have been developed by Sandia

National Laboratory (SNL). They have made advances in completion technology that include downhole perforation, cementing, and well-cleaning.

As the lead laboratory for high-temperature component development, SNL has been instrumental in providing, through both in-house projects and subcontractors, components needed for logging high-temperature geothermal wells. They have advanced hybrid circuit technology, and developed prototype logging tools (275°C) and a metal sheath cable. Sandia has also worked with the General Electric Company to produce a 275°C multiplexer and with the Harris Semiconductor Company to develop high-temperature (275°C) electronic components.

Materials Brookhaven National Laboratory (BNL) has developed and tested several high-temperature polymer concrete systems for cementing geothermal wells. BNL has also investigated nonmetallic materials such as plastics, ceramics, and refracting cements for handling hot brines and steam.

Direct-Use Idaho National Eng. Laboratory (INEL) has developed several direct-use demonstration projects at Raft River, Idaho. The laboratory has also provided technical assistance for the direct-use geothermal projects.

Hot Dry Rock Sponsored by DOE/DGE, the Hot Dry Rock (HDR) Geothermal Energy Development Program is managed through a field office at the Los Alamos National Laboratory (LANL). The HDR Program was established to investigate--and, if possible, to demonstrate--the usefulness of natural heat in the earth's crust as a commercial source of energy.

Fenton Hill, located in a geothermal area approximately 30 km west of Los Alamos, is the site of LANL's pioneering HDR heat-extraction experiments. In May 1980, HDR technology was used to produce electricity in an injection demonstration experiment at Fenton Hill. A 60-kVA, binary-cycle electrical generator was installed in the Phase I surface system and heat from about 3 kg/s of geothermal fluid at 132°C was used to boil Freon R-114. The produced vapor was used to drive a turbo-alternator.

A Phase II system that should approach commercial requirements, consisting of a pair of 3-km deep wells into granite at 275°C, is now being constructed at Fenton Hill. other work at Fenton Hill includes environmental monitoring, development of equipment, instruments and materials for technical support, development of several kinds of mathematical models, and analysis of data collection from extensive resource investigations which was then assembled into a geothermal gradient map of the U.S.

National Energy Software Center (NESC) Argonne National Laboratory (ANL) operates the National Energy Software Center (NESC) which makes computer programs available to interested users in all areas of energy research. NESC maintains a software library with full documentation. software codes can be requested by all types of organizations worldwide, and NESC's services are provided at very nominal cost with no royalty charges for the programs. As an example, NESC has evaluated and adapted for distribution five computer programs developed at LBL for geothermal reservoir engineering applications (reservoir simulation, wellbore flow, well test analysis). Numerous requests for these programs have shown that NESC can be effective in transferring new methodology into engineering practice.

LBL'S ROLE AND ACCOMPLISHMENTS IN THE FIELD OF GEOTHERMAL RESERVOIR ENGINEERING Since the emphasis of this conference is on reservoir engineering, this section will be limited to a summary of LBL's past and present work in this area. This work is classified into several sections and discussed below.

Cerro Prieto Cooperative Project LBL is coordinating the U.S. technical activities being carried out at Cerro Prieto under an agreement between WE and Comisión Federal de Electricidad of Mexico. This multidisciplinary program includes geological, geophysical, geochemical, subsidence, and reservoir engineering studies with the purpose of developing a hydrogeological model of the geothermal system and to analyze its response to large-scale fluid production.

Some of the more important results obtained by the various American (e.g., U.S.G.S., U.C. Riverside and LBL) and Mexican groups involved in the program are as follows:

(1) The lateral boundaries and the temperature distribution within the geothermal anomaly have been generally established.

(2) The general distribution of deltaic and marine lithofacies in the field has been determined and is continuously revised as new well data become available.

(3) A general picture of the heat and mass flow pattern in the system has been developed. The hot fluids are recharged from the east and northeast and are moving laterally towards the west along the base of shale units. The fluids move upward through gaps in these shale units until they finally leak to the surface. After large-scale production began in 1973, colder waters began moving into the geothermal reservoir from shallower aquifers and from the edges of the field. A more detailed flow regime is being presently developed.

(4) Repeated surface geophysical surveys (dipole-dipole resistivity) have monitored changes in the reservoir caused by its exploitation. Apparent resistivity increases have

been detected over the older (western) part of the field at depths of 1 km or greater. On the other hand, large zones of decreased apparent resistivities have been observed west and east of that area. Modeling studies are being made to establish whether changes in salinity, temperature, and/or steam saturations of the reservoir fluids can explain the observed changes.

(5) Based on chemical and reservoir engineering data it was concluded that mixture with cooler waters rather than boiling is the dominant cooling process in the natural state, and that production causes displacement of hot water by cooler water, and not by vapor. Local boiling occurs near most wells in response to pressure decreases, but no general vapor zone has formed.

It is felt that the success of a multidisciplinary project like the Cerro Prieto study will strongly depend on the technical and managerial capabilities of the organization coordinating the effort and flow of information between the participating groups, as well as this organization's ability to be actively involved in the research phase. A national laboratory with its resources in manpower, laboratories, and shops is well suited for such technical and managerial roles.

Low-Temperature Research In 1981, DOE asked LBL and INEL to develop and implement jointly a new program in reservoir engineering methodology and reservoir assessment techniques specific to low- and moderate-temperature hydrothermal systems. Until that time, little effort had been devoted to the understanding of these reservoirs. Accomplishments to date include development of a computational model for thin, fault-charged hydrothermal reservoirs, development of well testing instrumentation, compilation and publication of case studies of low to moderate-temperature reservoirs and preparation of a handbook with reservoir engineering guidelines for potential developers.

High-temperature Research Since 1976, LBL has conducted a sizeable research effort in high-temperature geothermal reservoir engineering. Some of the highlights are as follows:

(1) International cooperation - Through a number of international cooperative projects (Italy, Iceland, Mexico, New Zealand), it has been possible to obtain access to geothermal operating experience and field performance data. This has facilitated recognition of technological problems and has made possible the development of novel methods for geothermal reservoir engineering. Much valuable information has been made available to the geothermal community in the United States.

(2) GREMP - LBL developed the Geothermal Reservoir Engineering Management Plan (GREMP) for DOE as a guidance for R&D policy in geothermal reservoir engineering. A comprehensive extramural research program was implemented, and LBL administered and technically monitored research contracts and disseminated the results to the geothermal industry.

(3) Reservoir Modeling - LBL's in-house research efforts have integrated talent from various disciplines (geology, hydrology, geophysics, reservoir engineering, physics, mathematics) to develop quantitative methods for geothermal reservoir evaluation and performance analysis. Emphasis has been placed on the development of sophisticated yet easy-to-use computer programs such as SHAFT79 and PT (or CCC), which would be viable tools for engineering applications. Novel methods have been demonstrated through generic studies, as well as through applications to field data. A workshop was held to instruct engineers from the geothermal industry in the use of these computer programs. LBL staff continues to advise interested individuals and organizations in the application of advanced geothermal reservoir engineering methods.

We believe that our reservoir modeling work has already had a significant impact on geothermal development planning in the United States, and will continue to facilitate design and optimization of exploitation strategies.

Energy Utilization - The Utilization Technology Group at LBL has had as its focus the binary-cycle energy conversion process. The binary-cycle is the leading candidate for utilization of moderate and low-temperature resources for electricity generation. Optimization of the working fluid and cycle state point as functions of resource temperature and economic conditions has been studied using the powerful code "GEOTHM" developed at LBL. Cycles using supercritical mixtures of light hydrocarbons have been shown to be optimal at present cost levels.

Heat exchangers constitute a major portion of the binary-cycle power plant cost, and the performances of both novel and conventional heat exchangers have been studied under field conditions. Laboratory measurements have also been performed to establish heat transfer coefficients for butane/isopentane mixtures. A 500-kW direct-contact heat exchanger pilot plant has been designed, built, and tested at East Mesa. LBL is presently supporting the Heber Binary Demonstration Power Plant by participating in design reviews and in the design of the data acquisition system for the plant.

Field Testing - At the onset of government programs to stimulate the development of geothermal resources in the United States, there was a need to develop improved methodology for testing geothermal wells and geothermal reservoirs. Because well testing is the most common and reliable technique for providing data on the in situ reservoir parameters, it is essential to have a well-developed test methodology. As part of the LBL Geothermal Reservoir Engineering Program, well testing methods, procedure,

instrumentation, and interpretation have been investigated.

Well testing methods developed for geothermal well testing have followed the lead of the petroleum industry. Three types of tests--production tests, injection tests, and interference tests--assimilated from the petroleum industry were determined to be the most suitable to geothermal reservoirs. To make these techniques applicable to geothermal reservoirs, the theory has been modified to include the effects of two-phase (steam-water) nonisothermal flow in the reservoir, two-phase and nonisothermal wellbore flow with variable rate, and fracture flow. For highly saline or gaseous reservoirs, an accurate equation of state must be developed and included in the calculations. To date very little data exist on the properties of saline and gaseous brines at elevated temperatures and pressures. This is a major area of on-going research intended to facilitate the development of geothermal reservoirs.

In the past, a major obstacle to the implementation of well testing techniques has been the lack of instrumentation and measurement devices for high-temperature and high-pressure application. Temperature, pressure, and flow must be measurable both downhole and at the surface, at sufficient accuracy to obtain reliable estimates of the reservoir parameters. In 1976, there were only two systems available for obtaining downhole pressure: a mechanical device designed for the oil and gas industry, and an electronic device rated to 150°C. Obtaining downhole pressure, temperature, and flow data at temperatures greater than 150°C was limited by lack of high temperature electronics, transducers, seals, cable heads, and cable. Now, as the result of the development of high temperature electronics at Sandia, the potential exists to develop instruments suitable for use at temperatures of up to 275°C. Concurrent to the Sandia program, the reservoir engineering group at LBL has concentrated on developing tools that use only surface electronics. Using this philosophy, a downhole pressure/temperature/flow tool rated to 225°C has been developed. It incorporates a Bell and Howell CEC 1000-4 series pressure transducer, an RTD, and a modified Kuster spinner. A spinner (downhole flow meter) and a temperature tool, both rated to 300°C, have also been developed and fabricated.

FUTURE POSSIBLE RESEARCH AREAS A great deal of important work remains to be done by the national laboratories in geothermal reservoir engineering. Future challenging areas of research are:

(1) Injection studies - Many geothermal fields require injection in the very near future, and many important problems in this area have to be addressed as soon as possible.

(2) Fractured porous media studies - Because most geothermal reservoirs are highly fractured, it is important that pioneering work on fractured porous media done at LBL be continued.

(3) Geophysics - There is continued need for the monitoring of reservoir changes by geophysical means.

(4) Geochemical studies - There is great potential for future development and application of geochemical methods in reservoir engineering.

(5) Gas chemistry effects - Gas chemistry effects on reservoir analysis must be more thoroughly studied.

ckno We l the input from various s of the geothermal group at LBL in particul Norman Goldstein, Karsten Pruess, Marcel Lippmann, Sally Benson, Robert Ful and Mar Bodvarsson. Their assistance and cooperati s efull appreciated. This work was supported by the Assistant t for Conservat and Renewable E y Office of Renewable :t Division of l and Hydropower Technologies of the a ment of Energy under Contrac No. ENG

Proceedings Seventh Workshop Geothermal Reservoir Engineering
Stanford, December 1981. SGP-TR-55.

GEOTHERMAL RESERVOIR ENGINEERING: THE ROLE OF THE U.S. GEOLOGICAL SURVEY

Wendell A. Duffield

U.S. Geological Survey
345 Middlefield Rd.
Menlo Park, CA 94025

Introduction The U.S. Geological Survey has a legislated mandate to assess and inventory the Nation's geothermal resources. Accordingly, principal objectives of the Survey's Geothermal Research Program are: (1) to determine the geologic, geochemical, geophysical, and hydrologic characteristics of all types of geothermal systems; (2) to improve and develop techniques of exploration for and assessment of geothermal resources; (3) to characterize the seismicity, ground deformation, and hydrologic changes that may be induced by the production of geothermal fluids and their subsequent injection back into the subsurface; and (4) to determine the amount of geothermal energy that exists as a national resource and periodically to update this assessment as new information becomes available. Research that addresses objectives 1, 2, and 3 is designed to provide information that permits an increasingly accurate assessment of the Nation's geothermal resources.

Reservoir-Related Research Since its formal establishment in 1971, the Survey's Geothermal Research Program has supported field, laboratory, and theoretical studies in geology, geophysics, geochemistry, and hydrology. Duffield and Guffanti (1981a,b) have recently sumnarized the history of the program from 1971 through 1980. The program's broad-based, multidisciplinary character reflects the fact that any comprehensive understanding of geothermal systems requires studies of rocks, fluids, and a host of canplex interactions between the two. If reservoir engineering, the subject of this workshop, is defined in a broad sense to include all studies that either directly or indirectly help to characterize a geothermal reservoir, most of the research of the Survey's Geothermal Research Program addresses some aspect of today's topic.

Some of the Geological Survey's geothermal research is quite directly related to reservoir engineering. Laboratory experiments, development of theory, and computer-assisted numerical modeling have attempted to describe the characteristic behavior of a vapor-dominated hydrothermal system; computer-assisted numerical modeling has also been applied to hot-water and two-phase hydrothermal systems. Precise measurement of ground deformation at The Geysers, California, has suggested a correlation between steam production and subsidence. Similarly, precise measurements of gravity at The Geysers have suggested a correlation between steam production and changes in the strength of the gravity field. Research in well-logging equipment has resulted in development of an acoustic televiewer that can map the size, orientation, and position of fractures in high-temperature geothermal boreholes. Laboratory measurements of the electrical and magnetic properties of rocks under simulated geothermal conditions help constrain all modeling of geothermal reservoirs.

Geologic studies of the Survey's Geothermal Research Program have provided information on the nature of the heat source, the lithology of reservoir rocks, and the inferred nature of permeability for several geothermal systems. Several geoelectric techniques have been used to map the electrical conductivity of the crust and upper mantle; relatively deep probing techniques have provided information on heat sources, and shallower probing techniques have helped to outline the size and position of geothermal reservoirs themselves. Research using active and passive seismic techniques has identified crustal zones of low seismic velocity that may reflect the presence of magma, has outlined structures important to delineating geothermal reservoirs, and has discovered apparent anomalies in the elastic properties of rocks that may constitute geothermal reservoirs. Monitoring of seismicity at The Geysers has shown a correlation between areas of steam production and small-magnitude earthquakes. Measurements of temperature gradient and thermal conductivity in crustal rocks have delineated several broad regions of characteristic and differing heat flow and have provided considerable information on the thermal budget of specific hydrothermal convection systems. Hydrologic studies have

defined the water budget of some geothermal areas and, coupled with chemical analyses of waters, have provided a powerful tool for defining the origin and tracing the general path of fluids in hydrothermal systems.

Geochemical study of fluids probably has been the most fruitful single area of research for characterizing hydrothermal systems; many widely used geochemical techniques have been pioneered by the Geological Survey. The chemistry of surface fluid samples has been used to discriminate between vapor-dominated and hot-water systems, to estimate subsurface temperatures, to constrain the possible origins of fluids and their recharge areas, and to estimate the residence time of fluids in many hydrothermal systems. In recognition of their cost-effective exploration potential, a variety of chemical geothermometers are used in the early stages of geothermal evaluation worldwide. Techniques have also been developed to adjust geothermometer temperatures for dilution of thermal water with cool shallow ground water during convective flow to the surface. Analyses for deuteriun, oxygen-18, and tritium commonly are used to estimate the origin and residence time of hydrothermal fluids. Current research holds some promise for developing additional means of estimating residence time, through analysis of various radionuclides in hydrothermal fluids. Moreover, geochemical monitoring of fluids from areas under production--for example, at Larderello, Italy, and Cerro Prieto, Mexico--has provided considerable insight into the functioning of geothermal reservoirs; time-dependent changes in the composition of produced fluids, especially when considered together with such more traditional production data as temperature and pressure, provide information critical to successful long-term exploitation strategies of such reservoirs. Duffield and Guffanti (1981a,b) have sumnarized the findings of other Geological Survey research that addresses various aspects of geothermal reservoirs.

Research Trends Field-oriented studies of geothermal reservoirs may conveniently be grouped into surface (including shallow heat-flow drilling) and subsurface categories. With rare exception, the Geological Survey's geothermal research has been of the surface variety. Recent research drilling, however, reflects program policy to seek opportunities to make measurements in and study samples from boreholes. Geological Survey research drilling funded by the U.S. Department of Energy demonstrated in July 1981 a potential geothermal resource for nonelectrical use in the vicinity of Mount Hood, Oregon; a pumping test produced 380 L/min from an 80°C aquifer at about 1,200-m depth. At Newberry caldera, Oregon, research drilling funded and carried out by the Geological Survey in 1981 discovered a 265% permeable zone in the bottom few meters of a 932-m-deep borehole; a 20-hour flow test from this zone produced a sample of geothermal fluid whose chemical analysis should provide considerable information on the composition and thermodynamic state of the reservoir fluid. The recovery of nearly continuous core from the Newberry hole provides abundant opportunities for studies of the reservoir and overlying rocks.

Such sampling of reservoir fluids and rocks is the most direct way to test inferences made from surface studies. The Survey's Geothermal Research Program is philosophically comnitted to seeking opportunities for research drilling that make this type of direct sampling possible. The Survey plays an active role in promoting the goals of the Continental Scientific Drilling Committee of the U.S. National Academy of Sciences, specifically the proposal of this organization's Thermal Regimes Panel to drill into the roots of a hydrothermal system at roughly 500°C and 6- to 7-km depth. Research drilling into increasingly hotter and deeper parts of geothermal reservoirs may be the tool needed for major advances in our understanding of hydrothermal systems.

References

Duffield, W. A., and Guffanti, Marianne (1981a), The Geothermal Research Program of the Geological Survey: U.S. Geological Survey Open-File Report 81-564, 108 p.

------ (1981b), The Geothermal Research Program of the Geological Survey: U.S. Geological Survey Circular, in press.

Proceedings Seventh Workshop Geothermal Reservoir Engineering
Stanford, December 1981. SGP-TR-55.

GEOTHERMAL RESERVOIR ENGINEERING DEVELOPMENT THROUGH INTERNATIONAL COOPERATION

F. G. Miller
H. J. Ramey, Jr.

Stanford University
Stanford, CA USA

Introduction About twenty years ago when the Geysers Geothermal Steam Field in California first started producing steam in significant quantities for the generation of electricity there were probably no more than five or six people in the U.S.A. who could qualify as geothermal reservoir engineers. Then as now, the Geysers field was the only field in the U.S.A. producing steam in significant quantities on a commercial basis. We are now entering a new era, however, and can expect steam production in this country to rise markedly in the next few years.

In 1960 there were at least a few thousand persons in the U.S.A. who were practicing reservoir engineering in the petroleum industry and in groundwater management organizations. Thus the U.S.A. had at its disposal a great deal of talent and expertise but very little experience in either the operation of natural underground steam reservoirs or in the development of needed geothermal reservoir engineering technology. In contrast, various other countries had been producing natural underground steam reservoirs for many years and had developed from practical experience a considerable fund of knowledge about reservoir behavior. However, these countries had no reservoir engineers in the sense we now conceive this profession, and there was no common awareness of the need for new technology.

What we conceive as reservoir engineering is of importance in the preparation and understanding of international cooperative agreements in geothermal energy. Reservoir engineering is related to other branches of engineering involved in the development and operation of geothermal-fluid reservoirs. As examples, it is related to drilling, production, and process engineering. It is also related to management functions pertaining to development and production.

The conventional concept limits its scope mainly to: (1) Analyses of well logs, (2) Analyses of reservoir pressure, temperature, production and well-effluent composition histories, (3) The design implementation, and analysis of field tests, (4) theoretical studies of reservoir behavior, reservoir modeling, and studies of physical models in the laboratory. All this is for the purpose of developing and applying techniques to forecast well and reservoir deliverabilities and ultimate economic recoveries under different operating conditions.

In some instances the concept of reservoir engineering is much broader, encompassing additional functions which may include land management, drilling, engineering, production geology, production engineering, pipeline transportation of products to local storage facilities or power plants, and managerial decision-making regarding such things as redrills, selection of sites for new wells, processing facilities, or power plants. This broad concept places the reservoir engineer in the role of reservoir manager and in this capacity he would also initiate feasibility studies and arrange for research along lines that appear best to him.

In the geothermal community the conventional concept of reservoir engineering has been adopted generally although it has been subject to change, and often to additions as more is learned about new factors affecting reservoir behavior.

Binational cooperative geothermal research programs were developed as a logical means to benefit both the U.S.A. and the countries participating with it. Some binational programs covered a number of areas of research on geothermal energy, but from the outset, reservoir engineering became widely recognized as an important subject of general concern.

Efforts were made early in binational studies to develop new geothermal reservoir engineering technology through applications and modifications of existing petroleum and groundwater technology. These studies led to a better understanding of the physical nature of geothermal reservoirs, a deeper appreciation of the physical differences between steam, petroleum, and groundwater reservoirs; and they helped researchers avoid duplication of effort.

Laboratory studies of physical models were made, computer models were developed, and reservoir engineering field studies were made. Generally accepted methods of approach were followed in making field studies. Field performance data were used to formulate hypotheses regarding the nature of reservoirs. These hypotheses were then tested using physical or mathematical models, or both. The physical laws involved in the performance of the reservoirs could then be recognized so that pertinent engineering equations could be derived and solved. If results from such equations appear valid based on comparisons to field performance data, then it is possible to study various methods of field development and production, and to forecast performance.

Bilateral programs active during recent years have been the source of a substantial fund of knowledge, useful new technology, and transfers of technology to the U.S.A.

These technical gains for participating countries would not be possible without well understood written agreements carefully prepared in advance of joint research activities. Some comments on these agreements follow.

Comments on The Execution of International Cooperative Agreements International cooperative research has been government-sponsored, an outgrowth of private consulting, or a necessity for industrial development. Regardless of how they came about or how they were implemented, binational programs in which the U.S.A. has been a participant have been of benefit to this country.It is important that participants sign international agreements with a spirit of good will. Both sides should be well aware of the non-technical problems which can confront them. There are many such problems. Joint determination of the specific research to be undertaken is one of them. Another is the manner in which joint research proposals are to be submitted to government sponsors. Another is naming in the proposals the researchers from the participating countries and delineating the distribution of work among them. Less significant but also important are the plans that must be made for working together in each others home offices and laboratories. This involves the need for travel plans. It has become clear that binational cooperative research, if it is to be successful, demands that participants work together at fairly frequent intervals and write their reports together. Doing so is unmistakable evidence of cooperation. If each side works mainly alone and a mere exchange of reports takes place at the end of a contract period, the research cannot be judged as truly cooperative.

Researchers and research managers on both sides should be tolerant regarding language problems which might arise. They should recognize that social, cultural, and economic differences are ever present but will not cause difficulties if both sides act in good faith and display good will. The ways of doing business in one country are not the same as in another. Researchers and research managers should accept this fact and consider their pursuit of joint objectives as a contest to be won through patience and the best use of their abilities and resources.

International Cooperative Studies In the ensuing paragraphs we discuss some of the international cooperative work that has been done in geothermal energy in recent years. By necessity our treatment of this subject is sketchy because there have been so many cooperative arrangements, formal and informal. Published information on many of these apparently is either scarce or nonexistent. Moreover, we recognize that compiling available data for a more comprehensive treatment could become a virtually impossible task, but would not alter our views if the cooperative arrangements covered in our discussion are representative of the whole. Lastly, we admit that making our selection was naturally influenced by projects we are most familiar with and those are the ones which have involved Stanford either directly or indirectly. We do not mean to imply in any way that Stanford's role in the development of geothermal reservoir engineering has been any more important than those of many other organizations concerned with geothermal energy problems.

Our purpose is to disclose benefits to participating countries, to indicate the practicality of these benefits, technically and economically, and to show that international cooperative work can accelerate the development of the geothermal industry and thereby ease energy shortage problems.

Costa Rica - In 1980 Professor H.J. Ramey, Jr., of Stanford University consulted for the government of Costa Rica on the Miravalles geothermal field. He made pressure transient analyses, designed well tests, and made engineering assessments. He presented a talk on the Miravalles field in the fail of 1980 in one of the weekly seminars of the Stanford Geothermal Program.

One of the geothermal engineers at Miravalles, Eduardo Granados, an employee of the Costa Rican government utility, ICE, was invited to come to Stanford during the winter of 1980-81 as a visiting scholar. After completing his visit Mr. Granados applied for admission to the graduate geothermal study program at Stanford and was admitted. This kind of interaction with practicing engineers throughout the world yields worthwhile benefits not only to graduate students and faculty at Stanford, but also to the U.S.A. as a whole. It provides an important indirect aid

to our national geothermal development program.

El Salvador - In 1975 Professor W.E. Brigham of Stanford University did some consulting work for El Salvador on that country's Ahuachapan geothermal field. This work concerned the possibility of increasing the size of the power plant, the longevity of the field, locations for new wells, and possible reinjection of produced water. The questions which arose characterized the type of development planning that uses reservoir evaluations as a basis for decision-making. The Ahuachapan field is the first hot water field in the western hemisphere that produced from volcanic sediments. Since 1975 a number of other similar fields have been found, however, in Central America and the U.S.A.

Consulting assignments of the kind taken by Professor Brigham in El Salvador expand the experience background of reservoir engineers, augment their understanding of geothermal reservoir behavior and improve the skills they need to forecast reservoir performance. The new technology gained is of primary value to the U.S.A. as an aid in the development of the American geothermal industry.

Iceland - Several years ago there was a formal agreement in effect between the Atomic Energy Commission in the U.S.A. and the Iceland Energy Authority. This agreement called for cooperation between the two countries in the field of geothermal energy. It was broad in scope and dealt more with conventional engineering matters at the ground surface than with geosciences. Apparently it was in force for a period of about five years but used in only a few instances. Experience disclosed that formal procedures were not necessary for these.

By means of the agreement the U.S.A. was seeking access to the extensive background knowledge Iceland had accumulated on non-electrical applications such as direct heating with geothermal water. The U.S.A. used no particular method to gain its objectives. Generally the activities of the U.S.A. were limited to visits to plants and to other installations. These visits also could have been arranged informally.

Reservoir engineering was not mentioned in the agreement, probably because this branch of engineering was relatively unknown in the geothermal community at the time and it had been applied to few geothermal systems.At about the end of the 1970's decade the agreement was due for renewal, but neither of the two countries took the initiative to see that this was accomplished. Their passive attitude may have been due to the agreement's shortcomings. It was quite general, outlining no specific programs which should be undertaken or any specific problems which should be attacked. Moreover, no special funding for the work was provided for. Thus, interest waned.

Some benefits to both countries did accrue, however, as a result of informal cooperative arrangements. Lawrence Berkeley Laboratory (LBL) in the U.S.A. and various institutions in Iceland worked together on the Krafla high-temperature area of northeast Iceland. Iceland was interested in having work &ne at LBL on the troublesome Krafla reservoir. It was the first high-temperature reservoir in the country to produce less than what was expected originally.

Iceland has not yet developed the experience to deal with complex reservoirs except for low-temperature reservoirs where classical groundwater hydrology can be applied. Icelanders working in geothermal energy have broad experience, but only a limited part is specifically in reservoir engineering.

Although the problems at Krafla have not yet been solved the cooperative effort with LBL has provided some insight into the processes underlying these problems. The U.S.A. gains technologically from its involvement with these problems.

Italy - In the early part of the 1970's, Professor H.J. Ramey, Jr. of Stanford University discussed possible cooperative research between the U.S.A. and Ente Nazionale per l'Energia Elettrica (ENEL) in Italy. He delivered lectures in Italy on reservoir engineering and geothermal reservoir behavior. In the spring of 1975 Dr. Graziano Manetti and Engineer Antonio Barelli, both with ENEL came to the Petroleum Engineering Department of Stanford University as visiting scholars, for a period of about two months. Cooperative work between the U.S.A., through Stanford, and ENEL was discussed at length. Tentative plans were made after many discussions and seminars.

Later the proposed program was reviewed and discussed on a more formal basis with Dr. Raffael Cataldi of ENEL and some of his associates. Dr. Cataldi had already discussed with Professor Ramey in Italy the prospective Stanford-ENEL cooperative effort, before the visit of Dr. Manetti and Engineer Barelli. During the period of Dr. Cataldi's visit joint meetings were held. Those present included Professors F.G. Miller and H.J. Ramey, Jr. from Stanford, Professor P.A. Witherspoon and Drs. R. Schroeder and J.H Howard from LBL, Dr. L.J.P. Muffler from the USGS, and Dr. Cataldi and his associates from ENEL.

These activities led to a five-year agreement on cooperative research in geothermal energy which was signed in 1975 by both countries and extended in 1980 for a second five years. The agreement was between Ente Nazio-

nale per l'Energia Elettrica (ENEL), Italy, and the Energy Research and Development Administration (ERDA), now the U.S. Dept. of Energy (DOE), U.S.A. Six major areas for joint research were involved. One of these, Project 3, was on "reservoir physics and engineering and resource assessment", and is the one of interest here.

Through this agreement and resultant DOE contracts, Stanford and LBL with ENEL, have used the Larderello region of geothermal steam fields in Italy as an experimental laboratory to develop new reservoir engineering technology. Field data are available back to 1945. Under the cooperative research program field tests have been designed and implemented and the results analyzed. Important results have been published, attention being invited particularly to Project 3 papers presented at two ENEL–DOE Workshops for Cooperative Research in Geothermal Energy. The first was held at ENEL facilities in Larderello, Italy, Sept. 12–16, 1977. The papers presented were published in the Workshop Proceedings and iater in a special issue of thermics.

The second Workshop was held at Lawrence Berkeley Laboratory, Berkeley, California, October 20-23, 1980. Presented papers are published in the Workshop Proceedings.

An example of an important transfer of technology to the U.S.A. is a successful new method developed to forecast steam production. It was developed from studies made in the Gabbro field in Italy, and can be applied to similar fields in the U.S.A. The results are published in the 1980 Workshop Proceedings.

Another example of a transfer of technology to the U.S.A. is a method of engineering analysis developed to estimate flow patterns and fracture trends in certain geothermal steam reservoirs in which a principal producing well penetrates a vertical fracture extending part way to the bottom of a reservoir, hypothesized as a boiling water interface. The method was developed from well interference studies made on the Travale steam field in Italy. Results are published in the foregoing special issue of Geothermics.

Japan - Contacts between Stanford University and the Japanese geothermal industry were initiated as a result of participation in that industry by postgraduates. An informal cooperation has been in effect for the last two years. Professor Roland N. Horne of Stanford has spent two months in Japan during that time. His activities included consulting arrangements for reservoir evaluations and the teaching of a geothermal reservoir engineering short course with 63 attendees, done in cooperation with the Japan Geothermal Energy Center which is now a part of the New Energy Development Organization (NEDO). This organization in Japan is approximately equivalent to the Department of Energy in the U.S.A. Professor Horne also delivered various lectures and made a number of site visits. This interaction proved invaluable from the U.S.A. geothermal standpoint because a wide range of Japanese geothermal experience hitherto buried in Japanese language publications came to light. The subsequent presentation of the impact of reinjection experience in Japan has evoked controversy in U.S.A. geothermal reservoir engineering circles and has stimulated new research as the apparent implications are confirmed or disproved.

Contact between Stanford University and Japanese geothermal agencies is now extensive. These agencies include NEDO, New Energy Foundation, University of Tokyo, Kyushu University Geological Survey of Japan, Electric Power Development Company, Kyushu Electric Power Company, Japan Metals and Chemical Company, Mitsubishi Metals Corporation, Mitsubishi Heavy Industries, Toshiba International, Nippon Steel Corporation, Japan Oil Engineering Company and West Geothermal Energy Company. In January 1982 Stanford University will welcome its first Japanese geothermal exchange visitor. He is from the Electric Power Development Company and will join two Japanese students currently in residence.

Cooperation between the geothermal communities of the U.S.A. and Japan is formalized also through Japanese financial and technical participation in the Los Alamos Hot Dry Rock Program. The enthusiasm and technical expertise which Japan is applying to geothermal utilization is certain to be of benefit to the U.S.A. if joint relations continue at their present or an increased level.

Mexico - Two cooperative agreements have been in effect in recent years. One of these, signed in 1977, was between the U.S. Energy Research and Development Administration (now DOE), represented by Lawrence Berkeley Laboratory, and the Comision Federal de Electricidad (CFE), Mexico. The other agreement, signed in 1980, and supported by the DOE, is between the Petroleum Engineering Department of Stanford University and the Instituto de Investigaciones Electricas, Mexico. Together these agreements involve field tests, reservoir modeling and laboratory research.

The cooperative research of LBL and CFE is based on a formal bi-national agreement. Stanford-IIE cooperative research is based on a memorandum of understanding, akin to a letter of intent or gentlemen's agreement. For the joint purposes of Stanford and IIE this more informal arrangement, which was recommended by DGE, seems more practical.

Objectives of the Stanford–IIE proposed program were discussed with the U.S. Division of Geothermal Energy in early 1980 by Professors Miller and Ramey, of Stanford University, and Dr. Pablo Mulas del Pozo of IIE. In the early part of 1980 three engineers from IIE, Dr. Francisco Cordoba, Ing. Vicor Arellano, and Alberto Yanez, spent about three months at Stanford as visiting scholars participating in many seminars relating to the prospective cooperative research effort. This led to the DOE–Stanford Contract for joint research with IIE. Prior to this, however, Stanford professors F.G. Miller and Heber Cinco–Ley, in 1979, performed consulting services for the United Nations, assisting IIE with its plans for research facilities and a research program.

Long term reservoir performance data needed by the U.S.A. to develop new technology are being made available from the Cerro Prieto Geothermal Steam Field and from other Mexican fields.

During fiscal year 1981, Stanford–IIE work included investigations of: (a) the use of pressure gradients and profiles in well analysis, (b) Tracer analysis for fractured systems, (c) Interference tests in flashing reservoirs, and, (d) Lumped parameter modeling of the Cerro Prieto reservoir.

New Zealand - Most of the scientific interchange between the U.S.A. and New Zealand is probably at the personal level. New Zealand government laboratories frequently provide office space for short term appointments of the fellowship type to scientists of the U.S.A. wishing to work closely with New Zealand colleagues. Similarly, the U.S. Geological Survey (USGS) and U.S. universities frequently provide opportunities for New Zealand scientists to spend time in the U.S.A. pursuing their research and exchanging ideas with American colleagues.

A major contribution of New Zealand to the U.S.A. geothermal program is an open supply of data from developed geothermal fields in New Zealand. Data from Wairakei, for example, are available in the U.S.A. through an exchange arrangement in which the USGS is the U.S. coordinator.

Professor Michael O'Sullivan of the Theoretical and Applied Mechanics Department of the University of Auckland spent a year recently at the Lawrence Berkeley Laboratory doing research on reservoir simulations. Earlier he did similar work on New Zealand's Wairakei and Broadlands fields. Conversely, Dr. Michael Sorey who is an American scientist with the USGS recently spent two years with the Department of Scientific and Industrial Research (DSIR) in New Zealand. Dr. Sorey had earlier gained experience with reservoir simulation work on the Long Valley geothermal area of California. While he was in New Zealand he did similar work on the Wairakei field.

What is believed to be the first reservoir engineering study of a New Zealand geothermal reservoir was made by Professors R.E. Whiting and H.J. Ramey, Jr., in the early 1960's. Both men were faculty members of Texas A&M at the time. A report on their work, published by the Society of Petroleum Engineers of AIME, dealt with the development of material-and-energy balance equations for the Wairakei field.

Two recent managers of the Stanford Geothermal Program came from New Zealand, Professor Roland N. Horne who is now a faculty member of the Stanford Petroleum Engineering Department, and Dr. Ian G. Donaldson, who is a scientist with the DSIR in New Zealand. Both men have made important contributions to the development of geothermal reservoir engineering technology applicable in the U.S.A.

Nicaragua - In 1977 H. Dykstra and R.H. Adams, both formerly with the Standard Oil Company of California were engaged by the Nicaraguan government to make a reservoir engineering study and conduct field tests in the Momotombo geothermal reservoir. Both of these men are experienced and highly qualified.

Dykstra reported the principal results of their studies at Stanford's Third Workshop on Geothermal Reservoir Engineering held in December 1977. Flow tests and pressure measurements were made on a group of five wells in the Momotombo reservoir. The purpose was to evaluate this hot water reservoir, to determine well interference effects, to determine reservoir boundary conditions and to obtain mass flow rates and enthalpy.

Bottom hole pressures were measured in four wells, static pressures in three of these and both flowing and shut–in buildup pressure in the fourth. Flow tests were made on all five wells.

Although Dykstra and Adams could not accomplish all their objectives throuqh analysis of their carefully planned and executed tests, they were able to shed light on the performance behavior of the Momotombo reservoir and to explain in logical fashion why the reservoir behaves as it does.

Most important they brought back to the U.S.A. some valuable experience on a hot water reservoir in a volcanic environment which adds to our meager fund of knowledge on the subject.

Taiwan - Professor H.J. Ramey, Jr. of Stanford University visited Taiwan on a consulting assignment in 1979. He made studies on the Chingshui geothermal steam field, near the northeastern coast of Taiwan. This field

produces hot water with some carbon dioxide from six wells.

Carl Chang of the Chinese Petroleum Corporation and Professor Ramey performed pressure transient tests jointly and analyzed the results. Their work led to four publications at the Fifth Workshop on Geothermal Reservoir Engineering at Stanford in December 1979. These publications all related to the Chingshui field. They dealt with a preliminary study of the Chingshui geothermal area, a well interference test, pressure buildup tests, and an application of the Horner method to the estimation of static reservoir temperature during drilling operations. These publications present pressure and temperature transient data from field testing, and data interpretation. Field information of this kind is valuable to engineers and scientists in this area of research.

Following the 1979 Workshop, Carl Chang spent a quarter in residence at Stanford as a visiting scholar.

Concluding Remarks It is clearly evident from this brief review of international cooperation in geothermal energy development that the countries involved have made important additions to their fund of knowledge on geothermal energy. Efforts made are easing energy shortages, revealing this source as a viable alternative to oil and gas throughout many parts of the world.

Technically, much has been gained from new engineering methods and scientific techniques which shed light on the physical and chemical nature of geothermal-fluid reservoirs. These methods and techniques help explain why reservoirs behave as they do and they thereby facilitate forecasts of performance- Geothermal energy development appears to be on the threshhold of a new expansion. Much has been learned and there is still much to be learned.

Looking ahead, we must consider problems now surfacing. A few questions which arise are how can we make better use of geochemical data to explain past reservoir behavior and explain future behavior? To what extent can these data be best applied to determine underground flow patterns? How can we best advance reservoir analysis by applying to steam zones the knowledge we now have on vapor pressure lowering and liquid adsorption? How can we best design tracer studies so that they will yield needed information on reservoir size and configuration and on fracture size, orientation, and distribution? What compaction and fracture effects can be expected from the reinjection of cool water? Can land subsidence become a major problem in residential, industrial or farm areas? What are the economic implications? What should be done to further develop well testing theory so that the results of field tests can be interpreted more easily and with more confidence? How can we extract heat economically from reservoir rocks after rates of fluid production have become uneconomic? We have, of course, developed partial answers but more complete answers are needed.

International cooperation generally offers economic incentives which should not be minimized. At least as an approximation, the work force on a binational research investigation is twice what it would be for either of the two participating countries considered alone. Easy access to each other's experience background promotes rapid growth of new ideas.The growth that we can anticipate can be similar to the explosion in technology which occurred in the 1930's and 1940's in the petroleum industry. We can foresee that the prospects for continuing an expanded geothermal energy development should remain very good if enough encouragement and support are forthcoming from the governments and private companies involved. International cooperation can be an important factor in this growth.

Proceedings Seventh Workshop Geothermal Reservoir Engineering
Stanford, December 1981. SGP-TR-55.

RESOURCE DEVELOPMENT

C. L. Ritz

Republic Geothermal, Inc.
11823 E. Slauson Avenue
Santa Fe Springs, CA 90670

RESOURCE DEVELOPMENT*

The resource assessment techniques utilized in geothermal reservoir engineering are a combination derived from the disciplines of groundwater hydrology and petroleum engineering. As the geothermal industry has developed, these techniques have been modified to take into account phenomena normally ignored in aquifer management and oilfield practice. Details of multiphase flow and heat transfer need to be incorporated into the geothermal reservoir engineer's repertoire. The purpose of this presentation is to (1) comment on how several established groundwater and petroleum reservoir engineering techniques (reservoir modeling and wellbore flow simulation) are currently utilized in the geothermal industry to speed the development of large and small prospects, and (2) suggest areas where future government-funded research might be directed in order to assist the geothermal industry in the development of geothermal resources.

Mathematical models of wellbore flow have been used to extend our understanding and make predictions on well productivity, heat loss, and the relationship of temperature to pressure in a flowing and flashing well. Examples of satisfactory fits of theory to experiment in a well with very high salinity (200,000 ppm TDS) and high concentration of CO_2 will be presented. Suggestions for improvements to currently available wellbore flow models will be made.

Sophisticated numerical simulators have been used to predict reservoir performance and compare resource output as a function of well placement and development scenarios. Unfortunately, such studies have not increased the utilities or investors confidence in a reservoir's ability to deliver its estimated reserves. This has resulted in a reassessment of field development plan and a subsequent emphasis on stepwise, modular development rather than a large scale, all-at-once exploitation of a geothermal resource. As an example, various development scenarios of the East Mesa field will be presented along with advantages and disadvantages of each approach. Recommendations for future studies of resource development will also be given.

In comparison to the development of a large geothermal resource such as East Mesa, the smaller, low temperature geothermal resources capable of only direct heat utilization rather than electric power generation present an interesting challenge. The reason for the interest is that the nature of the flow of the hot water is incompletely understood and must be inferred from a combination of subsurface geology and well test data. This, in turn, leads to questions of delicately balancing resource recharge with production and reinjection. An example of a small resource, along with the reservoir parameters needed for well-test design and resource assessment, will be given. Recommendations for future studies regarding the exploitation of small geothermal resources will also be presented.

Concluding remarks will deal with the present versus future role of the geothermal reservoir engineer in evaluating and predicting reservoir performance. Emphasis will be on recommendations that can put the credibility of the geothermal reservoir engineer on a level equal to that given to reservoir engineers in the petroleum industry. The useful role that government funding can play is raising the credibility of the geothermal reservoir engineer. The point will be raised that funding efforts need to be increased in the areas of field studies and case histories, development of high temperature well logging instrumentation, and evaluation of materials capable of withstanding geothermal conditions.

* This is only a summary of the actual presentation.

Proceedings Seventh Workshop Geothermal Reservoir Engineering
Stanford, December 1981. SGP-TR-55.

GEOTHERMAL RESERVOIR ENGINEERING - UTILITY INDUSTRY PERSPECTIVE

Vasel W. Roberts

Electric Power %search Institute
P. O. Box 10412
Palo Alto, CA 94303

The perspective of the utility industry, concerning geothermal energy, has not changed dramatically during the past year. There have been minor changes, but most were positive and all were small increments. This is somewhat surprising given the dramatic down turn in the federal research and development program and delays encountered by three of the key pacing geothermal power plant projects. It indicates an unexpected strength in the industry.

Some of the key issues and changes in utility industry perspective are discussed herein, recognizing that a consensus of opinion is sometimes slow to form and that most measures of perspective are indirect and not very accurate.

Strong Interest Continues Utility interest in geothermal energy has never been greater. Evidence of this interest is manifest in modest increases in the utilities estimates of future generating capacity, roughly 10 percent last year. The problems associated with finding an adequate steam supply for the 50 MWe power plant at Baca, the necessity to shut down the East Mesa binary plant for modification, and the negative report by the California Public Utilities Commission on the Heber flash plant were disappointing of course but apparently have not diminished interest. These events simply tend to confirm the view of some that not all issues have been resolved and suggest that strong continuing commitments will be necessary for the commercialization of geothermal resources. Most of the geothermal utilities are willing to consider such commitments.

Value vs Price One of the key issues is still the cost of geothermal power. While the cost of geothermal heat is usually calculated by accountants and economists and the price established by negotiation, both are based on reservoir performance data developed by the reservoir engineer. Most utilities do not have sufficient information or knowledge about the reservoir to calculate the cost of producing geothermal energy and must prepare for price bargaining based on its value to the company. The value may not be the same for different companies.

Different geothermal fluids may have different temperatures and enthalpies, and do not all have the same intrinsic value. A first order estimate of the value of a particular geothermal heat source from the utility perspective can be established by comparing conversion efficiencies. Geothermal energy must be converted to electricity at temperatures significantly lower than for fossil and nuclear fuels, therefore, the conversion efficiency is lower, the heat rate higher. For example, the Heber binary plant is expected to have an overall thermal efficiency of about 12 percent while a conventional fossil plant would be around 36 percent, or possibly higher. Therefore, a Heber BTU is worth only one-third that of a fossil BTU in that area for power generation. This concept can be further refined by including second order factors for such things as differences in inherent availability factors for different power plant types, capital cost, operations and maintenance costs, etc. The alternate energy source might range from "avoided cost," to dominant energy source or a mix of all energy sources, depending on the needs of the utility, to establish an equivalent value for geothermal energy. The value thus established can then be used as the basis for negotiating price.

Reliability of Energy Supply Perhaps the most frequently cited concern relates to the reliability and longevity of new reservoirs. This has been a persistent issue and efforts to resolve it have been slow. EPRI with the help of Stanford has been trying to partially overcome this problem by developing a utility oriented reservoir assessment manual. The idea is to make the utilities more comfortable with the subject matter and increase their capability in this area. The problem with most of the existing literature is that it is not tutorial and is not geared to utility needs.

The utility has a vital interest in the iterative path that combines the various technical disciplines and diagnostic activities designed to assess the value of specific geothermal energy deposits. In a logical sequence of decisions, the utility contemplating a geothermal project must be able to assess the probability

of success of the project. It must also determine whether the project is a sound business venture and allocate some level of importance to the project within the company. To accomplish these efforts, close interaction between the utility counterpart and the reservoir engineering activity is essential. Physical and thermal models of the reservoir together with reservoir capacity and sustainable production rates are key sets of information needed to convey confidence that a project can be successful. Estimates of the reliability of energy supply are difficult to develop but may be inferred in a crude way from reservoir data on producing potential.

Plant Type and Size Once a reservoir has been shown to be interesting enough for a power plant project, feasibility studies will follow. During this phase, the quality of the energy is the next most important set of information. Information about temperature, enthalpy, presure and well production rates are necessary to allow the utility to determine the type and size of plant to be built. Generally it is not a question of selecting a power plant type, but matching the type with the thermodynamic characteristics of the geothermal fluid for optimum busbar cost and resource utilization.

The utility perspective on power plant size has changed somewhat during the past year. While most utilities still prefer 50 MWe plants, or larger, for commercial use, some have an interest in small plants down to one MWe and most are now interested in smaller plants from one MWe to 20 MWe as the first unit on each new field. A strong interest in wellhead units has also emerged, as a means of achieving early involvement in field development, assessing reservoir potential, and developing design criteria for larger plants to follow. Wellhead units can also be useful in assessing the economics of distributed systems compared to central plants. Interest in this concept stems from speculation that the economics of quantity might outweigh economics of scale for some geothermal systems. Also small units are more easily recycled in the event of reservoir or well failure. This aspect may be attractive where the producing potential of the reservoir has not yet been proven.

Accurate and complete geothermal fluid chemistry is essential for developing requirements for scale and corrosion control, and also requirements for environmental control systems and design criteria for these systems.

Other Issues The concern for the reliability of long term energy supply is one of the main issues, as noted, and busbar energy cost runs a close second. Other issues of high priority with the utilities include capital availability, land use, and future potential of the resource. While licensing can be a difficult issue, environmental protection is thought to be practical since the threat to the environment is low and present environmental control technology appears to be capable of meeting most existing standards. Issues that arise later in the project include plant type, plant size, cooling water availability and scaling and corrosion. EPRI's Geothermal Program is attempting to address a number of these issues, as a part of its current research and development plan.

Conclusion While the capability of the utilities is still deficient in the area of geothermal reservoir assessment, interest in geothermal power is high. Filling this gap by cooperative exchange, consultation and increasing in-house capability can only accelerate geothermal development.

Proceedings Seventh Workshop Geothermal Reservoir Engineering
Stanford, December 1981. SGP-TR-55.

APPLICATION OF A LUMPED PARAMETER MODEL TO THE CERRO PRIETO GEOTHERMAL FIELD

J. D. Westwood* and L. M. Castanier

Petroleum Engineering Dept.
Stanford University
Stanford, California 94305

Abstract In this paper, a lumped parameter mathematical model for hot water geothermal reservoirs is developed and applied to the Cerro Prieto geothermal field in Mexico.

The production and pressure histories of Cerro Prieto were assembled from field data. A computer program was then used to perform sensitivity studies on reservoir size, porosity, aquifer recharge, and temperature of recharge fluid. Two types of depletion schemes were investigated; in the first, the reservoir remains essentially one-phase liquid, and in the second, the reservoir becomes two-phase at a point early in its history. A satisfactory match of the history of the field has been obtained. This paper shows the usefulness of a lumped parameter model in clarifying the basic behavior of a hot water geothermal system and in giving focus to more complex two- and three-dimensional modeling efforts. The results obtained specifically for the Cerro Prieto field will also be of value to the scientists and engineers studying this reservoir.

Introduction Typically, a geothermal power plant must have a lifetime of thirty years to be economic. Because of the large increments of investment necessary at each successive stage of development, it is especially important to be able to forecast the future performance of a field from existing knowledge. Geothermal reservoir models attempt to serve this predictive function. In the beginning of the life of a field, when relatively little is known, the simplest models, which require the least amount of information, are appropriate. Later, as more information is accumulated about the geologic, geochemical, hydrodynamic, and thermodynamic characteristics of the field, these models may be refined and a better understanding of the resource achieved. One of the simplest types of mathematical models is the so-called "lumped parameter" model. The purpose of this kind of simulator is to match average reservoir behavior. The reservoir is treated as a homogeneous body, whose characteristics change as quantities of mass and energy enter and exit. The value of a particular parameter throughout the model reservoir is the average value of that parameter in the real system.

*Now with Marathon Oil.

In this paper, a lumped parameter approach to geothermal modeling is investigated. The amount of data required is minimal compared to finite-difference models. The Cerro Prieto geothermal field in Mexico was the subject of the modeling study; the lumped parameter model is most appropriate here since the field is still "young," having entered its eighth year of commercial production.

Some examples of lumped parameter models can be found in the literature. Whiting and Ramey (8) first used this concept in 1969 to model the Wairakei reservoir in New Zealand. Brigham and Morrow (2) in 1974 developed three models appriate for closed, vapor-dominated reservoirs. In 1979 Brigham and Neri (3) modeled the Gabbro zone of the Larderello field. Castanier, Sanyal, and Brigham *(4)* included heat transfer in the recharge region to simulate the behavior of the East Mesa reservoir.

To date, there have been no lumped parameter studies of the Cerro Prieto field similar to those reviewed above. However, a few preliminary simulation efforts have been made. In 1978, Lippmann, Bodvarsson, et al. (6), formulated a simplified three-dimensional, finite-difference model of the reservoir. In 1979, Lippmann and Goyal presented the results of two three-dimensional, finite-difference, hydrogeologic models of Cerro Prieto (7). Liguori (5) in 1979 used a simplified finite-difference reservoir model coupled to a wellbore model.

The Cerro Prieto Field The Cerro Prieto field is located about 30 km south of Mexicali, Mexico. This study is concerned with modeling the area of the field shown in Fig. 1, which supplies Units 1 and 2 and which has been in production since 1973. The wells have a perforated interval of 100-200 m at an average depth of 1200-1300 m. However, because of the complex interbedding, it is not obvious what the thickness of the reservoir is in this area. Porosity ranges from .15 to .35 in sand or sandstone, but is lower in shales. Various estimates of the permeabilities range from 40 to 100 md. The temperature of most wells in the Unit 1 and 2 area is about 300°C. Noncondensable gases, predominantly CO_2 and H_2S, are present in sufficient quantity to affect both the compressibility and the phase behavior.

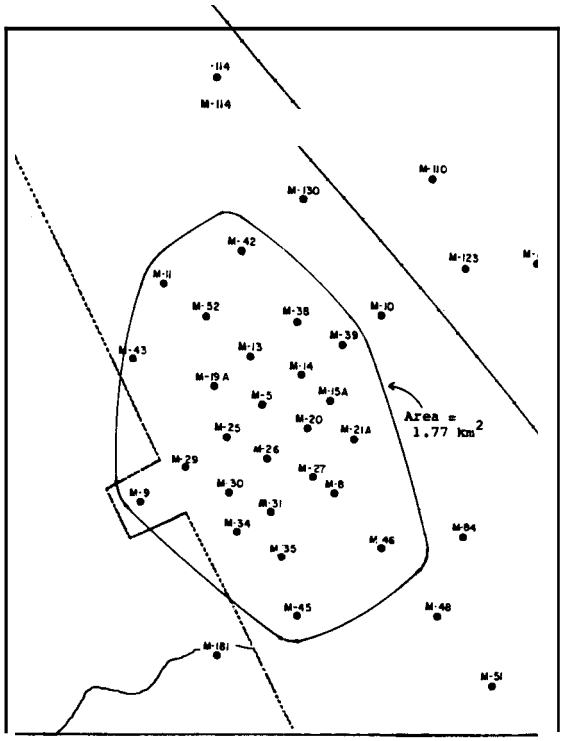

Fig. 1: The Units 1 and 2 Production Area

In the lumped parameter model, reservoir and fluid properties are considered to be uniform throughout. During a time step, quantities of mass and heat enter and exit, changing the reservoir from its initial state to its final state. The model in this paper neglects conductive heat transfer and convective movement of mass and heat across reservoir boundaries. For a complete description of the model, please see references 4 and 8.

Data Analysis Modeling requires two general types of data: field properties and field history. Some field properties such as reservoir area, rock matrix compressibility, density and heat capacity are known well. Others, such as thickness, porosity, and fluid compressibility of the production zone as well as geometry, permeability, and temperature of the recharge aquifer are not known accurately.

The history of reservoir behavior is deduced from logging, geochemical, and well production data. The model requires the history of mass flowrate, specific enthalpy of produced fluid, average reservoir pressure, and average reservoir temperature.

The history of average pressure in the production zone was developed from a set of isobaric maps which were presented by Bermejo, et al. (1) Using the four maps in their paper, the average pressure was determined in the production zone during 1973, 1975, 1977, and 1979. These four points are the basis for the curve of observed pressure history which is drawn for reference in Fig. 2.

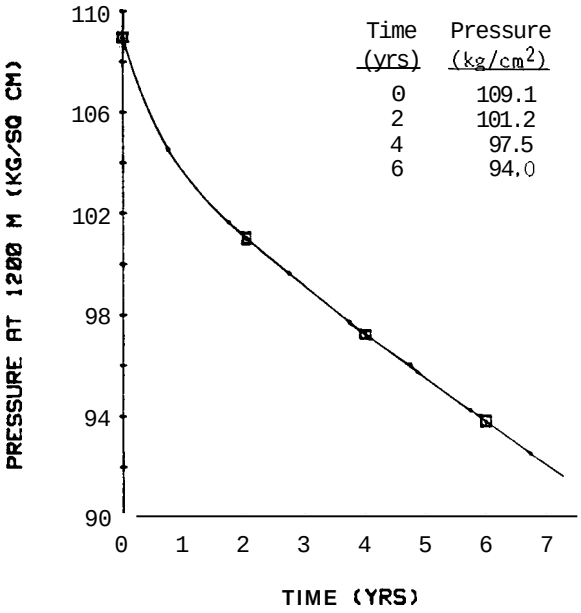

Fig. 2: History of Average Field Pressure

The initial temperature in the production zone is calculated from the enthalpies of the producing wells in 1973. The enthalpy should correspond to that of liquid water because the steep decline in pressure during this period indicates that the reservoir fluid was essentially one-phase liquid. After neglecting the cold wells M-9, M-34, and M-39, and M-29 because they were producing from a cold shallow zone during this time, the average liquid enthalpy was calculated to be 316 kcal/kg. This enthalpy corresponds to an initial temperature of 296°C. It is generally believed that the temperature has declined steadily at a rate of 1-3°C per year to about 285°C in 1979.

If the reservoir is uniformly two-phase, then the pressure and temperature must follow the saturation line. Unfortunately, the vapor pressure curve is not certain because of the effects of water salinity, non-condensable gases, and capillarity in the pore space. With this in mind, it is more appropriate to determine the position of the saturation curve empirically.

After examining the enthalpy and pressure histories, it was decided that if the reservoir flashed at all (in the sense of a lumped parameter model), it flashed sometime around the beginning of 1974. It is at this time that the initial steep decline in pressure due to liquid decompression perhaps levels out somewhat because of the growth of two-phase conditions. The fluid enthalpy also rises above the average enthalpy of liquid water at the initial temperature. The specification of two-phase conditions starting at the beginning of 1974 determines the initial point on the "pseudo" vapor pressure curve as 104.7 kg/cm³ and 296°C. The rest of the curve is constructed according to

the shape of the actual vapor pressure line for water. The rate of temperature decrease, which is dictated by the rate of average pressure decline, matches the observed rate (Fig. 3).

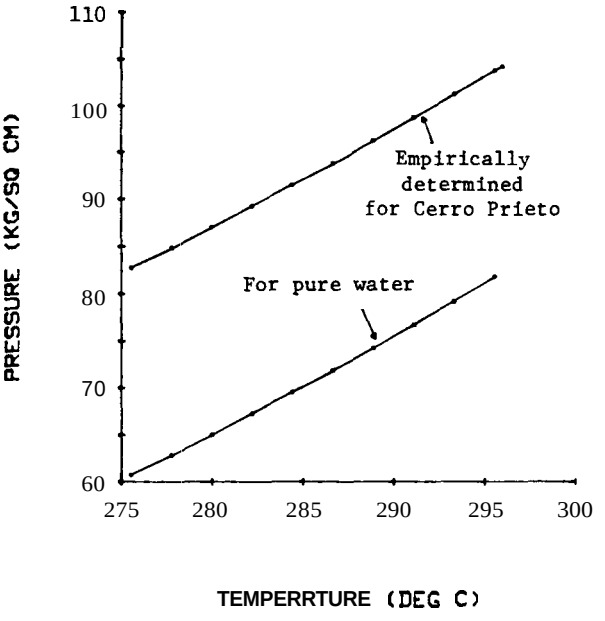

Fig. 3: Vapor Pressure Curves

History Matching In the simulation of a two-phase scenario for the reservoir, the behavior outlined above was assumed. As an alternative for comparison purposes, the reservoir was also modeled as a one-phase system with a large compressibility.

Various sensitivity studies were performed under each depletion scheme in order to investigate the effect: of varying reservoir parameters.

Several factors were considered in obtaining a satisfactory match of the history at Cerro Prieto. On the basis of the sensitivity studies, it was felt that a two-phase scheme would offer the best chance of matching the pressure behavior.

Figure 4 shows the results of history matching. The match is quite good over the entire 7.5 year period. The parameters used in obtaining this match are realistic except for aquifer size. The thickness of the production zone is 380 m; the porosity is 22%; and the recharge temperature is 260°C. However, the cross-sectional area of the aquifer is 18 x 10^6 m^2, which is about 3.5 times the total surface area of the production zone. The strength of the recharge indicates that a radial or spherical influx may be closer to actual conditions. In any case, the results in this report with a linear recharge system indicate that strong recharge is occurring at Cerro Prieto. One additional possibility is bottom water influx into the reservoir. This would explain the behavior shown by the pressure and enthalpy

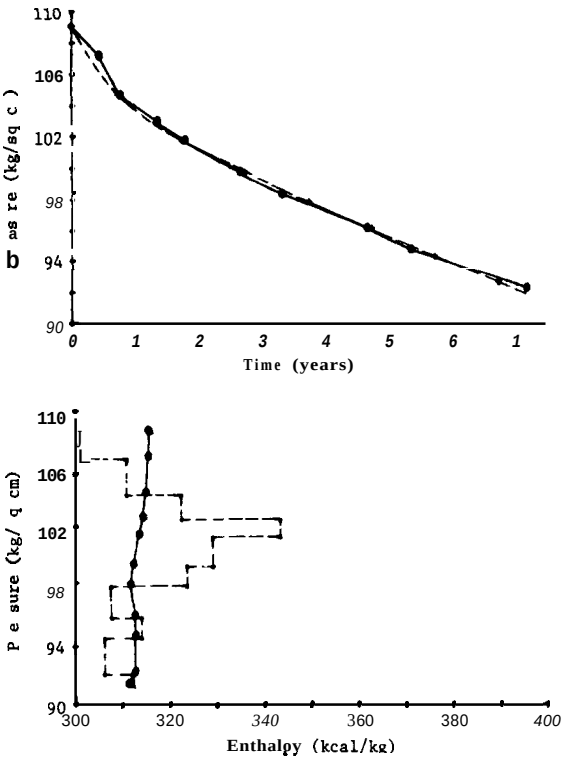

Fig. 4: History Match

observations. As shown by the results of the sensitivity studies presented later, a satisfactory match of the reservoir by a one-phase scheme is impossible. A two-phase scheme presents a sharp decline in pressure until the reservoir reaches the pseudo-vapor pressure curve. It then flashes and the pressure decline rate decreases while the enthalpy in the reservoir rises. In order to match both the pressure and the produced-enthalpy curves, it is necessary to assume a large aquifer recharge. At the same time, this would slow the pressure decline rate at the beginning of production and then lower the enthalpy at the end by reducing the steam quality into the reservoir.

A sensitivity study on the temperature of recharge water showed that raising the temperature of fluid influx would cause the pressure decline to be more gradual. Decreasing the reservoir thickness would counteract this effect, and would cause the enthalpy rise to be slower. In order to obtain agreement with the enthalpy history, a large aquifer would be necessary to provide a cool mass of recharge water. As the volume of the production zone became smaller relative to the cold aquifer, the decline in pressure along the saturation line would increase. Figure 5 shows an example of a sensitivity study in which the temperature of the recharge water is varied, assuming a two-phase depletion scenario. In this case, the size of the aquifer was too small to match either the pressure or the enthalpy observed.

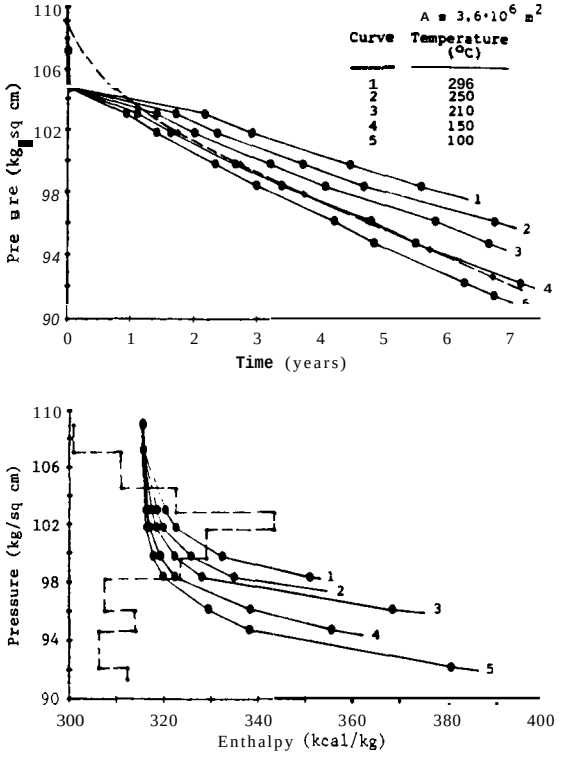

Fig. 5: Sensitivity Study of Temperature of Recharge Fluid (Two–Phase)

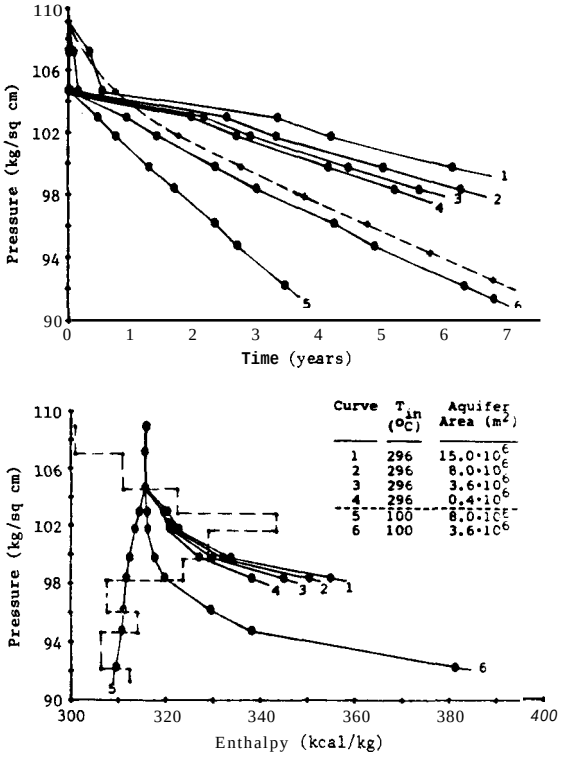

Fig. 6: Sensitivity Study of Aquifer Size (Two–Phase)

Figure 6 shows the effect of a change in aquifer size.

An additional point to address in this work is the sensitivity of the model to the location of the arbitrary zones; particularly, the intermediate zone extent may effect the validity of the results.

Figure 7 shows the drop in pressure and the rate of rise of produced enthalpy when the length of the intermediate zone increases. Geological data and temperature surveys must be used carefully in order to input this parameter properly.

Due to the complex faulting and difficult geology of Cerro Prieto, the thickness of the producing interval is difficult to estimate. In Fig. 8, we varied this parameter from 250 to 750 m. The best history match was obtained for a thickness of 380 m. The porosity was changed from .15 to .25. As can be expected, the model is not very sensitive to this parameter, because the total heat content in the reservoir is not very dependent on the porosity.

The history match obtained here is not unique. Other matches, which were not as good, were possible for a smaller reservoir and a warmer and stronger recharge. A temperature of 260°C is the minimum for which it is possible to get good enthalpy and pressure matches. Below this temperature, a smaller aquifer must be

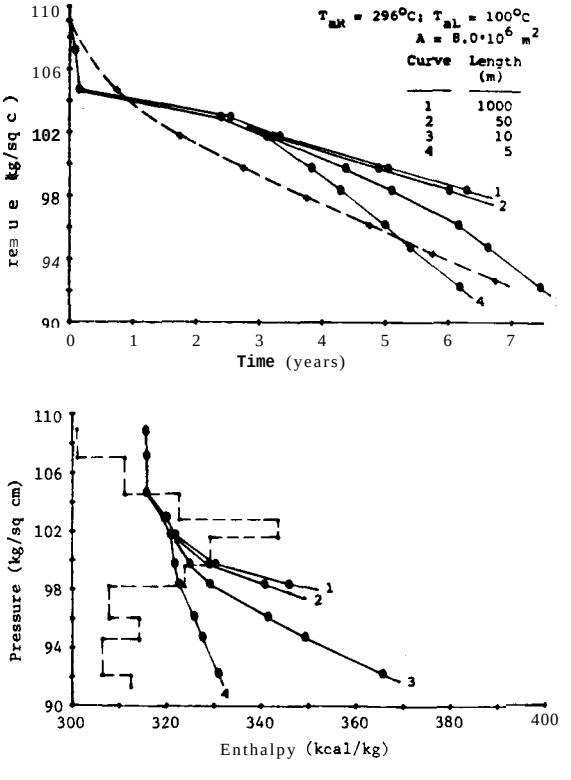

Fig. 7: Sensitivity Study of Length of Thermal Zone (Two–Phase)

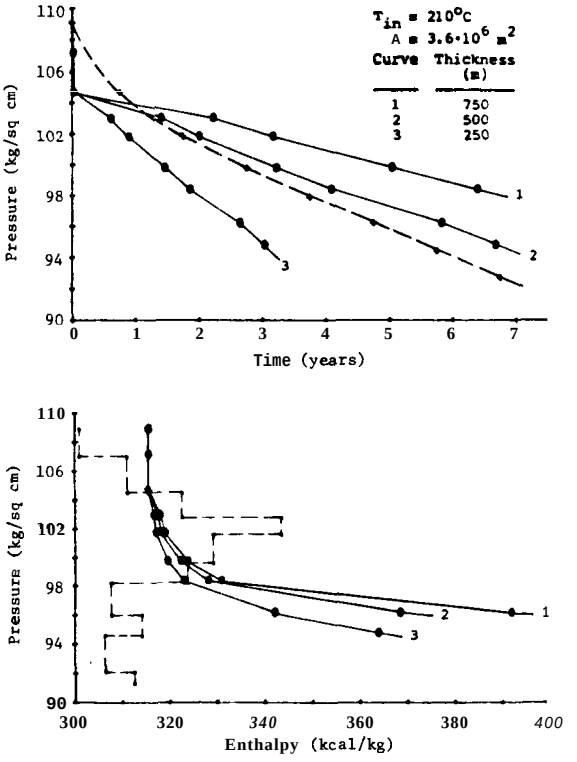

Fig. 8: Sensitivity Study of Reservoir Thickness (Two-Phase)

specified to reproduce the pressure trend, but the enthalpy becomes too high because the reservoir mass is depleted too rapidly. Above this temperature, it is possible to obtain simultaneous pressure and enthalpy matches, but the discrepancy between aquifer size and reservoir volume becomes larger.

The history match has been extrapolated out to a 30-year lifetime. A flowrate of 2000 tons/hr is assumed, and the produced enthalpy is approximately equal to the enthalpy of the reservoir fluid. No attempt is made to account for the effect of production in other areas of the field. After thirty years, the pressure has declined to 67 kg/cm^2, the temperature to 256°C, and the reservoir fluid is 5% quality steam with an enthalpy of 286 kcal/kg.

Conclusions Although the information that was required for the lumped parameter model of Cerro Prieto Units 1 and 2 is minimal compared to distributed parameter models, considerable judgment was still necessary to formulate a consistent set of data from the diverse and sometimes conflicting sources that are available. However, the simple nature of the lumped parameter approach allows rapid insight into relationships between physical reservoir characteristics and production behavior. The following conclusions may be drawn:

1) A depletion scheme in which the production zone becomes two-phase early in its history best fits observed behavior at Cerro Prieto.

2) A potent aquifer recharge has prevented the enthalpy of the fluid in the reservoir from rising in response to high rates of production from a relatively small volume. The geometry of the recharge system is probably radial or spherical, rather than linear.

3) The temperature of the recharge water is about 260°C. If the temperature is below 260°C in the model, then either the pressure decline is too steep or the enthalpy in the reservoir increases. If the temperature is above 260°C, the history matches are not as good, and the reservoir description becomes less physically realistic.

Acknowledgments The authors would like to thank Coordinadora Ejecutiva de Cerro Prieto through its Department of Studies, who, through Lawrence Berkeley Laboratory, kindly contributed field pressure and temperature data used in this work. This work forms part of the cooperative program between Stanford University, California and the Instituto de Investigaciones Electricas, Mexico, with support from U.S. Department of Energy contract number DE-AT03-80SF11459.

References

1. Bermejo, F. J., Navarro, F. X., et al. "Pressure Variation at the Cerro Prieto Reservoir During Production," in Proc. of the Second Sym. on the Cerro Prieto Geothermal Field, Mexicali, 1979, 494-496.

2. Brigham, W. E., and Morrow, W. B. "P/Z Behavior for Geothermal Steam Reservoirs," SPEJ, Dec. 1977, 407-412.

3. Brigham, W. E., and Neri, G. "Preliminary Results on a Depletion Model for the Gabbro Zone," in Proc. Fifth Workshop on Geothermal Reservoir Engineering, Ramey, H. J., and Kruger, P., eds. SGP-TR-40, 229-240.

4. Castanier, L. M., Sanyal, S. K., and Brigham, W. E. "A Practical Analytical Model for Geothermal Reservoir Simulation," SPE 8887, Annual California Regional Meeting of the SPE, Pasadena, 1980.

5. Liguori, P. E. "Simulation of the Cerro Prieto Geothermal Field Using a Mathematical Model," in Proc. of the Second Sym. on the Cerro Prieto Geothermal Field, Mexicali, 1979, 524-526.

6. Lippmann, M. J., Bodvarsson, G. S., et al. "Preliminary Simulation Studies Related to the Cerro Prieto Field," in Proc. of the First Sym. on the Cerro Prieto Geothermal Field, San Diego, 1978, LBL-7098, 375-383.

7. Lippmann, M. J., and Goyal, K. P. "Numerical Modeling Studies of the Cerro Prieto Reservoir," in Proc. of the Second Sym. on the Cerro Prieto Geothermal Field, Mexicali, 1979, 497-507.

8. Whiting, R. L., and Ramey, H. J., Jr. "Application of Material and Energy Balances to Geothermal Steam Production," J. Pet. Tech. (July, 1969), 893-900.

Proceedings Seventh Workshop Geothermal Reservoir Engineering
Stanford, **December 1981. SGP-TR-55.**

WELL LOG ANALYSIS APPLIED TO CERRO PRIETO GEOTHERMAL FIELD

M. Castaneda*, A. Abril**, V. Arellano*, R. L. McCoy***

*Instituto De Investigaciones Electricas
**Comision Federal De Electricidad
Coordinadora Ejecutiva De Cerro Prieto
Mexicali B. C. Mexico
***Patterson, Powers and Associates, Inc.
Houston, Texas

Introduction :

The Cerro Prieto Geothermal Field is a liquid-dominated geothermal system located 30 km southeast of Mexicali Baja, California, Mexico, in the Mexicali Valley. Although some wells were drilled and completed in the late 60's, it was April, 1973, when the geothermal power plant began operating with a capacity of 75 MW of electric power. Presently, the power plant installed capacity is 150 MW but this amount is expected to increase as further field development is planned to take place in the coming years. A number of questions are being presently asked as this field development continues. What will the deliverability of this geothermal field be in relation to planned installations? Will reinjection be required to supplement aquifer recharge? What will be the reservoir life and ultimate recovery?

This concern has resulted in a joint project, where Comision Federal De Electricidad, Instituto De Investigaciones Electricas and INTERCOMP Resource Development and Engineering, Inc., of Houston, Texas are presently involved in performing reservoir simulation studies on the Cerro Prieto Field.

An integral part of this project is the analysis of geophysical well logs to determine basic reservoir parameters. There are three primary sources of data on the petrophysical properties of a reservoir: core analysis, well tests and well logs. Core analysis data are limited because of the expenses involved in obtaining the core samples and performing the analysis. Well test analysis provide reservoir properties averaged over a large volume and therefore is not detailed. Well log analysis then, is the prime means of obtaining detailed data from the reservoir. A distribution of material parameters can be obtained from this analysis and the reservoir can be better defined for simulation purposes.

Data Gathering. In late 1976, as a result of the DOE/CFE Cooperative Agreement, The Lawrence Berkeley Laboratory (LBL) of the University of California began a systematic digitization of selected geophysical logs in order to permit computer analysis of the Cerro Prieto well logs. Selected wells throughout the field were chosen for this study. Before any computer techniques were applied, the digitized well logs were visually compared with the original blue prints to make sure that only reliable data could be used in making any interpretation. Special care was taken for any possible depth shift on logs run in each well and when such depth shift was present, a correction was made for this effect.

Selecting the Reservoir Interval of Study. The structural geology of the Cerro Prieto Field has been presented in several proceedings related to this field and it is well known. The formation is of sedimentary type with alternating shale and sandstone layers resting on a highly fractured granitic basement. There are some structural interpretations of this field based on temperature and electrical logs in the literature. For this study, basically the lithologic column presented by Abril and Noble in 1978[1] was selected. Figure 1 presents a typical field cross-section resulting from that work and Figure 2 shows its location on the field. From this lithologic column, intervals L_2 and Reservoir A were of special interest for the following reasons: a) for simulation studies, these zones will be of interest because most of the existing wells are completed here and consequently, all reservoir data (production data, well tests) come from these zones, and b) although the formation temperature begins to increase rapidly in Zone N, this zone presents a high content of carbonate ions in solution resulting in many well completion and scaling problems.

Determination of Effective Porosity. The computer program used for all calculations was INTERCOMP's Log Analysis Program. This program permits the use of petrophysical relationships whether they be standard industry accepted equations or derived empirical relationships. This program is full explained in Reference 11.

For a clean sandstone lithology, the density log is usually the most reliable porosity device. When shale is present, a correction has to be applied to density log readings for determining effective porosity. From the density log:

$$\phi_D = \frac{\rho_{ma} - \rho}{\rho_{ma} - \rho_f}$$

ρ = Density Log Reading

ρ_{ma} = Matrix Density

ρ_f = Formation Fluid Density

and:

$$\phi_e = \phi_D - V_{sh}\,\phi_{Osh}$$

where:

ϕ_e = Effective Porosity

ϕ_D = Porosity from Density Log

V_{sh} = Shale Volume

ϕ_{Dsh} = Shale Porosity

The shale volume can be obtained from gamma ray or Sp logs.

From the gamma ray log:

$$V_{sh} = \frac{GR - GR_{min}}{GR_{max} - GR_{min}}$$

From the SP log:

$$V_{sh} = 1 - \left(\frac{Sp - Sp_{min}}{Sp_{max} - Sp_{min}}\right)$$

In order to obtain maximum and minimum log values, the gamma ray and Sp log responses were histogrammed in each interval. Figure 3 presents a typical histogram for well M27. It is well known that both logs tend to over estimate shale volume. In our case, shale volume was evaluated from both logs and the minimum value was used for the effective porosity determinations. The exception to this was the case where the baseline drifts in the self potential log were apparent and this log was not used or when just one of these logs was run in a particular well.

An average effective porosity was obtained by arithmetically averaging the incremental determined porosity in each zone. Porosity values greater than 40% were disgarded on the averaging procedure. Figure 4 presents the obtained effective porosity values for both intervals. At this time, no consistent core data was available to verify the reliability of the obtained porosity data. Core samples from selected wells are being presently analyzed at IIE Petrophysical Laboratory. As this is done, reservoir permeability, another basic reservoir parameter, will be determined by means of some sort of porosity-permeability transform.

Evaluation of Water Salinity. The methods used to determine water salinity from well logs are reported and discussed elsewhere in the literature [3,9] and will not be reviewed here. Three of those methods that can be applied to the Cerro Prieto Field were selected for this purpose. They are different in the way the formation water resistivity (R_w) is determined. A brief description is as follows:

Method I - Requires only the spontaneous potential log. So at any depth:

$$R_w = (R_{mf})^{10(SSP/K)}$$

where:

$K = 61 + 0.133\,T$, T in °F

R_{mf} = Mud Filtrate Resistivity (from log headings and temperature log)

SSP = Static Spontaneous Potential Value

Method II - Evaluates R_w using an electrical log and a porosity log. At any depth:

$$R_w = \frac{R_t\,\phi_e^{\,m}}{a}$$

m = Cementation Factor

a = Constant in Archie's Formula $F = a\phi^{-m}$

R_t = True Formation Resistivity

Method III - Uses a Simandeoux water saturation equation (total shale equation)[14]. In this case, water saturation is assumed to be 100% and the only remaining unknown is the formation water resistivity, R_w. That is:

$$R_w = \frac{\phi_e^{\,m}}{a(1-Vsh)\left(\frac{1}{Rt} - \frac{Vsh}{Rsh}\right)}$$

where:

ϕ_e, m, a, V_{sh}, R_t are defined before in this paper.

R_{sh} = Shale Resistivity.

After R_w is obtained from any of the three methods described above, total disolved solids (water salinity) can be found from a correlation for Na Cl solutions reported in the literature[7].

$$\text{Na Cl eq} = 10^x$$

$$x = \frac{3.562 - \text{Log}\,(R_{w75} - 0.0123)}{0.955}$$

and:

$$R_{w75} = R_{wT}\,\frac{T + 6.77}{(75 + 6.77)}, \quad T \text{ in } ^oF$$

Some facts have been taken into account in evaluating the resistivity terms. It is a well known effect that both the invasion of drilling mud into the formation and temperature measurements or calculations of true formation resistivity (R_t) and some authors[5] have proposed various methods to overcome this problem. In our

case, when possible, R_t was corrected for mud invasion effects according to the method presented by Bateman et al. (1978). Regarding temperature effects, this is not a serious problem as long as enough data is available to determine true or initial formation temperature. If the temperature profile deviates radically from a linear relationship, this profile must be considered. Although some methods for determining static reservoir temperature during drilling operations, have been presented in the literature [6,8,13], they could not be used because there was not enough required drilling data for this purpose. Instead, the stabilized shut-in well temperature profile obtained during the observation period was selected as an approximation to true formation temperature. For some fractured geothermal fields this temperature profile is not representative of reservoir temperature because of the existence of internal flows within the well[10] but Cerro Prieto is of sedimentary type field and it was suggested recently[4] that this phenomenon was unusual in this field,

The water salinities determined from these three methods were compared with laboratory data[12] and the results are shown in Figure 5. As we can observe, water salinities evaluated from the self potential log (Method I) and those evaluated using the Simandeoux's Equation (Method III) were lower than the laboratory reported data. Water salinities calculated from resistivity logs and density logs (Method II) were closer to the actual water salinity values. This has been found to be the case in other geothermal fields[5].

final Remarks

The obtained information will be of great help for the planned reservoir simulation studies of this geothermal field. As more wells are being analyzed, more data regarding reservoir parameters will be known. At the present time, some wells are being drilled and completed into the deeper reservoir B interval. That portion of the reservoir will also be analyzed and included in the simulation study.

Acknowledgements

The authors would like to thank Coordinadora Ejecutiva De Cerro Prieto through its Department of Studies, and also the Instituto De Investigaciones Electricas for the opportunity given to them for presenting this paper.

REFERENCES

1. Abril, G. A., Noble, J. E., (1978). "Geophysical Well Log Correlations Along Various Cross-Sections of the Cerro Prieto Geothermal Field," First Symposium on the Cerro Prieto Geothermal Field, Baja, California, Mexico, Sept. 1978, pp. 41-46.

2. Bateman, R. M., Konen, C. E., (1978), "The Log Analyst and the Programmable Pocket Calculator: Part IV, Dual Induction - Late - Rolog 8", The Log Analyst, May-June, 1978.

3. Brown, L. S., Gobran, B. D., Sanyal, S. K, (1980), "Determination of TDS in Geothermal Systems by Well-Log Analysis", Proceeding of the Sixth Workshop Geothermal Reservoir Engineering, Stanford University, Stanford, California, Dec. 16-18, 1980.

4. Castaneda, M., Horne, R. N. (1981), "Location of Production Zones With Pressure Gradient Logging", Geothermal Resources Council Trans., Vol. 5, pp. 275-281.

5. Davis, D. G., Sanyal, S. K. (1979), "Case History Report on East Mesa and Cerro Prieto Geothermal Fields", Informal Report LA 7889-MS, Los Alamos Scientific Laboratory, June, 1979.

6. Dowdle, W. L., Cobb, W. M. (1975), "Static Formation Temperatures From Well Logs: An Empirical Method", J. Pet. Tech., V. 27, pp. 1320-1330.

7. Dresser Atlas (1980), "Log Interpretation Charts."

8. Edwardson, M. J., Girner, H. M., Parkinson, H. R., Williams, C. D., (1962), "Calculation of Formation Temperature Disturbances Caused by Mud Circulation", J. Pet. Tech., V. 14, pp. 416-426.

9. Gobran, B. D., Brown, L. S., Sanyal, S. K. (1981), "A Hand-Held Calculator Program for Estimating Water Salinity From Well Logs", The Log Analyst, Vol. XXII, No. 2, (March-April, 1981).

10. Grant, M. A. (1979), "Interpretation of Downhole Measurements in Geothermal Wells", New Zealand Department of Scientific and Industrial Research, Report AMD-88.

11. INTERLOG, A Petrophysical Program: User's Guide, (1981), INTERCOMP Resource Development and Engineering, Inc., Houston, Texas.

12. Laboratory Department, Internal Report. Coordinadora Ejecutiva De Cerro Prieto, Mexicali, B. C., Mexico.

13. Roux, B., Sanyal, S. K. (1979), "An Improved Approach to Estimating True Reservoir Temperature From Transient Temperature Data", Proceedings of the Fifth Workshop Geothermal Reservoir Engineering, Stanford University, Stanford, CA., Dec. 12-14.

14. Schlumberger, (1972), "Log Interpretation, Volume I - Principles."

FIGURE 1 - TYPICAL FIELD CROSS-SECTION (FROM ABRIL AND NOBLE, 1978)

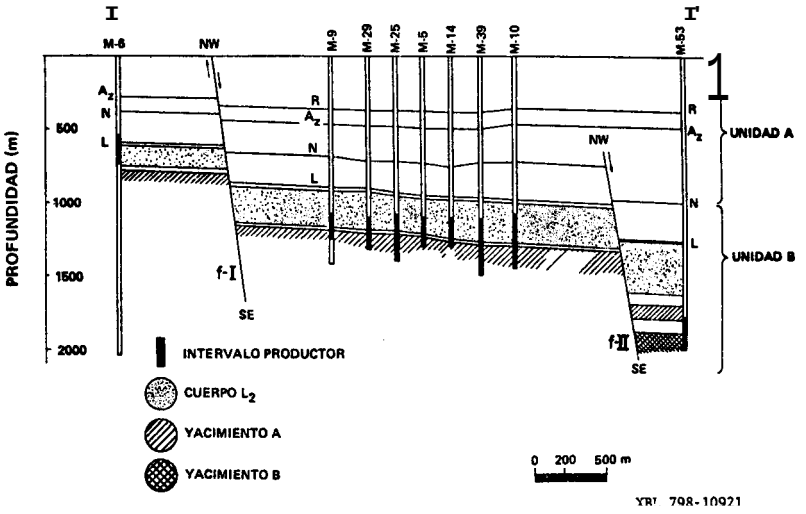

FIGURE 2 - LOCATION OF THE FIELD CROSS-SECTIONS (FROM ABRIL AND NOBLE, 1978)

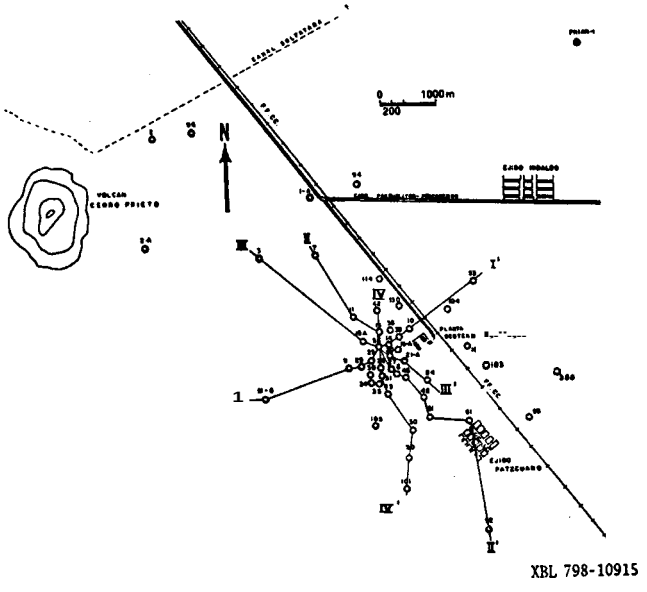

FIGURE 3 - GAMMA LOG RESPONSE
HISTOGRAM FOR WELL M27

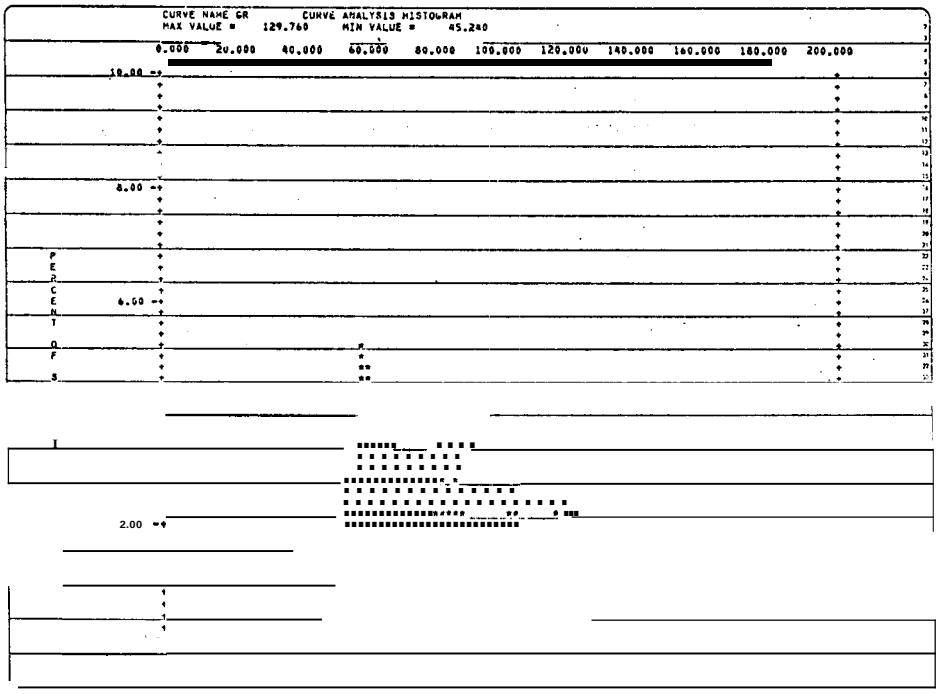

FIGURE 4 - AVERAGE POROSITY VALUES FOR INTERVALS L_2 AND A

WELL	ZONE	INTERVAL (ft)	POROSITY (%)
M19A	L_2	2900 - 3750	19.7
	A	3800 - 4270	16.0
M25	L_2	2900 - 3800	20.2
	A	3850 - 4580	12.0
M27	L_2	3100 - 4000	19.7
	A	4050 - 4210	13.2
M29	L_2	3450 - 3700	15.7
	A	3750 - 4180	13.3
M43	L_2	2930 - 3730	19.0
	A	3800 - 4090	15.4
M45	L_2	3100 - 3860	16.4
	A	3900 - 4570	14.5
M46	L_2	3000 - 3800	15.9
	A	3850 - 4650	11.5
M50	L_2	3050 - 3900	16.5
	A	3950 - 4120	17.0
M101	L_2	3590 - 4350	16.5
	A	———	
M102	L_2	3900 - 5350	19.1
	A	5500 - 6300	12.9
M107	L_2	4500 - 6060	17.1
	A	———	———

FIGURE 5 - AVERAGE WATER SALINITY DATA AS

PPM NaCL equiv CALCULATED FROM THREE

DIFFERENT METHODS

WELL	INTERVAL (ft)	*WATER SALINITY (PPM) METHOD I	METHOD II	METHOD III	LABORATORY DATA
M19A	3600-4240	1650	10465	6013	13812
M25	3580-4590	4266	13499	6504	15054
M27	3600 -4240	1958	9306	4840	11794
M29	3608-4250	1151	17037	9664	13044
M43	3772-4100	3127	14617	8512	13076
M45	3900-4120	730	10806	4477	11060
M46	3930- 4640	1278	10885	5650	10113
M50	3750-4120	1348	9329	3002	13278
M53	6050-6550	—	15225	8793	14446

*Salinity at reservoir conditions

Proceedings Seventh Workshop Geothermal Reservoir Engineering
Stanford. December 1981. SGP-TR-55.

RECENT RESULTS OF TEE WELL DRILLING PROGRAM AT CERRO PRIETO

Bernardo Domínguez A.[1], Marcelo J. Lippmann[2] and Francisco Bermejo M.[1]

[1]Coordinadora Ejecutiva de Cerro Prieto
Comisión Federal de Electricidad
Mexicali, Baja California, México

[2]Lawrence Berkeley Laboratory
Earth Sciences Division
Berkeley, California 94720

Abstract

The results of the 1980 and 1981 well drilling activities at the Cerro Prieto geothermal field are summarized. Details are given on the new series of deeper wells completed in the western ("older") part of the field (Cerro Prieto I), and on the development and step-out wells drilled in the eastern part of the field (Cerro Prieto II and III). Production characteristics of on-line and stand-by wells are discussed. Recent changes in well completion procedures are also described.

Introduction

During the last two years significant advances have been made in the development of the Cerro Prieto field. The purpose of this paper is to update the information presented during the Fifth Geothermal Reservoir Engineering Workshop (Alonso et al., 1979).

The installed electrical power capacity at the field continues to be 150 MW (four 37.5-MW high-pressure turbogenerators). A 30-MW lower-pressure unit has been undergoing testing since mid-1981. Before going into full operation, some installations of the flashing plant for this unit will have to be modified to improve its performance. At this plant, water at about 169°C separated from the high-pressure steam is flashed at 4.36 and 2.11 kg/cm^2 abs. The construction of two 220-MW power plants, each with two 110-MW turbogenerators, has begun. These plants are scheduled to go into operation during 1983 and 1984, respectively.

Drilling program

In November 1981 there were five drilling rigs and two work-over rigs active in the area; about 96 deep wells have been completed. Between December 1979 and November 1981 27 wells were drilled. These wells are shown in Figure 1, with the exception of well G-1, located about 6 km ENE of well NL-1. The total depths and maximum temperatures measured in these wells are given in Table 1.

TABLE 1

CERRO PRIETO
WELLS DRILLED BETWEEN DECEMBER 1979 AND NOVEMBER 1981
TOTAL DEPTHS AND MAXIMUM MEASURED TEMPERATURES

Well	Total Depth (m)	Max. Temp. (°C)	Well	Total Depth (m)	Max. Temp. (°C)
E-1	1996	338	M-115	under construction	
E-2	1945	328	M-117	2495	360
E-3	1814	333	M-118	2664	299
E-4	1767	333	M-122	under construction	
E-5	1966	322	M-125	2315	354
E-7	under construction		M-132	3268	284
G-1	3000	<100*	M-133	2356	310
H-2	3535	288	M-137	2506	>233
M-47	1730	>219	M-139	under construction	
M-73	1885	324	M-147	1908	353
M-79	1813	245	M-157	2545	331
M-109	2396	355	M-172	3287	282
			M-189	3495	267
			T-328	2695	349
			T-364	2926	320

NOTE:
* well filled with drilling mud

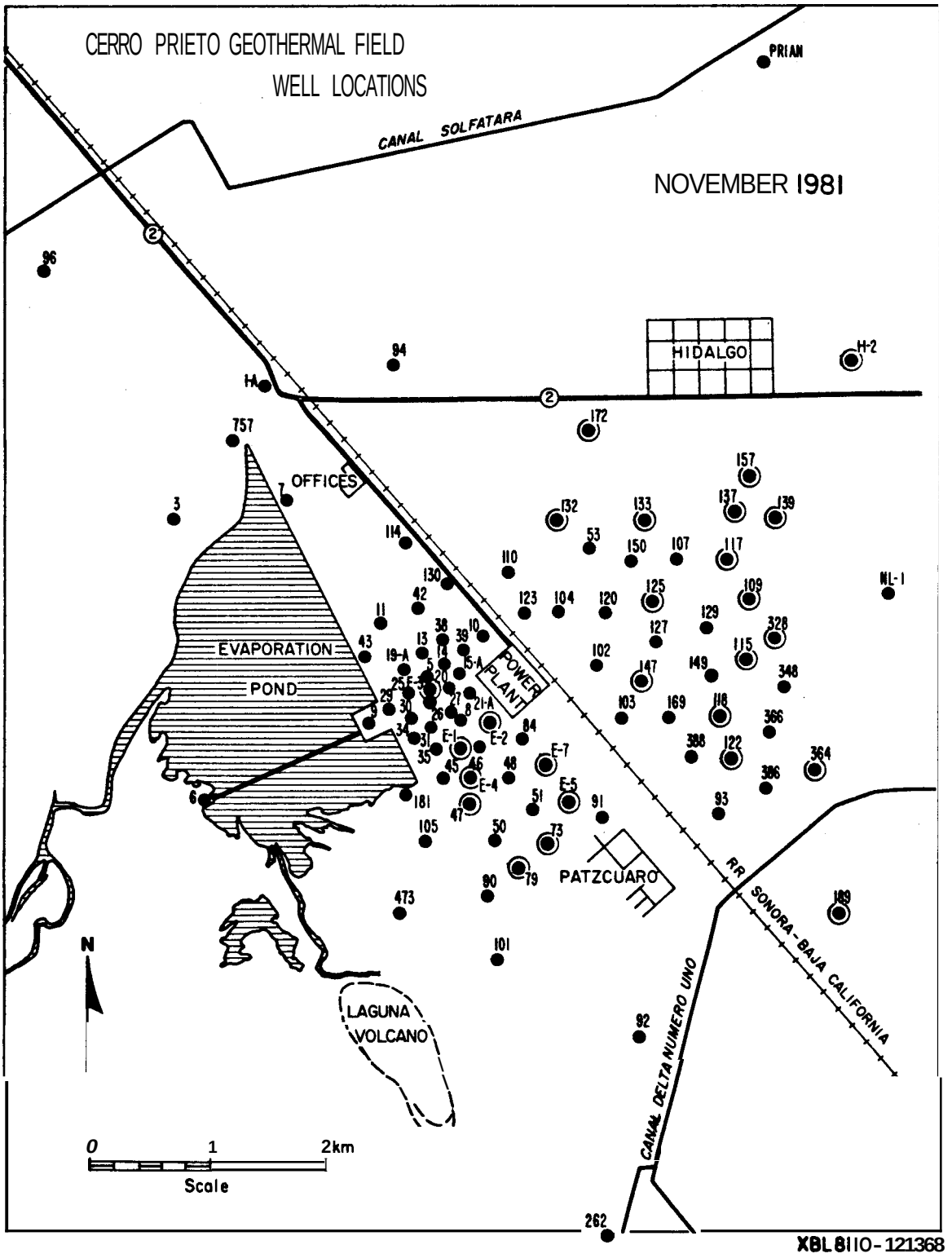

Figure 1. Location of wells at Cerro Prieto. Wells Indicated with concentric circles were drilled between December 1979 and November 1981.

In the eastern part of the field the purpose of the drilling activity has been to increase the number of product-ion wells for the power plants under construction, and to explore for the boundaries of the geothermal system. The temperature profiles obtained in the most recently drilled wells confirmed the temperature distributions developed earlier this year by Castillo et al. (1981) (See Figures 2 and 3). The wells drilled during 1980 and 1981 have essentially delineated the northern, eastern and southeastern boundaries of the thermal anomaly. Outside of this region, the 1977 Prian well (3496 m depth) and the recent G-1 well (3000 m depth) have shown very low temperatures.

In the western part of the field, new production and stand-by wells were drilled for the existing power plant. In that region the wells of the deeper "E-series" (average total depth: 1900 m) have confirmed the presence of a hotter aquifer (about 335°C) below the reservoir which has been under exploitstion since 1973, and whose average temperature and depth are about 280°C and 1250 m, respectively.

Well pressures and production rates

Shut-in wellhead pressures in the northwestern part of the field (CP I Norte), excluding the E-wells, have reached up to about 800 psi; in the southwestern part (CP I Sur) about 900 psi; in the southeastern part (CP II) about 1300 psi; and in the northeastern region (CP III) about 1200 psi.

In CP I Norte (excluding the deeper E-wells) the maximum steam production ever measured in a well was 125 t/h. In CP I Sur, some wells reached 140 t/h of steam. In CP 11, where the reservoir is at 2700-3000 m depth, steam productions of up to 300 t/h have bten measured. In CP III, the reservoir is at 2000-2500 m depth, and some wells have produced above 100 t/h of steam. (Domínguez and Sánchez, 1981).

The production characteristics of the wells supplying steam to the power plant as of August 1981 are given in Table 2. At that time, the average electrical power generation

TABLE 2

CERRO PRIETO WELLS ON LINE
PRODUCTION CHARACTERISTICS
(AUGUST 1981)

Well	Orifice diam. (in)	Pressure (in psig) Wellhead	Separator	Production (metric tons/h) Steam	Brine	Enthalpy (cal/g)
M - 5	7 7/8	110	98	25.7	69.4	304
M - 11	4	119	104	13.5	47.9	281
M - 14	3 7/8	168	107	20.5	70.5	284
M - 19A	7 7/8	110	100	56.3	135.7	315
M - 25	4	240	112	38.5	73.1	344
M - 29	7 7/8	120	113	15.8	60.5	277
M - 30	7 7/8	110	100	41.4	106.1	309
M - 31	5	106	97	16.7	38.8	318
M - 35	7 7/8	122	105	53.8	130.1	316
M - 42	8	190	104	43.7	146.5	285
M - 43	8	108	107	18.7	54.0	300
M - 48	8	130	106	46.1	72.3	364
M - 50	8	125	108	75.4	167.8	326
M - 51	8	122	110	78.2	133.1	355
M - 53	8	124	103	17.3	25.2	370
M - 84	8	100	95	41.4	22.3	489
M - 90	8	108	106	41.4	129.0	292
M - 91	8	112	109.5	67.4	133.1	339
M - 101	8	104	102	17.6	27.9	361
M - 102	5	100	96	22.0	8.2	528
M - 103	4	185	104	48.5	48.3	418
M - 104	6	132	103	63.4	25.6	522
M - 105	8	130	115	56.1	81.6	375
M - 114	8	105	104	41.6	136.8	287
M - 130	8	115	107	53.3	131.8	315
E - 1	4 112	410	130	103.6	172.4	363
E - 2	3 1/8	872	131	64.4	108.7	361
E - 3	3 1/2	580	98	41.1	121.8	295
			TOTALS:	1223.4	2478.5	

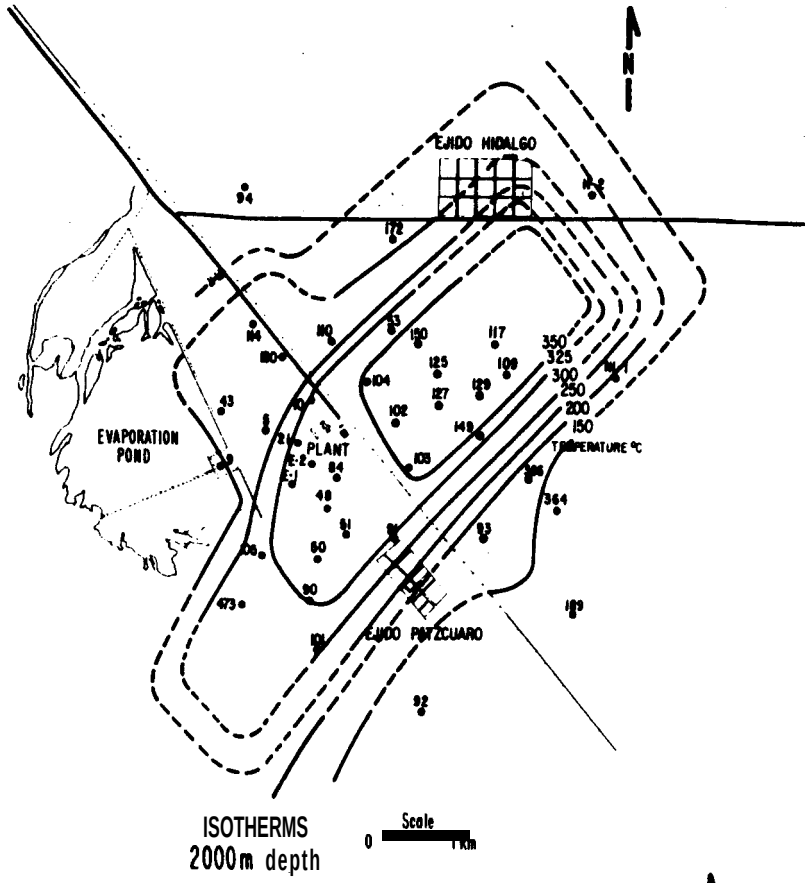

Figure 2.

Cerro Prieto; isotherms at 2000 m depth. (modified from Castillo et al., 1981)

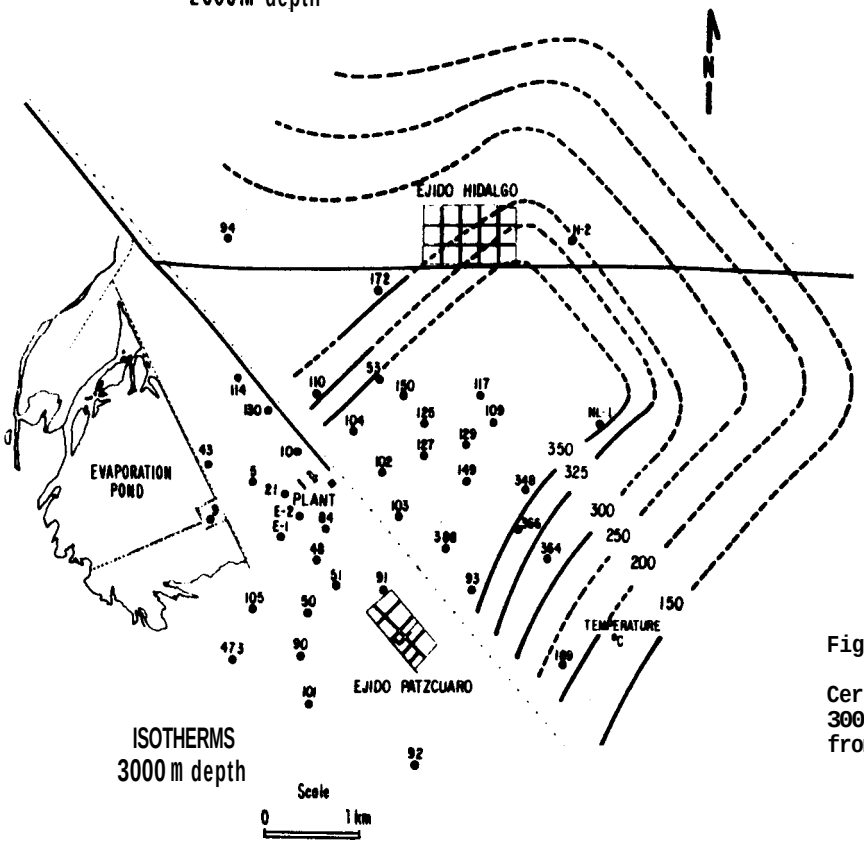

Figure 3.

Cerro Prieto; isotherms at 3000 m depth. (modified from Castillo et al., 1981)

XBL 8111-4870

was 112.5 MW (only three of the four turbogenerators were on line because of repairs to one of the cooling towers). Table 3 shows the production characteristics of the stand-by wells.

Well completion

A number of modifications have been made in the way the wells are completed at Cerro Prieto, partly because deeper production and exploration wells are being drilled, and partly to reduce mechanical and corrosion problems in the casings (Table 4).

The casing completion described by Alonso et al. (1979, Table 2) using production casings with API N-80 tubing was not very successful. The lifetime of these casings is about 6 months (Dominguez et al., 1981). Corrosion, collapses and fractures have been detected.

Up-to-date results have shown that the wells completed during 1977-78 using API K-55 production casings have performed well. These heavier, soft steel casings have shown greater resistance to mechanical stresses and corrosion. The damages observed in some of the 1977-78 wells are believed to be related to faulty cementing of the casings caused by circulation losses and/or failure of casing accessories during the cementing operations.

Presently API C-75 grade production casings are being installed at Cerro Prieto (Table 4). Because of the recent installation, it has as yet not been possible to evaluate their performance.

To reduce circulation losses while cementing long strings of casings (up to 2000 m long), low-density cement slurries have been used. Recently, good results have been obtained by adding small diameter ceramic spherules to the slurry, reducing its specific gravity to about 1.3 (10.8 lb/gal).

In some wells, mainly because of circulation losses, none of the cement slurry returns to the surface. Recently, the non-cemented annular space behind casings has been filled by pouring fine silica sand. It not only reduces the open space behind the partially cemented casing, but also gives it mechanical support. Up to now the wells where this procedure was used have not shown problems.

Final remarks

The drilling of production and exploration wells will continue at Cerro Prieto. The immediate goal is to drill enough wells to satisfy the long-term steam requirements of the power plants. It is estimated that the existing plant will need 30 wells (6 MW/well), while each of the two power plants under construction will require the steam from about 25 wells (8.8 MW/well) to reach a total generating capacity of 620 MW_e by 1984.

In order to establish the areal extent and the energy potential of the southern parts of the field (CP I Sur and CP II) a number of wells are planned to be drilled soon in the area between wells M-101, 93, 189 and 92.

TABLE 3

CERRO PRIETO STAND-BY WELLS
PRODUCTION CHARACTERISTICS

Well	Date	Orifice diam. (in)	Wellhead Pressure (psig)	Production (metric tons/h) Steam	Water	Enthalpy (cal/g)
M - 7	7/25/79	5	100	15.0	101.5	235
M - 73	7/29/81	8	182	100.1	165.0	357
M - 93	6/22/79	8	170	80.7	186.0	320
M - 94	9/03/80	4	100	6.5	76.9	210
M - 110	11/18/79	10	220	185.3	335.7	346
M - 120	4/21/80	10	129	121.7	148.7	392
M - 129	2/12/80	5	700	216.0	301.2	376
M - 147	2/05/80	6	670	297.1	249.6	438
M - 149	3/02/80	8	104	66.4	124.8	342
M - 169	3/28/80	9	183	123.3	204.9	356
M - 172	9/09/81	6	101	23.3	117.3	253
T - 366	7/29/79	8	291	223.5	269.5	383
T - 386	10/07/81	10	110	86.0	159.5	343
T - 388	5/22/80	7	324	169.8	278.5	357
Q - 757	12/05/79	3	101	5.8	51.4	222

TABLE 4

CERRO PRIETO
PRESENT CASING COMPLETIONS

Casing	Size O.D. (in)	API Grade	Weight (lb/ft)	Joint Threads	Approximate Depth (m)
		PRODUCTION WELLS			
Conductor	30	B	98.9	Welded	0 - 50
Surface	20	5-55	106.5	RT.8T.SC.	0 - 300
Intermediate	13 3/8	K-55	68.0	BT.	0 - 1200
Production	9 5/8	c-75	47.0	SEU.HT.	0 - 2500
Liner	7	c-75	29.0	SEU.HT.	2450 - 3000
		EXPLORATION WELLS			
Conductor	20	H-40	94.0	RT.8T.SC.	0 - 100
Surface	13 3/8	K-55	54.5	BT.	0 - 500
Intermediate	9 5/8	c-75	47.0	SEU.HT.	0 - 1600
Production	7	c-75	29.0	SEU.HT.	1550 - 3300
Liner	4 112	c-75	13.5	CS.HT.	3250 - 3800

Notes
BT. = Buttress thread
RT.8T.SC. = Round thread, 8 threads/in, short joint
SEU.HT. = Super E.U. Hydrill thread
CS.HT. = C.S. Hydrill thread

Acknowledgments

The authors express their gratitude to the authorities and personnel of the Coordinadora Ejecutiva de Cerro Prieto of the Comisión Federal de Electricidad for their support and encouragement. Part of this work was supported by the Assistant Secretary for Conservation and Renewable Energy, Office of Renewable Technology, Division of Geothermal and Hydropower Technologies of the U.S. Department of Energy under Contract No. W-7405-ENG-48.

References

Alonso E.,H., Domínguez A., B., Lippmann, M.J., Molinar C., R., Schroeder, R.E., and Witherspoon, P.A., 1979. Update of reservoir engineering activities at Cerro Prieto. In Proceedings, Fifth Workshop Geothermal Reservoir Engineering, Stanford Geothermal Program, SGT-TR-40, pp. 247-256.

Castillo,F., Bermejo,F.J., Domínguez,B., Esquer, C.A., and Navarro, F.J., 1981. Temperature distribution in the Cerro Prieto geothermal field. In Proceedings, Third Symposium on the Cerro Prieto Geothermal Field, Lawrence Berkeley Laboratory, LBL 11967 (in preparation).

Domínguez, B., and Sánchez, G., 1981. Comments on some geothermal drilling and well completion problems at Cerro Prieto. In Proceedings, Third Symposium on the Cerro Prieto Geothermal Field, Lawrence Berkeley Laboratory, LBL 11967 (in preparation).

Domínguez,B., Vital,F., Bermejo,F., and Sánchez, G., 1981. Performance of casings in Cerro Prieto production wells. In Proceedings, Third Symposium on the Cerro Prieto Geothermal Field, Lawrence Berkeley Laboratory, LBL 11967 (in preparation).

Proceedings Seventh Workshop Geothermal Reservoir Engineering
Stanford, December 1981. SGP-TR-55.

DESIGN OF A TRACER TEST FOR THE GEOTHERMAL FIELD OF LOS AZUFRES, MICHOACAN, MEXICO: PROGRESS REPORT

Eduardo R. Iglesias and Gerardo Hiriart

Instituto de Investigaciones Eléctricas
Apartado Postal 475
Cuernavaca, Morelos, México

Comisión Federal de Electricidad
Oklahoma #85, 6° Piso
México 18, D.F., México

ABSTRACT

A tracer test will be conducted at the Los Azufres geothermal field to detect possible high permeability flowpaths interconnecting reinjection and production wells, in order to asses reinjection feasibility in the Tejamaniles area. This test will be the first of its kind to be conducted in t h i s geothermal field. Tracers will be injected in wells **A-7** and **A-8**; **A-2 will** constitute the main observation well. This study suggests that other wells, including probably **A-16, A-1, A-22** and **A-18,** should also, be mnitored. Continuous production/reinjection will provide the driving force for interwell flow. To speed up results, simplify logistics, and reduce costs, slugs of two different tracers, each identifying a particular well, will be simultaneously injected. We *chose* anions as tracers because they propagate through reservoir formations with negligible absorption, and considering the availability of equipment for their analysis. Several bromide, iodide and thiocyanate salts were considered as prospective tracer sources. The unknown background iodide concentrations in the reservoir were determined by us. We estimated the amounts of the prospective salts to be injected by means of Lenda and Zuber's method, and computed the corresponding costs. Considering these amount-cost calculations and that bromide and iodide have been extensively tested in geothermal environments, we chose these anions as the main tracers for the test. As a complement, we propose to conduct a field experiment to evaluate thiocynate as a geothermal tracer.

INTRODUCTION

The Los Azufres geothermal field is located 19°49'N, 100°39'W on the Transmexican **Neo-**Volcanic Axis. The field consists of highly fractured neo-quaternary volcanic deposits. Production horizons are mstly andesites, but in some cases include dacite. Because of the tightness of these igneous **rocks** the main production is believed to proceed through fractures.

The reservoir is liquid-daminat&, but there is a steam cap located near wells **A-6** and **A-17,** in the Tejamaniles region. Produced waters are of medium salinity: TDS ~ 5000-8000 ppm for separated brines (Templos y García, 1981) These brines contain silica **(900-1300** ppm), boron **(150-250** ppm), arsenic **(15-30** ppm), and traces of mercury (Templos y García, 1981). Such amounts of ecologically nocive substances are not suitable for untreated surface disposal. Thus, reinjection of the spent brines is considered as one alternative for disposal.

&injection of relatively cold spent brines, apart from solving the disposal problem, *may* be beneficial to maintain reservoir pressure (e.g. Cuellar et al, **1978**; Home, **1981**). But thermal interference may also result from reinjection (e.g. Einarsson et al, **1978**; Home, **1981**), with potentially serious economic consequences due to enthalpy drawdown. Tu avoid the detrimental effects of thermal interference, two reinjection strategies may be adopted: (a) to reinject into formations hydraulically isolated from the producing reservoir; or (b) to reinject at a distance from the producing wells such that the reinjected water has time to reheat before being produced. This "safe distance" depends sensitively on the details of the local pemability. For example, in Ahuachapan a tracer arrived at a well 400 m distant from the reinjection well in two days, but the corresponding arrival times far two other wells located **450** m and **1000** m from the injector were several weeks (Einarsson et al, **1978**). Thus, identification of high permeability paths interconnecting planned reinjection-and production-wells should preceed the actual implementation of a reinjection *schene.* Tracer tests constitute an unsurpassed reservoir engineering tool to detect such short circuiting flowpaths.

This paper reports on the design of a tracer test that will be run in the Los Azufres geothermal field. The test will involve wells **A-7** and **A-8** as reinjectors, and well **A-2** as the producer. The main goals are (a) to detect possible high permeability flowpaths linking the planned reinjector wells with **A-2**; and (b) to interpret the data, either in terms of fracture conductivity or of matrix permeability.

In the following sections we describe the test area, and discuss the design of this first

tracer test in Los Azufres.

TEST AREA

The test area lies in the Tejamaniles region (or module, as they have been termed), in the southern prtion of the field (Fig. 1).

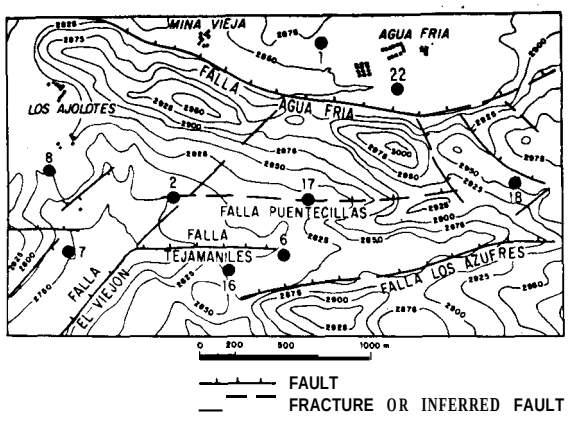

Fig. 1. Map of the Tejamaniles and Agua Fria modules.

Planned reinjection wells A-7 and A-8 lie on the western *edge* of the field, as inidicated by geologic and resistivity data (Garfias, 1981). Their depths, open intervals, and distances to other wells located in the Tejamaniles and Aqua Fria modules are given in Table 1. East fran A-7/A-8 the distribution of temperature is dome-like, with its maximum *near* wells A-6 and A-17. This is reflected in the depths of the wells drilled in the Tejmiles module.

Production well A-2 is located several hundred meters East from the planned reinjectors. The completions and lithological columns of wells A-2, A-7 and A-0 are shown in Figure 2. The production and reinjection intervals intersect mstly microlitic andesites, with *some* interspersed dacite and porphyritic andesite in well A-7. In these tight ingneous rocks the flaw is thought to come mainly through fractures. Note that the reinjection intervals lie deeper than the production interval of A-2, except for the upper slotted interval of well A-I which overlaps it. This is a desirable feature for a reinjection scheme because the negative bouyancy of the colder and denser reinjected water tends to delay thermal interference: but my add some difficulty to the recovery of tracers. However, there is indication of hydraulic connection of wells A-7 and A-8 With A-2, from an BY-lier interference test (Hiriart, 1980).

Other neighboring wells, in addition to A-2, were included in Table 1 for completeness. Of these, A-16 is the second closest to the reinjection area. Well A-16 was first drilled vertically to a depth of 2500 m. High temperatures but low permeabilities were found. Recently the well was reentered and directional drilling began from a depth of ∿ 500 m. At the time of this writing the directional well had succesfully intersected the Tejamaniles fault. The depth and distances to well A-7 and A-8 given in Table 1 were estimated *by* us. At the time of this writing the productivity test had not started. Thus, it is not known whether *dry* steam or a two-phase mixture will be produced. If the produced fluid turns out to be two-phase, it is *expected* that A-16 will be kept bleeding through a small diameter line throughout the duration of the tracer test. In that *case,* the separated water will be monitored for tracers.

Farther East from the reinjection area lie wells A-6 and A-17. These relatively shallow wells produce *dry* steam. The chemical tracers we *are* planning to use in this first test partition negligibly into the gas phase. Therefore these wells will not be mnitored during the tracer test.

Next in increasing distance fran the reinjection area is well A-1, located to the NE of A-7/A-8 in the *Agua* Fria module (Fig. 1). This well is currently producing 30 tons/h with a water/steam ratio of 2:1. It is *expected* that this flowrate will be kept constant throughout the duration of the tracer test. If that is the case, the separated water will be mnitored for tracers.

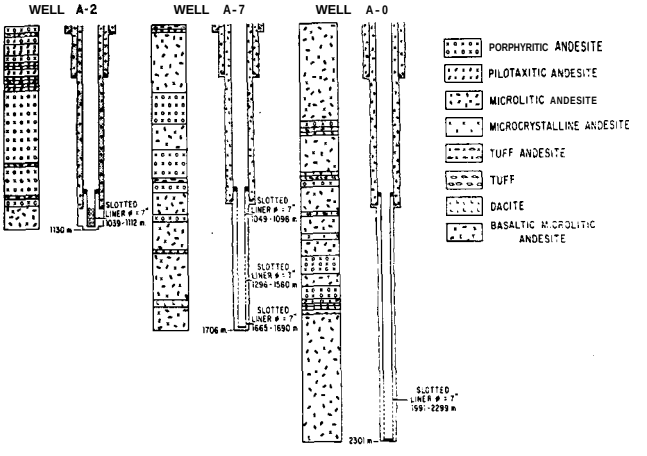

Fig. 2. Lithological columns and completions of wells A-2, A-7 and A-8.

Finally, wells A-22 and A-18, in the Agua Fria and Tejamaniles modules respectively, are the farthest from the reinjection area. These wells are *expected* to be kept bleeding through small diameter lines throughout the duration of the tracer test. Due to their negigible productions and great distances from the injection pints, there is little hqp of actually detecting tracers in these wells. Nevertheless they will be mnitored on a low priority basis throughout the test.

TEST DESIGN

General Remarks

The test will be conducted in multitracer, continuous production/reinjection mode, as follows. Simultaneous production/reinjection will begin some time before actual tracer injection to allow as much stabilization of the flaw in the reservoir as practically possible. Separated water being produced from A-2 will be concomitantly reinjected in wells A-7 and A-8. After a convenient stabilization time has elapsed, short injections of two different tracers, each identifying a particular well, will be inserted in the lines feeding A-7 and A-8. Sampling of well A-2 will begin immediately afterwards. During the first several hours samples will be extracted every half hour; subsequently, the rate of sampling will decrease monotonically. The rationale for this sampling strategy is to record possible early rapid buildup of tracer concentration in A-2 due to high permeability path(s) extending from one or both reinjection wells; as arrival times increase so do dispersions, and tracer concentration buildups become slower, therefore sampling frequency can be safely decreased.

Tracers used in hydrogeology and in the oil and geothermal industries include radioactive substances and chemicals. Use of radioactive tracers involves lengthy proceedings to obtain licenses and equipment currently unavailable to us. For simplicity chemical tracers were adopted.

The main advantage of the approach described in the preceding paragraphs is that the multitracer configuration insures a significantly shorter test. Consequently, logistics can be made simpler, costs (e.g. associated with personnel and equipment) can be reduced, and results will be available earlier.

Tracers

The popular chemical tracers mentioned in the literature can be broadly divided in fluorescent dyes and salts with detectable cations or anions. Fluorescent dyes tend to be retained in the reservoir rocks (Wagner, 1977) and were not considered for this test. Experience has indicated that cations do not propagate through reservoir formations as easily as anions. Thus, only anions were considered as tracers. After screening, the following candidate salts were selected: sodium bromide (NaBr), sodium iodide (NaI), potassium iodide (KI), ammonium thiocyanate (NH_4SCN), and sodium thiocyanate (NaSCN). These salts have suitable anion to molecule molecular weight ratios and high solubilities (Table 2). High solubilities are desirable because they determine the maximum concentration attainable at the point of injection, which generally should be as high as possible in slug injection tests to insure detectability over long distances.

Chemicals with high tracer-anion/salt mass ratios are convenient to keep munts of salts injected and costs dawn. Iodide and bromide have been succesfully used as tracers in geothermal environments (e.g. McCabe et al, 1980, 1981; Tester et al, 1979); thiocynate (although fairly common in the oil industry) has not, to our knowledge.

Background Concentrations

The natural (background) reservoir concentrations of the chemicals used as tracers are important for tracer test design because they are related to the amounts of tracers to be injected, as shown later in this paper. In the following paragraphs the background concentrations of iodide, bromide, and thiocyanate in the test area are discussed.

Bromide concentrations are routinely determined by CFE's* geochemistry group in Los Azufres. Average values for separated waters from wells A-2, A-7 and A-8 are 0.29 ± 0.28 ppm, 0.35 ± 0.10 ppm, and 0.2 ± 0.2 ppm respectively (Lopez and Templos, 1980).

Iodide concentrations are not routinely determined in Los Azufres. Sampling and analysis was conducted by an IIE† team in October 1981; CFE personnel collaborated taking downhole samples from well A-7. Iodide concentration resulted as follows: for separated water from A-2, 0.35 ± 0.01 ppm; for two downhole samples from A-7, corresponding to depths of 1075 m and 1420 m, 0.18 ± 0.01 ppm and 0.17 ± 0.01 ppm respectively; for water from the disposal pond of well A-18 (samples taken near the discharge tube), 0.23 k 0.01 ppm.

Allowing for dilution of the samples from separated water, and considering the known downhole values, we conservatively adopted reservoir "background concentrations" of 0.40 ppm and 0.25 ppm for bromide and iodide respectively. Thiocyanate is generally absent from geothermal waters. Its concentration in the reservoir brine was assumed not to exceed 0.01 ppm.

Amounts and costs

The amount of tracers to be injected were estimated following a method devised by Lenda and Zuber (1970). Normalized breakthrough curves for line injection between two impermeable layers computed by these authors were used. This method assumes that the flow takes place in a homogeneous porous medium with matrix pemability. These assumptions might not apply to the igneous formations characteristic of the test area. Nonetheless, they provide a conservative, "worst case" approach to the tracer flow: generally, in a two well injection

* Comisión Federal de Electricidad

† Instituto de Investigaciones Electricas

Table 1 Wells directly involved in test, and wells in nearby areas

	Tejamani East Module							Agua Fria Module	
Well	A-8	A-7	A-2	A-16+	A-5	A-17	A-18	A-1	A-22
Wellhead height above sea level (m)	2775	2750	2750	2825	2800	2810	2950	2875	2875
Depth (m)	2301	1706	1130	1285*	900	627	1328	2173	1560
Open intervals (m)	1991-2299	1049-1095 1296-1580 1665-1690	1039-1130	1072-1285 *	548-581	361-622	1013-1324	1725-2160	1007-1350
Distance to A-7 (m)	500	-	700	740*	1250	1460	2670	1950	2180
Distance to A-8 (m)	-	500	730	960*	1450	1550	2760	1800	2130

+ Well directionally drilled * Estimate by the authors

Table 2. Chemical properties of prospective tracers*

Tracer	Ratio of molecular weights (anion/ molecule)	Solubility(g/100 c.c.) In cold water	In hot water
NaBr	0.768	116	121
NH_4SCN	0.763	128	very soluble
NaSCN	0.716	139	225
KI	0.764	128	208
NaI	0.846	184	302

*From the Handbook of Chemistry and Physics, 60th Edition, CRC Press.

Table 3. Tracers amounts vs. costs

Tracer	Relative price* per unit mass	Peak anion concentration in breakthrough curve (ppm)	Relative amounts of salts to be injected Well A-7	Well A-8	Relative cost of salt to be injected Well 17	Well 18
NaBr	1.00	0.60	1.000	1.148	1.000	1.148
NH_4SCN	1.37	0.10	0.168	0.192	0.230	0.263
NaSCN	1.42	0.10	0.179	0.205	0.254	0.291
KI	14.51	0.35	0.586	0.673	8.503	9.765
NaI	18.23	0.35	0.530	0.608	9.662	11.084

* From the Chemical Marketing Reporter (October 1981)

configuration greater dispersion of the tracer is expected in transport through a porous matrix than in fracture flow.

We have adapted Lenda and Zuber's method, which in its original form applies to radioactive tracers, for use with ionic tracers derived from highly dissociating salts. Briefly, the modified method estimates the mass of salt to be inyected, m, from

$$m = (\mu_{salt}/\mu_{ion})(c/c_D)\ x^2\ \phi h\ (D_x/D_y)^{-1/2} \quad (1)$$

Where c is the minimal concentration of the anion at the maximum of the breakthrough curve which assures a proper recording of *the* whole *curve,* c_D *the* dimensionless peak concentration in the dimensionless breakthrough *curve,* x the interwell distance, ϕ the porosity and h the height of the confined aquifer, and D_x and D_y the dispersion coefficients parallel and normal to the direction of flow respectively. The dimensionless ratio (D_x/vx), where v is the mean velocity of flow in the x direction, parametrizes the breakthrough curves. Whithin the range of parameters considered c_D decreases with increasing values of (D_x/vx). Therefore, from equation (1) greater values of m correspond to higher values of (D_x/V) for a given distance. Values of (D_xv) range fran a few centimeters for fine sands to about 100 m for fissured rocks (Lenda and Zuber, 1970). Thus, we adopted $(D_x/v) = 100$ m in order to obtain conservative estimates of the mass of tracer to be injected.

An extra safety factor is provided by the ratio (D_x/D_y) appearing in equation (1). For liquids, theoretical and experimental values of this ratio lie between 1 and 20 for Bodenstein numbers (= effective grain diameter × man flow velocity/ coefficient of molecular diffusion) ranging from 4×10^{-1} (slow laminar flow) to 10^5 (fast turbulent flow) (Lenda and Zuber, 1970 and references therein). In *our* calculations we set &/%) = 1, effectively enhancing the safety marg of *our* estimates.

We adopted $c = c_{bck} + 10\varepsilon$, where c_{bck} is the background concentration of the anion in the reservoir fluid and ε is the resolution of the corresponding method of analysis. Standard methods of analysis adequate for the concentrations of interest here have typical resolutions of 0.02 ppm, 0.01 ppm, and 0.01 ppm for bromide, iodide, and thiocyanate respectively. The vales of c thus computed are shown in Table 3.

Taking $\phi h = 1$m, a typical value for the test *area,* we computed the estimates *shown* in Table 3. For convenience these results are expressed in terms of the mass of NaBr to be injected in well A-7, The greater distance of well A-8 to well A-2 results in a practically negligible ~ 15% increase of the mass of tracer to be injected over the values corresponding to A-7. The background concentrations of the tracers have a more pronounced effect in this particular case. The small amounts of thiocyanates estimated indicate the advantage of using as tracers substances that are naturally absent in the brines, and for which sensitive analysis techniques exist.

Table 3 also *shows* the relative costs of the mass to be injected for each salt considered. Not surprisingly, the smallest costs, by far, correspond to thiocyanates. Note also that the relatively low background concentration of iodide compensates for its higher price per unit mass.

Although thiocyanates look very attractive from the pint of view of their low costs, they have not been extensively tested in geothermal environments. Bromide and iodide are better known as geothermal tracers, and their costs are reasonable for the planned test (US $1009 for NaBr in A-7). Therefore, we conclude that bromide and iodide are the indicated tracers for the first test in Los Azufres.

Finally, a usefull extension of *this* work is suggested *by* our results. We propose to conduct a field experiment to evaluate thiocyanate a5 a geothermal tracer. The experiment would consist of injecting this anion in parallel with the main tracers in wells A-7 or A-8. Comparison of the corresponding breakthrough curves would provide valuable information about the characteristics of thiocyanate as a geothermal tracer.

ACKNOWLEDGMENTS

We thank Ing. C. Miranda from CFE for taking downhole fluid samples, and Dr. D. Nieva from IIE for conducting the iodide analysis and for useful discussions.

This work forms part of the cooperative geothermal program between Instituto de Investigaciones Electricas and Stanford University.

REFERENCES

. Cuellar, G., Choussy, M., and Escobar, D. (1978) "Extraction-reinjection at Ahuachapan Geothermal Field", Pmc. 2nd Invitational Well-testing Symp., Report LBL-8883, pp 15-25.

. Einarsson, S., Vides, A., and Cuellar, G. (1975) "Disposal of Geothermal Waste Water by Reinjection", Proc. 2nd United Nations Symp. on the Development and Use of Geothermal Resources, pp 1349-1363.

. Garfias, A. (1981), personal communication.

. Hiriart, G. (1980) "Prueba de interferencia sector Tejamaniles", Oficina de Evaluación y Estudios, Comisión Federal de Electricidad, September 1980.

. Home, R. (1981) "Geothermal Reinjection Experience in Japan", Society of Petroleum Engineers of AIME, paper SPE 9925, pp 423-433.

. McCabe, W., Manning, M., and Barry, B. (1980)

"Tracers Tests, Wairakei", Geothermal Circular WJMcC 2, Institute of Nuclear Sciences INS-R-275, DSIR, New Zealand.

- McCabe, W., Manning, M, and Barry B. (1981) "Tracer Tests, Broadlands 1980", Geothermal Circular WJMcC 3, Institute of Nuclear Sciences INS-R-288, DSIR, New Zealand.

- Lenda A., and Zuber,A. (1970) "Tracer Dispersion in Groundwater Experiments., in Isotope Hydrology 1970, IAEA, Vienna pp 619-641.

- Lopez, J. M and Templos, L. (1980) "Estudios Químicos del Agua Separada de los pozos productores del campo geotérmico de Los Azufres, Michoacán", Memoria 3a. Reunión Nacional de Geotecnia y Geotermia.

- Templos, L. and García, G. (1981) "Pruebas de inyección de agua separada en el Módulo de Tejamaniles, Campo Geotérmico de Los Azufres, Michoacán, México", CFE División del Eje Neovolcánico, April 1981.

- Tester, J. Bivins, R., and Potter, R. (1979) "Interwell Tracer Analysis of a Hydraulically Fractured Granitic Geothermal Reservoir", Society of Petroleum Engineers of AIME, paper SPE 8270.

- Wagner, O. (1977) "The use of Tracers in Diagnosing Interwell Reservoir Heterogeneities-field Results", Journal of Petroleum Technology, Nov. 1977, pp 1410-1416.

Proceedings Seventh Workshop Geothermal Reservoir Engineering
Stanford, December 1981. SGP-TR-55.

ANALYSIS OF FLOW DATA FROM SEVERAL BACA WELLS

T. D. Riney and S. K. Garg

Systems, Science and Software (S^3)
P. O. Box 1620
La Jolla, California 92038

Abstract Analyses are presented of the downhole pressure buildup data for wells located in the Redondo Creek area of the Baca Geothermal Field. The downhole drilling information and pressure/ temperature surveys are first interpreted to locate zones at which fluid enters the wellbore from the fractured formation and to estimate the initial reservoir temperature and pressure in these zones. Interpretation of the buildup data for each well considers wellbore effects, the CO_2 content of the fluid and differentiates between the single-phase and two-phase portions of the data. Different straight-line approximations to the two portions of the data on the Horner plot for a flow test yield corresponding estimates for the single and two-phase mobilities. Estimates for the formation kh are made for the wells.

Introduction The Baca Geothermal Field is located in the Valles Caldera in north central New Mexico, 60 miles north of Albuquerque, and about 35 miles northwest of Santa Fe. Analysis of the downhole data from wells drilled in the Redondo Creek area of tne field indicates that the bulk of the formation permeability is in a fracture network. Consequently, the performance of a well depends largely upon whether it intersects one or more fractures, how large each intersected fracture is and the degree to which it is connected to the rest of the network. The reservoir pressures identified from the downhole analysis define a vertical gradient of 0.348 psi/ft.

Chemical analyses of the discharge fluids from Baca wells indicate that the reservoir fluid is of low salinity ($\leq$ 8,000 ppm) with an incondensible gas content (principally CO_2) of about 0.4 to 1.5 percent by mass (a = 0.004 to 0.015). The effect of the incondensible gas content on the fluid state may be examined using an equation of state for a mixture of pure water and carbon dioxide (Pritchett, et al. [1981]). Figure 1 illustrates the effect in p-T space for a = 0.01. The probable extent of the initial two-phase region in the Baca reservoir and the extent to which the wells will induce

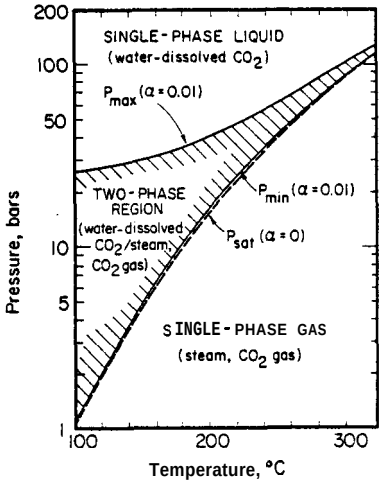

Figure 1. Phase diagram for water with CO_2 mass fraction α=0.01. Saturation curve for pure water (α=0) is dashed.

flashing in the formation upon production are very sensitive to the CO_2 content of the fluid.

The S^3 reservoir simulator CHARGR was recently employed in a series of radial flow calculations to investigate the response of initially single-phase and initially two-pnase reservoirs undergoing production or injection from a single well (Garg and Pritchett [1980]). Figure 2 shows the Horner plot for the simulated buildup history of an initially single-phase reservoir that undergoes flashing upon production. The initial buildup behavior (wellbore storage effects were not simulated) is governed by the two-phase region of the reservoir; the slope on the Horner plot of the curve yields a value for the total kinematic viscosity ν_t which is characteristic of the two-phase region created during drawdown. The detailed calculations show that the pressure buildup is accompanied by the propagation of a condensation front, originating at the well, into the formation; the condensation front eventually engulfs the

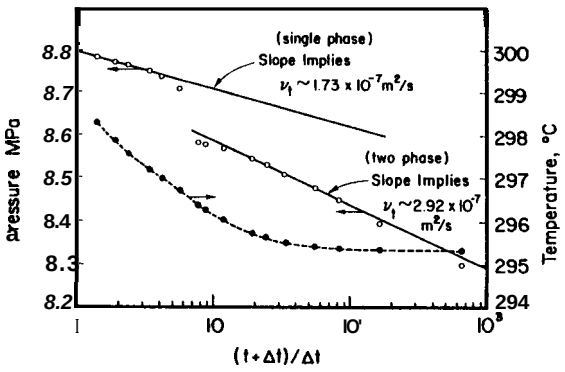

Figure 2. Pressure and temperature buildup data for Case B-1 simulated well test (Garg and Pritchett [1980]).

entire two-phase region after which the buildup behavior is essentially that of a single-phase fluid. The two-phase buildup extends over a full log cycle; the slope of this straight line implies a kinematic viscosity which is in fair agreement with the actual two-phase value. The single-phase buildup in this case extends over less than one-half cycle; the slope of this straight line implies a kinematic viscosity which is about 40 percent larger than the actual single-phase value. This example, and other cases treated, illustrate the importance of selecting the correct straight line.

We have used the results of the numerical simulations to provide guidance in our interpretation of the flow data from several Baca wells. The interpretation considers the effects of the CO_2 content and fracture permeability of the reservoir. The analysis also accounts for the fact that the downhole pressure/temperature gages are usually located several hundred feet from the primary production zone. In the following we will present representative buildup analyses of data from two Baca wells.

Well Baca No. 4 Figures 3 and 4 present selected temperature and pressure profiles recorded in well B-4. Survey S8 was taken prior to any production testing, but the well had been deepened from 5048 ft (4301 ASL) to 6378 ft (2987 ASL) five weeks earlier. Temperature survey S11 was made 17 days after a 9-day production test and is in close agreement with S8 for depths less than 5000 ft. For very long shutin times the measured temperatures (profiles S24 and S40) are much higher than for the shorter shutin times (profiles S8 and S11) except for close agreement at the bottom of the hole. This is attributed to the influx of hot fluid from a minor entry near the bottom of the well. Survey S16 was recorded two days after shutin following a 64-day drawdown

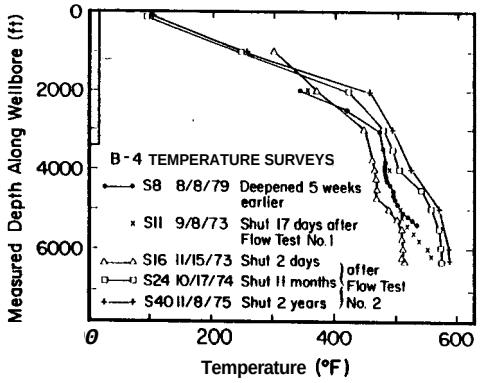

Figure 3. B-4 temperature surveys before, during and after Flow Test No. 2.

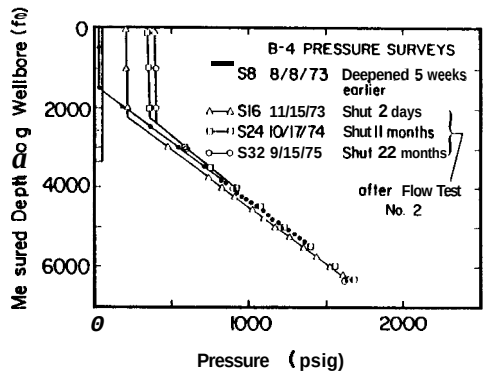

Figure 4. B-4 pressure surveys before, during and after Flow Test No. 2.

period. The primary production is apparently located at ~ 4800 ft (4546 ASL); the reservoir rock is cooled by the flashing of the fluid within the production zone. The corresponding pressure profile (S16 in Figure 4) shows that the fluid in the wellbore two days after shutin is liquid below 2100 ft. The long-term stable profiles (S24 and S32) cross the early time profile (S8) at ~ 4500-5000 ft. Pressure equilibrium between the wellbore and reservoir fluid is maintained at the zone of primary permeability ~ 4800 ft.

In summary, the zone of primary permeability in B-4 is located at ~ 4800 ft (4546 ASL) with minor entries located near the wellbottom and at shallower depths noted during drilling. The initial temperature and pressure at 4800 ft are estimated to be 1170 psig (~ p(a) = 81.4 bars)* and ~ 500°F (260°C).

Although B-4 has been flow tested three times, downhole measurements are available only for the buildup period following Flow Test No. 2 (9/10/73-11/13/73). During the 64-day drawdown portion of this test the fluid flowed to a separator vessel and the

steam and water phases were measured individually. After 50 days, the flow rate stabilized with a wellhead pressure of 120 psig and a separator pressure of 113 psig (Hartz [1976]). At separator conditions the steam fraction and total fluid enthalpy were reported to be 27.5 percent and h_t = 556.1 BTU/lbm. The mass flow rate and the duration of Flow Test No. 2 are taken as

$$M = 172{,}500 \text{ lbm/hr} \sim 21.73 \text{ kg/s}$$
$$t = 1538 \text{ hours.}$$

Figure 5 shows a semi-log plot of the buildup data recorded by Union at a depth of ~ 6350 ft (3000 ASL). Since the measurements

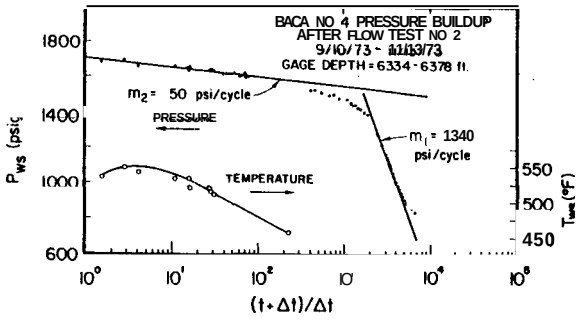

Figure 5. B-4 pressure and temperature buildup following Flow Test No. 2.

were made so far below the primary production zone at 4800 ft (4546 ASL), we must account for the pressure difference in the data interpretation.

During drawdown the wellbore is filled with two-phase fluid which enters from the primary production zone. The reservoir rock is cooled by the flashing of the fluid within the production zone. After shutin the temperature within this zone recovers along with pressure until condensation occurs; it subsequently recovers slowly, primarily by conduction. From the temperature survey made on 11/15/73 (S-16) we estimate the temperature in the wellbore at 4800 ft (4546 ASL) after condensation is initiated to be ~ 464°F (240°C).

The CO_2 content of the discharge fluid from B-4 has been measured to be 0.85-1.1 percent (a = 0.0085-0.011). Although the in-situ value may be different (Pritchett, et al. [1981]), we assume for the moment that a = 0.01. Then according to Figure 1,

* Here and in the sequel we add 10 psi (0.7 bars) to the gage pressure to correct for tne atmospheric pressure at ~9000 ASL.

the pressure required to ensure that the 464°F (240°C) wellbore fluid be single-phase liquid is P_{max} = 812 psia (56 bars). Correspondingly, the recorded shutin pressure at ~ 6350 ft (3000 ASL) must satisfy the inequality $p_{ws} > 812 + 0.35\ (4546-3000) = 1353$ psia = 1343 psig

This value is attained at ~ 43 minutes after shutin; hereafter there is a constant hydrostatic head of 541 psi between the gage pressure and the corresponding pressures in the production zone. Only the single-phase portion of the Horner plot (Figure 5) may be used in this case (a = 0.01) in evaluating formation properties of the production zone.

Further, if the CO_2 content were 1 percent (a = 0.01), then from Figure 1 we see that the initial reservoir conditions (81.4 bars, ~ 260°C) would correspond to single-phase liquid. During drawdown the formation fluid flashes in the vicinity of the wellbore and the flash front propagates laterally into the producing zone. After shutin, condensation commences but a two-phase region created during drawdown would not return to single-phase liquid until the pressure builds up to the value of P_{max} associated with ~ 260°C, i.e., P_{max} = 67 bars (972 psia). The corresponding pressure at the recording depth of 6350 ft (3000 ASL) is given by $p_{ws} = 972 + 0.35\ (4546-3000) = 1513$ psia = 1503 psig. This value is close to the transition pressure (~ 1575 psig) between the two-phase and single-phase behavior shown in Figure 5.

We note in passing that if we had ignored tne presence of CO_2 and assumed the fluid to be pure water (α_0 = 0), we would compute that the producing zone at 4800 ft would recover from two-phase to single-phase water when the pressure builds up to p_{ws} = 1212 psig. This value is considerably below the observed transition pressure (~ 1575 psig).

Because of the uncertainty in the values of a and the initial temperature in the production zone, it is of interest to determine the values of these parameters which correspond to the two-phase to single-phase transition pressure indicated by the Horner plot. The equation-of-state for CO_2/water mixtures (Pritchett, et al. [1981]) has been used to determine those points (α_0, T_0) which correspond to a pressure in the production zone of P_{max} = 1575 - 541 = 1034 psig = 1044 psia (72 bars). The estimated initial temperature (T_0 ~ 500°F) corresponds to the higher measured value of CO_2 in the discharge fluid (α_0 = 0.011) whereas the lower measured value (α_0 = 0.0085) corresponds to an intial temperature of T_0 ~ 512°F (~ 267°C). These values are within the uncertainties of the measurements.

The slope m_2 = 50 psi/cycle = 3.44 x 10^5 Pa/cycle in the single-phase portion of the Horner plot reflects the buildup behavior in the production zone and extends over two full log cycles. It can, therefore, be used to estimate the kinematic mobility-thickness product from the relation

$$\frac{kh}{\nu_t} = \frac{1.15\ \dot{M}}{2\pi m} = \frac{1.15\ (21.73)}{2\pi(3.44 \times 10^5)} = 1.16 \times 10^{-5}\ \text{ms}$$

To estimate the formation kh product we need an approximate value for the total kinematic viscosity of the reservoir fluid during the single-phase portion of the buildup response. We use the viscosity of liquid water at the initial conditions of the producing zone (81.4 bars, 260°C), $\nu_t = \nu_\ell$ = 1.315 x 10^{-7} m^2/s and compute

$$kh = 1.52 \times 10^{-12}\ m^3 = 5050\ \text{md-ft.}$$

Well Baca No. 20 The temperature surveys, in Figure 6 especially S5 and S10, indicate that relatively low temperature fluid enters the wellbore at approximately 4000 ft (5165 ASL). This implies that the primary production zone is located at 4000 ft and the fluid entering the wellbore at this depth during buildup subsequent to Flow Test No. 4 has been cooled by flashing within the formation. Below 5000 ft (4237 ASL) there appears to be conductive heating of the wellbore fluid (see S5 and S10).

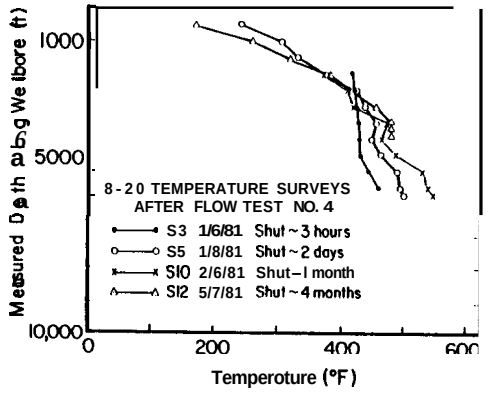

Figure 6. 8-20 temperature surveys following Flow Test No. 4.

The initial pressure at 4000 ft is estimated from S2 (not shown) and S12 (Figure 7) to be ~ 975 psig (p(a) = 67.9 bars). Since no stable temperature profile is available, we extrapolate S12 from 3500 ft to estimate the initial temperature at 4000 ft to be ~ 485-515°F (252-268°C). From S3 the temperature in the primary production zone at 4000 ft (5165 ASL) is estimated to be reduced to ~ 432°F by the in-formation flashing.

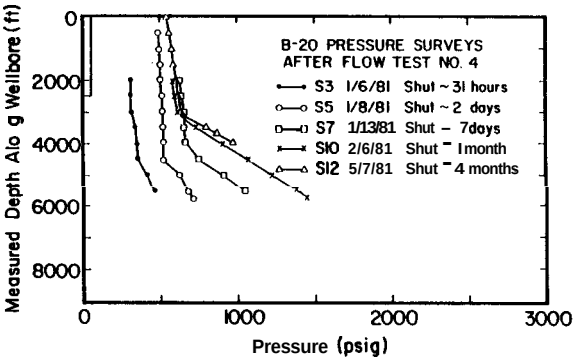

Figure 7. 6-20 pressure surveys following Flow Test No. 4.

Four flow tests have been performed on 6-20 but only Flow Test No. 4 (9/24/80-1/6/81) was of sufficient duration (104 days) and with sufficient pressure transient measurements to warrant analysis. During the flow test the well was flowed through a vertical separator. The wellhead pressure and total flow rates varied over the test period but stabilized over the last two months. For the purposes of analysis we use

M = 56,100 lbm/hr (averaged over last 10 days)

~ 7.06 kg/s

t = 2,653 hours (equivalent production time)

Time t is calculated by dividing the cumulative fluid mass produced during the 104-day Flow Test No. 4 (148,830,000 lbm) by the total mass flow rate averaged over the last ten days of the production.

Figure 8 presents a semi-log plot of the pressure buildup at a depth of 4500 ft (4700 ASL) where most of the downhole recordings were made. Since the primary production is

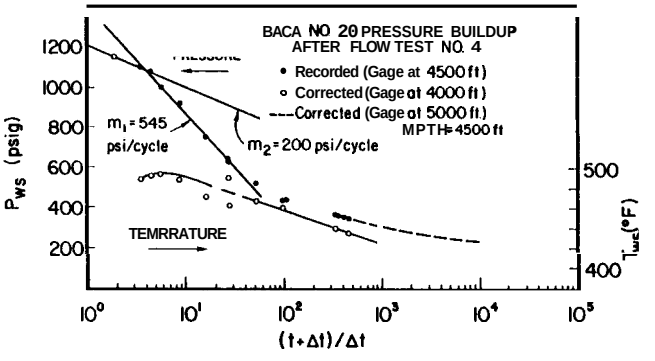

Figure 8. 6-20 pressure and temperature buildup following Flow Test No. 4.

at 4000 ft and the bulk of the pressure data were recorded at 4500 ft, it is necessary to account for the pressure difference in interpreting the data. The pressure profiles in Figure 7 show that the wellbore fluid is

two-phase during the buildup period. The fluid below 4500 ft is two-phase at three hours (S3) and two days (S5) after shutin. After seven days (S7) the fluid below 4500 ft is single-phase liquid, the fluid above 4000 ft is single-phase gas and there appears to be a two-phase section at 4000-4500 ft. After one month there is liquid below 3000 ft with a gas cap above this depth.

Since the wellbore pressure at the gage depth must be corrected by different amounts at different buildup times, we have replotted the Horner plot in Figure 9. The data points at 4000 ft (5165 ASL) recorded during profile surveys are indicated as are the estimates made from surveys in which recordings were only made at 4500 ft (4700 ASL). In this case the estimates for the primary production depth (4000 ft) contain corrections which account for changes in the wellbore state with changes in buildup time. From the corrected plot (Figure 9) we see that the transition from slope m_1 to m_2 is actually completed at $p_{ws} > \sim 900$ psig rather than the much larger apparent value inferred from Figure 8.

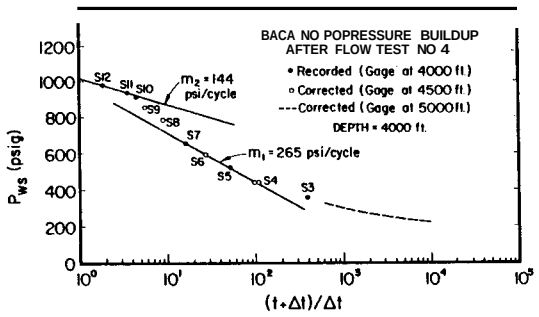

Figure 9. Corrected 6-20 pressure buildup following Flow Test No. 4.

A CO_2 mass fraction of 1.47 percent has been measured in the discharge fluid from well 6-20. This is higher than that measured in all but one other well and may be higner or lower than the in-situ value (Pritchett, et al. [1981]). If we assume that the CO_2 content in the primary production zone is in fact the same as measured in the discharge fluid, then the zone at 4000 ft would be initially two-phase for any temperature within our range of uncertainity (~ 252-268°C). According to the equation-of-state for CO_2/water mixtures, at 252°C the initial in situ gas saturation would be $S_g = 0.077$ whereas the temperature of 268°C would imply $S_g = 0.409$. In this case, the transition from slope m_1 to slope m_2 in Figure 9 would merely reflect the recovery of the production zone to its initial conditions.

On the other hand, if we assume the change in slope corresponds to a transition from two-phase to single-phase behavior during buildup, then the equation-of-state for CO_2/water mixtures may be used to determine the set of permissible points (T_0, α_0) for which P_{max} = 62.8 bars (910 psia = 900 psig). A value of $T_0 = 252°C$ would imply $\alpha_0 = 0.01$ whereas a value of $T_0 = 268°C$ would imply $\alpha_0 = 0.003$.

Because of the uncertainty in α_0 and T_0 we cannot establish if the primary production zone is initially single-phase liquid (e.g., P_0 = 67.9 bars, T_0 = 252°C, $\alpha_0 = 0.01$) or initially two-phase (e.g., P_0 = 67.9 bars, T_0 = 252°C, $\alpha_0 = 0.0147$). In either case, however, the slope m_1 in Figure 9 approximates the two-phase portion of the pressure build-up for a full log cycle and this portion of the data can be used to infer formation properties.

From the value of m_1 = 265 psi/cycle (18.3 x 10^5 Palcycle) we can calculate the corresponding value of the two-phase kinematic mobility-thickness product

$$\frac{kh}{\nu_t} = \frac{1.15\ \dot{M}}{2\pi m_1} = \frac{1.15\ (7.06)}{2\pi(18.3 \times 10^5)} = 7.06 \times 10^{-7}\ \text{ms}$$

To estimate the formation kh product we first note that during the last ten days of Flow Test No. 4 the wellhead pressure and effective (total) enthalpy of the produced fluid were essentially constant: WHP = 116 psig; h_t = 794.3 BTU/lbm. We have used these values, and an isenthalpic model for two-phase flow in the wellbore that assumes no slippage between the liquid and gas components, to estimate the downhole flowing conditions during the final ten days of drawdown. The calculated pressure at 4000 ft (5165 ASL) is p_{wf} = 180 psig (p(a) = 13.1 bars) and the corresponding downhole flowing kinematic viscosities of the liquid and gas components and the mass ratio of the mixture entering the wellbore are as follows:

$$\nu_\ell = 1.59 \times 10^{-7}\ m^2/s$$

$$\nu_g = 2.29 \times 10^{-2}\ m^2/s$$

$$m_g/m_\ell = 1.12$$

The linearized equations in the Appendix can now be used to estimate ν_t. From Eq. (A-5) we compute

$$\frac{k_{rg}}{k_{r\ell}} = 1.12\ \frac{22.9}{1.59} = 16.2$$

If we assume that the flow within the formation is primarily through a fracture

network then from Eq. (A-6) we can calculate the individual relative permeabilities $k_{rg} = 0.942$ and $k_{r\ell} = 0.058$. From Eq. (A-2) we estimate the total kinematic viscosity during the last ten days of drawdown.

$$\nu_t = \left(\frac{0.058}{1.59 \times 10^{-7}} + \frac{0.942}{2.29 \times 10^{-6}}\right)^{-1}$$

$$= 1.29 \times 10^{-6}\ m^2/s$$

We assume that the kinematic viscosity during the two-phase portion of the buildup is approximated by this value. An estimate of the formation kh product from the two-phase portion of the buildup data can now be made.

$$kh = (1.29 \times 10^{-6})\ (7.06 \times 10^{-7})$$

$$= 90.8 \times 10^{-14}\ m^3 = 3030\ md\text{-}ft$$

Discussion The objective of this paper was to illustrate an analysis procedure which is based on the synthesis of field measurements and theoretical results in interpreting geothermal well flow data. The interpretation given here for well B-4 is based on the single-phase portion of the buildup data and yields a value of kh which is in reasonable agreement with the value of 4207 md-ft estimated by Hartz [1976] from a conventional Horner plot analysis. The interpretation given for well 6-20, however, is based on the two-phase portion of the buildup data and a correction of the Horner plot to account for the fact that gage is located several hundred feet from the primary production zone. A conventional Horner analysis would not be applicable.

Acknowledgements This work was performed under Contract 4514510 with the Lawrence Berkeley Laboratory as part of the evaluation of the Baca reservoir being conducted under a cooperative agreement between Union Oil Company and the Department of Energy. The assistance of Ms. Mary Margaret Pierce is gratefully acknowledged.

References

Garg, S. K. and J. W. Pritchett (1980), "Pressure Transient Analysis for Hot Water and Two-Phase Geothermal Wells: Some Numerical Results," Topical Report No. DOE/ET/27163-5, Prepared by Systems, Science and Software Under Baca Geothermal Demonstration Project, October.

Grant, M. A. and S. K. Garg (1981), "Interpretation of Downhole Data from the Baca Geothermal Field," Topical Report No. DOE/ET/27163-12 Prepared by Systems, Science and Software Under Baca Geothermal Demonstration Project, May.

Hartz, J. D. (1976), "Geothermal Reservoir Evaluation of the Redondo Creek Area, Sandoval County, New Mexico," Union Oil Company of California, Santa Rosa, California, September 9 and November 23.

Pritchett, J. W., M. H. Rice and T. D. Riney (1980), "Equation-of-State for Water-Carbon Dioxide Mixtures: Implications for Baca Reservoir," Topical Report No. DOE/ET/27163-8, Prepared by Systems, Science and Software Under Baca Geothermal Demonstration Project, October.

Appendix Several authors (e.g., Garg and Pritchett [1980]) have obtained approximate analytical solutions for a geothermal reservoir undergoing two-phase production at a constant rate. In these studies the balance equations for radial two-phase flow in porous media are linearized by assuming that the total and the component kinematic mobilities are related as follows:

$$\left(\frac{k}{\nu}\right)_t = \frac{k\,k_{r\ell}}{\nu_\ell} + \frac{k\,k_{rg}}{\nu_g} \qquad (A\text{-}1)$$

$$\frac{1}{\nu_t} = \frac{k_{r\ell}}{\nu_\ell} + \frac{k_{rg}}{\nu_g} \qquad (A\text{-}2)$$

Given the flowing enthalpy h_t of the two-phase mixture, it is also possible to obtain the separate kinematic mobilities.

$$\frac{k\,k_{r\ell}}{\nu_\ell} = \left(\frac{k}{\nu}\right)_t \left[\frac{h_g - h_t}{h_g - h_\ell}\right];\quad \frac{k\,k_{rg}}{\nu_g} = \left(\frac{k}{\nu}\right)_t \left[\frac{h_t - h_\ell}{h_g - h_\ell}\right] \qquad (A\text{-}3)$$

The expression

$$h_t = m_g\, h_g + (1-m_g)\, h_\ell \qquad (A\text{-}4)$$

relating the total and fluid component enthalpies may be used with Eqs (A-3) to write

$$\frac{k_{rg}}{k_{r\ell}}\frac{\nu_\ell}{\nu_g} = \frac{m_g}{m_\ell} = \frac{m_g}{1-m_g} \qquad (A\text{-}5)$$

Here m_g and $1-m_g$ are the gas and liquid components of the fluid flow.

If we assume that the flow within the formation is primarily through a fracture network, then

$$k_{r\ell} + k_{rg} = 1 \qquad (A\text{-}6)$$

Proceedings Seventh Workshop Geothermal Reservoir Engineering
Stanford, December 1981. SGP-TR-55.

FRACTURE STIMULATION EXPERIMENTS AT THE BACA PROJECT AREA

C. W. Morris & M. J. Bunyak

Republic Geothermal, Inc.
11823 E. Slauson Avenue
Santa Fe Springs, CA 90670

Abstract

The DOE-sponsored Geothermal Reservoir Well Stimulation Program group performed hydraulic fracture treatments on two wells located in Union's Baca Project Area in north-central New Mexico. The treatment in Baca 23 was conducted on March 22, 1981, utilizing a cooling water pre-pad followed by a high viscosity frac fluid carrying a mixture of sintered bauxite and resin-coated sand as the proppant. A non-productive 231-foot interval from 3,300 feet to 3,531 feet was isolated for the treatment. Post-stimulation surveys and production tests indicated a fracture had been successfully created; however, the production rates declined to noncommercial levels because of the low formation temperature in the open interval and reduced relative permeability caused by two-phase flow effects in the formation.

The second treatment was conducted in Baca 20 on October 5, 1981, again utilizing a cooling water pre-pad followed by a high viscosity frac fluid carrying only sintered bauxite as the proppant. A 240-foot interval from 4,880 feet to 5,120 feet, which was indicated to have produced only a small portion of the well's 56,000 lb/hr total mass flow, was isolated for the job. The temperature in this interval (540°F) gave Baca 20 the distinction of being the hottest well to be fractured in the United States to date. Post-stimulation tests and analyses indicate a fracture was created with a vertical height of only about 100 feet at the bottom of the open interval. The productivity of the well is poor, probably because of the low permeability formation surrounding the artificially created fracture. An acid cleanout operation is planned to remove possible damage to the fracture conductivity caused by the calcium carbonate fluid-loss additive.

Introduction

The U.S. Department of Energy-sponsored Geothermal Reservoir Well Stimulation Program (GRWSP) was initiated in February 1979 to pursue industry interest in geothermal well stimulation work and to develop technical expertise in areas directly related to geothermal well stimulation activities. Republic Geothermal, Inc. (RGI) and its principal subcontractors (Maurer Engineering, Inc. and Vetter Research) have completed seven field experiments. Two experiments have been performed in the low temperature reservoir at Raft River, Idaho (Morris, et al., 1980); two experiments in the moderate temperature reservoir at East Mesa, California; one experiment in the high temperature, vapor-dominated reservoir at The Geysers; and two experiments, reported herein, in the high temperature reservoir at Baca, New Mexico.

The Baca reservoir lies within the Jemez Crater, Valles Caldera, and is defined by more than twenty wells completed to date in the Redondo Creek area by Union Geothermal Company of New Mexico (Union). The main reservoir, 4,000 to 6,000 feet in thickness, is composed of volcanic tuffs with low permeability and a primary flow system of open fracture channels. In the Redondo Creek area, wells have encountered a high temperature (500°F+) liquid-dominated reservoir, but several wells have not been of commercial capacity, primarily because of the absence of productive natural fractures at the wellbore.

It is believed that hydraulic fracture treatments can create the fractures required to make these wells commercial and that such a well stimulation may be an attractive alternative to redrilling. The relatively large amount of reservoir data available and the high reservoir temperature made this field a good candidate for field experiments in the evaluation of geothermal stimulation techniques, fracture fluids, proppants, and mechanical equipment.

After considering several candidate wells, RGI and Union agreed that Baca 23 and subsequently Baca 20 were the best sites for the fracture treatments. These wells, shown in Figures 1 and 5, were selected because: (1) they were noncommercial or a poor producer; (2) the fracture system is present in the area as proven by the surrounding wells; (3) the wells could be recompleted to isolate the stimulation interval; (4) observation wells were available within 1,500 feet; (5) the wellsite was large enough for the frac equipment; and (6) in the case of Baca 23 the rig was already on location.

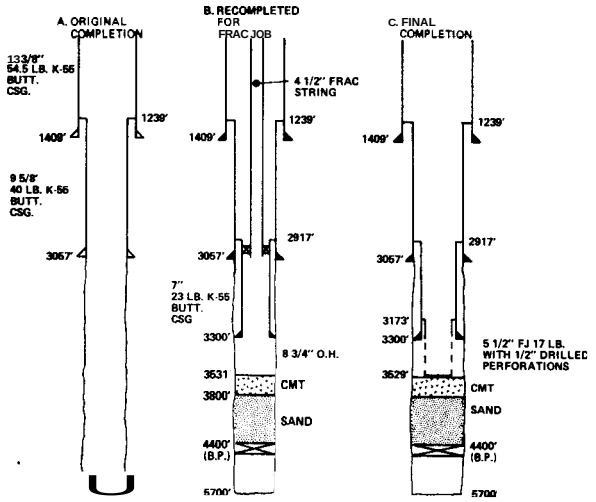

FIGURE 1 BACA 23 COMPLETION DETAILS.

The experiments were cost-shared by Union and the GRWSP. Union paid the cost of rig mob li-zation and demobilization plus the cost of recompleting the wells for the treatments. The GRWSP paid for the stimulation treatment and other directly related costs totaling about $450,000 for Baca 23 and about $581,000 for Baca 20.

Baca 23

Well Recompletion - Baca 23 was originally completed as shown in Figure 1A with a 9-5/8" liner cemented at 3,057 feet and 8-3/4" open hole to 5,700 feet. The well was flow tested and at that time would not sustain flow. An interval from 3,300 feet to 3,500+ feet in the well was selected for fracture stimulation. Good production had previously been encountered near this depth approximately 200 feet away in Baca 10. The interval is now cemented off be-hind casing in Baca 10. Fracturing a more shallow interval, immediately below the shoe of the 9-5/8" casing, was considered to have a substantial risk of comnunication with lower temperature formations above. The temperature in the zone selected was approximately 450°F.

Since the top of the selected interval was deeper than the existing 9-5/8" liner, a 7" liner was cemented to a depth of 3,300 feet to exclude the interval above. The lower portion of the hole was sanded back to 3,800 feet and plugged with cement to 3,531 feet to contain the treatment in the desired interval. This recompletion is shown in Figure 1B. The treatment interval was totally nonproductive after being isolated for the stimulation treatment.

Treatment Summary - A hydraulic fracture treatment was performed on the well consisting of 7,641 bbl of fluid and 180,000 lb of 20/40-mesh proppant pumped in eight stages. The stages are detailed in Table 1 and the pressure/rate history is shown in Figure 2.

TABLE 1

BACA 23 TREATING SCHEDULE

STAGE NO.	PLANNED SIZE (bbl)	ACTUAL SIZE (bbl)	PROPPANT (LB/GAL)	PROPPANT (SIZE)	FLUID
1	4,000	3,582	0	–	PRODUCED WATER WITH FLUID LOSS ADDITIVE (FLA)
2	500	502	0	–	POLYMER GEL WITH FLA
3	500	502	2	100-MESH	POLYMER GEL WITH FLA
4	500	526	0	–	POLYMER GEL WITH FLA
5	900	905	1	20/40-MESH	POLYMER GEL
6	1,000	1,000	2	20/40-MESH	POLYMER GEL
7	600	562	3	20/40-MESH	POLYMER GEL
8	58	62	0	–	PRODUCED WATER
	8,058	7,641			

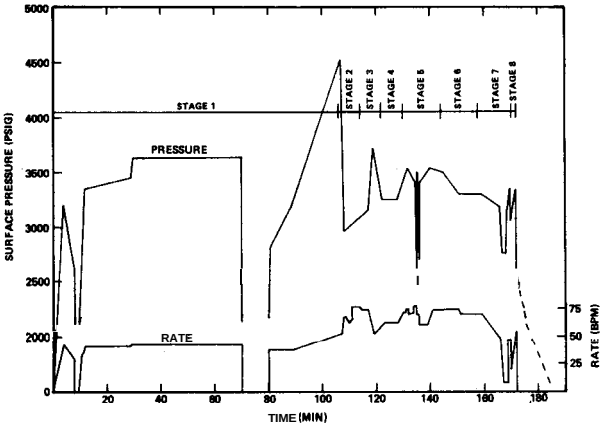

FIGURE 2 BACA 23 FRACTURE STIMULATION PRESSURE PRESSURE/RATE HISTORY.

The treatment was pumped through a 4-1/2" tubing frac string with a packer set near the top of the 7" liner as shown in Figure 1B. The frac string was necessary to isolate liner laps in the well from the treating pressure.

Although the job was basically a conventional hydraulic fracture treatment, the high formation temperature (450°F) dictated special design and materials selection requirements. Therefore, 50 percent of the frac fluid was dedicated to wellbore and fracture pre-cooling with the final 50 percent of the fluid used to place the proppant. While frac fluid properties are known to degrade rapidly at high temperature, these effects were minimized by pre-cooling, by pumping at high rates (up to 75 BPM), and by limiting the frac interval to 231 feet. Proppants were selected for their insensitivity to the high temperature (Sinclair, et al., 1980). Both resin-coated sand and sintered bauxite were used. Chemical work included compatibility studies of the frac materials with the formation fluids and the use of chemical tracers to monitor fluid returns.

The job was separated into eight stages. In Table 1 the eight stages are shown with the

planned and actual stage sizes. The fluid used for pre-cooling the formation (Stage 1) was produced geothermal water stored in a pit near the location. The job ran short by 418 bbl of pre-pad water because the usable volume of the pit was underestimated. No harmful effects resulted from this short fall, however. Otherwise, the schedule was followed closely. The fluid for Stages 2-7 was a 60 lb/1,000 gal hydroxypropyl guar polymer gel pre-mixed using fresh water. The gel was crosslinked as it was pumped.

Finely ground calcium carbonate was selected as a fluid-loss additive (FLA) for Stages 1-4. About 5,700 lb of fine fluid-loss additive were used during the job. A larger fluid-loss additive consisting of 42,000 lb of 100-mesh sand was pumped in Stage 3 to slow leaks into the natural fractures of the formation.

Total proppant placed in the formation during the job was 180,000 lb. The original plan was to use a 50/50 mixture of sintered bauxite and resin-coated sand, both 20/40-mesh. The actual proportion of the proppants was 54 percent sintered bauxite and 46 percent resin-coated sand by weight.

Actual horsepower required for the job was 6,400 hhp versus the 5,880 hhp estimated by assuming an 80 BPM pump rate and 3,000 psi wellhead pressure. Higher than expected frac gradients were responsible for the increase. Frac gradients measured at the beginning, middle, and end of the job were 0.83, 0.92, and 1.175 psi/ft respectively. The buildup in frac gradient is difficult to interpret here, but nonetheless should be noted for consideration in planning and evaluating future fracture treatments.

Test Results and Analyses - During the fracture treatment, Los Alamos National Laboratory performed a fracture mapping experiment using Baca 6 as an observation well. A triaxial geophone system was placed in the well; and using techniques developed for the Hot Dry Rock Project, microseismic activity caused by the fracture job was mapped. The 14 discrete seismic events indicate northeast trending activity in a zone roughly 2,300 feet long, 650 feet wide, and 1,300 feet high. The rock failure, therefore, occurred in a broad zone and suggests the stimulation did not result in the creation of a singular monolithic fracture. These microseismic events would be expected to proceed in advance of any significantly widened, artificially created fracture and would not necessarily define a final propped flow path to the wellbore at Baca 23. Calculations of the theoretical fracture length were made assuming a 300-foot high fracture. The results suggest a fracture wing of 430 to 580 feet in length may have been created, depending on the assumptions utilized for the frac fluid, fluid efficiency, and fracture width.

As discussed above, the 231-foot interval isolated for stimulation was nonproductive prior to the treatment. This indicated that no significant natural fractures intersected the wellbore. Twelve hours after the frac job, a static temperature survey (shown in Figure 3 with a pre-frac survey) was obtained by Denver Research Institute. This survey showed a zone cooled by the frac fluids estimated to be more than 300 feet in height at the wellbore.

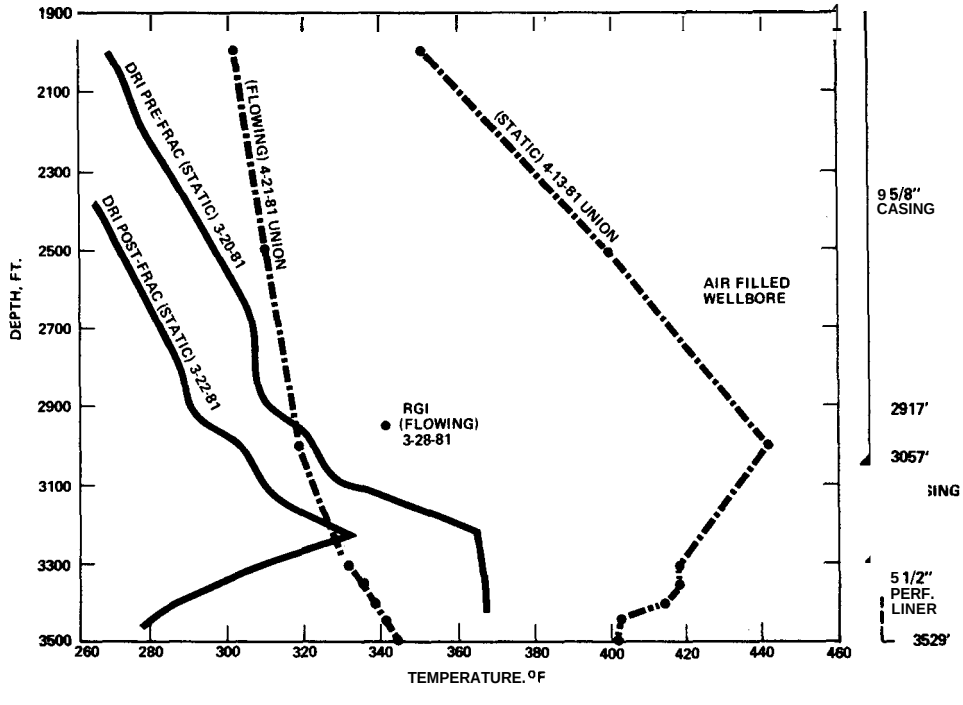

FIGURE 3 BACA 23 TEMPERATURE SURVEYS.

After the post-frac temperature survey was obtained, the frac string was pulled and the well was circulated with aerated water and allowed to flow to be sure that production of proppant into the wellbore would not interfere with subsequent testing. No significant amount of proppant was produced into the wellbore after the frac job. At this time it was determined that the well was worthy of final completion and further testing. A 5-1/2" pre-perforated liner was installed in the treatment interval as shown in Figure 1C.

On March 26, 1981, a six-hour production test through drillpipe was performed in which transient, downhole pressure and temperature measurements were obtained. A unique testing method was utilized to overcome the data gathering problems usually associated with flow testing a geothermal well. The procedure was a combination of conventional drillstem test (DST) methods (to eliminate large wellbore storage effects) and gas lift to maintain steady, single-phase flow to the wellbore. The gas lift was provided by injecting nitrogen gas at depth through coil tubing inside the drillpipe. As a result of this procedure, the well flowed at a low, steady rate (about 21,000 lb/hr) and the transient pressure data obtained downhole provided an indication of wellbore storage effects, fracture flow effects, and reservoir transmissivity.

A conventional Horner analysis (Figure 4) of the pressure buildup data yielded an average reservoir permeability-thickness of 2,500 md-ft. This compares closely with results from other noncommercial wells in the area and with the 6,000 md-ft average reservoir value obtained by Union from interference well tests (Hartz, 1976). Although the linear flow indicators were weak, the length of the fracture was calculated to be about 300 feet from the pressure versus square root of time analysis. A skin factor of -3.9 was also calculated. The maximum recorded temperature was 342°F which indicated that the near wellbore area had not recovered from the injection of cold fluids.

Following the modified DST, a 49-hour flow test was performed to determine the well's productive capacity. The results showed that the well could produce approximately 120,000 lb/hr total mass flow at a wellhead pressure of 45 psig, although the rate was continuing to decline. The chemical tracer data showed that the frac fluid stages were thoroughly mixed together in the return fluids and the frac polymer had thermally degraded by the end of this test.

Union performed a long-term flow test on the well during April-May 1981. A static temperature profile of the well prior to this test showed that the bottom-hole temperature still remained low (401°F). Temperature and pressure surveys run on April 21 (Figure 3) recorded a maximum temperature of 344°F and a maximum pressure of 120 psig at 3,500 feet. Therefore, two-phase flow was occurring in the formation, with the steam fraction estimated at more than 50 percent. This two-phase flow condition, has been observed in other wells in the field.

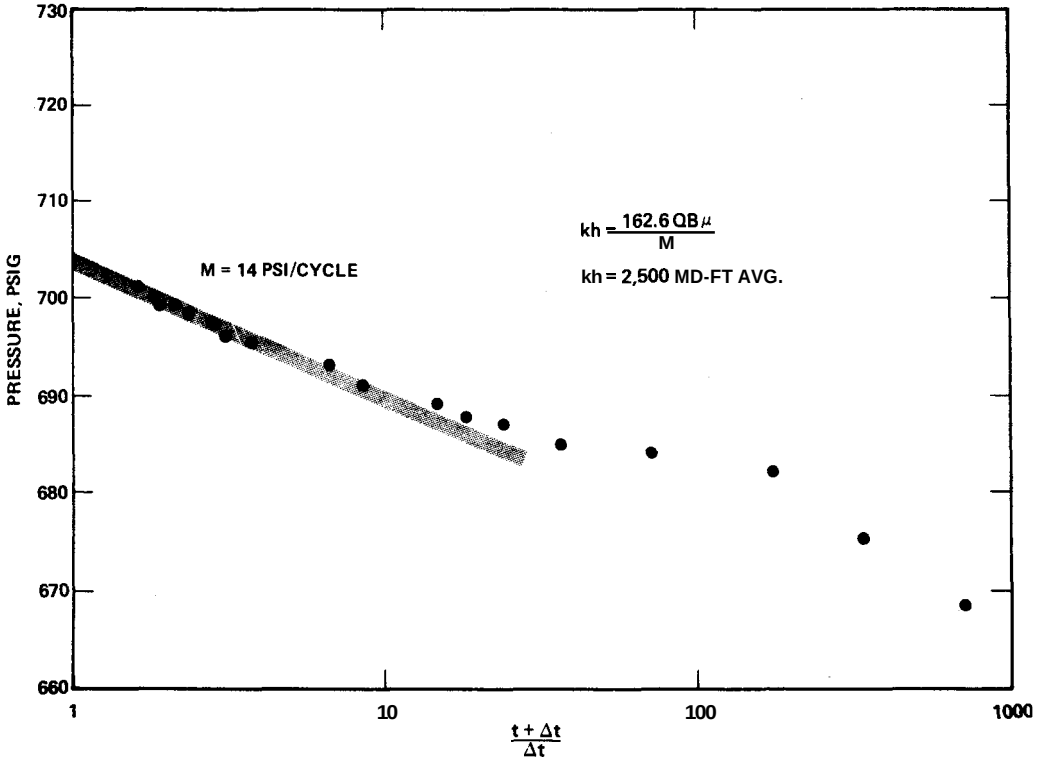

FIGURE 4 BACA 23 PRESSURE BUILDUP DATA—MARCH 26,1981

The formation cooling seen in the April 13 temperature survey is apparently a result of the temperature drop associated with flashing in the formation.

Of greater concern is the low productivity observed during this last test. The mass flow rate had dropped to 73,000 lb/hr (about 50 percent steam) with a wellhead pressure of 37 psig in May 1981. Since the well recovers productivity following each shut-in period and then exhibits the same decline again, the cause of the rate decline is probably not due to scaling in the formation. Partial closing of the fracture is possible, but the productivity loss is probably the result of relative permeability reduction associated with two-phase flow effects in the formation. The relatively low formation temperature in the completion interval also contributes to the well's poor productivity.

Baca 20

Well Recompletion - Baca 20 was originally completed as shown in Figure 5A with a 9-5/8" liner cemented at 2,505 feet and a 7" slotted liner hung at 2,390 feet with the shoe at 5,812 feet. The 7" slotted liner was pulled,

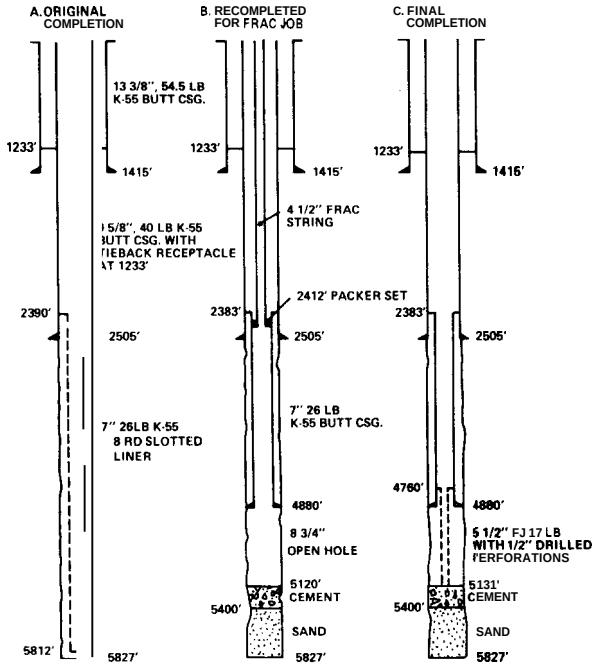

FIGURE 5 BACA 20 COMPLETION DETAILS.

lost circulation zones cured using cement plugs, and then a 7" blank liner was cemented in place at 4,880 feet in order to isolate the desired treatment interval. Since the frac interval was to be from 4,880 feet to 5,120 feet, a sand plug was placed from 5,827 feet total depth to 5,400 feet and then capped with cement to 5,120 feet. The recompletion is shown in Figure 5B. This particular 240-foot interval was chosen primarily because the best production in the area has been found near the bottom of the Bandelier Tuff and because of its high reservoir temperature (540°F).

Treatment Summary - The hydraulic fracture treatment was accomplished in the eleven stages defined in Table 2. The high formation temperature (540°F) once again dictated special design and materials selection.

TABLE 2

BACA 20 TREATING SCHEDULE

Stage No.	Planned Size (bbl)	Actual Size (bbl)	Proppant (lb/gal)	Proppant Size	Fluid
1.	2000	2000			FRESH WATER WITH FLUID LOSS ADDITIVE (FLA)
2.	500	639	0.39	100-MESH $CaCO_3$ (10,500 LB)	FRESH WATER WITH FLA
3.	500	350			FRESH WATER WITH FLA
4.	1500	1400			POLYMER GEL WITH FLA
5.	500	566	1.33	100-MESH $CaCO_3$ (31,500 LB)	POLYMER GEL WITH FLA
6.	500	500			POLYMER GEL WITH FLA
7.	1150	1168	0.46	16/20-MESH BAUXITE	POLYMER GEL
8. a	850	682	1.85	16/20-MESH BAUXITE	POLYMER GEL
b		378	2.77	16/20-MESH BAUXITE	POLYMER GEL
9.	300	450	2.11	12/20-MESH BAUXITE	POLYMER GEL
10.	750	451	4.21	12/20-MESH BAUXITE	POLYMER GEL
11.	150	151			FRESH WATER
	8700	8735			

The treatment was pumped through a 4-1/2" tubing string with a packer set at 2,412 feet, just below the 7" liner hanger. A 3,000 bbl fresh water pre-pad was used to cool the wellbore and fracture. The proppant selected was 119,700 lb of 16/20-mesh sintered bauxite, followed by 119,700 lb of 12/20-mesh sintered bauxite. The proppant was carried by a 60 lb/1,000 gal hydroxypropyl guar polymer gel mixed in fresh water. This fluid was a new high-pH crosslinked HP guar system having better stability at high temperature. The gel was crosslinked as it was being pumped. Chemical tracers were added to the injected fluid to monitor fluid returns.

Approximately 4,200 lb of 200-mesh calcium carbonate was added in Stages 1-6 to act as a fluid-loss additive. In an effort to stop leakage into the small natural fractures, 42,000 lb of 100-mesh calcium carbonate was pumped in Stages 2 and 5 in concentrations of 0.39 ppg and 1.33 ppg, respectively. The 100-mesh material was injected in "slugs" to enhance its chances of bridging on the fractures.

The majority of the treatment fluid was pumped at approximately 80 BPM. The rate was slowed to 40 BPM in Stage 10 when the proppant concentration was increased to 4.2 lb/gal. In anticipation of frac gradients of 0.9 psi/ft and higher, as seen in Baca 23, a total capacity of 11,000 hhp was made available and connected in the system. However, the actual peak hydraulic horsepower used was only 7,450 hhp because of lower frac gradients. An instantaneous shut-in pressure was measured soon after the treatment was initiated (1,000 psig) and again near the end of the job (1,300 psig), giving frac gradients of 0.63 psi/ft and 0.69 psi/ft, respectively. The pressure/rate history is shown in Figure 6.

Minor variations in the planned pumping schedule occurred during the treatment (Table 2), but all fluids and proppants were injected into the formation and the desired goal of ending the treatment at a relatively high proppant concentration was achieved. The variations occurred: (1) in Stage 7 when only 1/2 lb/gal of proppant was inadvertently added instead of the planned 1 lb/gal; (2) in Stage 8 when a higher proppant concentration was used to make up for the smaller amount used in Stage 7; and (3) in Stage 9 where the proppant concentration was increased to 3 lb/gal of the larger proppant instead of the planned 2 lb/gal. In Stage 10 the rate was slowed and the proppant concentration increased to 4.2 lb/gal to achieve a more widely propped fracture. The wellhead pressure and frac gradient were lower than expected, offering reasonable assurance that the proppant would not screen out at the lower rate and higher concentration.

Test Results and Analysis - During the fracture treatment Los Alamos National Laboratory again performed a fracture mapping experiment using Baca 22 as an observation well. A triaxial geophone system was placed in the well at a depth of approximately 3,000 feet and the microseismic activity caused by the fracturing job was mapped. A large number of discrete events (45) were recorded during the job, however, the orientation measurement of the tool was lost. Again the activity occurred in a broad zone which was roughly 2,000 feet long, 1,600 feet wide, and 1,700 feet high. Theoretical calculations of the artificially created fracture length would be 340-800 feet in a homogeneous matrix material, depending on the assumptions utilized for the frac fluid, fluid efficiency, and fracture height. These calculations were based primarily on the injected fluid and proppant volumes in a single, vertical fracture.

As discussed above, the 240-foot interval was nonproductive prior to the treatment, although there was a small rate of fluid loss during the well completion operations. This indicated that at least one lost circulation zone existed in the wellbore. Approximately 12 hours after the frac job the first of several temperature surveys, as shown in Figure 7, was obtained in the well. These temperature surveys showed a zone cooled by the frac fluids, estimated to be less than 100 feet in height, near the bottom of the open interval. In addition, the zone located behind the 7" liner casing at approximately 4,720 feet also indicated some cooling. This zone was apparently cooled by the workover fluids and possibly by

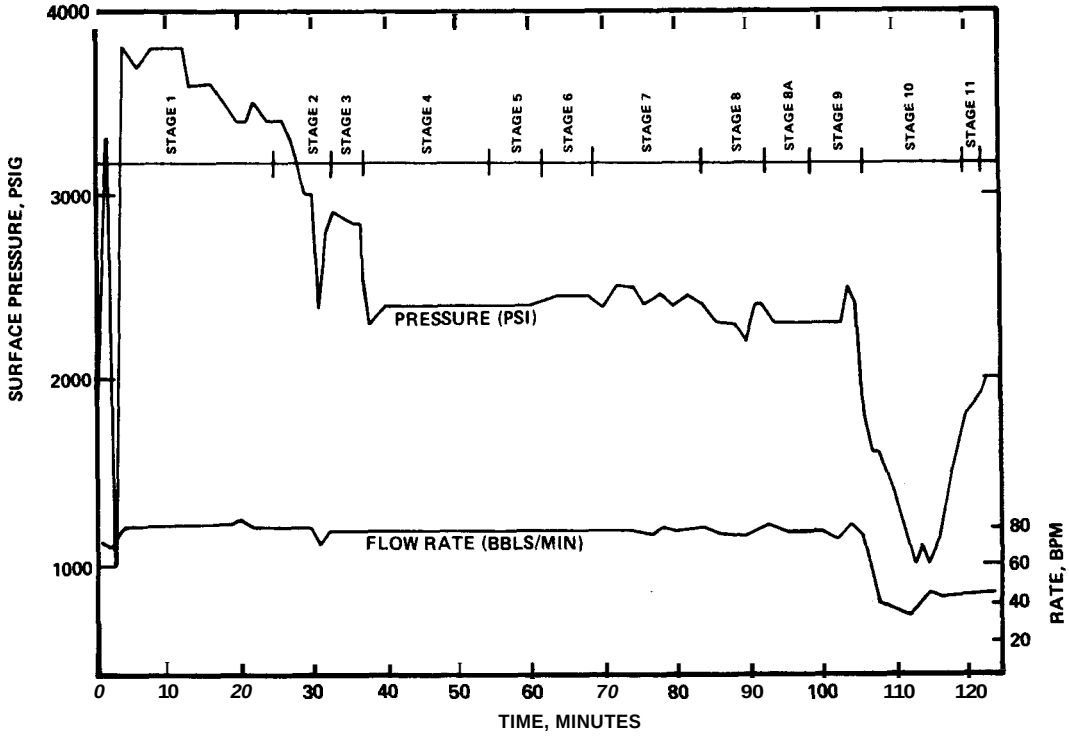

FIGURE 6 BACA 20 FRACTURE STIMULATION PRESSURE/RATE HISTORY.

the fracturing fluids; however, the communication between this zone and the open interval (if it exists) appears to be at some distance away from the wellbore. Electric log surveys were run in the open interval following the frac job. No significant new fracture zones (or high porosity) were observed, although several zones did show increased neutron porosity values.

At this time it was determined that the well was worthy of final completion and further testing. A 5-1/2" pre-perforated liner was installed in the treatment interval as shown in Figure 5C. On October 10-11, 1981, a 6-hour production test through drillpipe was performed in the same manner as the orillstem test at Baca 23. A steady rate of about 21,000 lb/hr single-phase flow was maintained to the wellbore. Transient pressure and temperature data were obtained downhole during the DST. A conventional Horner analyis of the pressure buildup data (Figure 8) yielded an average reservoir permeability-thickness of 1,000 md-ft. Evaluation of these data also indicated small wellbore storage effects and fracture (linear) flow near the wellbore. Although the indicators of linear flow were weak, the length of the fracture was calculated to be about 280 feet from the pressure data (pressure vs square root of time). A skin factor of -4.9 was also calculated. Numerical simulation of a high conductivity fracture in a low permeability formation supports this interpretation, although the solution is not unique. The maximum recorded temperature during the test was 320°F and indicated that the near wellbore area had not recovered from the injection of cold fluids. Additional temperature surveys were run in the well following the DST, as shown in Figure 7, which again indicated the fluid was entering (leaving) the wellbore in the lower part of the open interval.

Following the modified DST, a 14-day flow test was performed to determine the well's productive capacity. The well produced approximately 120,000 lb/hr total mass flow initially, but declined rapidly to a final stabilized rate of approximately 50,000 lb/hr (wellhead pressure of 25 psig) under two-phase flow conditions in the formation.

Because of the poor performance of the well, it was decided to perform an acid cleanout of the fracture. As indicated above, calcium carbonate was used as the fluid-loss additive during the hydraulic fracture treatment. This material was used with the expressed intent of performing an acid cleanout should the fracture conductivity show damage. The possibility of

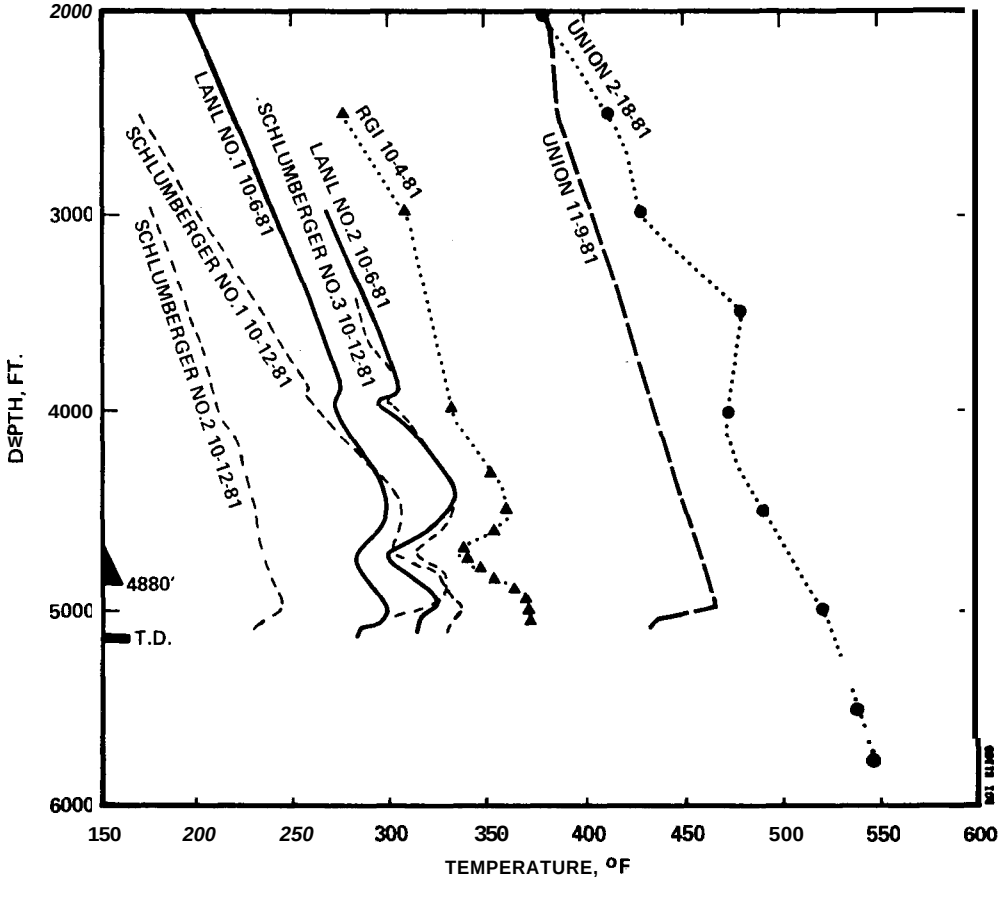

FIGURE 7 BACA 20 TEMPERATURE PROFILES—OCTOBER 1981.

such damage with insoluble fluid-loss additives (e.g., 100-mesh sand) has been a concern in prior stimulation experiments. Although the pressure data does not indicate that the fracture conductivity has been damaged, it does not preclude the possibility that the calcium carbonate has plugged the natural fractures and flow paths in the formation which intersect the artificial fracture.

Conclusions

1. Large hydraulic fracture treatments were successfully performed on both Baca 23 and Baca 20. Production tests indicated that high conductivity fractures were propped near the wellbore and communication with the reservoir system was established.

2. The productivities of Baca 23 and Baca 20 have declined to noncommercial levels since the fracture treatments. The probable cause is relative permeability reduction associated with two-phase flow effects in the formation.

3. The ability of Baca 23 to produce substantial quantities of fluid at a high wellhead pressure is limited because of the low formation temperature in the shallow treatment interval. The productivity of Baca 20 is severely restricted because of the low permeability formation surrounding the artificially created fracture.

4. Although the stimulation treatments did not result in commercial wells at Baca, the hydraulic fracturing techniques show promise for future stimulation operations and for being a valid alternative to redrilling in other reservoirs.

References

Hartz, J. D., Geothermal Reservoir Evaluation of the Redondo Creek Area, Sandoval County, NM, Union Oil Company Report, September 1976.

Morris, C. W., Verity, R. V., and Sinclair, A. R., "Raft River Well Stimulation Experiments," Geothermal Resources Council, Transactions, Vol. 4, September 1980.

Sinclair, A. R., Pittard, F. J., and Hanold, R. J., "Geothermal Well Stimulation," Geothermal Resources Council, Transactions, Vol. 4, September 1980.

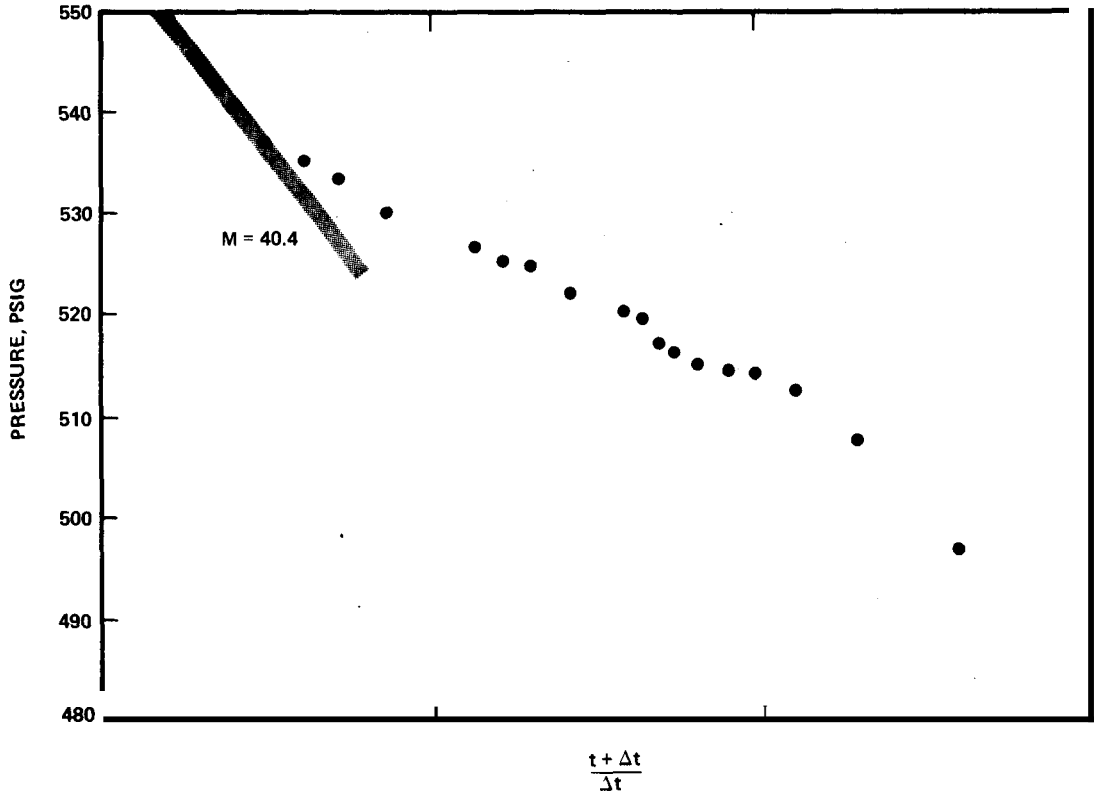

FIGURE 8 BACA 20 DST NO. 2, PRESSURE BUILDUP HORNER PLOT—OCTOBER 11,1981.

Proceedings Seventh Workshop Geothermal Reservoir Engineering
Stanford, December 1981. SGP-TR-55.

THE REYKJANES GEOTHERMAL FIELD IN ICELAND: SUBSURFACE EXPLORATION AND WELL DISCHARGE CHARACTERISTICS

J. S. Gudmundsson
T. Hauksson
J. Tomasson

Geothermal Division, Orkustofnun
(Iceland Energy Authority)
Reykjavik

Introduction The exploration and development of the Reykjanes geothermal field dates back to about 1956 when the first well was drilled. This well was 162 m deep and had a maximum temperature of 185°C. The chloride concentration of the deep brine was about 25% higher than that of ordinary seawater. The well produced *3-4* kg/s of a steam-brine mixture for over 10 years without a noticeable change in chemical composition (Bjornsson et al. 1971). The fact that the fluid produced was of brine origin but not rainwater affected greatly the course of exploration and development of the Reykjanes field. Most high-temperature geothermal fields in Iceland produce fluids of rainwater origin.

The Reykjanes field was investigated extensively in the years 1968-1970 (Bjornsson et al. 1970, 1971, 1972). This was done in relation to plans to produce 250,000 tonnes/year of not only common salt but various other sea-chemicals for export (Lindal 1975). The investigation showed that the field would be suitable for development. However, the proposed sea-chemicals scheme did not materialize at that time and further geothermal work in Reykjanes was terminated. Four years ago a company was formed to consider again the production of common salt and other sea-chemicals in Reykjanes. Since that time it has conducted pilot plant and other studies to investigate the feasibility of salt production, mainly for the Icelandic market, which is currently about 60,000 tonnes/year. The building of a demonstration plant has now been decided. It is therefore anticipated that the Reykjanes field will come under development in the next few years.

From the time geothermal work was terminated in Reykjanes 10 years ago, two other high-temperature fields have been explored and developed in Iceland (Gudmundsson et al. 1981). These are the Krafla field (Stefansson 1981) in the northeast and the Svartsengi field (Thorhallsson 1979) in the southwest. These two fields are still being developed. While the Reykjanes field waited for development the one production well drilled was kept on discharge. The purpose of this test was to learn about the long-term discharge characteristics of the well/reservoir system. In 1980 extensive output measurements were done on this well, showing both flowrate and enthalpy at various wellhead conditions. The main purpose of the present paper is to report on the long-term discharge test and the more recent output measurements. An important feature of the salt-making in Reykjanes is that the geothermal brine itself will be the source of chemicals, *so* that the steam-brine mixture produced by the wells will supply both the energy and raw material to the process. The long-term chemical characteristics of the production wells is therefore of great importance. The emphasis of this paper will therefore be on reporting the geochemical nature of the Reykjanes field and the one production well operated for nearly a decade. To provide some background information, the reported subsurface exploration work will be discussed. The extensive surface exploration work of Bjornsson et al. (1970, 1971, 1972) will, however, not be discussed. It is hoped that the present paper may contribute something to the near future drilling and development activities in the Reykjanes field. At the same time it may provide reservoir engineering and other information for those not familiar with geothermal resource developments in Iceland.

Subsurface Exploration In 1968 and 1969 seven boreholes were drilled in the Reykjanes geothermal area. Four of the wells (2, *3*, 4 and 8) were deep (301 m, 1165 m, *1036* m and 1754 m, respectively) and encountered both high temperatures and good aquifers, while three wells (5, 6 and 7) were relatively shallow (112 m, 572 m and 73 m) and did not penetrate the hot reservoir. The locations of all the boreholes are shown on Figure 1, which is the resistivity survey map of the area (Bjornsson et al. 1970, 1971, 1972). The surface area of the Reykjanes field has been estimated to be 1-2 km^2, which makes it one of the smallest in Iceland.

Drilling in the Reykjanes field proved to be difficult. Well 2 was never completed because it could not be controlled during drilling once the casing had been run to bottom-hole. Borehole *3* collapsed during initial discharge while well *4* produced for a few weeks before doing the same. This latter well was later

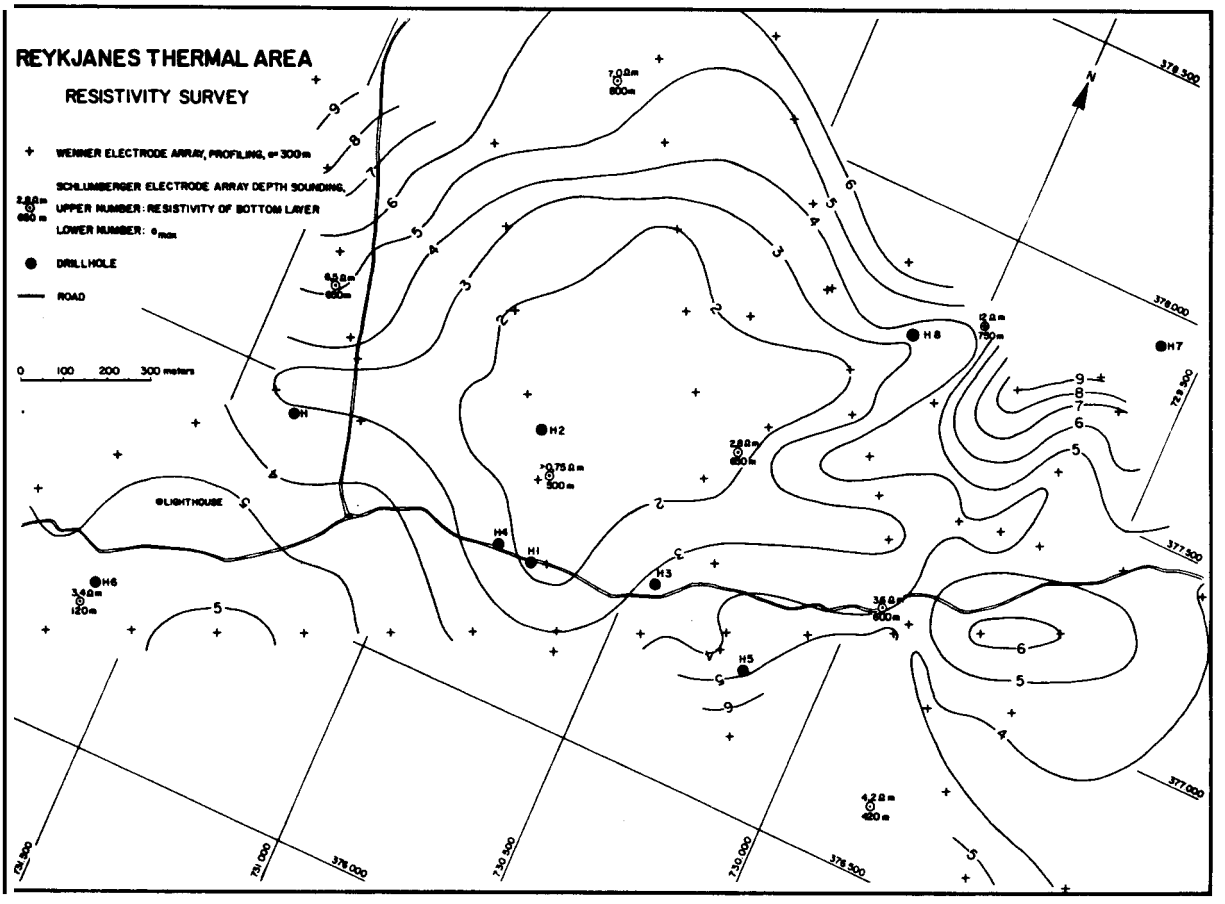

Figure 1: Resistivity survey map of the Reykjanes geothermal area, also showing the location of boreholes (Bjornsson et al. 1970, 1971, 1972).

abandoned after unsuccessful attempts to drill out the collapse. Because of the experiences with wells 3 and 4 it was decided to put a slotted liner to the bottom of well 8. It should be stated here that prior to 1968 it was not the practice in Iceland to put slotted liners in boreholes drilled in high-temperature areas. Until then open hole completion (without slotted liner) had been used with success in several fields. Well hole 8 turned out to be one of the best drilled in Iceland at that time. On initial discharge it delivered about 80 kg/s of a steam-brine mixture with an enthalpy of 1200 kJ/kg. Wells 2 and 4 delivered much less or about 30 kg/s and 20 kg/s, respectively.

The average concentrations of major elements in the deep brines feeding the geothermal wells in Reykjanes are shown in Table 1 (Hauksson 1981). The table shows that the brines are similar in total dissolved solids (TDS) to that of ordinary seawater. Also shown in Table 1 are the well depths and estimated inflow brine temperatures as derived from silica geothermometry. The chloride ion (Cl) concentration expresses salinity and is independent of water-rock thermal equilibria (Arnorsson 1978). It is clear from the table that salinity increases with decreasing well depth and therefore with decreasing brine temperature also. This increase is considered to be due to boiling of the geothermal brine as it rises toward the surface in the reservoir. It should be noted that while the total dissolved solids of the geothermal brines are similar to that of seawater, there are some differences in individual components. These differences are mainly due to ion exchange equilibria between rock and water. The geothermal brines are deficient in magnesium (Mg) and sulphate (SO_4) but enriched in potassium (K) and calcium (Ca). The change in sodium (Na) is not as marked, being less in well 8 than in seawater. The amount of silica (SiO_2) in the geothermal brines is an order of magnitude higher than in seawater, as would be expected from its increased solubility with temperature.

Table 1: Averaqe concentration (mq/kq) of chemical components in geothermal brine in Reykjanes and standard seawater. Also shorn are well depth and estimated brine temperature.

Component	Geyser	Well 1	Well 2	Well 4	Well 8	Seawater
SiO_2	569	414	355	452	588	6.0
Na	14,300	12,400	10,700	10,100	9 520	10,470
K	2,020	1,510	1,400	1,340	1 380	380
Ca	2,400	1,980	1,790	1,640	1 580	398
Mg	56	1.13	-	-	1.43	1,250
SO_4	155	82.2	75.6	74.5	40.8	2,630
Cl	28,900	23,700	20,500	19,800	19 200	18,800
F	0.25	0.15	-	-	0.15	1.26
TDS	50,900	-	34,800	33,800	33,300	33,900
CO_2	42.1	-	2,110	-	1,930	100
H_2S	-	-	43.1	-	36.5	-
H_2	-	-	-	-	0.24	-
Depth (m)	0	162	301	1,036	1,754	-
Temp. (^oC)	100	(220)	225	250	270	-

Subsurface stratigraphy of the Reykjanes field has been constructed by investigation of drill-cuttings and a few cores taken during the main exploration work from 1968-1970 (Tomasson and Kristmannsdottir 1972). It was found that hyaloclastic tuffs and breccias and tuffaceous sediments dominate in the uppermost 1000 m. At greater depths about half the rock is basalt and the rest tuffaceous rocks, mainly sediments. Although the hyaloclastite formation is highly porous, few good aquifers were encountered in the wells drilled. Numerous aquifers were, however, found in the interbeds of the deeper basalt formation. Contacts between lava flows and interbeds are expected to be porous and highly permeable. Faults and fissures seem also to form channels of substantial permeability.

The examination of the drill-cuttings showed that calcite ($CaCO_3$) was found throughout the rock. Although the amount of calcite varied with depth and location it was found to be most abundant in the uppermost *500-700* m. Calcite tends to precipitate out due to boiling when geothermal fluids flow toward the surface in boreholes and reservoirs. It seems likely that calcium rich rocks represent a region of initial boiling in the Reykjanes field. A further evidence for boiling in the upflow zone of the reservoir is the chloride concentration of the brine feeding the geyser and boreholes as shown in Table 1. The chloride concentration shows an increase between wells *8, 4* and *2* from 2% to 5% to 9% higher than that in seawater, the wells being *1754* m, 1036 m and 301 m deep, respectively. The corresponding values for well 1 are 26% and 162 m.

Tne Reykjanes Peninsula is rather flat. The Reykjanes geothermal field is about 20 m above sea-level while the Svartsengi field 15 km to the northeast is about *40* m above sea-level. The hydrostatic pressure on the Peninsula should therefore be rather uniform although there must be some regional gradient away from the hills and mountains to the east or northeast. The volcanic rocks that make up the bulk of the Reykjanes Peninsula are considered highly porous throughout. It is therefore not surprising to find that the ground is saturated with seawater even 30 km inland. Geohydrological studies have indicated that the bulk of the Peninsula is saturated with seawater which becomes more diluted as the hills and mountains are approached. On top of the seawater there is a freshwater lens which exhibits a classical freshwater-seawater interface of coastal aquifers. In the geothermal fields the freshwater lens does not exist because of the upflow of hot water and steam. It has been found that the water table within the Reykjanes field is similar to that of the groundwater table surrounding the system. It follows that there must be some boundary or separation that prevents the cold water from invading the field. It has been argued that accompanying the circulation of cold seawater toward the field and down into the ground, there must occur substantial precipitation of secondary minerals (mainly anhydrite) at the boundary of the thermal system, forming an impervious cap. This will lead to the separation of the hydrothermal system from the surrounding colder seawater. This separation is considered most advanced close to the surface and to decrease progressively downwards.

The amount of deuterium (D) in the deep brine in Reykjanes has been measured (Arnason 1976 and Olafsson and Riley 1978). It was found that the brine in well 8 contained about 23 o/oo less (δD=-23 o/oo) than standard seawater. Local rainwater contains about 48 o/oo less deuterium than seawater. The usual explanation for the low deuterium concentration of the Reykjanes brine has been that the reservoir fluid was a mixture of seawater and rainwater. The two would mix in near equal proportions (48% and 52%) to result in the measured deuterium value. But the chloride concentration of the geothermal brine is approximately the same as that of seawater as shown in Table 1. This "coincidence" has been attributed to continuous boiling and evaporation of the seawater/rainwater mixture. In the Svartsengi high-temperature field about 15 km away from Reykjanes, the deuterium concentration in the deep brine has been measured (Arnason 1976). Its value is also 23 o/oo less than that of seawater. Typical salinity (Cl) in the Svartsengi field is about 12,600 mg/kg (Thorhallsson 1979), which concentration has been explained as resulting from the mixture of 67% seawater and 33% rainwater (Kjaran et al. 1979). As in the Reykjanes field the δD = -23 o/oo value has been explained by continuous boiling and evaporation in the reservoir. However, the "coincidence" of both fields having δD = -23 o/oo but different salinities may require an explanation that also satisfies the "coincidence" previously mentioned. It is postulated here that the deuterium concentration in deep geothermal brines is mainly controlled by water-rock interactions. Deep brines are understood here to be geothermal fluids at depths greater than 1 km and which have not experienced evaporation in the main upflow zone of a geothermal field. It should be noted that hydrogen isotope fractionation between OH-bearing minerals and water have been demonstrated in the laboratory (O'Neil and Kharaka 1976, Suzuoki and Epstein 1976). The Reykjanes and Svartsengi fields are in similar geologic environments associated with interactions of seawater, basaltic rock and recent or active volcanism. The alteration minerals that form due to geothermal activity contain numerous hydroxyl (OH) groups that may take part in the proposed isotope interactions with circulating brine. This assumes that hydrothermal alteration progresses continuously during the lifetime of geothermal fields and that seawater behaves differently than freshwater. Seawater has higher ionic concentrations than freshwater so that chemical interaction processes are enhanced. This means that for the above postulate to hold the fractionation of deuterium between hydrothermally altered basaltic rock and geothermal brine could be chemically controlled. This tentative postulate could perhaps be examined by comparing the deuterium content of alteration minerals in Reykjanes with that found in high-temperature fields having water of rainwater origin.

Production Well The feasibility of most geothermal projects depends heavily on the success of drilling. The cost, deliverability and longevity of wells is therefore of major importance. Well 8 in Reykjanes is the only borehole there that has discharged for any length of time. An examination of the experience gained from the 12 years of its operation should therefore be most relevant to the future development of the Reykjanes geothermal field. Also to be considered is what information borehole measurements can contribute to our understanding of the reservoir/well system. Because the geothermal brine in Reykjanes will be put to direct process use as well as for energy purposes, in the production of salt, its chemical as well as other characteristics are of concern.

Well 8 was drilled to a depth of 1754 m. It has a 13 3/8" anchor casing down to 89 m and a 9 5/8" production casing to 297 m, both cemented. It has a 7 5/8" liner from 260 m to a depth of 1685. This liner was placed in the well about one year after drilling. The liner is slotted at four intervals 984-1037 m (49 m), 1122-1308 m (186 m), 1484-1535 m (50 m) and 1624-1685 m (61 m). These intervals were selected because circulation losses had been encountered there during drilling.

The drilling of well 8 was completed on November 28, 1969. Its temperature was measured both during and after drilling. Figure 2 shows a few of these measurements. The temperature log from November 9, 1969, indicated aquifers at depths of about 360 m (300-450 m) and 820 m (750-900 m). The well was first discharged about one year after drilling on October 24, 1970. At that time the bottom-hole temperature was 250-260°C and about 230°C at 750-850 m. On initial discharge the well was kept on a 10" critical lip-pressure nozzle for about two months until January 1971 when it was shut-down. On February 3, 1971, its temperature was measured as shown on Figure 2. The bottom-hole temperature had clearly increased to 280-290°C.

The temperature log taken after the first 2 months of production (February 3, 1971) is of particular interest as it may indicate where flashing starts in the well during discharge. If two straight lines are drawn through the temperature profile, they intersect at a depth of about 910 m. It must be remembered here that the first slots of the liner start at 984 m such that the total flowrate of the well had been developed at that point. The straight line below 910 m may represent the flow of liquid brine at about 290°C from near bottom, being mixed with colder brine as it passes the liner slots. The point of flashing represents the saturation temperature of the brine mixture from the various aquifers. Figure 2 shows this temperature to be about 270°C, the same as indicated in Table 1. Above 910 m the steam-brine mixture flashes continuously and cools

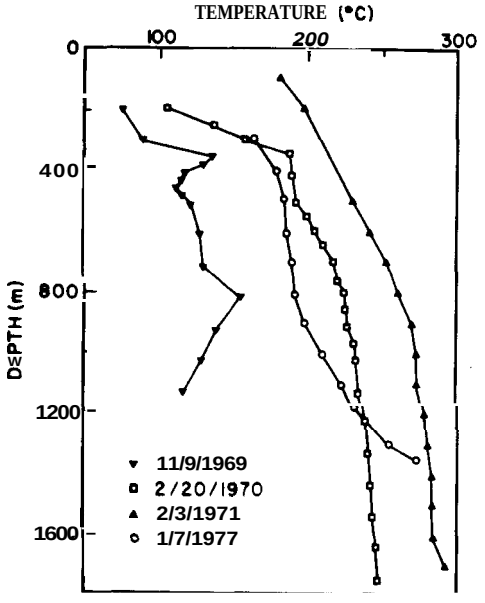

Figure 2: Temperature measurements in well 8 in Reykjanes

as it flows up the borehole. It should be noted that the temperature log of February 3, 1971, was not a flowing survey, but measured shortly after the well had been shut-in. Because the well had produced for a long time and reached stable thermal conditions, the temperature of its immediate surroundings may have approached the temperature profile existing in the well during discharge. It would be of great interest to compare the flashing point estimated above to theoretical borehole calculations for pressure drop and other characteristics of steam-water flows in geothermal wells.

The discharge history of well 8 has been presented by Thorhallsson (1977). Figure 3 shows the well discharge in the first four years of production, from October 1970 to October 1974. When the well was shut-down after the first two months the 10" nozzle was removed and replaced by an 8" one to carry out a deliverability test as discussed below. When this test was over, the well was again shht-down and fitted with a 4" nozzle. The well discharged through this nozzle for long periods but was temporarily (few hours) shut-domi and fitted with the 8" nozzle (critical lip-pressure) for all subsequent (instantaneous) flowrate measurements.

The initial discharge of well 8 was about 85 kg/s through the 10" nozzle to the atmosphere. When it was fitted with the 8" nozzle, two months later, its maximum flowrate was about 70 kg/s (deliverability test January 1971) whereas by 1974 this had decreased just below 60 kg/s, the well-head pressure being about 6 bar-a. Thorhallsson (1977) estimated that the long-term discharge of the well with the 4" nozzle may have been 45-55 kg/s during the first four years shown in Figure 3. The well was shut-in for three years from October 1974 to October 1977.

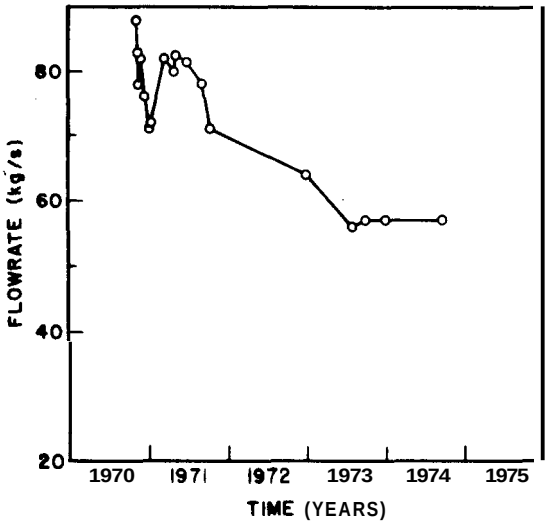

Figure 3: Discharge history of well 8 in Reykjanes

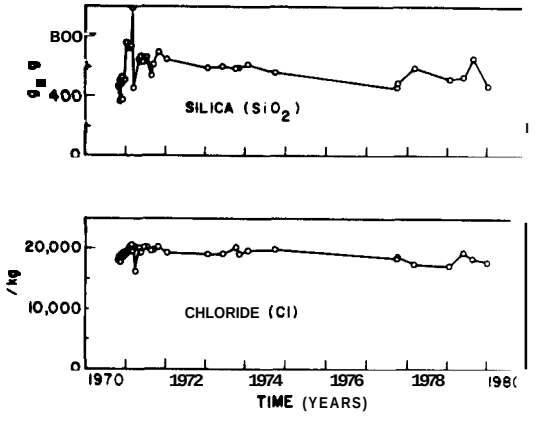

Figure 4: Silica and chloride concentration with time in the deep brine of well 8 in Reykjanes

The discharge history curve of well 8 in Figure 3 shows several features of interest. Before considering these the corresponding changes in deep brine chemistry will be examined. Figure 4 shows the silica (SiO_2) and chloride (Cl) concentrations with time, not only the first four years, but also later measurements (Hauksson 1981). The silica concentration changed from about 470 mg/kg in October 1970 to about 730 mg/kg in February 1971.

This corresponds to an apparent increase in deep brine temperature from about 250°C to over 280°C according to silica geothermometry. During the same period the chloride concentration increased from about 18,000 mg/kg to 20,000 mg/kg. From the time of initial discharge the concentration of most major elements in the deep brine have however been found to remain fairly constant (Hauksson 1981). It is perhaps of interest to note that the same conclusion had been arrived at from the monitoring of well 1 from 1956 to 1966.

During the first two months of full discharge the flowrate of well 8 decreased from about 85 kg/s to 70 kg/s. At the same time the silica concentration of the deep brine increased, indicating a temperature increase from about 250°C to 280°C. There appear to be two main explanations why the flowrate decreased and the indicated temperature increased during initial discharge. The first is that the well initially may have produced fluids that were influenced by cold water injected when the slotted liner was placed in the well. It must be remembered, however, that the slotted liner was run into the well about one year after the drilling finished. The second explanation is that the deeper feed zones (aquifers) of the well are more permeable than the upper feed zones. Therefore, when the well starts discharging at high flowrates (70-80 kg/s), there occurs greater drawdown in the upper feed zones compared to the deeper zones. The result of this would be that the contribution of the upper feed zones to the total well flowrate would decrease more rapidly with time than that of the deeper and hotter feed zones.

#en well 8 was put on long-term discharge through the 4" nozzle to the atmosphere in January 1971, the total long-term steam-brine flowrate decreased from the 70-85 kg/s in the initial period to the estimated 45-55 kg/s, as mentioned above. When the well was measured in March 1971 the total (instantaneous) flowrate through the 8" nozzle was 80 kg/s or about 10 kg/s greater than that measured with the 10" nozzle at the end of the initial two months' discharge period. The problem at hand is to explain why the flowrate increased. The silica concentration of the inflow brine seemed also to have decreased to a value at which it remained after that. A possible explanation is that at the lower long-term flowrate of 45-55 kg/s, as compared to 70-85 kg/s, there is less drawdown in the aquifers feeding the well. Each 8" nozzle test lasted a day or two during which time further drawdown presumably did not develop to affect the discharge flowrate. An instantaneous measurement using the 8" nozzle should therefore result in a higher flowrate than at conditions of greater drawdown when discharging for two months through the 10" nozzle.

From 1971 to 1974 the 8" nozzle (instantaneous) flowrate of well 8 decreased from over 80 kg/s to under 60 kg/s. The long-term flowrate (between each measurement) was much lower or 45-55 kg/s. An examination of Figure 3 shows that the total flowrate declines in a fashion where drawdown is increasing. It should be noted that the total flowrate declines smoothly with time, also, that the rate of decline 1971-1974 (flow 45-55 kg/s) is much lower than 1970 (flow 70-85 kg/s). There is some other evidence to support the above suggestion that drawdown in well 8 has increased with time. In 1970 the water level in the well was at about 40 m while in 1979 it was at 109 m (Bjornsson et al. 1971 and Gudmundsson 1980). In both instances the well was in near thermal equilibrium with the reservoir, i.e., not filled with cold water after drilling.

In the autumn of 1977 the wellhead of borehole 8 was overhauled after three years of shutdown (Thorhallsson 1977). The temperature in the well was measured as shown in Figure 2. It was found that the well was blocked at a depth of about 1370 m and that the temperature was very different from that measured before. The temperature profile had assumed an s-type curve with an inflection point at about 820 in depth. Several simple caliper (wire frame) measurements were made in the 7 5/8" slotted liner. It was found that in addition to a blockage at 1369 m, there appeared to be a minor restriction at 704 m and a major one at 841-845 m. The well was discharged on October 3, 1977, through an 8" nozzle. After two days the total flowrate was measured (critical lip-pressure method) to be 43 kg/s and the wellhead pressure 4 bar-a. On October 5, 1977, the well was shut-down temporarily and fitted with a 4" nozzle to produce 37 kg/s at a well-head pressure of 17 bar-a the following day. The discharge rate was therefore almost independent of wellhead pressure, indicating some restriction (choking) in the wellbore. #en the well was shut-in three years earlier the discharge through the 8" nozzle had been just under 60 kg/s so that the flowrate had decreased by about 1/3. It seems that this loss of production could be attributed to the wellbore blockages. Silica geothermometry of samples collected at the time of the above discharge measurements indicated deep brine temperatures just above 270°C as before. Because of the blockages found in well 8 in 1977, a difficulty arises with respect to the flowrate decline during 1971-1974 shown in Figure 3. It is possible that all or some of the decline was due to gradual wellbore blockage rather than drawdown in the main feed zones of the well. For the time being, however, it will be assumed that the two are separate because the flowrate decline is gradual while casing/liner failures are likely to occur suddenly, for example, when

wells are put on discharge after long standing periods. Well 8 was again shut-down in July 1978 for further simple caliper measurements which confirmed earlier results. The well was then kept on production until November 1978 when it was shut-down for repair in the following December. This repair or workover was done with a 6 3/8" drill-bit down to about 750 m and then a 6" drill-bit to bottomhole. The detailed results of this work-over are not yet well understood. After the work-over the well may have no liner at depths of 630-725 m and where the two main blockages were found as indicated above.

The deliverability of geothermal wells expresses their total flowrate against back pressure Two main deliverability measurements have been carried out on well 8, the first in 1971 and the second in 1980. The former was done using the critical lip-pressure method where the brine enthalpy was determined by silica geothermometry (Bjornsson et al. 1971). The latter was similarly based on the critical lip-pressure method but involved also the determination of the brine flowrate when the total mixture had flashed at atmospheric conditions. By this improved method the enthalpy of the steam-brine mixture could be determined independently (Gudmundsson 1980). The two deliverability tests are shown in Figure 5. The measurements in 1971 were carried out in one dav at the end of the initial discharge period (see above), The well was fitted with an 8" nozzle and the flowrate was adjusted by *e* valve, the readings being taken one or two hours later. The measurements in 1980 were taken over a period of four days. The well had been discharging almost continuously for one year with a wellhead pressure of 20-30 bar. The conditions under which the two deliverability tests were taken were therefore quite different. The 1980 test was carried out using 3", 5" and 7" nozzles. When changing nozzles the flow was directed through a by-pass line to minimize all pressure and temperature transients in the reservoir-well system. Each nozzle was allowed at least one day to adjust to stable wellhead pressure and flowrate values. Two sets of measurements were taken for each nozzle, the first after one day of adjustment and the second about 2 hours after decreasing the flowrate by a valve When using the 7" nozzle, however, two more sets of measurements were taken, also two hours after adjusting the flowrate.

The enthalpy of the steam-brine mixture was measured in the 1980 deliverability test. A chemical sample was also taken (January 8, 1980) and the temperature of the deep brine estimated from silica geothermometry. All these measurements are shown in Figure 6. The enthalpv of the steam-brine mixture was found *to* depend on the wellhead pressure and decreasing flowrate. This seems to indicate that the upper aquifers feeding the borehole are not as permeable as the deeper aquifers. Two measurements were taken for each nozzle/valve setting. When the wellhead pressure was increased the first time, for all the nozzles, the enthalpy did not change. However, after the second and third wellhead pressure changes when using the 7" nozzle, the enthalpy decreased. This may indicate that the pressure and thermal conditions in the reservoir-well system had not reached stable conditions. The deep brine temperature estimated from silica geothermometry is shown in Figure 6. It indicates basically the same enthalpy as obtained from the direct neasurements. The saturation curve for steam-water is shown in Figure 6 for reference.

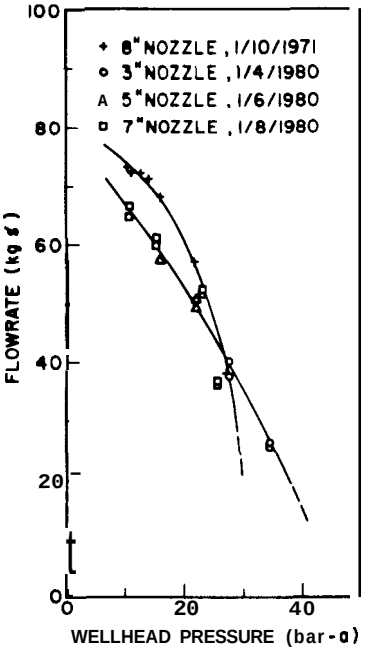

Figure 5: Deliverability measurements of well 8 in Reykjanes

Concluding Remarks Twenty-five years have now passed since the first exploration was initiated in the Reykjanes field. The main exploration work was, however, carried out about 10 years ago so that the early work (25 years ago) is mainly of historic interest. Nevertheless an important issue must be how the example of Reykjanes reflects on the future development of geothermal energy. In addition 'to what has already been stated above, the following aspects may be considered: (1) The results of the first exploration work influenced the way in which the resource may be used; (2) The pioneering nature of the sea chemicals scheme, as proposed about 15 years ago, was an important reason for the lack of development of the Reykjanes field; (3) Although the main

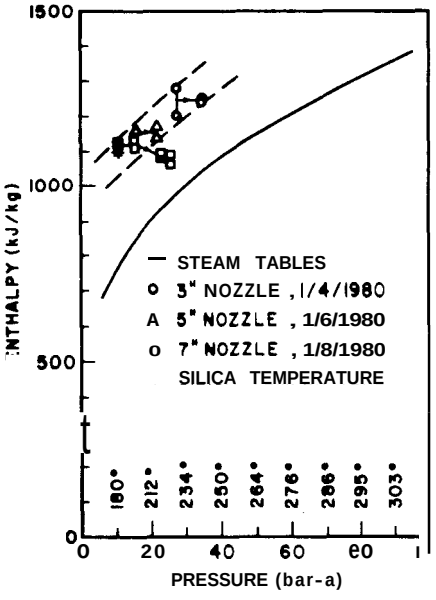

Figure 6: Enthalpy measurements of well 8 in Reykjanes

exploration phase (ten years ago) lasted only 3 years the basic results are still considered valid. There have, however, been advances in several areas of geothermal exploration and evaluation that should be applied to the field now.

The problems experienced in the drilling and discharging of the Reykjanes wells were new in Iceland. They had not been met in other fields and indicated that perhaps each geothermal area should be treated as unique. This view was, however, not arrived at until much later when further experience from other fields showed that experience gained in one geothermal field was not necessarily applicable to others.

Drilling in geothermal fields provides direct access to the energy resource in the ground. In exploration it should give information about the nature of the reservoir with respect to the translation of thermal energy into power. An important consideration in this translation must be the natural circulation of fluids in the geothermal reservoir. Geochemistry, both that of the water and the rock, has the potential of providing such information. It is well established that the Reykjanes field produces a deep brine having salinity similar to that of seawater. The origin of the geothermal brine is, however, still a subject of discussion. The isotope chemistry of the brine has puzzled investigators and will probably continue to do so for some time yet. In this paper a hypothesis is set forth as to the origin of the deep brine. It is suggested that water-rock interactions influence the deuterium content of the deep brine. This is very much a tentative suggestion but should nevertheless warrant consideration.

The feasibility of geothermal projects depends greatly on the success of drilling. Factors of importance in this success are the cost of drilling and also the deliverability and lifetime of boreholes. These two latter issues are explored in this paper by way of well 8 in Reykjanes as an example. The lifetime of boreholes, as the term is used here, concerns their mechanical condition mainly. It is evident that geothermal wells will generally experience difficult temperature and pressure transients. These may lead to failures resulting in permanent damage. The experience gained from well 8 in Reykjanes shows that great care is called for in the operation of high-temperature boreholes. The cementing of casings appears to be one of the most important factors in prolonging the lifetime of geothermal wells. Avoiding severe temperature transients in wells will aid in their successful operation In addition to casing and liner failures, problems may arise due to the deposition of calcite ($CaCO_3$) and other materials in the wellbore. Such problems tend to be field specific, while their solution (cleaning) usually involves drilling. Such workover operations will inevitably put strain on boreholes and may lead to failures as already mentioned.

Measurements of the deliverability of geothermal wells (well characteristics) are used for three main purposes: To specify steam-water transmission lines/equipment and power plants; To aid in the exploration for good production fields in geothermal areas, and; To monitor the performance of wells with time once under production. Such tests do not require the shut-down of wells and should therefore not introduce great temperature transients downhole. Deliverability tests will continue to provide the reservoir engineer with first-hand measurements of some of the dynamic fluid and heat flow processes taking place underground.

Acknowledgment

The authors would like to thank V. Stefansson, B. Steingrimsson and B. Lindal for reading the draft of this paper.

References

Arnason, B., 1976: Groundwater Systems in Iceland Traced by Deuterium, Soc. Sci. Isl., Pub. No. 42, 236 pp.

Arnorsson, S., 1978: Major Element Chemistry of the Geothermal Sea-water at Reykjanes and Svartsengi, Iceland, Mineral Mag., 42, 209-220.

Bjornsson, S., Arnorsson, S., and Tomasson, J., 1970: Exploration of the Reykjanes Thermal Brine Area, Proceedings, U.N. Symp. Development Utilization Geothermal Resources, 2, (2), 1640-1650.

Bjornsson, S., Arnorsson, S., Tomasson, J., Olafsdottir, B., Jonsson, J., and Sigurmundsson, S. G., 1971: Reykjanes--Final Report on Exploration, Iceland Energy Authority, 122 pp. (In Icelandic).

Bjornsson, S., Arnorsson, S., and Tomasson, J., 1972: Economic Evaluation of Revkianes Thermal Brine Area, Iceland, Am. Assoc. Pet. Geol. Bull., 56, (12), 2380-2391.

Georgsson, L. S., 1981: A Resistivity Survey on the Plate Boundaries in the Western Reykjanes Peninsula, Iceland, Geoth. Resources Council Trans., 5, 75-78.

Gudmundsson, J. S., 1980: Discharge Measurements of Well 8 in Reykjanes, Iceland Energy Authority, Note JSG-80/01, 16 pp. (In Icelandic).

Gudmundsson, J. S., Thorhallsson, S., and Ragnars, K., 1981: Status of Geothermal Electric Power in Iceland 1980, Proc. Fifth E.P.R.I. Annual Geoth. Conf. Workshop, 7/52-7/65.

Hauksson, T., 1981: Reykjanes--Concentration of Chemicals in Geothermal Brine, Iceland Energy Authority, Note TH-81/04, 53 pp. (In Icelandic).

Kjaran, S. P., Halldorsson, G. K., Thorhallsson, S., and Eliasson, J., 1971: Reservoir Engineering Aspects of Svartsengi Geothermal Area, Geoth. Resources Council Trans., 3, 337-339.

Lindal, B., 1975: Development of Industry Based on Geothermal Energy, Geothermal Brine and Sea Water in the Reykjanes Peninsula, Iceland, Proc. Second U. N. Symp. Development Use Geothermal Resources, 3, 2223-2228.

Olafsson, J., and Riley, J. P., 1978: Geochemical Studies on the Thermal Brines from Reykianes (Iceland), Chem. Geol., 21, 219-237.

O'Neil, J. R., and Kharaka, Y. K., 1976: Hydrogen and Oxygen Isotope Exchange Reactions Between Clay Minerals and Water, Geochimica et Cosmochimica Acta, 40, 241-246.

Stefansson, V., 1981: The Krafla Geothermal Field, Northeast Iceland. Ryback, L., and Muffler, L.J.P. (eds.), Geothermal Systems, Wiley, 273-294.

Suzuoki, T., and Epstein, S., 1976: Hydrogen Isotope Fractionation Between OH-bearing Minerals and Water, Geochimica et Cosmochimica Acta, 40, 1229-1240.

Thorhallsson, S., 1977: Well 8 in Reykjanee, Iceland Energy Authority, Note OS-JHD-7730, 9 pp. (In Icelandic).

Thorhallsson, S., 1979: Combined Generation of Heat and Electricity from a Geothermal Brine at Svartsengi in S.W. Iceland, Geoth. Resources Council Trans., 3, 733-736.

Tomasson, J., and Kristmannsdottir, H., 1972: High Temperature Alteration Minerals and Thermal Brines, Reykjanes, Iceland, Contr. Mineral. Petrol., 36, 123-134,

Proceedings Seventh Workshop Geothermal Reservoir Engineering
Stanford, December 1981. SGP-TR-55.

ANALYSIS OF WELL DATA FROM THE KRAFLA GEOTHERMAL FIELD IN ICELAND

G.S. Bodvarsson†, S. Benson†, O. Sigurdsson§
G.K. Halldorsson§, and V. Stefansson§

†Earth Sciences Division, Lawrence Berkeley Laboratory, Berkeley, California 94720
§National Energy Authority, Reykjavik, Iceland

Introduction As part of an informal agreement between Lawrence Berkeley Laboratory (LBL) and four Icelandic Institutions responsible for the exploration and development of geothermal energy in Iceland, well data from the Krafla geothermal field in Iceland have been analysed. The data consist of injection test data and production data. The injection test data were analyzed for the reservoir transmissivity and storativity. Analysis of the production data to determine the relative permeability parameters for the Krafla field is in progress. In this paper, the analysis of injection tests at the Krafla field will be described.

The Krafla geothermal field is located on the neovolcanic zone in north-eastern Iceland (Figure 1). The neovolcanic zone is characterized by fissure swarms and central volcanoes. The Krafla geothermal field is located in a caldera (8 x 10 km), with a large central volcano, also named Krafla.

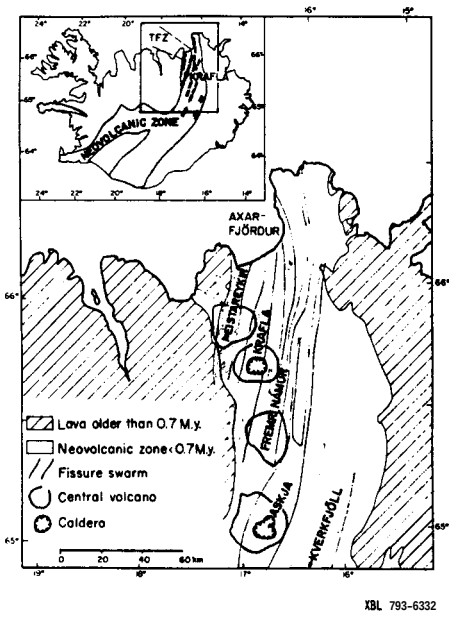

Figure 1 The location of the Krafla geothermal field in Iceland.

Surface geophysical exploration at Krafla was initiated in 1970. In 1974, two exploration wells were drilled, and the subsurface data indicated the presence of a high temperature (>300°C) geothermal field. Presently, 18 wells have been drilled at Krafla: the locations of the wells are shown in Figure 2.

Stefansson (1981) has presented a detailed description of the reservoir system at Krafla; his model is summarized below. In the old well field (wells 1-13, & 15) pressure and temperature data from the wells have indicated the presence of two reservoirs. The upper reservoir contains single phase liquid water at a mean temperature of 205°C. This reservoir extends from a depth of 200 m to a depth of about 1100 m. The deeper reservoir is two-phase, with temperatures and pressures following the saturation curve with depth. This reservoir directly underlies a thin confining layer at a depth of 1100-1300 m and it extends to depths greater than 2200 m (the depth of the deepest well). The two reservoirs seem to be connected near the gully, Hveragil. In the new well field (south of Mt. Krafla, wells 14, 16-18), the upper reservoir has not been identified, and only the twc-phase liquid dominated reservoir seems to be present.

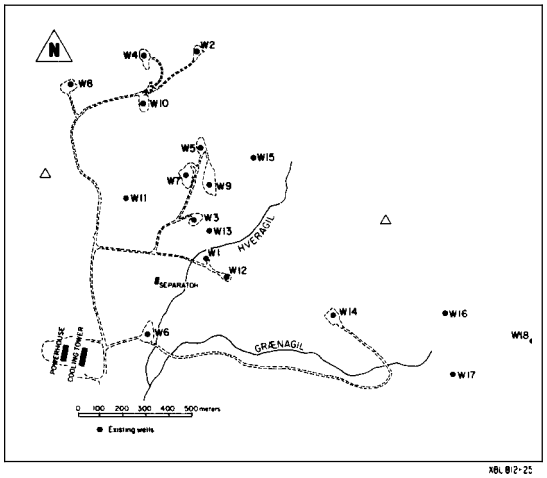

Figure 2 Well locations.

Well testing at Krafla A common procedure at Krafla is to perform an injection test soon after the drilling is completed. This procedure has been applied to the last 13 wells drilled at Krafla (wells 6–18). The purpose of the injection tests is twofold: 1) to attempt to stimulate the well, i.e., increase the water losses, and 2) to obtain data that can be analyzed to yield the transmissivity of the formation.

Experience obtained from injection testing of wells in Krafla, as well as in several other geothermal fields in Iceland, has shown that in many cases apparently dry wells (small water losses) have been sufficiently stimulated to become reasonably good producers. The reasons for this are not presently known, but several possible explanations are: 1) cleaning of fractures, 2) opening up of fractures due to increases in pore fluid pressure, or 3) thermal cracking close to the well, due to the temperature difference between the injected water and the hot reservoir water.

Conventional type curve analysis of the injection test data from Krafla has been reported by Sigurdsson and Stefansson (1977) and Sigurdsson (1978). In the present study the use of numerical simulators for well test analysis is illustrated.

Analysis of Injection Test Data The well KG–13 (W13) at Krafla was drilled in June–July 1980 (Figure 2). A simplified casing diagram for the well is shown in Figure 3. The well is cased (9 5/8 in casing) to a depth of 1021 m, below that a 7 5/8 in slotted liner extends to the well bottom. Thus the well is completed only in the lower, two-phase reservoir. The figure also shows the location of a major fracture feeding the well at a depth of 1600–1700 m.

A few days after drilling, two injection tests were performed (10th and-11th of July, 1980, respectively). During the tests a pressure

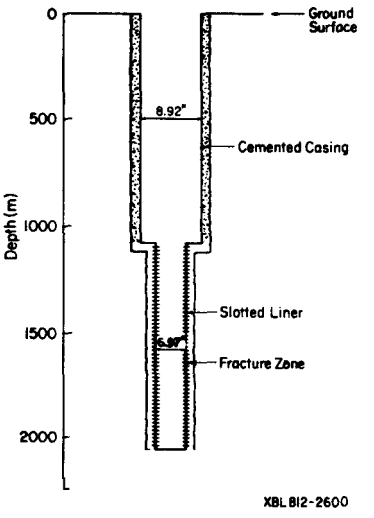

Figure 3 Simplified casing diagram for well KG–13.

transducer was located at a depth of approximately 220 m below ground surface, and continuous readings were obtained at the surface. The temperature of the injected water was approximately 20°C.

The injection rates at the surface are shown in Figure 4 along with the water level data for the second test. After the first injection test was completed (July 10th), injection was continued throughout the night at a stable injection rate of approximately 29 kg/s until initiation of the second test (see Figure 4). The second injection test consisted of an initial falloff, followed by three injection segments with increasing flow rates, and finally, a second falloff. During the test, a free surface water table was Present in the well, and since the injection tests are short, significant wellbore storage effects were present. Furthermore, analysis of the injection test was possibly complicated by thermal effects, as 20°C temperature water was injected into a two–phase reservoir of

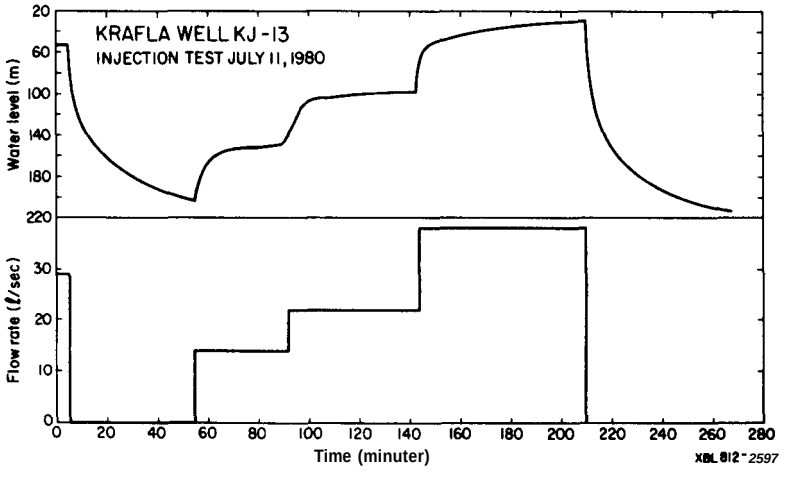

Figure 4. Flow rate and water–level data for injection test of well KG–13.

much higher temperature. For the present analysis, the fracture zone at 1600–1700 m depth was assumed to be the primary aquifer; the thermodynamic conditions at this depth correspond to a temperature of approximately 320°C.

The first step in the analysis of this well test was to correct for the wellbore storage effects. They were easily accounted for by using variable flow rate analysis, rather than the constant step-rate surface flow rates shown in Figure 4. Since the well head flow rate and the water level in the well were known, the sandface flow rate could be calculated on basis of simple mass balance as follows:

$$q_s = q_w - \pi r_w^2 \rho_w \Delta s \qquad (1)$$

where As denotes the change in the water level. Equation (1) simply states that the water entering the well (q_w) must leave the well (q_s) or be contained in the well, causing a change in the water level (As). Certainly after some time a steady state condition will be reached where the flow rates at the wellhead and at the sandface are identical and consequently the water level is stable (As = 0). However, for the Krafla wells (casing diameter 9 5/8 in), the wellbore storage effects will last for approximately one and one half hours, and therefore the variable flow rate approach must be employed in the test analysis.

Because of the two-phase nature of the Krafla reservoir and the non-isothermal effects introduced by the cold water injection, attempts were made to model the injection test data using the two-phase simulator SHAFT79 (Pruess and Schroeder, 1980) and the non-isothermal simulator PT (Bodvarsson, 1981). However, these attempts were unsuccessful, as a reasonable match with the water level data for entire test (the initial falloff, the three injection steps, and the second falloff) could not be obtained. Further attempts to simulate the injection test data were made using the variable flow rate Theis type model ANALYZE (McEdwards and Benson, 1981) and the numerical simulator PT in its isothermal mode. The best match obtained is shown in Figure 5.

The match is very good at all times, except for the third injection step, where the calculated water level values are slightly higher than the observed values. Figure 5 also shows the calculated sandface flow rates used in the simulation, as well as the well head flow rates.

The parameters obtained from the match were $kH/\mu = 1.52 \times 10^{-8} m^3/pa \cdot sec$ and $\phi\beta_t H = 8 \times 10^{-7} m/pa$.

The transmissivity (kH) of the reservoir could not be determined, as it was not obvious if the viscosity (μ) of the cold injection water or the hot reservoir water should be used in the analysis. Furthermore, the total compressibility (β_t) could not be explicitly calculated, as the porosity (ϕ) and the effective reservoir thickness (H) were not known. Further discussion of the reservoir parameters determined from the injection test is given later in this section.

Now let us examine the apparent isothermal behavior observed in the injection test data. Since the fluid viscosity changes by more than an order of magnitude for the temperature range 20° to 320°C, one would not expect isothermal pressure behavior in the data especially when the data is taken during both injection and falloff periods. The reason for this is that for a Theis-type reservoir, the pressure changes during injection will correspond to the cold water fluid properties,

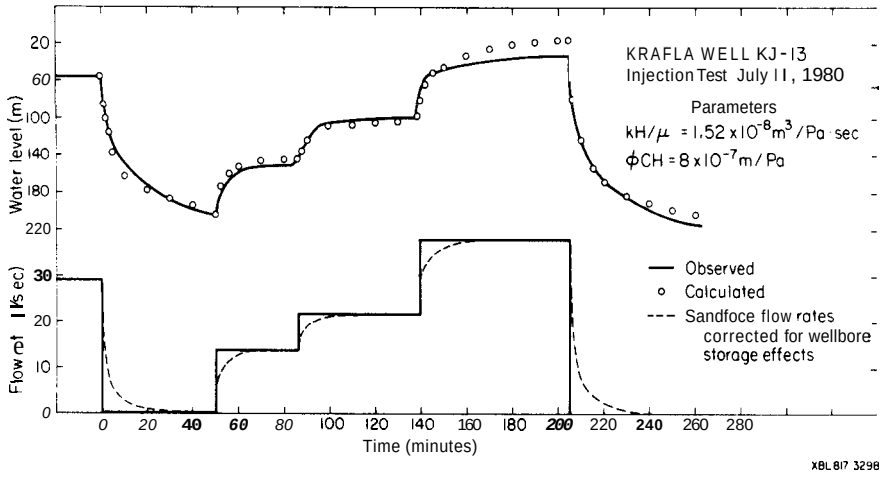

Figure 5. Comparison between observed and calculated water levels for injection test of well KG-13.

whereas during the falloff period, the pressure changes will correspond to the fluid properties of the hot reservoir (Bodvarsson and Tsang, 1980).

In an attempt to explain the isothermal behavior of the data from the injection test, two possibilities must be explored: 1) that the undisturbed reservoir conditions (e.g., T = 320°C) control the pressure response at the well; and 2) that the temperature of the injected water is the controlling factor. As cold water has been injected into the well at all times during drilling (approximately 45 days) and also during the few days after drilling, there must be a cold water zone around the well. Consequently, the first possibility seems unlikely. If the cold water zone around the well is to explain the isothermal behavior in the data, this zone must extend further from the well than the pressure disturbance during each injection step.

In order to study the advancement of the cold-water front along a fracture intercepting the well, the theory developed by Bodvarsson and Tsang (1981) was used. A single horizontal fracture, representing a permeable layer between lava beds, is assumed to absorb the total injection rate. Heat conduction from the rocks above and below the fracture retards the advancement of the cold water front. The equation governing the advancement of the cold water front along the fracture away from the well is:

$$r = \left(\frac{t \cdot q^2 \cdot (\rho_w c_w)^2}{4.396 \cdot \pi \cdot \lambda \cdot \rho_r c_r} \right)^{1/4} \qquad (2)$$

where r is the radial distance of the cold water front away from the injection well, q is the injection rate, λ is the thermal conductivity, and $\rho_w c_w$ and $\rho_r c_r$ are the volumetric heat capacities of the injected water and the rock matrix respectively. Figure 6 shows the advancement of the cold water front along the fracture versus time. The parameters used in the calculations are shown in Figure 6; they represent the average injection rate prior to the injection test, and average thermal properties for basaltic rocks. Figure 6 shows that, if one considers only the injection after drilling (2-3 days), the cold water front will have advanced approximately 50 m away from the well when the second injection test begins. It is of interest to note that this estimate is independent of the fracture aperature (Bodvarsson and Tsang, 1981).

In comparison, the radius of influence for the pressure disturbance due to a typical injection step can be calculated directly from the reservoir diffusivity as follows:

$$r = \sqrt{\frac{4kt}{\phi \mu \beta_t}} \qquad (3)$$

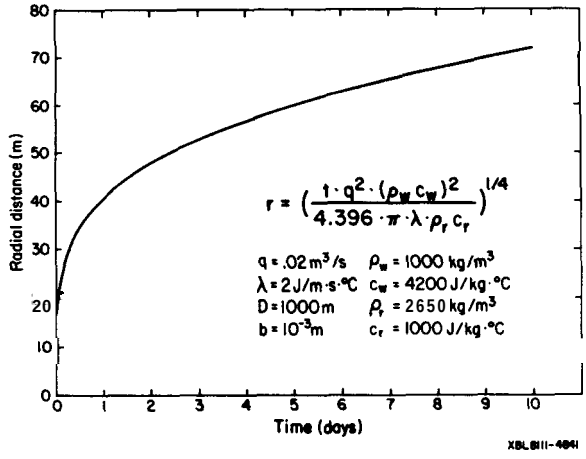

Figure 6 Advancement of the cold water front with time along a horizontal fracture.

Multiplying the numerator and the denominator by the effective thickness of the fracture zone H, the parameter groups determined from the well test (see equations 2 and 3) can be used to determine the radius of influence. For an injection step lasting 1 hour, a radius of influence of 16.5 m can be calculated. As this value (16.5 m) is less than the calculated radial extent of the cold water zone (~ 50 m), isothermal pressure behavior can be expected. If this analysis is correct, the fluid parameters corresponding to the cold injection water should be used, and consequently this implies a transmissivity of kH = 15 Darcy-meters.

The fracture zone (aquifer) feeding the Krafla well KG-13 is believed to be very thin, or on the order of 1 m (Stefansson, personal communication, 1981). If one assumes a value for the porosity (ϕ) for this zone, say $\phi = .10$, a very high total compressibility, $\beta_t = 8 \times 10^{-6}$ pa^{-1} can be calculated using equation (3). This high total compressibility can be explained by the two-phase conditions in the reservoir, or by high fracture compressibility. Due to the uncertainity in explaining the isothermal behavior of the test, both possibilities will be explored.

The compressibility of two-phase fluids is two to four orders of magnitude larger than those of single phase liquid or steam water (Grant and Sorey, 1979). The two-phase compressibility depends on many parameters, such as the temperature, saturation, porosity, and the relative permeability curves. Figure 7 shows the relationship between fluid compressibility and vapor saturation for various values of porosity. In calculating the curves shown in Figure 7 a reservoir temperature of 300°C and the Corey relative permeability curves are used. Comparison of the total compressibility β_t (previously determined $\beta_t = 8 \times 10^{-6}$ pa^{-1}) to Figure 7 yields a porosity value of $\phi \simeq .05$ and vapor saturation of $S_v < .20$. These values agree very well with values of porosity

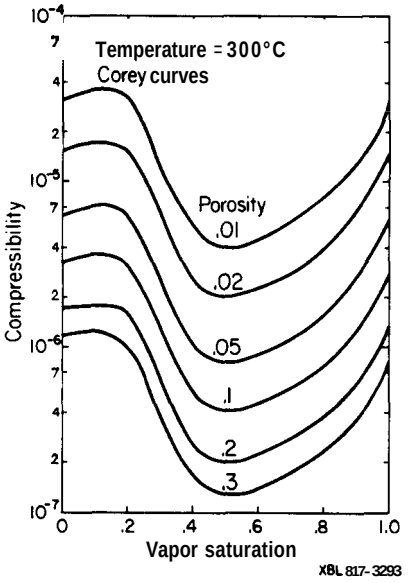

Figure 7 Fluid compressibility as a function of vapor saturation for various values of porosity.

and vapor saturation inferred from other field data (Stefansson, 1981). However, it is rather doubtful that the high compressibility determined from the injection tests is due to the presence of two-phase fluids, because of the cold water zone surrounding the well. It is possible that the high compressibility is due to deformable fractures. In that case, the increase in well losses during injection tests may be due to opening up of fractures caused by increased pore pressures.

The second injection test that was analyzed was performed on well KG-12 (W12). The well is cased (9 5/8 in casing) to a depth of 952 m, and below that to the bottom of the well (2222 m), a 7 in slotted liner is in place. This well is also completed in the lower two-phase reservoir. The major fracture zone is located at a depth of 1600 m, but some contribution to the production from the well may come from fractures located at a depth of 1000 m.

The injection test data, consisting of water level data and wellhead flow rates are given in Figure 8. As the figure shows, for several days prior to the test, cold water at a rate of 30 l/s was injected into the well. After an initial falloff lasting for approximately one and one half hours, four injection/falloff segments with increasing injection rates were used. On the average, each of the injection steps only lasted 40 minutes, so that wellbore storage effects are quite important.

Analysis of the injection test of well KG-12 was carried out using the simulator PT in its isothermal mode. Figure 9 shows the best match obtained between the observed and the calculated water level values. Figure 9 also shows the variable flow rate used in the

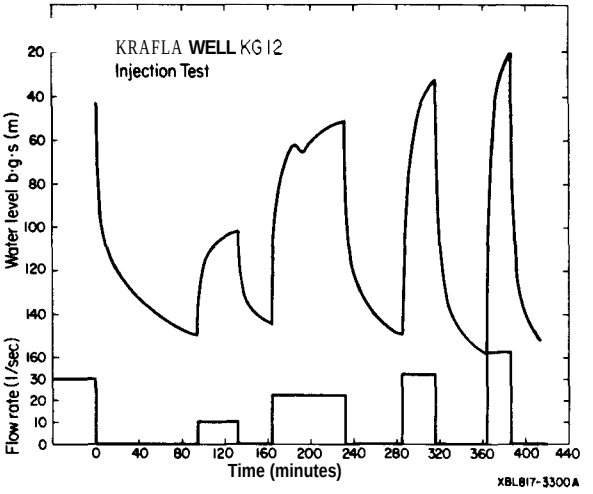

Figure 8 Injection test data for KG-12.

simulation (broken line) to account for the wellbore storage effects. As the figure shows, the calculated values compare very well with the observed data. However, the entire test could not be simulated using a constant value for kH/μ. For the initial falloff and the first injection-falloff cycle the data were matched reasonably well using $kH/\mu = 1.2 \times 10^{-8}$ $\frac{m^3}{pa.s}$; however, approximately 200 minutes after the injection test began, a decrease in the water level was observed, although the injection rate remained constant (Figure 9). This implies a change in the transmissivity of the reservoir. This is verified by the numerical simulation, since if the kH/μ factor is kept constant at $kH/\mu = 1.2 \times 10^{-8}$ over the entire simulation, the calculated pressure changes will greatly exceed the observed ones. Therefore, in the simulation the transmissivity had to be increased to account for the apparent stimulation due to the cold water

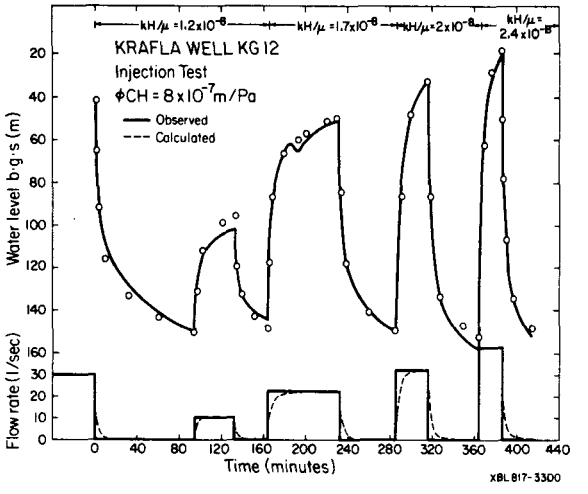

Figure 9 Match of calculated and observed water-level data at KG-12.

injection. In the simulation shown in Figure 9, the kH/μ was increased by a factor of two, from an initial value of 1.2×10^{-8} m^3 to a final value of 2.4×10^{-8} m^3. Injection test data from several other Krafla wells have shown similar increases in injectivity during injection. The experience at Krafla has indicated that cold water injection can stimulate tight wells into becoming fair producers. Similarily, increases in productivity of flowing wells due to thermal contraction have been reported by Stefansson and Steingrimsson (1980)

In the simulation shown in Figure 9 a constant storativity value was used, $\phi\beta_t H = 8 \times 10^{-7}$ m/pa. This value is identical to the value obtained from the analysis of well KG-13. This indicates either a rather constant distribution of the fluid reserves (ϕ and S_v rather uniform), or a fairly uniform fracture compressibility.

Conclusions Injection test data from the Krafla geothermal field in Iceland have been analyzed using numerical simulation techniques. The results indicate that although the injected water is of a much lower temperature than the undisturbed reservoir water, there are no apparent nonisothermal effects observable in the data. One possible explanation is that a cold water zone exists around the well due to the cold drilling water and that the pressure disturbance during the injection tests does not extend beyond the cold water zone. Thus, the reservoir parameters must be evaluated based on the fluid properties corresponding to the injected fluid.

Numerical modeling studies of injection tests from two of the Krafla wells (KG-12 and KG-13) yielded the transmissivity and storativity of the formation surrounding the wells. The results indicate that the injection test stimulated well KG-12, since an apparent increase in the transmissivity was observed during the test. Also, for both of the wells, the modeling results indicated a high total compressibility. The high compressibility can either be due to the two-phase condition in the reservoir or a high fracture compressibility.

Acknowledgements This research was performed as a part of a cooperative scientific investigation of the Krafla geothermal field between NEA, SEPW, ERI, and SI of Iceland and LBL of U.S.A. This work was supported by the Assistant Sceretary of Conservation and Renewable Energy, Office of Renewable Technology, Division of Geothermal and Hyropower Technologies of the U.S. Department of Energy under Contract No. W-7405-ENG-48.

References

Bodvarsson, G.S. (1981), "Mathematical Modeling of the Behavior of Geothermal Systems under Exploitation", (Ph.D. dissertation) Lawrence Berkeley Laboratory, Berkeley, California.

Bodvarsson, G.S., and Tsang, C.F. (1980), "Thermal Effects in Well Tests of Fractured Reservoirs," Proceedings, Third International Well-Testing Symposium, Lawrence Berkeley Laboratory (March 26-28).

Bodvarsson, G. S., and Tsang, C.F. (1981), "Injection and Thermal Breakthrough in Fractured Geothermal Reservoirs," to be published in the Journal of Geophysical Research, LBL-12698.

Grant, M.A., and Sorey, M.L. (1979), "The Compressibility and Hydraulic Diffusivity of Water-Steam Flows," Water Resources Research, vol. 15, no. 3, p. 684-686.

McEdwards, D.G., and Benson, S.M. (1981), "User's Manual for ANALYZE, Variable-Rate, Multiple-Well, Least Squares Matching Routine for Well-Test Analysis," Lawrence Berkeley Laboratory, Berkeley, California, LBL-10907.

Pruess, K., and Schroeder, R.C., (1980), "SHAFT79 User's Manual," Lawrence Berkeley Laboratory, Berkeley, California, LBL-10861.

Sigurdsson, O., and Stefansson, V. (1977), "Lekt i borholum i Kroflu", (in Icelandic) National Energy Authority of Iceland.

Sigurdsson, O. (1978), "Rennsliseiginleikar efra jardhitakerfisins i Kroflu," (in Icelandic) National Energy Authority of Iceland.

Stefansson, V. (1981), "The Krafla Geothermal Field, Northeast Iceland," Geothermal Systems, L. Ryback and L.J.P. Muffler (editors).

Stefansson, V., and Steingrimsson, B. (1980). "Production characteristics of wells tapping two-phrase reservoirs at Krafla and Namafjall" Proceedings. 6th Workshop Geothermal Reservoir Engineering, Stanford University, Stanford California, SGP-TR-50, 49-59

Proceedings Seventh Workshop Geothermal Reservoir Engineering
Stanford, December 1981. SGP-TR-55.

FIRST RESULTS OF A REINJECTION EXPERIMENT AT LARDERELLO

Anselmo Giovannoni, Giovanni Allegrini and Guido Cappetti
ENEL-Unit2 Nazionale Geotermica, Pisa, Italy
Romano Celati
CNR-Istituto Internazionale per le Ricerche Geotermiche, Pisa, Italy

Abstract Reinjection, which began at Larderello in 1974 as a means of disposing of excess steam condensate, is now envisaged as a method for improving heat recovery.

The behavior of the geothermal field when subjected to production and injection is difficult to predict because of the very heterogeneous fractured reservoir. More information is needed on circulation patterns and heat sweeping processes to estimate the long-term behavior of the reservoir and to avoid detrimental effects. A series of reinjection experiments is now under way in different parts of the Larderello reservoir, aimed at improving knowledge of these points before starting a wide-scale injection program.

This paper presents the results of about one year of injection in an area that has been exploited intensely for over 20 years.

During this test the following were noted:
- almost complete vaporization of the injected water;
- significant production increases and no temperature decrease in the wells around the injector.

Introduction Production from the Larderello field, under exploitation for more than 50 years, has been kept more or less constant during the last 30 years by drilling new wells.

This policy has proved to be less than satisfactory during the last few years because of the large decrease in pressure throughout the field (Fig.1), and in the more productive zones in particular (Ferrara et al.,1970; Celati et al.,1977a; Baldi et al.,1980).

The success of the new wells is tied to the possibility, still to be verified, of recovering fluids from zones outside the present margins of the field and from deep horizons of the reservoir (more than 2 km depth).

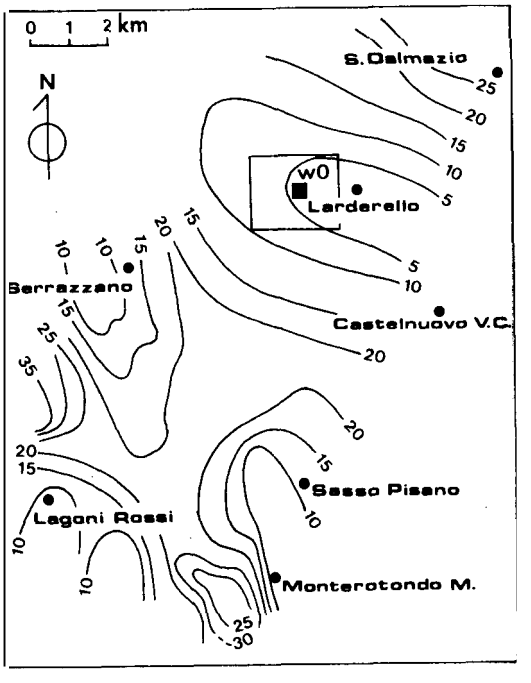

Figure 1 Pressure distribution at the top of the reservoir in the Larderello field, showing injection well wO and the study area. Pressure in bar.

Another possible approach is to inject large quantities of water back into the reservoir. Theoretically a "secondary recovery" of heat from this greatly depleted reservoir is possible as the temperature in most of the explored volume is still within the 240°-260°C range;

temperature values of more than 300°C have also been recorded more or less everywhere at depths below 2 km.

Mathematical models and a limited field experience (Celati et al.,1977b; Celati and Ruffilli,1980; O'Sullivan and Pruess,1980; Schroeder et al.,1980) have shown that it is possible to increase both the recovery factors in the long term and the production rates in the short term, by exploiting reservoirs with pressures below saturation values.

Favourable conditions for obtaining significant production increases can be found in the horizons most exploited nowadays, over the wide zones of Larderello characterized by high permeability and low pressures.

In the present energy situation this seems to be a highly attractive possibility. At the moment, however, we have not a sufficient knowledge of the spatial distribution of the fractures, nor, consequently, of the path taken by the injected fluid in the reservoir and the sweep efficiency attainable. "Short-circuits" have frequently occurred between wells at the drilling stage, after a circulation loss, and productive wells.

For these reasons, before defining a large-scale injection program for the Larderello field, the decision was taken to run a series of tests in different places and situations. The objectives of these tests are to study field behavior, select the most suitable sites for injection wells and develop some tracing methods capable of throwing light on the evolution of the phenomena.

First injection test The zone chosen for the first reinjection test is that shown in Fig.1. The main reasons for choosing this zone were:

- high permeability tied to a diffuse fracturing. The initial flow-rate in some of these wells exceeded 300 t/h;
- high density of productive wells and, hence, possibility of studying the propagation of the effects of injection (Fig.2);

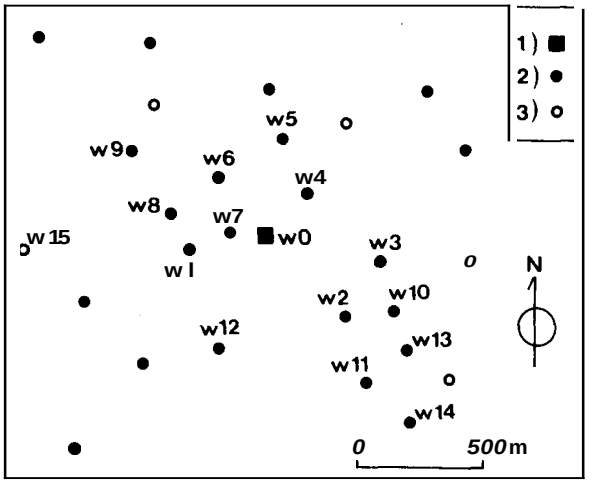

Figure 2 Location of the wells 1)injection well; 2)productive wells; 3) shut-in wells.

- marked decrease in production and reservoir pressure with time (Fig.3), with temperatures remaining around 240°-260°C;
- marked stability of the chemical characteristics of the fluids during the last few years, and more or less uniform spatial distribution of the isotopic composition around the injection well.

All the wells in the area vary in depth from 400 to 600 m, their steam entries lying within the carbonate-evaporitic formation.

The first test was conducted from January to August 1979, keeping the flow-rate of the injected water on quite low values (usually 30 and 50 m^3/h, and about 105 m^3/h for a short period only). After a 3 month break injection began again with higher flow-rates.

All the wells from wl to w14 in Fig.2 were affected to varying degrees, in the form of production increases and changes in fluid composition. The most significant changes were those affecting the isotopic composition of the fluid (Nuti et al.,1981).

Figure 4 shows the flow-rate of the injected water, the total production increase of wells wl-w14, the wellhead

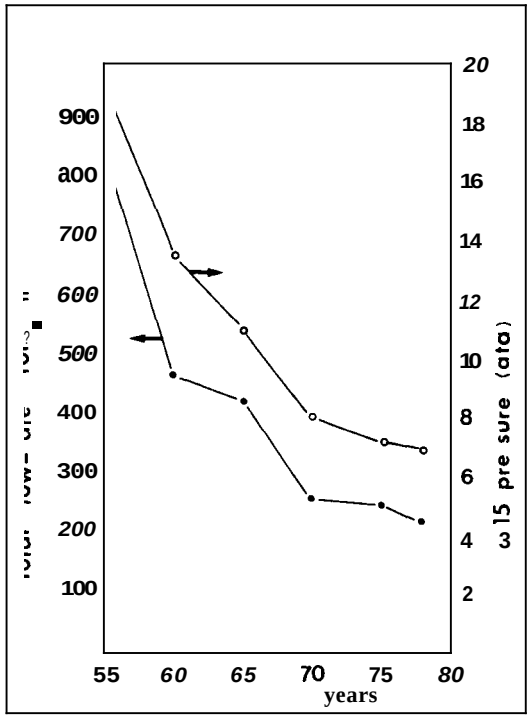

Figure 3 Decline in total flow-rate in wells w1 to w14 and in shut-in pressure in well w15.

pressures and temperatures of the seven most productive wells in the area and the average gas content of wells w1 - w14. The steam flow-rate was strongly affected by the variations in wellhead pressure, which increased notably during this period as a result of certain operations in the power-plants. The increase in flow-rate was lower than the amount of water injected. Wellhead temperature in the productive wells varied very little, even in the wells nearest the injector. The average gas content of the fluid decreased to 70% of its pre-injection value, which, along with increased pressure, led to an increase in conversion efficiency. The variations in the gas/steam ratio appear to be tied to the flow-rate of injected fluid. The latter has a negligible gas content so that the steam it produces merely dilutes the gas in the original steam.

The studies of the isotopic composition of the fluid have shown that it is possible to calculate the contribution of the injected water to the production of the various wells (Nuti et al.,1981). Systematic analyses of the isotopic composition of the fluid have been made on four wells only (w1,w2, w7 and w11). We can thus estimate how much of the steam produced by the injected water joins the fluid produced by these wells. Figure 5 shows that they produce about 60% of the injected water and that this contribution alone is higher than the increase in flow-rate observed throughout the area.

Towards the end of the injection period (204th day in Fig.5) an isotopic survey was made of all the wells affected by reinjection. According to the results of Nuti et al., more than 90% of the flow-rate of injected water was reproduced by the wells. The variations in the gas/steam ratio can also be used to evaluate, albeit approximately, the contribution of injected water to production in the area, assuming that the fluid produced is a mixture of original steam with a constant gas content and injected water containing no gas. This calculation, however, is incorrect as the gas content in the original steam flowing to any given well is not constant because the flow pattern in the reservoir is altered by reinjection. The error made in computing gas dilution can be reduced by using the average gas/steam ratio in the fluid produced from all the wells in the area, but it cannot be eliminated altogether. Nevertheless, the gas/steam ratio is known for all the wells affected by reinjection and for the entire duration of the test; we can thus estimate approximatively the fraction of the water injected in the total fluid produced in the area. Figure 5 shows that the contribution of injected water to production, calculated in this way, is more or less the same as the injection rate.

On the whole we may conclude that, in this first test phase of small injection rates, almost all the water injected is vaporized and joins the fluid produced. The total increase in flow-rate, however, is much smaller than this contribution, which means that the flow of original steam towards the wells decreased during injection. In this case, the phenomenon was mainly

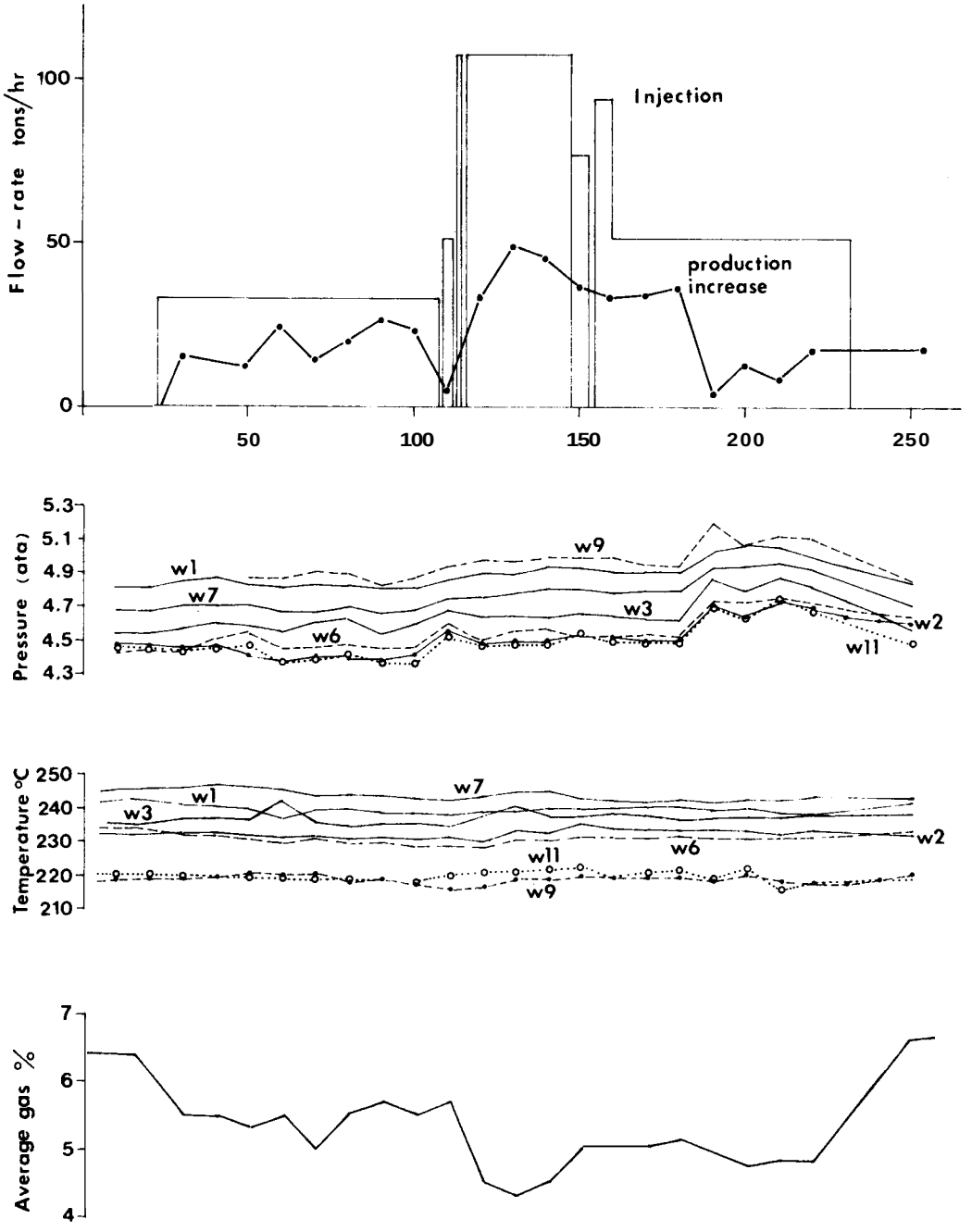

Figure 4 Injection rate in well w0 and total production increase in wells w1 to w14. Wellhead temperature and pressure in the seven most productive wells of the area. Average *gas* content in wells w1 to w14.

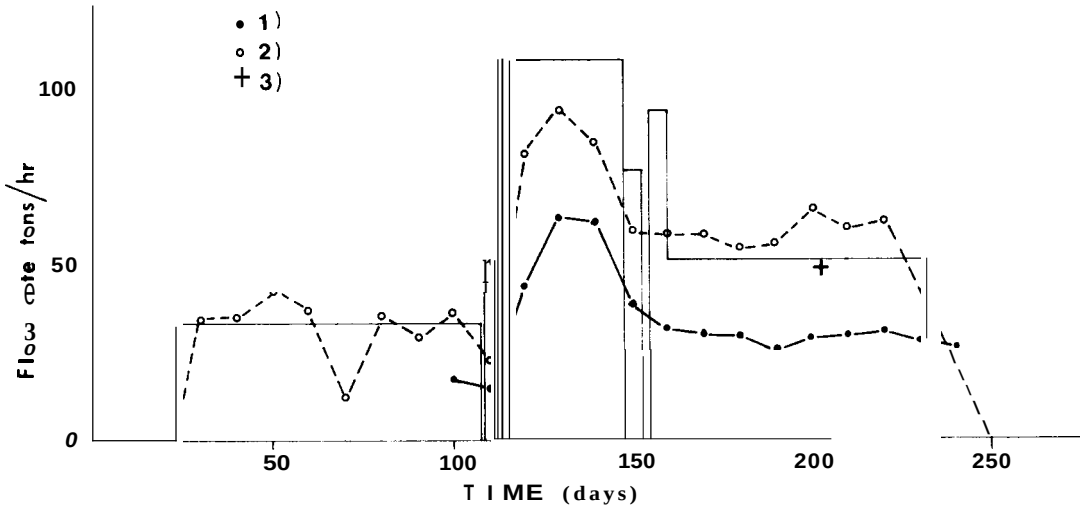

Figure 5 Injected water recovered through wells w1,w2,w7 and wl , from isotopes,1); injected water recovered through wells w1 to wl4, from gas content,2) and from isotopes,3).

caused by the back-pressure increases on the wells, deriving from operations in the power-plants. These back-pressure increases have a considerable effect on the rise of steam from great depths and a much lesser effect on the steam coming from the shallower, very permeable formations. These observations are in agreement with the results of the numerical simulation (Schroeder et al.,1980), indicating that effects of this type can also have a certain importance when producing at constant wellhead pressure.

Figure 6 shows the trend of fluid flow-rate and the contribution of injected water to production for wells w7 and w9. In w7, which is very near the injection well, this contribution is much higher than the increase in flow-rate, whereas in w9, relatively further away from the injection point, the increase in flow-rate is higher than in w7, but the contribution of injected water is very low. The flow of original steam thus decreases in w7, and increases in w9 as a consequence of an increase in reservoir pressure.

Reinjection was always conducted with

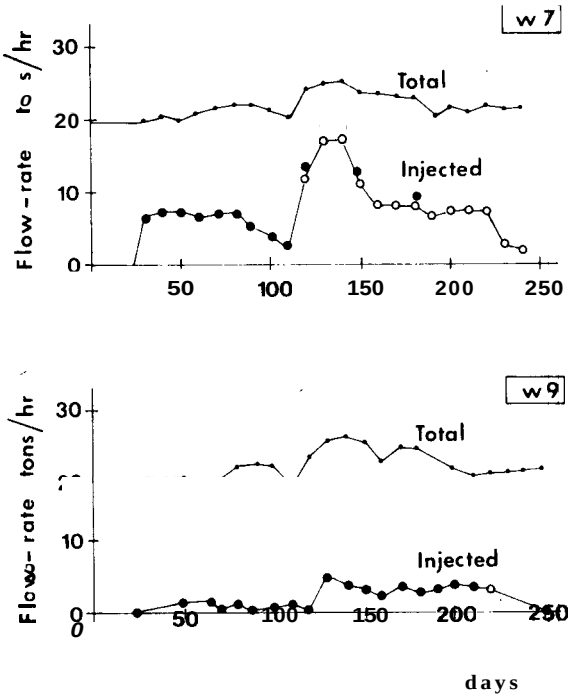

Figure 6 Fluid production and injected water recovered in wells w7 and w9. 'From isotopes. *From gas content.

no back-pressure at the wellhead, and

the injectivity of the well showed no variations throughout the duration of the test; the pressure at the top of the permeable sector of the borehole never varied more than 0.5 ata from static pressure.

Despite the fact that a total of 2.3 x 10^5 m^3 of water was injected into well wO during this first phase, at an average rate of 50 m^3/h, the well had already reached its usual shut-in pressure at wellhead 10 minutes after injection ended, and no liquid phase was found in the borehole. The well was kept shut for twenty days, during which the pressure remained constant and the temperature in the bore was at saturation values. On opening the well the steam rapidly became superheated and the wellhead temperature quickly rose to 185°C after only 8 days (Figure 7), and 220°C at wellbottom after 40 days production.

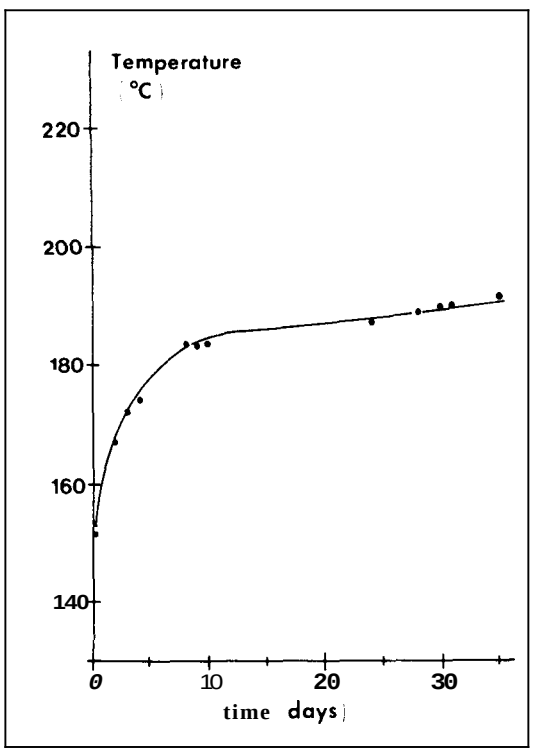

Figure 7 Wellhead temperature in wO, producing at the end of the injection period.

Conclusions No breakthrough phenomena were observed during this first phase of the experiment with low injection rates, even with such a reduced well spacing. On the contrary, the conditions appear to be favourable for a good penetration of the water into the fractured medium, and for a good rock-fluid thermal exchange.

A second injection phase is now under way to verify the earlier results when injecting at higher flow-rates. Other experiments are beginning in nearby areas with productive wells deeper than the injection wells. These tests hopefully will also shed light on the penetrating capacity of the injected fluid at depth.

References

Baldi,P.,Bertini,G., Calore,C.,Cappetti,G.,Cataldi,C., Celati,R. and Squarci, P.(1980)," Selection of Dry Wells in Tuscany for Stimulation Tests", Proc. Second DOE-ENEL Workshop for Cooperative Research in Geothermal Energy, Berkeley,p.98-115.

Celati,R.,Squarci,P.,Stefani,G.C. and Taffi,L.(1977a),"Study of Water Levels in Larderello Region Geothermal Wells for Reconstruction of Reservoir Pressure Trend", Proc. of Simposio International sobre Energia Geotermica En America Latina, Ciudad de Guatemala, 1976, IILA, Rome, p.501-526.

Celati,R.,McEdwards,D.,Ruffilli,C., Schroeder,R.,Weres,O. and Witherspoon, P.(1977b),"Study of Effect of Reinjection with a Mathematical Model",Proc. ENEL-ERDA Workshop,Larderello,1977,p. 256-298.

Celati,R. and Ruffilli,C.(1980),"Simulazione numerica della iniezione in sistemi a vapore-dominante", ENEL-CNR Report,Pisa, 19 pp.

Ferrara,G.C., Panichi, C., Stefani, G. (1970), "Remarks on the geothermal Phenomenon in an intensively exploited field. Results of an experimental well", Geothermics, Special Issue 2, v.2, pt.I, p.578-586.

Nuti, S.,Calore,C. and Noto,P.(1981) "Use of Environmental Isotopes as Natural Tracers in a Reinjection Experiment

at Larderello", Proc.7th Workshop Geothermal Reservoir Engineering, Stanford, 15-17 Dec., 1981.

O'Sullivan,M.J. and Pruess,K.(1980)"Numerical Studies of the Energy Sweep in Five-Spot Geothermal Production-Injection Systems",Proc.6th Workshop Geothermal Reservoir Engineering, Stanford, 16-19 Dec.,1980,p.204-212.

Schroeder,R.C.,O'Sullivan,M.J.,Pruess, K.,Celati,R. and Ruffilli,C.(1980), "Reinjection Studies of Vapor-Dominated Systems", Proc.2nd DOE-ENEL Workshop for Cooperative Research in Geothermal Energy, Berkeley, 1980,p.381-433.

Proceedings Seventh Workshop Geothermal Reservoir Engineering
Stanford, December 1981. SGP-TR-55.

USE OF ENVIRONMENTAL ISOTOPES AS NATURAL TRACERS IN A REINJECTION EXPERIMENT AT LARDERELLO

Sergio Nuti, Claudio Calore and Pietro Noto

Istituto Internazionale per le Ricerche Geotermiche, (CNR),
Via del Buongusto 1,
56100 Pisa, Italy

Abstract Reinjection of the discharge from the power-plants of a geothermal field can cause serious, irreversible damage to the field itself, so that such operations must be mnitored continuously. Tracer techniques are particularly useful for this purpose.

In some reinjection studies tritiated water was used as a tracer, but this methcd has certain disadvantages as well as advantages, one disadvantage being the destruction of the natural tritium balance in the reservoir.

The natural abundances of tritium at Larderello were, and are still, used to study field recharge from meteoric waters, so that another tracing methcd had to be applied to avoid disrupting these studies. The discharge fluid from the power-stations is traced naturally by its ^{18}O and D compositions with respect to the steam ccmposition of the field. As these isotopes do not create the same difficulties as tritium we are checking their possible utilization as tracers.

This paper presents the results obtained by applying this methcd in the first phase of a reinjection experiment now under way in a central area of the field which has been exploited for long periods. Some limits of this method are also discussed.

Introduction Because of the limited natural recharge of the Larderello geothermal field (Petracco and Squarci, 1975), the decision was taken to study the possibility of recharging it artificially by reinjecting the waste from the geothermoelectric pier-plants back underground in some suitable points of the field itself. This procedure would also solve the problem of getting rid of these effluents whose ccmposition is such that they cannot be discharged into the runoff waters or the shallow aquifers.

In a vapour-dominated field such as that of Larderello, with a heterogeneous reservoir and fracture-derived permeability, one cannot predict with any certainty the effects induced by reinjection. For example, one could expect a decrease in steam enthalpy and/or in the amount of steam produced. In order to avoid eventual irreversible negative effects to the field sane experiments must be made prior to launching a full-scale reinjection programme.

These experiments will provide useful information on the complex phenomenology of vapour-dominated systems only if the tools used are adequate.

In this respect the tracer tests assume a role of considerable importance, as they can provide informtion on the processes occurring in the reservoir and on eventual modifications to these processes; they can also be used to calculate the m u n t of injected water reappearing as steam in the fluids produced and individuate any preferential pathways of the fluids

The problem is to find a routine work method that creates as little disturbance as possible to the system, but which also produces the maximum of data.

In the reinjection tests currently being conducted in a central area of the Larderello field, which has been exploited for the past 20-odd years, a study is being made of the potential of the stable isotopes ^{18}O and D as tracers.

The reasons for undertaking a reinjection programme at Larderello, the problems connected with this programme and the results from the engineering viewpoint are described in a paper by Giovannoni et al. (1981).

Enviromtal isotopes as natural tracers In some geothermal fields tritiated water has been used as a tracer in reinjection studies, as in The Geysers (Gulati et al., 1978) and at

Ahuachapan (Einarsson et al.,1975). As outlined by Gulati et al., this method has its negative as well as positive aspects. Among the former are the fact that the method requires expensive and time-consuming enrichment analyses and that its application destroys the natural tritium balance in the reservoir.

The natural tritium abundance at Larderello has been, and is still, used in studies of field recharge by meteoric waters (Panichi et al.,1974,1978). Another tracer method had thus to be adopted to avoid compromising these studies.

Environmental tracers have, on the other hand, been used for some time now in geological studies in merit of their being natural tracers.

The isotopic abundances of oxygen-18 and deuterium in the waters have helped to solve many hydrogeological problems. Problems more closely tied to an exploited geothermal field have also been investigated by means of the stable isotopes. During recent years especially, some interesting conclusions have been reached on subjects such as deep temperatures, physical state of the water and origin of some components of the geothermal fluid (Noto et al., 1979; Panichi et al.,1979; Nuti et al.,1980).

In the reinjection experiment now under way at Larderello, in an area with high temperatures and pressures of about 5 ata, the steam from the monitored productive wells had a composition ranging between -1.5 and -3 in $\delta^{18}O$ and -37 to -42 in δD. All the δ values given in this paper refer to differences permil fran VIENNA-SMOW, the international isotope standard for waters defined by the International Atomic Energy Agency of Vienna (Gonfiantini, 1978).

After leaving the turbines the steam is condensed, and the condensed water passes to the cooling towers where a considerable fraction is lost to the atmosphere in the form of vapour. Because of this process the residual water is greatly enriched in the heavy isotopes oxygen-18 and deuterium. Throughout the experiment the isotopic composition of the injected water was in fact more or less constant with respect to $\delta^{18}O$ and δD, both being near to a value of +5, and far from the value of the "undisturbed" wells.So the discharge water is traced naturally by its stable isotopic canposition and no artificial or radioactive tracers need be added to the system, avoiding all the negative effects this type of interference entails, including those to the environment. The only disturbance is thus that brought on by reinjection itself.

The sampling and analysis techniques can be carried out as routine field operations, which are easy to apply and cheaper than tritium measurements.

Moreover,this method, as opposed to the pulse techniques, permits us to monitor the system systematically throughout the reinjection test, so that we can immediately obtain information on any variations underqone by processes occurring in the reservoir. Theoretically some negative aspects could exist in this method.There could be an isotopic exchange between the water and the rocks, but this phenomenon, if it did take place, would affect the oxygen only. Again, an isotopic re-equilibration could take place between the water and gas species, but this is a theoretical possibility only, as the latter represents only 2.8 miles percent of the geothermal fluid at Larderello and could, therefore, have little effect on the isotopic composition of the water. Furthermore, 90% of the gas is CO_2, so that the hydrogen would, again, be unaffected.

The last, and most serious, negative aspect is the possibility of an isotopic fractionation of the water during phase change.

Results of the tracing experiment The injection well chosen for the experiment, WO, lies in a central area of the field, where exploitation has been under way for more than 20 years but temperatures have remained high (more than 240°C in the reservoir).

The monitored wells are distributed all round well WO, at distances of 150 to more than 700 metres (Fig.1). The isotopic composition of the steam produced by the wells in this zone is nearly uniform, so that it would be only sliqhtly affected by any change in the original fluid flow pattern ensuing from reinjection.

In the first phase of this experiment a total of 30-35 m^3/h of water was injected for about 3 months, 105 m^3/h for about 20 days and 50 m^3/h for another 3 months.

After iiijection began the isotopic composition of the fluid in the monitored wells shifted towards the positive values of the reinjected water, and began decreasing when reinjection was reduced to 50 m^3/h.

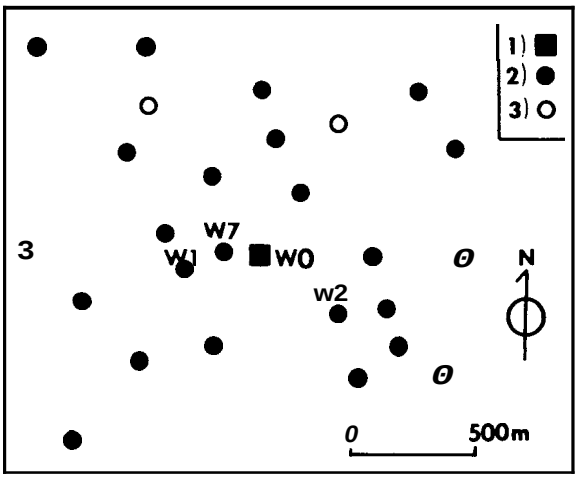

Figure 1 Location of the wells in the area west of Larderello affected by the reinjection test. 1) reinjection well; 2) production wells; 3) shut-in wells.

Once the test ended the canposition returned to its earlier "undisturbed" values, while well WO started producing steam whose isotopic composition was slightly more positive than that of the nearby wells (Fig.2). The deuterium showed the same behaviour as the oxygen-18. This alone shows that at least part of the injected water vaporizes and that this steam joins the fluid produced by the surrounding wells.

Figure 3 shows the trend of the isotopic composition of the fluids produced in wells W2 and W7 during this phase of reinjection, in a δD-$\delta^{18}O$ diagram. The high linear correlation coefficients and the position of the points along straight lines joining the "undisturbed" canposition of the wells to that of the reinjected water suggest that a simple mixing process has taken place, with no disturbing phenomena related to isotopic exchange or fractionation. The fact that no isotopic fractionation has occurred suggests that the vaporization process does not produce two phases but a steam phase only, i.e., every portion of the injected water participating in the boiling process is completely vaporized.

In these conditions the m u n t of injected water returning in the fluid produced by the wells can be calculated by the following balance equation:

$G_I = G_{WH} (\delta_{WH} - \delta_R / \delta_I - 6,)$, where G is the flaw-rate, I, WH and R are subscripts representing the fluid coming from injected water, fluid produced by the wells and original fluid respectively.

Figure 4 shows the the spatial distribution of the fraction of injected water versus the to-

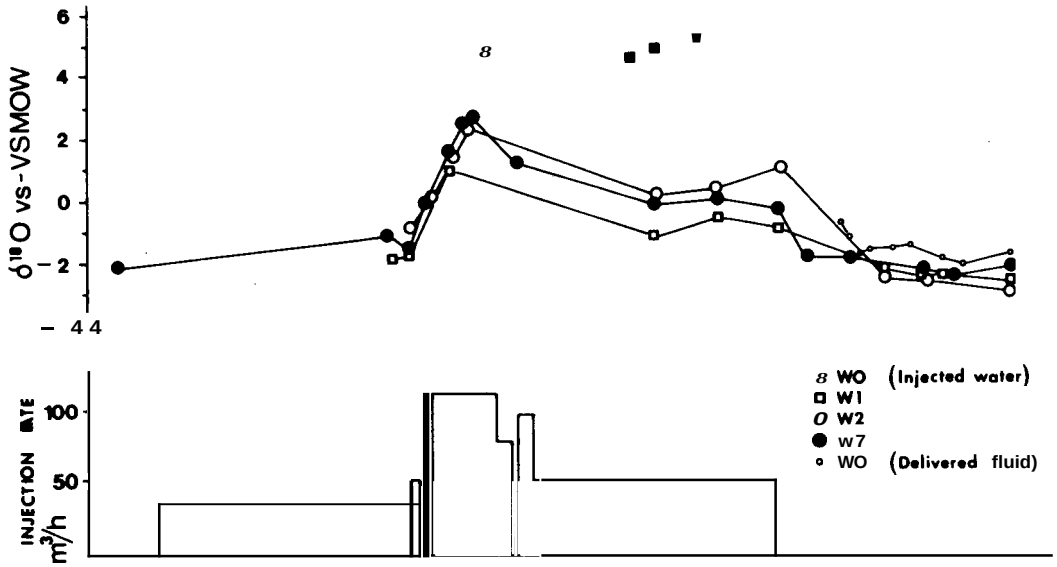

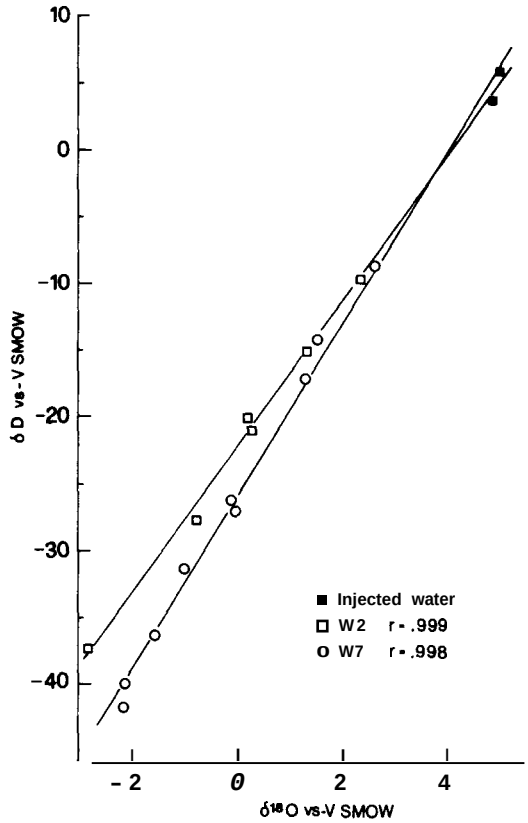

Figure 3 Variation in isotopic composition, in a $\delta D - \delta^{18}O$ diagram, of the condensate of the fluid produced by wells W2 and W7 during the reinjection test.

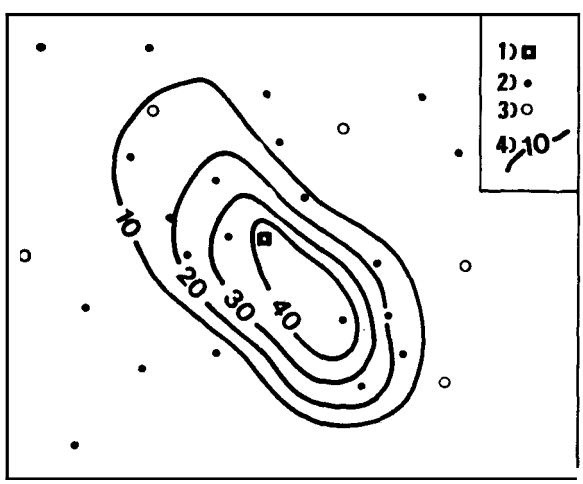

Figure 4 Contribution of injected water to production. 1),2) and 3) as in Fig.1; 4) percentage ratio of injected water recovered as steam to the total fluid produced by the wells.

tal fluid produced by the wells about 20 days before the test ended.

The fact that the wells most affected by reinjection lie *along* a NW-SE alignment, the lack of correlation between the distance from the reinjection well to the others and the contribution of reinjected water in their steam *show* that the injected water has found preferential pathways in the underground.

This consequently confirms that the reservoir cannot be compared to a homogeneous and isotropic porous medium.

In conclusion, artificial tracers are unnecessary in vapour-dominated fields with certain favourable conditions, as the stable isotopic composition of the reinjected water already acts as a natural tracer. By mnitoring the isotopic composition of the condensate of the productive wells in the area affected by reinjection we were able to ascertain that the injected water vaporizes and contributes to production, to calculate the amount of injected water re-entering the surrounding wells and to individuate the preferential pathways taken by this water in the underground.

In *our* opinion these results prove that tritium is not always the best tracer for reinjection studies in vapour-dominated geothermal systems.

References

Einarsson,S.S.,Vides,A. and Cuellar,G. (1975), "Disposal of Geothermal Waste Water by Reinjection". Proc.2nd U.N.Symp., San Francisco,Vol.2, 1349-1363.

Giovannoni,A.,Allegrini,G.,Cappetti,G. and Celati,R. (1981),"First Results of a Reinjection Experiment at Larderello". Proc. 7th Workshop Geothermal Reservoir Engineering, Stanford, 16-18 December,1981.

Gonfiantini,R. (1978),"Standards for Stable Isotopes Measurements in Natural Compounds". Nature, Vol.271, 534-536.

Gulati,M.S., Lipman,S.C. and Strobel,C.J.(1978), "Tritium Tracer Survey at The Geysers". Geothermal Resources Council,Trans. 2,237-239.

Noto,P.,Nuti,S.,Panichi,C. and Gonfiantini,R. (1979) "Environmental Isotopes in Geothermal Water Investigation". Proc.2nd Workshop on Isotopes in Nature, Leipzig.

Nuti,S., Noto,P. and Ferrara,G.C.(1980) "The System $H_2O - CO_2 - CH_4 - H_2$ at Travale, Italy:

Tentative Interpretation". Geothermics, Vol.9-3/4, 287-296.

Panichi, C., Celati, R., Noto, P., Squarci, P., Taffi, L. and Tongiorgi, E. (1974) "Oxygen and Hydrogen Isotope Studies of the Larderello, Italy, Geothermal System". In: Isotope Techniques in Groundwater Hydrology, Vol.2, IEAE, Vienna, 3-28.

Panichi, C. and Gonfiantini, R. (1978) "Environmental Isotopes in Geothermal Studies". Geothermics, Vol.6-3/4, 143-161.

Panichi, C., Nuti, S. and Noto, P. (1979), "Use of Isotopic Geothermometers in the Larderello Geothermal Field". In: Isotope Hydrology 1978, Vol.2, IAEA, Vienna, 613-630.

Petracco, C. and Squarci, P. (1975), "Hydrological Balance of Larderello Geothermal Region". Proc. 2nd U.N. Symp. on the Development and Use of Geothermal Resources, San Francisco, Vol.1, 521-530.

Proceedings Seventh Workshop Geothermal Reservoir Engineering
Stanford, December 1981. SGP-TR-55.

TEMPORAL EVOLUTION OF THE COMPOSITION OF THE FLUID FROM SERRAZZANO ZONE (LARDERELLO)

Franco D'Amore, Claudio Calore and Romano Celati

Istituto Internazionale per le Ricerche Geotermiche (CNR)
Via del Buongusto 1,
56100 Pisa, Italy

Abstract A temporal evolution in fluid composition has been noted during exploitation of the Serrazzano geothermal area, on the northwestern margin of the Larderello field. Strong variations have been recorded in the contents of NH_3, H_3BO_3, HCl and the uncondensable gases. The largest variations were recorded in the 1955-70 period, when new boreholes were being drilled.

One possible explanation of these changes may lie in the fact that the fluid discharged from the wells comes from diverse sources and that exploitation has gradually modified the contribution from each of these sources.

Introduction During the last few years there has been an increase in interest in time and space variations of fluid composition in vapour-dominated fields. The studies of fluid composition at Larderello and The Geysers have already shown interesting possibilities of the application of geochemical methods in field development and reservoir engineering (Celati et al., 1973; Panichi et al., 1974; D'Amore et al., 1977; Truesdell et al., 1977; Truesdell and Nehring, 1978; Mazor, 1978; D'Amore and Truesdell, 1979; Calore et al., 1980).

The long production histories of Larderello reveal different trends of fluid composition in different areas of the field, both as regards space distribution and time evolution. Space distribution appears to be controlled by two major phenomena: 1) mixing of original reservoir fluid with recharge waters and 2) gradual condensation of steam flowing from vaporization zones towards the field boundaries.

Time variations observed in some old wells of the central area of Larderello have been interpreted as the consequences of changes in the contribution of different steam sources to fluid production (D'Amore and Truesdell, 1979).

Serrazzano area, where space distribution appears to be controlled by steam condensation (Calore et al., 1980) has now been studied from the point of view of evolution of fluid composition during about 40 years of production.

This paper describes the first attempt at defining a conceptual model of Serrazzano reservoir capable of explaining the observed fluid composition history. We assume that, during exploitation, different steam sources contribute, to varying degrees, to fluid production.

Evolution of steam composition at Serrazzano We consider a limited zone, including the old densely drilled area and the productive wells north of it (Fig.1). The geological features are well known (Calore et al., 1980).

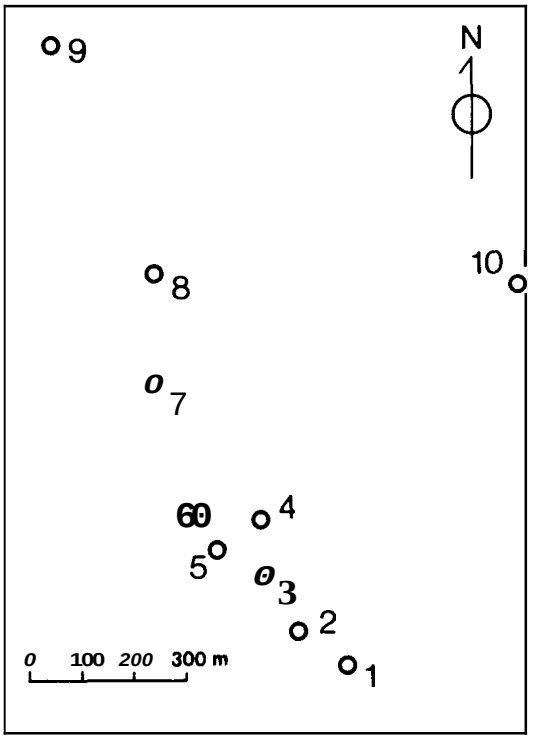

Figure 1 Producing wells in Serrazzano area

Wells nos.1 to 6 were drilled in the period

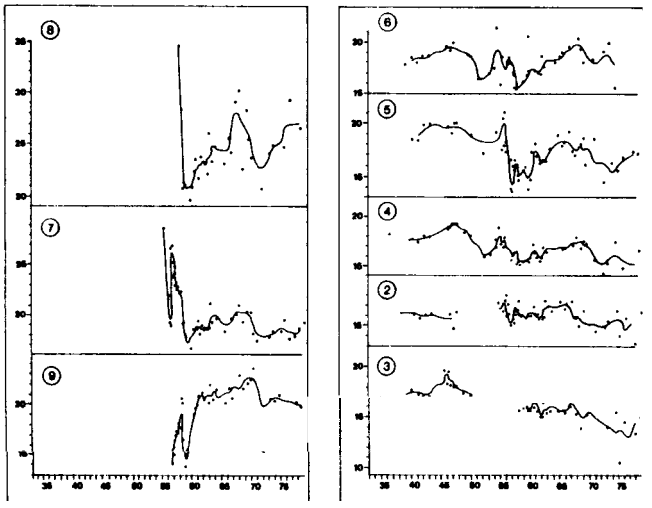

Figure 2 Gas/steam ratio in the steam of the producing wells of Serrazzano area (litres S.T.P./kg)

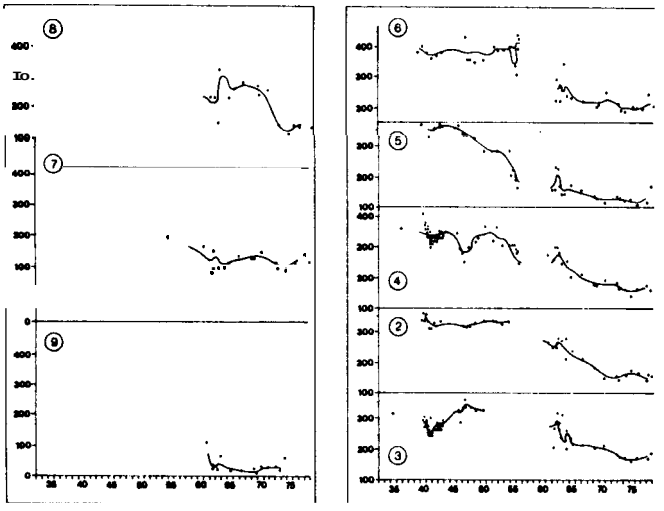

Figure 3 H_3BO_3 in the steam of the producing wells of Serrazzano area (ppm)

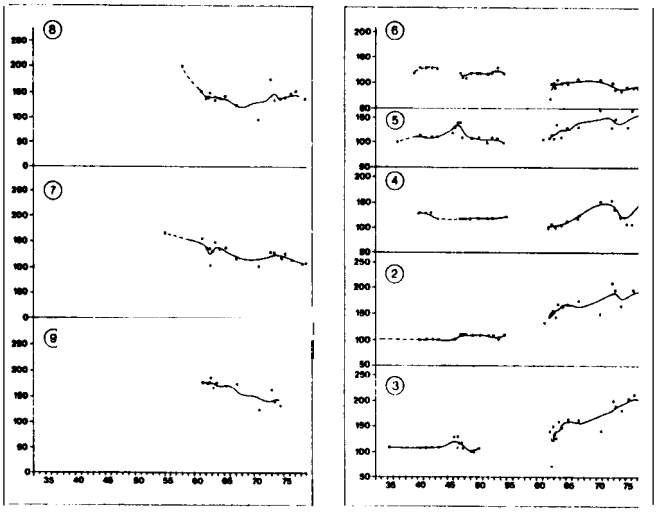

Figure 4 NH_3 in the steam of the producing wells of Serrazzano area (ppm)

1928-1941, with a very reduced spacing, close to surface manifestations.

From 1941 to 1954 no new wells were drilled in the area; wells 7,8 and 9 started production between 1954 and 1957 and well 10 in 1966.

The gas/steam ratio, boric acid and ammonia concentrations are generally available from 1940 on, while other chemical and isotopic analyses are relatively recent in this area.

Figures 2,3 and 4 show the changes with time of the gas/steam ratio and boron and ammonia in wells 2 to 9. Figure 5 shows the available Cl^- data for the wells in which its concentration was detectable.

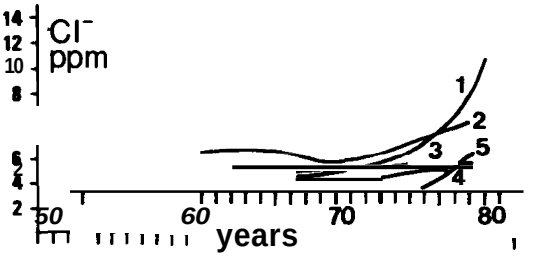

Figure 5 Cl^- (ppm) in the steam of the wells at Serrazzano. Wells not reported in the figure have undetectable Cl^- concentrations.

By smoothing the data some definite trends appear and in different wells show some correlation. Minor features are apparent in the gas/steam ratio only, as no boric acid and ammonia data are available for certain periods.

Discussion The study of space variations in fluid composition throughout Serrazzano area led to a conceptual model for this part of the field (Calore et al.,1980) that has now been tested to explain the time changes. A sketch of this model is shown in Fig.6.

A steam source is assumed to exist in a high temperature (about 270°C) zone east of the small area of our present study. This steam initially flowed towards the north, north-west boundaries, condensing on its way. The condensation should have been very effective near the 'cold walls' at the top of the reservoir and on the northern boundary, where there are low permeability formations, with the added probability of being cooled by a limited meteoric water infiltration through the ophiolitic

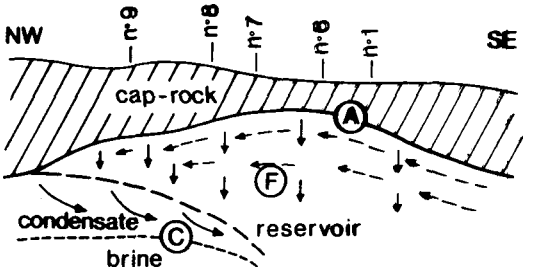

Figure 6 Conceptual model of Serrazzano reservoir.

rocks outcropping north of the study area. Along the vertical we can distinguish three different portions of the reservoir:
1) upper condensation zone, A, characterized by high fracture-derived permeability (Celati et al.,1975), high initial liquid saturation and a fluid very rich in boron and poor in ammonia and CO_2;
2) intermediate two-phase zone, F, with a lower permeability and low water saturation, capable of producing a fluid rich in CO_2 and NH_3 and poor in H_3BO_3;
3) lower liquid-saturated zone, C, whose existence is documented by the wells in the northern area and is inferred elsewhere; the liquid-two-phase boundary descends towards the south, so that the continuous liquid phase is close to the bottom of the wells in the northern part, gradually moving away as we move southwards.

We assume this liquid is made up of a high salinity water, surmounted by a layer of condensate, thinning from north to south; the effect of this condensate probably becomes negligible on the southern edge of the densely drilled zone.

Both in A and F, NH_3 and CO_2 gradually increase and H_3BO_3 decreases as we move towards the north. The deep liquid is assumed to be generally very poor in CO_2, boron and ammonia, but boron and ammonia increase towards the south where the brine contribution becomes significant.

Prior to 1954 only wells 1 to 6 were producing. During the second world war, from 1941 to 1946, when production probably decreased, some condensation occurred in the reservoir and the gas/steam ratio continually increased in wells 3 to 6. In 1946 production returned to normal and in a few years the fluid composition re-

turned more or less to pre-war values: the gas accumulation was depleted and the condensate deposited vaporized. Boron and ammonia data are scarce for this period; however, a decrease in boron and a contemporaneous increase in ammonia are clear in a few wells.

Production in this period came mainly from the upper section A of the reservoir. Before 1954 the gas/steam ratio was increasing, probably due to an increase in the contribution to fluid production from section F and from the north. This trend was halted by the start of production in new wells (no.7 in 1954, no.9 in 1955, n0.8 in 1957). Production from these wells was more than total production from the wells producing previously in the area. There was a strong interference between the new and old wells as shown in Fig.7: reservoir pressure is not available for the period 1954-1957 but the sharp decrease in total flow-rate of wells 2, 4, 5 and 6 clearly shows this interference.

The flow pattern in the reservoir was completely altered; the new wells exhibited a large and rapid decrease in gas/steam ratio and ammonia as they drained fluid from the south and the pressure decrease induced liquid boiling. The interference from the new wells brought on more boiling in the old zone too, and interrupted the previous flow of fluid from the north, so that a fast decrease also took place in the gas/steam ratio. The effects of the new wells were felt first in the upper zone A, due to its high permeability. Unfortunately boron and ammonia data are missing for this period.

The flow pattern continued to vary in the reservoir: the contribution from the two-phase intermediate zone F increased in all the wells, thus increasing the gas/steam ratio. The behaviour of the northern (nos.6,7,8 and 9) and southern (nos.1,2,3,4 and 5) wells differed in this period.

For the northern wells the two-phase zone F has a limited thickness, the deep, continuous liquid phase is close to the bottom of the wells and becomes rapidly the main source of the fluid produced. The steam generated at the top of the deep liquid phase is very poor in gas, boron and ammonia, so that the concentrations of all these components decrease in time.

For the central wells zone F eventually becomes the main source of fluid, with a minor contribution also from C. Thus, while boron decreases continuously in the period of decreasing A contribution, ammonia increases with the in-

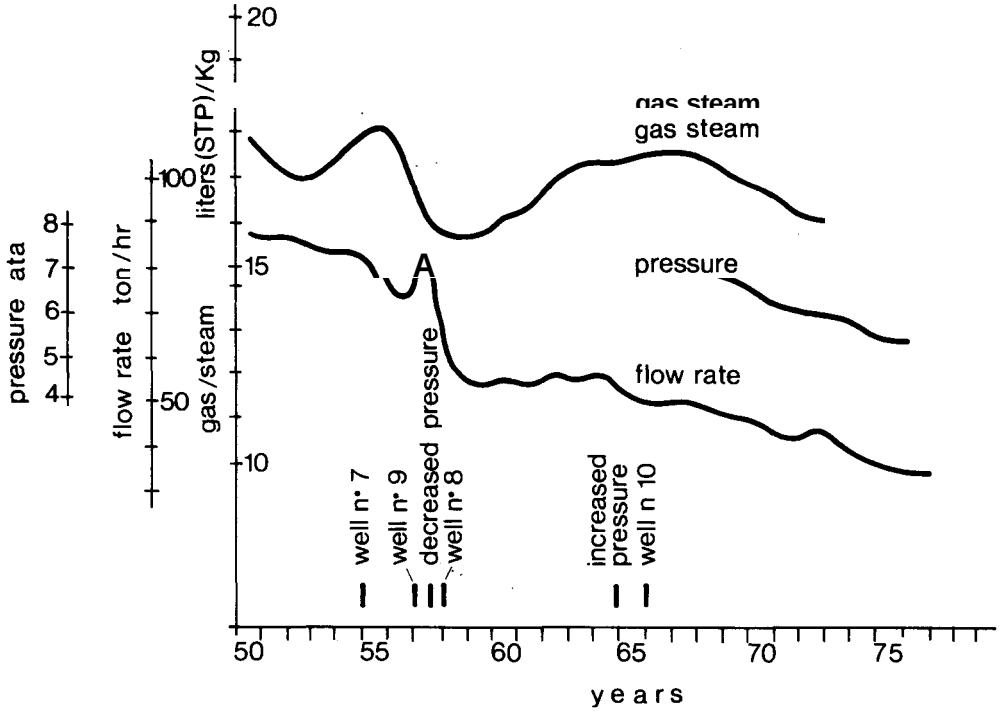

Figure 7 Total steam flow-rate and average gas/steam ratio of wells nos.2, 4, 5 and 6. Reservoir pressure and the date of starting production in new wells are also reported.

crease in contribution from F and C.

In the southernmost wells the contribution from the brine is responsible for the relatively high NH3 content and for the appearance or increase in Cl^-.

These processes are accelerated by the entry into production of well 10 and its consequent interference to already producing wells. In Fig.7 this interference is apparent both in the trend of reservoir pressure (measured in a shut-in well) and in the production of the old wells: both start decreasing after a period of rough stabilization. The contribution of deep liquid continues to increase, with a decrease in the gas/steam ratio in the majority of the wells and essentially a levelling-off of boron and ammonia.

The three-sources model applied by D'Amore and Truesdell(1979) to some wells of the central area of Larderello has been applied to the wells at Serrazzano. This model assumes that three sources, A, F and C, each delivering a fluid of constant composition, contribute to the production of each well. The three sources differ from one well to another.

The chemical characteristics attributed to the fluid coming from the different sources (Table 1) and the variations in their relative contribution to well production were chosen so as to be consistent with the conceptual model just described and to give a good match of the geochemical history of Serrazzano. The space variations of the F sources are consistent with a process of condensation of steam flowing from ESE to NNW (Fig.8).

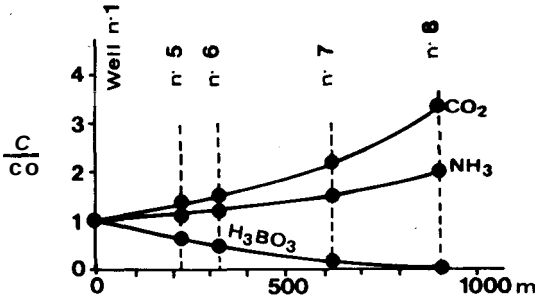

Figure 8 Space distribution of the assumed concentration changes of H_3BO_3, NH_3 and CO_2 in steam source F.

Figures 9 and 10 show the variations in time of the contributions from the different sources, along with the experilental data (dots) and model results (circles) for *two* wells characteristic of northern and southern zones.

These simple models roughly confirm the hypotheses outlined above. Obviously, these models are not completely adequate to describe the well behaviour in this area.In fact, they totally ignore horizontal flow of fluid in the reservoir. Strictly speaking, only a distributed parameter model would be capable of simulating this system adequately.

Table 1 Concentrations in the steam delivered by the sources A, F and C.

Well	Source	Gas/steam (litres STP/kg)	H_3BO_3 (ppm)	NH_3 (ppm)	HCl (ppm)
No.8	A	22.5	375	125	0
	F	75.0	20	400	0
	C	0.0	55	40	0
No.7	A	17.5	425	110	0
	F	52.0	40	300	0
	C	0.0	65	50	0
No.4	A	12.0	500	65	0
	F	30.0	120	230	0
	C	0.0	85	100	5
No.2	A	12.0	500	40	0
	F	22.5	170	200	0
	C	0.0	110	150	15

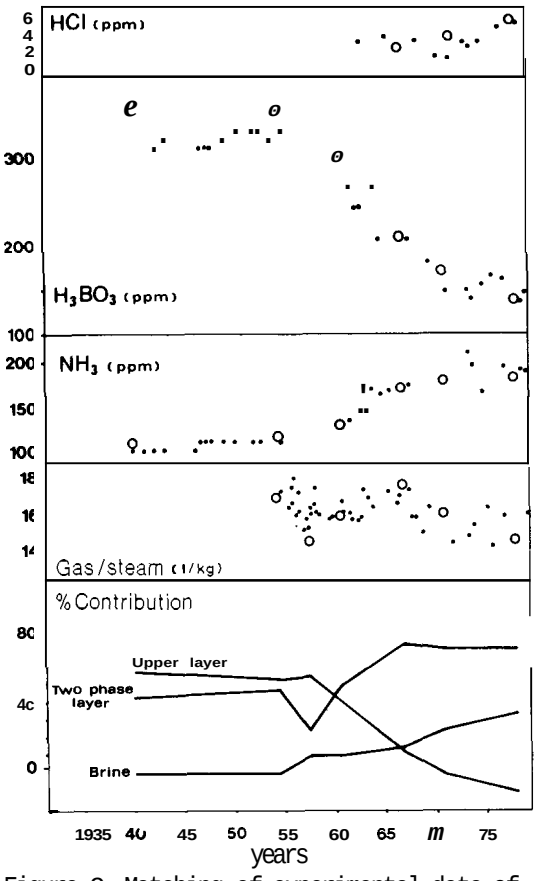

Figure 9 Matching of experimental data of well no.2 with a three-source model, and contribution of the three sources.

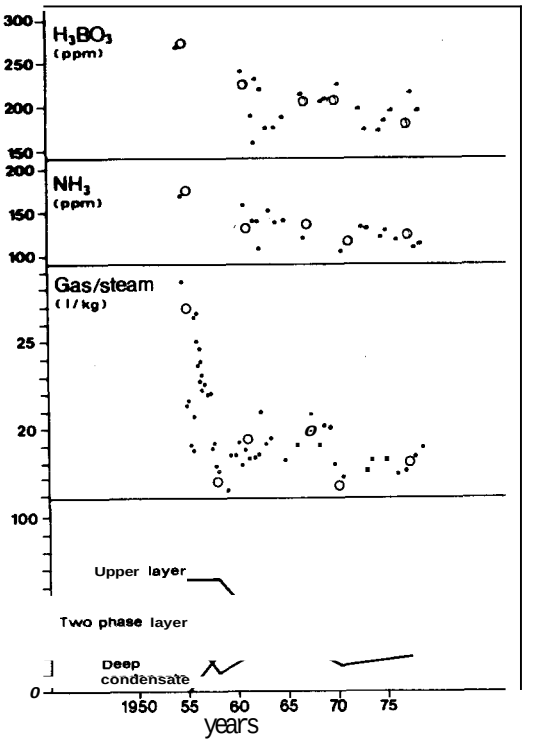

Figure 10 Matching of experimental data of well no.7 with a three-source model and contribution of the three sources.

References

Calore,C.,Celati,R.,D'Amore,F.,Squarci,P. and Truesdell,A.H. (1980),"A Geologic,Hydrologic and Geochemical Model of the Serrazzano Zone of the Larderello Geothermal Field". Proc.6th Workshop Geothermal Reservoir Engineering (H. J.Ramey,Jr. and P.Kruger,Eds.),Stanford,16-18 December,1980, 21-27.

Celati,R.,Noto,P.,Panichi,C.,Squarci,P. and Taffi,L. (1973), "Interactions between the Steam Reservoir and Surrounding Aquifers in the Larderello Geothermal Field".Geothermics, Vol.2-3/4,174-185.

Celati,R.,Neri,G.,Perusini,P. and Squarci,P. (1975), "An Attempt at Correlating kh Distribution with the Geological Structure of Larderello Geothermal Field". Geothermal Reservoir Engineering,Stanford,Geothermal Program, 15-17 December,1975, 37-41.

D'Amore,F.,Celati,R.,Ferrara,G.C. and Panichi, C. (1977),"Secondary Changes in the Chemical and Isotopic Composition of the Geothermal Fluids in Larderello Field",Geothermics,Vol.5, 153-163.

D'Amore,F. and Truesdell,A.H.(1979)"Models for Steam Chemistry at Larderello and The Geysers". Proc.5th Workshop Geothermal Reservoir Engineering,11-14 December,1979,283-297.

Mazor,E. (1978),"Noble Gases in a Section Across the Vapor-dominated Geothermal Field of Larderello,Italy",Pure and Applied Geophysics,Vol. 117,262-275.

Panichi,C.,Celati,R.,Noto,P.,Squarci,P.,Taffi, L. and Tongiorgi,E. (1974),"Oxygen and Hydrogen Isotope Studies of the Larderello (Italy) Geothermal System". In:Isotope Techniques in Groundwater Hydrology,1974,IAEA,Vienna,Vol.2, 3-28.

Truesdell,A.H.,Nehring,N.L. and Frye,G.A. (1977) "Steam Production at The Geysers,California, Comes from Liquid Water Near the Well-bottom". (Abs)Geol.Soc.Am.Abstracts with Programs,Vol.9, 1206.

Truesdell,A.H. and Nehring,N.L. (1978),"Gases and Water Isotopes in a Geochemical Section across the Larderello,Italy,Geothermal Field". PAGEOPH, V01.117, 276-289.

Proceedings Seventh Workshop Geothermal Reservoir Engineering
Stanford, December 1981. SGP-TR-55.

SUMMARY OF HOT DRY ROCK GEOTHERMAL RESERVOIR TESTING 1978 TO 1980

Z. V. Dash and H. D. Murphy (Editors)

Los Alamos National Laboratory
Los Alamos, NM 87544

Abstract Experimental results and re-evaluation of the Phase I Hot Dry Rock Geothermal Energy reservoirs at the Fenton Hill field site are summarized. This report traces reservoir growth as demonstrated during Run Segments 2 through 5 (January 1978 to December 1980). Reservoir growth was caused not only by pressurization and hydraulic fracturing, but also by heat extraction and thermal contraction effects. Reservoir heat-transfer area grew from 8000 to 50 000 m^2 and reservoir fracture volume grew from 11 to 266 m^3. Despite this reservoir growth, the water loss rate increased only 30%, under similar pressure environments. For comparable temperature and pressure conditions, the flow impedance (a measure of the resistance to circulation of water through the reservoir) remained essentially unchanged, and if reproduced in the Phase II reservoir under development, could result in "self pumping." Geochemical and seismic hazards have been nonexistent in the Phase I reservoirs. The produced water is relatively low in total dissolved solids and shows little tendency for corrosion or scaling. The largest microearthquake associated with heat extraction measures less than -1 on the extrapolated Richter scale.

Introduction The HDR reservoirs at Fenton Hill are located in the Jemez Mountains of northern New Mexico. The reservoirs were formed between two wells, GT-2B and EE-1, drilled into hot, low permeability rock and hydraulically fractured. Reservoir performance was first evaluated by a 75-day period of closed-loop operation from January 28 to April 13, 1978 (Tester and Albright, 1979). The assessment of this first reservoir in EE-1 and GT-2B is referred to as "Run Segment 2" or the "75-day test." (Run Segment 1 consisted of a 4-day precursor experiment conducted in September 1977.) Hot water from GT-2B was directed to a water-to-air heat exchanger where the water was cooled to 25°C before reinjection. Makeup water, required to replace downhole losses to the rock surrounding the fracture, was added to the cooled water and pumped down EE-1, and then through the fracture system. Heat was transferred to the circulating water by thermal conduction through the nearly impervious rock adjacent to the fracture surfaces.

Run Segment 3 (Expt. 186), the Hiqh Back-Pressure Flow Experiment (Brown, in preparation) was run during September and October 1978 for 28 days. The purpose of this experiment was to evaluate reservoir flow characteristics at high mean-pressure levels. The hiqh back pressure was induced by throttling the production well. Following Run Segment 3, the EE-1 casing was recemented near its casing bottom to prevent leakaqe of fluid into the annulus. An enlarged reservoir was then formed by extendinq a hydraulic fracture from an initiation depth of 2.93 km (9620 ft) in EE-1, about 200 m deeper than the first fracture in EE-1. The fracturing was conducted in March 1979, with two fracturing experiments. These experiments are referred to as "massive" hydraulic fracturing (MHF) Expts. 203 (March 14) and 195 (March 21). Preliminary evaluation of the new reservoir was accomplished during a 23-day heat-extraction and reservoir-assessment experiment that began October 23, 1979 (Murphy, 1980). This segment of operation with the EE-1/GT-2B well pair was Run Segment 4, or Expt. 215.

The long-term reservoir characterisics were investigated in Run Segment 5, or Expt. 217, which began March 3, 1980 (Zyvoloski, 1981). Because of the large size and resultinq slow thermal drawdown, a lenqthy flow time of 286 days was necessary to evaluate the reservoir. Run Segment 5 ended with the 2-day Stress Unlocking Experiment (SUE) (Murphy, 1981).

In the three years during which these reservoir tests were conducted, our understanding of reservoir behavior has steadily improved. Simplified models that were developed for Run Segment 2 were significantly modified by the time of Run Segment 5. Consequently, the previous tests were reanalysed in a consistent manner using the latest models. Further, the growth of the reservoir with time was traced and periods of growth attributed to thermal contraction and heat extraction effects were identified as apposed to qrowth caused by pressurization and hydraulic fracturing.

Heat Production and Heat-transfer Modeling Heat-transfer modeling of the reservoirs has been performed with two numerical models. Both models use two-dimensional simulators in

which heat is transported by conduction within the rock to the fractures. The most recently developed model (the multiple-fracture model) assumes that the reservoir consists of three parallel fractures idealized as rectangles in which the flow is distributed uniformly along the bottom of each fracture and withdrawn uniformly across the top. The flow is thus one-dimensional, and the streamlines are straight vertical lines. Consequently fluid dynamic considerations do not directly enter into the heat-extraction process, the sweep efficiency is implicitly assumed to be 100%. However, a rigorous two-dimensional heat-conduction solution is incorporated for the rock between the fractures, and this permits valid consideration of thermal-interaction effects between the fractures. In contrast, the older model (the independent-fractures model), assumes that the fractures (two in number) are circular and allows proper local positioning of the inlet and outlets, i.e., the point-like intersection of the injection well with the fracture can be modeled, as can the intersection of the main hydraulic fractures and the slanting joints that provide the connections to GT-2B. However, as was cautioned earlier, while the fluid dynamic effects of the joints/outlets can be faithfully modeled, the heat-transfer effect of the joints cannot; the area of the joints must be lumped with the main fractures. In view of this more faithful representation of inlet and outlets, and the fact that a complete two-dimensional solution to the Navier-Stokes fluid dynamic equations is incorporated, the independent-fractures model results in a more realistic assessment of the effect of fluid dynamics and sweep efficiencies upon heat extraction. The penalty, however, is that in the present two-dimensional version of the code, thermal interaction as the temperature waves in the rock between fractures overlap cannot be realistically represented, as it is with the multiple-fracture model.

Independent-Fractures Modeling The first application of this model was to the earlv research reservoir, when only a small single hydraulic fracture existed. This reservoir was tested extensively during Run Segment 2. Based upon spinner and temperature surveys in the production well, the depths of the intersections of the production well with the slanting joints were estimated as well as the flow rates communicated by each joint. In the calculations, the actual temporal variations of production and injection flow rates were utilized. With this information, estimates of the thermal drawdown were calculated with the model for various trial values of fracture radii and vertical position of the fracture inlet. A fracture radius of 60 m with an inlet located 25 m above the fracture bottom resulted in a good fit to the measurements. A radius of 60 m implies a total fracture area (on one side) of 11 000 m^2; however, because of hydrodynamic flow sweep inefficiencies the net area effective in heat exchange was only 8000 m.

During Run Segment 3 (the high back-pressure experiment) thermal drawdown suqgested that, according to the independent-fractures model, the effective heat area was nearly the same. However, flow rate (spinner) surveys in GT-2 indicated that because of the higher pressure level most of the flow was entering GT-2B at positions that averaged 25 m deeper than during Run Segment 2. In effect the reservoir flow paths were shortened about 25%. It was concluded that while pressurization did indeed result in partial short circuiting of the streamlines, it also resulted in a notable decrease in impedance, which afforded better fluid sweep and bathing of the remaining area. The reservoir was enlarged during the fracturing operations of 1979, the MHF Expts. 195 and 203. For the independent-fractures model the enlarged reservoir is portrayed as two fractures, the old one operative in Run Segments 2 and 3, with a new and larger one. The enlarqed reservoir was evaluated during Run Segment 4 and Run Segment 5. To summarize the Run Segment 4 studies, it was found that the old fracture had an effective heat-transfer area of 15 000 m^2 and the new fracture had an effective area of at least 30 000^2 m . The area determined in Run Segment 4 for the old fracture was at least twice that determined in Run Segment 2. This trend of increasing area is now attributed to thermal stress cracking effects (Murphy, 1979).

Better estimates of the total effective heat-transfer area of both fractures were obtained in Run Segment 5, during which the thermal drawdown was only 8°C. The mean outlet temperature actually increased slightly during the early portion of Run Seqment 5. This temporary increase is due to transport of deeper, hotter water to the production well, as well as to some interaction of the fractures. For simplicity the effect was neglected in the independent-fractures model as it is fairly small, less than 2°C. The data are fit very well by a model with a combined area of 50 000 m^2, some 5000 m greater than the area tentatively estimated during Run Segment 4.

A summary of the heat-exchange areas determined with the independent-fractures model is presented in Fig. 1. As can be seen, a steady increase, from 8000 to 50 000 m^2, is indicated. As indicated by the question marks in Fig. 1, the area increase due to the MHF experiments (195 and 203), is uncertain. The heat-transfer area was not measured until the later stages of Run Segment 4. Consequently, the area increase measured is due to the combined effects of all the fracturing and Run Segment 4 operations, and cannot be individually ascribed to the separate operations.

Multiple-Fracture Modeling For the multiple-fracture model the following procedure was used to fit the data.

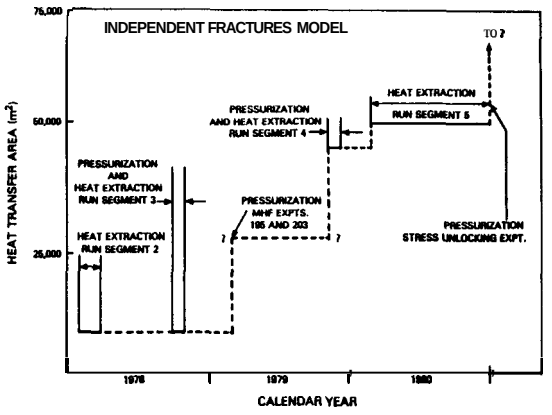

Figure 1 Heat transfer area growth determined by the independent fractures model in the Phase I reservoirs during Run Segments 2 through 5

- o The measured GT-2B flow rate and estimated reservoir inlet temperature were programmed as functions of time.
- o The initial fracture area was adjusted to obtain the best fit at early times.
- The fracture area was allowed to increase so as to provide a good fit to the remaining data. For computational simplicity, the area increase was assumed to occur in discrete steps rather than in a smooth, piece-wise linear, fashion.

As indicated earlier, the independent-fractures model was not able to detect any increase in the effective heat-transfer area during actual drawdown, but the multiple fracture model indicates that the heat-transfer area increased by a factor of two.

Similar modeling was carried out for Run Segments 3, 4 and 5. Figure 2 summarizes the growth of the heat-exchange area, according to the multiple-fractures model, throughout Phase I. The general similarity with the summary of the independent-fractures model, Fig. 1, is noted, but there are differences in detail.

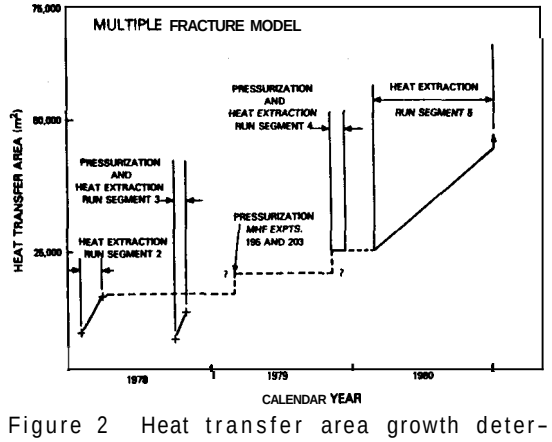

Figure 2 Heat transfer area growth determined by model fits to drawdown data and wellbore temperature logs in the Phase I reservoirs during Run Segments 2 through 5

The initial area of 7500 m^2 was established by many pressurizations and some cooling. This area grew to 15 000 m^2 in Run Segment 2. As indicated earlier the high back pressure of Run Segment 3 caused a redistribution of flow resulting in fluid dynamic short-circuiting. However, unlike the independent-fractures model, the new model indicates that the initial heat-exchange area was actually less than that of Run Segment 2, starting at 6000 m^2; but it then grew to 12 000 m^2 during the 28-day test. The system was pressurized to high pressures several times during MHF Expts. 203 and 195 and Run Segment 4 but no area or volume measurements were made until Run Segment 4. After Run Segment 4, the EE-1 temperature logs indicated that between 6000 and 9000 m^2 had been added to the lower part of the reservoir by the recementing and pressurization prior to and during Run Segment 4. This increased the measured heat-exchange area to between 21 000 and 24 000 m^2. The area measurements during Run Segment 5 are somewhat uncertain. The best estimates are that the heat-exchange area was greater than 45 000 m^2 at the end of the experiment. The lack of recovery of the outlet temperature indicates that the additional area is in the depleted upper half of the reservoir or was partly added to the lower half as Run Segment 5 proceeded.

Tracer Studies and Fracture Volume Growth The main objectives of reservoir tracer studies are to assess the volume changes associated with the creation of the Phase I system and to determine dynamic behavior of the system volume as the system undergoes long-term heat extraction. The fracture modal volume is simply the volume of fluid produced at GT-2B between the time the tracer pulse was injected and the time the peak tracer concentration appeared in the produced fluid. The wellbore volumes are subtracted from the total volume produced to give the true fracture modal volumes. The modal volume is considered the most reliable indicator of reservoir volume change. Large changes in the modal volume are observed after the hydraulic fracturing of the system between Run Segments 3 and 4 and during the SUE, which followed Run Segment 5.

A complete review of the tracer-test data from Segments 2 through 5 has revealed pertinent information regarding the growth of the reservoir due to heat extraction and pressurization effects. The reservoir growth due to heat extraction is, to be precise, really a thermal-contraction effect -- as the rock surrounding the fractures shrinks, the fractures, and consequently, the measured volumes, expand. In spite of nonlinear coupled effects of thermal contraction, pore and fracture inflation due to sustained pressurization, and local irreversibilities resulting in fracture propagation, a simple correlation between ΔV and ΔE exists. Furthermore, this simple relationship persists even in the presence of the confining stresses surrounding the active reservoir,

which induce a constrained behavior. For practical purposes, the region between the low-pressure data and the free thermal volume 1ines defines an envelope of reservoir operating conditions. As stresses are relieved, for example during SUE, or the high back-pressure test of the original reservoir (Run Segment 3), or the high-pressure, hydraulic-fracturing stage at the beginning of Run Segment 4, one moves away from the normally constrained condition toward the free thermal expansion line.

Perhaps the most promising aspect of the tracer tests is their potential for estimating the effective heat-transfer surface area of a reservoir. This becomes clear when the modal volume (plotted vs time in Fig. 3) is compared to the corresponding heat-transfer area (plotted vs time in Figs. 1 and 2); the similarities of the growth of area and volume are quite striking. This can be quantified by considering the relationships between area, volume, and aperture (or effective fracture opening). The volume, V, is simply the product of the area, A, and the mean aperture, w: $V = A \cdot w$. During heat extraction and/or pressurization, the area and aperture can both vary; therefore the volume is a function of two variables rather than one. For constant aperture, the tracer volumes should scale directly with heat-transfer area. Further development of this empirical correlation could provide a direct and independent method of determining reservoir heat-transfer area without requiring thermal drawdown, which is time consuming and expensive to obtain, particularly so for the larger Phase II reservoir under development.

Impedance Characteristics The impedance of a circulating geothermal reservoir is usually defined as the pressure drop between the inlet and outlet of the fracture caused by flow in the fracture, divided by the exit volumetric flow rate. Its units are pressure-s/volume, and in this report we typically use Giga Pascals per cubic meter per second (GPa s/m^3) or in English customary units, pounds per square inch per gallon per minute (psi/gpm). Because pressures are usually measured at the surface, a "buoyancy" correction should be made for the difference in hydrostatic pressures in the hot production well and the cold injection well. The depth at which this correction is calculated corresponds to the bottom of the injection well, that is, buoyancy inside the fracture is included in the hot leg. Impedances of about 1 GPa s/m^3 are considered desirable. For example, in the deeper and hotter Phase II reservoir being completed now, such a low value of impedance could actually result in "self-pumping" of the reservoir because of buoyancy effects.

Figure 4 summarizes the impedance history over Segments 2 through 5 and the SUE experiment. Impedance is dependent on fracture aperture, w. Theoretically, it decreases as $1/w^3$ in both laminar and turbulent flow. Aperture may be increased in several ways: (1) by pressurization of the fracture, (2) cooling of the surrounding rock, (3) dissolution of minerals lining the crack by chemical treatment of the fluid, and (4) by geometric changes resulting from relative displacement of one fracture face with respect to the other. Run Segments 2 and 3 were especially useful in demonstrating the correlation between impedance and pressure and temperature. The impedance changes observed after SUE were probably due to additional "self-propping" caused by slippage along the fracture faces near the exit or by other pressure-induced geometric changes.

The concentration of impedance near the exit, shown in all the low back-pressure flow experiments, may be desirable when the system impedance is reduced by multiple fractures. In this mode of reservoir development, the possibility of unstable "runaway" (one fracture cooling and taking much of the flow) exists, and the exit impedance concentration will prevent this until reservoir cooling has been extensive. Eventually, the problem of flow control in the individual fractures may arise,

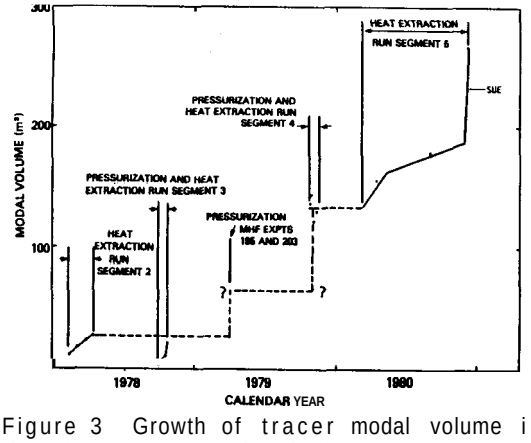

Figure 3 Growth of tracer modal volume in the Phase I reservoirs during Run Segments 2 throuqh 5

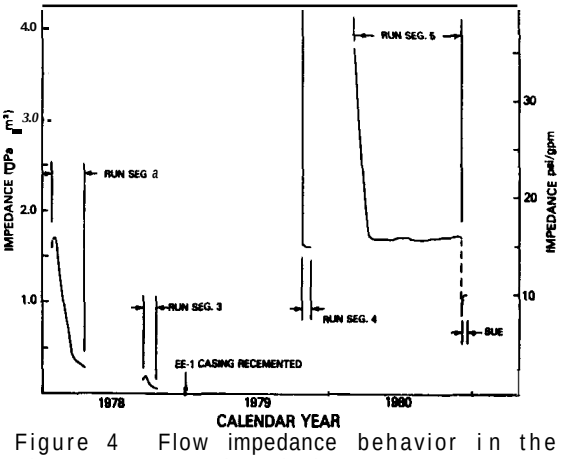

Figure 4 Flow impedance behavior in the Phase I reservoirs during Run Segments 2 through 5

and methods of flow control near the fracture entrance may be required.

During normal, low back-pressure conditions fracture impedance appears to be concentrated near the exit well, at least after a short period of operation, and total impedance does not depend strongly on wellbore separation. Impedances are sufficiently low to allow operation of efficient HDR geothermal energy-extraction systems. The impedance in a large system does not change rapidly, and the prognosis for operation of the multiple-fracture, Phase II system seems favorable.

Water Losses The water loss of an HDR system is very important because this water must be provided from some outside source. This information can be vital for environmental as well as economic reasons. The water-loss rate, that is, the rate at which water permeates the rock formation surrounding the fracture system, is the difference between the injection rate and the produced, or recovered, rate at GT-2B. This loss rate is a strong function of system pressures and flow rate and would also be expected to be a function of reservoir size.

The water-loss flow-rate data of each experiment contain many transients due to operation shutdowns, pump limitations, and various leaks. Consequently, the accumulative volume of water loss is best suited for comparisons since many of the transients are smoothed out, and this comparison is presented in Figure 5, for Run Segments 2, 3, and 5. Run Segment 4, only 23 days long, was excluded from this comparison because of the disparate conditions under which it was conducted.

Comparisons between Run Segments 2 and 5, both conducted under normal, low back-pressure conditions, can be made as follows. Direct comparisons indicate that the water loss for Run Segment 5 is approximately 40% higher than that of Run Segment 2 at comparable times after the beginning of heat extraction. However, because the operating pressure was 10% higher during Run Segment 5, the water

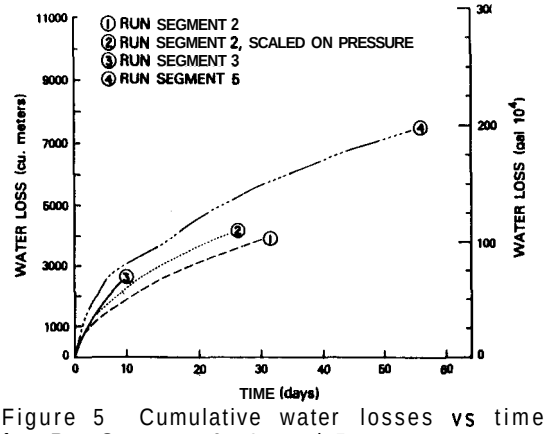

Figure 5 Cumulative water losses vs time for Run Segments 2, 3, and 5

loss for Run Segment 2 should be scaled up by 10% as in curve 2 of the figure, in order to be directly comparable to Run Segment 5. Then it is seen that the Run Segment 5 water loss is only 30% higher than Run Segment 2, despite a several-fold increase in heat-transfer area and volume. An obvious conclusion is that the heat-exchange system utilizes only a small portion of a much larger fracture system that controls water loss. This large, potential fracture system was not altered to any large extent by the MHF experiments of Segment 4. Furthermore, in comparison to the heat-transfer areas, these other areas did not grow siqnificantly from Run Segments 2 throuqh 5.

Fluid Geochemistry Analysis of the fluid-chemistry data from the Phase I reservoirs shows several interesting features that are pertinent to the size of the reservoirs. Strong evidence from each of the Phase I heat-extraction experiments indicates the existence of essentially two parallel flow paths: (1) a fracture-dominated flow path (perhaps consisting of multiple fractures) that includes the heat-transfer surfaces, and (2) a high-impedance flow path consisting of the connected microfractures and pores in the rock surrounding the heat-extraction portion of the reservoir. Displacement of the indigenous pore fluid contained in this high-impedance flow path is the single most important geochemical effect observed in the heat-extraction experiments to date. This is discussed further by Grigsby et al. (1981).

In summary, several conclusions should be drawn from geochemistry results to date. First of all, the overall circulating fluid quality in a HDR system is largely fixed by the pore-fluid concentration and displacement rate. Under the very worst conditions (that is, 100% of the produced fluid is pore fluid) the maximum concentration of dissolved solids would be around 5000 mg/ℓ for this reservoir -- within the Environmental Protection Agency (EPA) water quality standard for continuous irrigation of salt-tolerant plants. However, the steady-state concentration of total dissolved solids is typically 2500 mg/ℓ -- similar to water used for human consumption in many parts of the country. The pH of the water is 6.5 ± 0.5, nearly neutral, and problems with corrosion or deposition upon surface equipment such as piping, heat exchangers, and pumps have been minimal.

A second conclusion from the fluid-geochemistry studies concerns the very large volume of pore fluid that has been displaced from the rock surrounding the fracture system into the fracture system. Because this fracture system is everywhere pressurized above hydrostatic pressure, circulating fluid should be continuously lost to the surrounding matrix, which is subhydrostatic. Porefluid from this subhydrostatic pressure field would have to flow against a pressure gradient in order

to enter the flowing system. However, secondary flow paths with impedance intermediate to that of the main fracture system and that of the unfractured reservoir rock provide a means for the pressure level in the main fracture(s) to displace the pore fluid into the flow system. Finally, the flow from these secondary paths appears to be partially sensitive to the pressure difference between the inlet and outlet and probably, to the overall level of pressurization of the reservoir.

Seismicity Seismic monitoring was conducted for all the run segments with a surface seismic array and during portions of Run Segments 4 and 5, and SUE, with downhole geophone packages positioned in the reservoir vicinity. The objective of this monitoring was to evaluate potential seismic risks associated with HDR geothermal energy extraction. The largest event detected in Run Segment 4 with the downhole package had a magnitude of -1.5. The energy release of a -1.5 magnitude microseismic event is roughly equivalent to that of a 10 kg mass dropped 3 m. Furthermore, this event occurred during the high back-pressure stage. During the low back-pressure stage, more typical of ordinary heat-extraction conditions, the largest event was -3. During the 286-day Run Seqment 5, 13 microearthquakes ranging between -1.5 and 0.5 were recorded by the surface seismic array. These events were located about 200 m north of EE-2 at a depth of about 1 km. The events are not related to Run Segment 5 activities, but rather to the drilling of EE-2 and EE-3.

Conclusions The reservoirs of the Phase I HDR geothermal energy system have exhibited growth through all segments of operation. This growth resulted from pressurization, cooling (thermal contraction), and fracture-face displacement or movement. During the early time experiments (Run Segments 2 and 3) thermal drawdown was significant due to the small size of the reservoir involved (90°C for Segment 2 and 37°C for Segment 3). In the later experiments, drawdown was much less significant due to the larger reservoir. No drawdown was observed during Segment 4, and during Segment 5 operations, the reservoir sustained only an 8°C thermal drawdown after 286 days. Modeling of the Phase I reservoirs led to an estimated heat-transfer area of 8000 m^2 for Run Segment 2, while by the end of Run Segment 5 the heat-transfer area was estimated to be 45 000 to 50 000 m^2, about six times larger. Measured tracer volumes suggested a fracture area of 80 000 m^2 by the end of Segment 5. Modal volume of the reservoir has grown from 11 to 266 m^3 through the course of Phase I experiments.

Water losses were very encouraging because, for comparable operating pressure conditions, only a 30% increase of water loss was observed for a sixfold increase in heat-transfer area. The impedance remained constant throughout Run Segment 5 at about 1.6 GPa s/m^3. This is in contrast with the Run Segment 2 reservoir that exhibited a sharp decline in the impedance, presumably due to the large thermal drawdown that the system experienced. Geochemical monitoring of the system provided valuable insight concerning pore-fluid displacement and flow connections in the reservoir. The concentrations of dissolved chemicals in the produced water were relatively low and the pH was near neutral, so the produced water was of good quality and problems with corrosion or scaling of surface equipment have been minimal. Seismic activity in the Phase I reservoirs has been insignificant. Events associated with heat extraction have measured less than minus one on the extrapolated Richter scale,

Acknowledgments This work was supported by the Division of Geothermal Energy, U.S. Department of Energy. The contributions of R. L. Aamodt, R. G. Aguilar, D. W. Brown, D. A. Counce, H. N. Fisher, C. O. Grigsby, H. Keppler, A. W. Laughlin, R. M. Potter, J. W. Tester, P. E. Trujillo, Jr., and G. A. Zyvoloski to this summary report are gratefully acknowledged.

References

Brown, D. W. (ed.), "Results of Expt. 186, The High Back-Pressure Flow Experiment," Los Alamos National Laboratory report LA-8941-HDR (to be published).

Grigsby, C. O., J. W. Tester, P. E. Trujillo, D. A. Counce, J. Abbott, C. E. Holley, and L. A. Blatz, "Rock-Water Interactions in Hot Dry Rock Geothermal Systems: Field Investigations of In Situ Geochemical Behavior," submitted to J. of Volcanol. and Geotherm. Res., 1981.

Murphy, H. D. "Thermal Stress Cracking and the Enhancement of Heat Extraction from Fractured Geothermal Reservoirs," Geothermal Energy 7, 22-29 (1979).

Murphy, H. D. (ed.), "Preliminary Evaluation of the Second Hot Dry Rock Geothermal Energy Reservoir: Results of Phase 1, Run Segment 4," Los Alamos Scientific Laboratory report LA-8354-MS (May 1980).

Murphy, H. D. (ed.), "Relaxation of Geothermal Stresses Induced by Heat Production," Los Alamos National Laboratory report LA-8954-MS (August 1981).

Tester, J. W. and J. N. Albright (eds.), "Hot Dry Rock Energy Extraction Field Test: 75 Days of Operation of a Prototype Reservoir at Fenton Hill," Los Alamos Scientific Laboratory report LA-7771-MS (April 1979).

Zyvoloski, G. (ed.), "Evaluation of the Second Hot Dry Rock Geothermal Energy Reservoir: Result of Phase I, Run Segment 5," Los Alamos National Laboratory report LA-8940-HDR (August 1981).

Proceedings Seventh Workshop Geothermal Reservoir Engineering
Stanford. December 1981. SGP-TR-55.

DISPERSION IN TRACER FLOW IN FRACTURED GEOTHERMAL SYSTEMS

Roland N. Horne
Fernando Rodriguez

Dept. of Petroleum Enginering
Stanford University
Stanford, CA 94305

Abstract Recent field experiments in Japan have emphasized the importance of performing tracer tests in any geothermal utilization in which reinjection is in use or is planned. This is because rapid short-circuiting between reinjection and production wells may occur due to the fractured nature of the system. In cases where fracturing is such that preferred pathways exist in the reservoir, the result may be a rapid thermal drawdown of the field production. Tracer testing provides a method of evaluating the magnitude of such problems. Previous methods used to analyze the Onuma, Hatchobaru, and Otake tracer tests have used early and long time data, this paper discusses the use of the field concentration/time profile in fractured systems, and the likely forms of dispersion likely to dominate in the process.

Introduction Reinjection of waste hot water is practiced in many liquid-dominated geothermal fields (namely Ahuachapan, Otake, Onuma, Kakkonda, Onikobe, Hatchobaru, Mak-Ban, East Mesa, Brawley, and Raft River). The fundamental purpose of reinjection is to dispose of the unused hot water, although it has often been suggested that the reservoir productivity may be increased concurrently. In fact there has been only scant evidence to show support of reservoir performance by reinjection (see Horne 1981), and in fact in some cases it has been seen to be detrimental to production due to early invasion of the cooler injected water through high permeability paths in the reservoir. Furthermore, observations on the effects of reinjection have emphasized the need to pay close attention to the fractured nature of geothermal reservoirs.

The benevolence or malevolence of reinjection in geothermal reservoirs has been seen to be closely related to the degree of fracturing. The degree of fracturing has been most successfully determined by using tracer tests. For example, tracer tests summarized in Horne (1981) indicated a high degree of fracturing in Wairakei, Kakkonda, and Hatchobaru, a moderate or mixed degree in Onuma and Ahuachapan, and a low degree in Otake. In view of the subsequent experience in reinjection it was concluded that understanding the fracture system through the use of tracers should be the first step in designing a reinjection program. Unfortunately however, the methods of analysis appropriate to tracer flow in fractured systems are not yet fully developed, most surveys to date having used only the early time (or in one instance the late time) data. A method of analyzing the full tracer return profile is demonstrated in this work, and a discussion offered on the form of the appropriate transfer function.

Existing Tracer Analysis Methods The classic petroleum reservoir methods for analysis of tracer tests have commonly been based on uniform "sweep" flow through a porous medium in a given configuration (usually a 5-spot) - see for example Brigham and Smith (1965), Baldwin (1966) and Wagner (1977). In these analyses the system is modelled as a "stack" of non-connecting layers of porous media which are uniform but which nevertheless have differing properties. The tracer "breaks through" different layers at different times, giving rise to the characteristic multiple hump return illustrated in Figure 1. Geothermal systems however show very different returns because of the limitation of flow to fractures and commonly show a single hump return as in Figure 2. The absence of more than one strong tracer return itself emphasizes the highly fractured nature of geothermal reservoirs. It is clearly inappropriate to use the uniform sweep model of the petroleum industry in such instances.

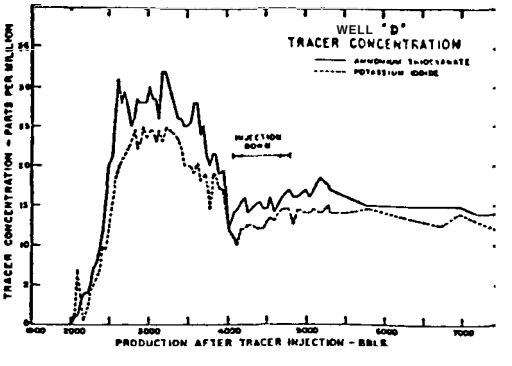

Figure 1: Multiple breakthrough tracer return - from Brigham & Smith (1965)

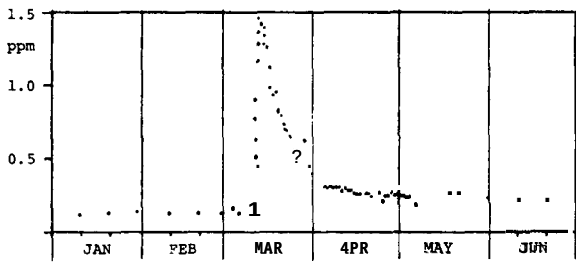

Figure 2: Onuma geothermal tracer test - from Ito, Kubota & Kurosawa (1978)

Without resorting to a flow model there are two important items of informatin which can be derived from a tracer test. The first is simply the speed of first return between an injector and permeability connection between the two. A "connectivity" map of the reservoir can be drawn from such results. The second item is the long term dilution of tracer in a test in which the produced tracer is recycled (as is often the case in an operational system). This long term dilution has been used by Ito, Kubota, and Kurosawa (1978) to estimate the volume of fluid circulating through the system at Onuma field.

These two calculations involve the use of only the early and late measurements in the test. In the petroleum literature, Brigham and Smith (1965) demonstrated a method of "matching" the intermediate time tracer return concentration, essentially by a trial and error apaproach. Their analysis was based on a model of the reservoir as a series of non-connecting layers with different permeabilities which gave rise to separate "peaks' in tracer return. Yuen, Brigham, and Cinco (1979) later extended the method of analysis to calculate the permeabilities of various layers by matching the concentrations at the various peaks with the analytical solution. Both of these studies considered a 5-spot configuration, however the methodology would be applicable to other configurations. Despite the considerable extra information that this "intermediate time" analysis can provide, it still essentially uses only data at the peaks of the response curve. Also, the analysis is based on a layer model that may hold for hydrocarbon reservoirs, but which would be inappropriate for most geothermal systems.

Features of Geothermal Tracer Tests Geothermal reservoirs are usually very highly fractured. As a result, and as an indication of this fact, the tracer response almost always shows just a single peak. Thus, although the early and late time analyses are still possible, the analysis of the single peak concentration would provide little extra information, and does in any case require the formulation of a flow model. Thus, there exists a need to formulate a means of analyzing the shape of the single humped tracer response with specific reference to flow in fractures. An attempt to isolate the features of tracer transport in fractures is reported here.

Tracer Transport in Fractures Methods of signal analysis are readily applicable to the interpretation of tracer return concentration histories, reducing the observed profile to the sum of its component signals. For example, the tracer concentration in a producing well that receives flow from an injection well through two intervening fractures will demonstrate the superposed transfer function corresponding to tracer flow through those two fractures. The difficulty in decoupling the response into its component parts depends on defining the features of those component parts. For example, tester, Bivins, and Potter (1979) describe a method to represent the tracer concentration C at a production point in terms of M independent components, thus:

$$C = \sum_{j=1}^{M} \xi_j C_j (X_m, \theta_j, Pej) \qquad (1)$$

where ξ_j is the fraction of flow in "path"; and non-dimensional distance and time are defined by:

$$X_j = \frac{x_j}{L_j} \qquad (2)$$

$$\theta_j = \frac{q_j t}{V_j} \qquad (3)$$

where x_j, L_j, q_j and V_j are the position within, length of, flow rate through and volume of the j-th "path" through the system. Pe_j represents the Peclet number of flow through the j-th path, defined as:

$$Pe_j = \frac{u_j L_j}{\eta_j} \qquad (4)$$

where η_j is the diffusivity (or dispersion coefficient) of tracer during transport.

Tester, Bivins, and Potter (1979) proposed the analysis of N measured values of exit tracer concentration C_i by minimizing the objective function F, where:

$$F = \sum_{i=1}^{N} (C - C_i^*)^2 \qquad (5)$$

and C is given by equation (1). Decision variables will be Pe_j, q_j, and V_j.

This method can straightforwardly provide estimates of the Peclet numbers associated with the various flow paths, and their relative (but not absolute) rates of flaw and relative (but not absolute) values. It does however depend strongly upon the transfer function $C_j(X_j, \ _j, Pe_j)$ assumed in equation (1) for the transport of the tracer. Brigham and Smith (1965) based their determination of the transfer function on flow through a porous medium between wells in a five spot formation. Tester, Bivins, and Potter (1979) determined transfer function for one- and two-dimensional flow through porous media.

Convective Dispersion in Fracture Flow These two studies do not, however, correctly represent the flow through a fracture in that a tracer front is modelled as propagating perpendicularly to the direction of flow. In a fracture, however, in either laminar or turbulent flow, the fluid will be transported faster in the center of the fracture than on the walls (in fact, due to boundary layer effects, it will not be transported along the walls at all). This is illustrated in Figure 3.

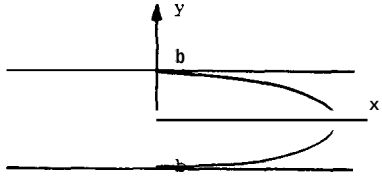

Figure 3: Fracture flow configuration

The profile across the span of the fracture for laminar flow is given by:

$$u(y) = -6\frac{U}{b^2}\left(y^2 - b^2\right) \qquad (6)$$

where U is the average velocity and b is the half-width of the crack. Equation (6) is the well known parabolic velocity distribution and gives rise to a maximum velocity at the center of the crack (at y=0) of 3/2 U.

Now, if a continuous slug of tracer were to be injected at time t=0, the distance x moved by the tracer front, assuming no dispersion, will be given by:

$$x(y) = u(y)t \qquad (7)$$

and thus the tracer will have "arrived" at x over a range of y given by the equation:

$$-6\frac{U}{b^2}\left(y^2 - b^2\right) = \frac{x}{t} \qquad (8)$$

the solution of which is:

$$y = \pm\sqrt{b^2 - \frac{3b^2}{2U}\frac{x}{t}} \qquad (9)$$

The mean concentration at point x is then given by:

$$c = \frac{y}{b} \qquad (10)$$

$$\text{or} \quad c = \sqrt{1 - \frac{t^*}{t}} \quad \text{for } t > t^* \qquad (11)$$

where t^* is the first arrival time of tracer and is given by:

$$t^* = \frac{2}{3}\frac{x}{u} \qquad (12)$$

In a practical case, of course, the tracer would not be injected continuously nor would it be injected at a concentration of 100%. Equation (11) may however be used to superpose the behavior of the leading edge and trailing edge of a tracer slug of initial concentration C_o, after which:

$$C = C_o\left[\frac{H(t - t^*)\sqrt{1 - \frac{t^*}{t}} - H(t - \Delta t - t^*)}{\sqrt{1 - \frac{t^*}{t - \Delta t}}}\right] \qquad (13)$$

where H(x) is the Heaviside step function:

$$H(x) = \begin{cases} 1, & x > 0 \\ 0, & x < 0 \end{cases} \qquad (14)$$

and t is the length of time the tracer is injected.

Figure 4 shows the normalized tracer return concentration C/C_o as a function of normalized time t/t^* for various values of injection time t/t^*. The similarity between Figures 4 and 2 should be noted.

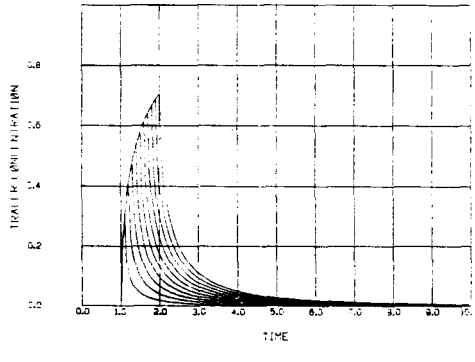

Figure 4: t/t^* 0.1 to 1.0, increments of 0.1

The end result of this non-uniform "convective" displacement of the tracer slug's leading and trailing edges is a dispersion of the tracer slug over the entire distance between the injection point and the

observation point. This smearing of the slug may be termed the "convective dispersion" of the tracer, although it must be remembered that the effect is literally to disperse the tracer and not to diffuse it. The "dispersivity" of this process may not be determined in the common sense of the term, however a qualitative impression of its order of magnitude may be estimated. Comparing Equation (13) with the solution for a purely dispersive transport:

$$C = C_o \left\{ \operatorname{erfc} \frac{L}{2\sqrt{\eta t}} - \operatorname{erfc} \frac{L}{2\sqrt{\eta (t+\Delta t)}} \right\} \qquad (15)$$

it is seen that, since the error function is roughly linear over its early range, there is a rough correspondence between the reciprocal square root of time terms in the two equations. Thus it may be observed that $4/L^2$ behaves like $1/t^*$ which is itself $1.5U/L$. The effective dispersivity of the convection process is therefore like:

$$\eta_{eff} = \frac{3}{8} UL \qquad (16)$$

and the effective Peclet number is always of order 8/3.

Taylor Dispersion in Fracture Flow Even thouqh molecular diffusion in the axial direction is several orders of magnitude smaller than all other effects (typically the Peclet number for molecular diffusion may be 10^{-9} compared to the value 8/3 determined for convective dispersion), the convective smearing of the tracer gives rise to large concentration gradients across the narrow width of the fracture. With this large concentration gradient molecular diffusion tends to rapidly equalise the tracer concentration across the fracture, thus counteracting the effect of convective dispersion. Figure 5 shows the molecular diffusion of a tracer slug across the width of a cavity.

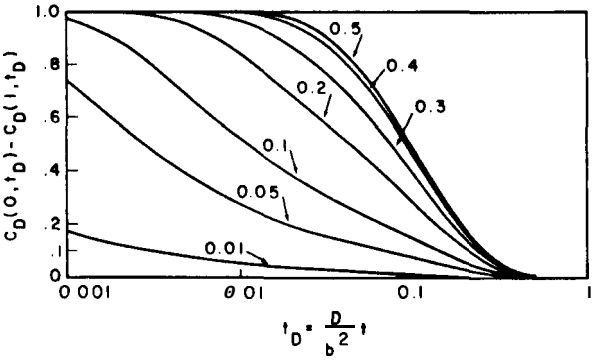

Figure 5: Concentration difference between wall and centerline as a function of time and initial tracer penetration across the fracture

For initial slug widths ranging from 0.01 to 0.5 of the total cavity width, the difference between the centerline and wall concentrations of tracer reduces effectively to zero within a dimensionless time t_D of 0.5 in every case. The molecular diffusivity D may be of order 10^{-5} cm^2/sec and the fracture half-width b may be of order 0.5 mm, suggesting that the transverse diffusion will equalise any concentration differences within 125 seconds (during which time the tracer slug could be considered to move no further than 40 cm). Clearly this transverse diffusion will rapidly overcome the convective dispersion in a field case.

This combination of transverse diffusion and convective dispersion is known as "Taylor Dispersion" and was described for pipe flow by Taylor (1953). The net result of Taylor dispersion is that the tracer front propogates with the mean speed of the flow in spite of the fact that the fastest moving fluid in the center of the channel moves at twice the speed in the case of pipe flow, or 3/2 times the speed in the case of fracture flow. The net longitudinal dispersion was determined by Taylor for pipe flow, and was derived during this investiqation for fracture flow to be:

$$\eta = \frac{2}{105} \frac{b^2 U^2}{D} \qquad (17)$$

It should be noted that the Taylor dispersivity is inversely proportional to the molecular diffusivity, hence net dispersion is greater when molecular diffusion is smaller. This analysis cannot be extrapolated to zero molecular diffusivity because of assumptions made in the derivation, however the maximum dispersivity in that case would be that determined in Equation (16).

With a mean flow speed of 3 cm/sec and a fracture width of 1 mm, a typical value of the dispersivity would be 40 cm^2/sec. For a 100 m long fracture this would give rise to a Peclet number of order 1000.

Turbulence Turbulence would tend to increase the rate of tracer diffusion across the fracture and would thus decrease the total effective dispersivity and increase the Peclet number.

Discussion Various dispersion mechanisms have been discussed. Comparing their individual relevance to the field problem of flow through fractures it is seen that: (1) Longitudinal molecular diffusion is insignificant, (2) Taylor dispersion will dominate over convective dispersion, (3) Turbulence will reinforce the effects of Taylor dispersion, (4) The Peclet number for one-dimensional flaw will therefore typically be greater than 1000.

In actual fact, field studies on the fracture system at Los Alamos (Tester, Bivins and Potter, 1979) indicated values of the calculated Peclet numbers of order 2. The further reduction in total transfer Peclet number is due to the fact that the tracer spreads in two or three dimensions away from the injection point and converges again towards the production point, thus being further dispersed. The single field result from Los Alamos suggests that this multi-dimensional dispersion effect is in fact at least 3 orders of magnitude greater than the simple one-dimensional dispersion mechanisms. This conclusion is being tested in this continuing study by calculation of typical flow configurations. However the principal and somewhat unsatisfying conclusion of this work so far is that the tracer return is dominantly determined by the large scale flow configuration.

Acknowledgement This work forms part of the cooperative qeothermai program between Stanford University and Instituto de Investigaciones Electricidad, Mexico. Funding for Stanford University's participation in this work was provided by the U.S. Department of Energy under contract number DE-AT-03-80SF11459.

References

Baldwin, D. E., Jr.: "Prediction of Tracer Performance in a Five-Spot Pattern," J. Pet. Tech. (Apr. 1966), 513.

Brigham, W. E., and Smith, D. H.: "Prediction of Tracer Behavior in Five-Spot Flow," paper SPE 1130 presented at the SPE-AIME 40th Annual Fall Meeting, Denver, Colorado, Oct. 1965.

Horne, R. N.: "Geothermal Reinjection Experience in Japan," paper SPE 9925 presented at the 1981 California Regional Meeting of SPSE, Bakersfield, California, March 1981, (to appear in J. Pet. Tech.).

Ito, J., Kubota, Y., and Kurosawa, M.: "Tracer Tests of the Geothermal Hot Water at the Oruna Geothermal Power Station," Japan Geothermal Energy Association Journal, Vol. 15, no. 2, (series 57), (June 1978) p. 87, (in Japanese).

Taylor, G. I.: "Dispersion of Soluble Matter in Solvent Flowing Slowly Through a Tube," Proceedings of the Royal Society (1953), p. 186.

Tester, J. N., Bivins, R. L., and Potter, R. M.: "Interwell Tracer Analysis of a Hydraulically Fractured Anonitic Geothermal Reservoir," paper SPE 8270 presented at the SPE-AIME 54th Annual Fall Meeting, Las Vegas, Nevada, Sept. 1979.

Wagner, O. R.: "The Use of Tracers in Diagnosing Interwell Reservoir Heterogeneities - Field Results," J. Pet. Tech. (Nov. 19771, 11410.

Yuen, D. C., Brigham, W. E. and Cinco-L., H.: "Analysis of Five-Spot Tracer Tests to Determine Reservoir Layering," U. S. Department of Energy Report SAN-1265-8.

Proceedings Seventh Workshop Geothermal Reservoir Engineering
Stanford, December 1981. SGP-TR-55.

LOW-TEMPERATURE GEOTHERMAL RESOURCE ASSESSMENT OF THE UNITED STATES

Michael L. Sorey and Marshall J. Reed

U. S. Geological Survey
Menlo Park, CA 94025

Introduction

Geothermal resource assessment is the estimation of the amount of thermal energy that might be extracted from the earth and used at costs competitive with other forms of energy at a foreseeable time under reasonable assumptions of technological improvement. A regional or national resource assessment provides a framework for long-term energy policy and strategy decisions by government and industry. A resource assessment is not intended to establish specific reserve figures for short-term investment and mdrketing decisions, but instead to give an overall perspective at a particular time, using uniform methodology and data.

The first systematic effort to estimate the geothermal resources of the United States was published in 1975 as U.S. Geological Survey Circular 726 (White and Williams, eds., 1975). This assessment and a followup assessment published in 1979 as Circular 790 (Muffler, ed., 1979) focused on the quantities of geothermal energy available in regional conductive environments, igneous-related geothermal systems, hydrothermal convection systems, and geopressured-geothermal systems. Estimates were given of the thermal energy recoverable from hydrothermal convection systems at temperatures above 90°C and geopressured systems. In addition, the 1979 assessment included a compilation of data on the occurrence of low-temperature geothermal water less than 90°C (Sammel, 1979), but no attempt was made to estimate the quantities of thermal energy associated with such occurrences.

Low-temperature geothermal resources occur in two types of geohydrologic environments. These include hydrothermal convection systems, comnonly involving upward flow of thermal water along faults in areas of above-normal heat flow, and conduction-dominated areas such as sedimentary basins where aquifers of large areal extent occur beneath a thick insulating blanket of rocks having low thermal conductivity. As discussed by Sammel (1979), low-temperature geothermal resources occur throughout the United States, with some at relatively shallow depths, and appear to have the potential for significant utilization in space heating and agriculture on a local basis.

To provide estimates of the quantities of thermal energy stored in and recoverable from low-temperature reservoirs in the United States, the Geological Survey has made a new assessment based on an updated inventory of low-temperature geothermal occurrences and on the development of new methodology for estimating recoverable energy. We have been aided in this task by the data gathered under programs of many state agencies and several private contractors which are supported by the State Coupled Geothermal Program of the Department of Energy's Division of Geothermal Energy. The assessment is nearly complete; results will be published as a USGS circular in 1982. We present here an outline of the methods used and general descriptions of the results obtained.

Methods for Assessing Geothermal Resources

Assessment of geothermal resources involves a two-step process of first determining the location, extent, and geohydrologic characteristics of each resource area and then estimating the amount of thermal energy stored in each reservoir (the resource base) and the amount of energy which can be produced at the land surface (the resource). Identified resource areas ideally should meet the criteria that a reservoir exists with sufficient permeability to supply long-term production and that reservoir temperatures exceed some minimum temperature-depth relation. As depicted in figure 1, we have used a lower-temperature limit which is 10°C above the mean annual air temperature at the surface and increases at a rate of 25°C/km with depth. This avoids consideration of the enormous quantity of cool, shallow groundwater while enabling us to include areas with anomalous concentrations of heat associated with hydrothermal convection systems and deep sedimentary basins or coastal embayments where temperatures increase relatively rapidly with depth.

The resource base for each low-temperature area identified in this assessment is calculated as:

$$q_R = \rho c \cdot a \cdot d \cdot (t - t_{ref}) \qquad (1)$$

where:

q_R = resource base (stored thermal energy)
ρc = volumetric specific heat of rock plus water (2.6 $J/cm^3°C$)
a = reservoir area

d = reservoir thickness
t = reservoir temperature
t_{ref} = reference temperature (15°C)

Statistical methods outlined in Circular 790 were used to quantify the uncertainty in these calculations and to provide probability distributions for total resource base, resource, and beneficial heat estimates. For each reservoir, estimates were made of the minimum, maximum, and most likely characteristic values for various parameters; these values were then used to form triangular probability densities from which the mean and standard deviation for each parameter and for the various energy quantities were calculated.

The approach used in previous assessments to estimate recoverable energy, or wellhead thermal energy, was to assume a recovery factor of 25 percent of the stored thermal energy. This value is based on a process involving injection of cold water into the reservoir to replace hot water withdrawn during production and to sweep out the energy stored in the rock. In uniformly-permeable reservoirs, up to 50 percent of the stored energy can be recovered before cold-water breakthrough occurs (Nathenson, 1975); 25 percent recovery was assumed to account for commonly-encountered non-uniform permeability conditions.

In the present assessment, wellhead thermal energy calculations were made both for a recovery factor of 25 percent for small systems and for a development plan involving production wells discharging for 30 years in the absence of cold-water injection for large systems. In this production model, wellhead thermal energy is given by:

$$q_{WH} = (\rho c)_f \cdot N \cdot Q \cdot (30 \text{ years}) \cdot (t - t_{ref}) \qquad (2)$$

where:
q_{WH} = energy recovered at the wellhead over 30 years
$(\rho c)_f$ = volumetric specific heat of fluid (4.1 J/cm3"C)
N = number of production wells
Q = average discharge rate of each well

This approach is believed to yield more realistic estimates of recoverable energy for most low-temperature areas, where lower energy content of the resource fluid and relatively large reservoir areas make the economics of injection much less attractive than for higher-temperature geothermal areas.

Limited hydrologic data precluded determination of optimum values for N and Q in equation (2) for most of our identified low-temperature reservoirs. Instead, we selected a production plan involving evenly-spaced wells discharging at 0.0315 m^3/s (500 gpm) for 30 years with a maximum drawdown of 152 m (500 ft). Then for a range of realistic values of reservoir transmissivity and storage coefficient and of confining-bed properties, we developed corresponding curves relating reservoir area to well area, defined as the square of the well spacing. An example, calculated using the leaky-aquifer solutions of Hantush (1960) with confining-bed properties considered typical for sedimentary basins, is presented in figure 2.

The curves in figure 2 show several significant features of a production model which does not involve injection. Most notable is the fact that as reservoir area increases the appropriate well spacing increases because of drawdown interference between wells. Only for very large-area reservoirs, such as the Madison limestone and Dakota sandstone in the northern Great Plains, does the well spacing become constant with reservoir area thereby permitting the number of wells to increase in proportion to the size of the reservoir. For smaller reservoir areas, the number of wells a reservoir can support does not increase in proportion to the size of the reservoir. Consequently, under this production plan, the energy recoverable from a 100 km^2 reservoir is only about 1.5 times that from a 10 km^2 reservoir with the same hydraulic characteristics. Equivalent recovery factors with this production stratagy vary from about 0.1 percent for the largest-area reservoirs in sedimentary basins to 25 percent for the smallest-area reservoirs associated with thermal springs. The 25 percent figure is approached for small reservoir areas where breakthrough of cold, induced recharge from surrounding regions rather than drawdown interference limits energy recovery.

Curves such as those in figure 2 can be used to estimate minimum, maximum, and most likely values for the well area, a_w, which define the corresponding triangular probability density and the mean value %. The assumption was made in developing these curves that each reservoir area was uniformly transmissive. The uncertainty associated with this assumption is treated in a manner similar to that used with the recovery factor approach by assigning a correction factor k to the estimated number of production wells with minimum, maximum, and most likely values of 0, 1, and 0.5, respectively. The effects of this correction factor are to decrease the estimate of N and to increase the confidence limits on estimates of $\overline{q_{WH}}$ and beneficial heat. The mean value for N is then given by $(\overline{ka}/\overline{a_w})$ and the mean wellhead thermal energy becomes:

$$\overline{q_{WH}} = (\rho c)_f \cdot (\overline{ka}/\overline{a_w}) \cdot M \cdot (\overline{t_{WH}} - t_{ref}) \qquad (3)$$

where:
M = (0.0315 m^3/s)·(30 years)
= 3 x 10^7 m^3
$\overline{t_{WH}}$ = mean wellhead temperature (≃ mean reservoir temperature).

For small-area reservoirs, our resource estimates based on equation (3) are close to those based on a recovery factor of 25 percent, but

for large-area reservoirs the well-spacing calculation yields a much smaller value. Differences between these estimates reflect the importance of time-scale over which production continues and the choice of injection versus no-injection developments. Maximum recovery fractions are obtained with an efficient injection plan designed to give cold-water breakthrough at the end of the designed life of the development. If cold water is not injected, high recovery fractions can still be attained for small-area reservoirs over a 30-year period, but for large-area reservoirs production would have to continue for much longer times to obtain high recovery fractions. Despite low recovery fractions, total energy recovery from sedimentary basins could be large because the estimated reservoir areas are so large.

The amount of each resource that can be directly applied to non-electric uses is termed beneficial heat, q_B. Whereas wellhead thermal energy, q_{WH}, represents energy above a reference state, beneficial heat represents energy that can be applied to specific processes such as heating air. Estimates of beneficial heat from geothermal fluid can be compared with thermal energy obtainable from other fuels. Selection of appropriate uses for low-temperature geothermal water depends partly on the reservoir temperature, and different uses involve different rejection temperatures for the geothermal waste water. We have used the following equation to calculate the mean temperature drop, Δt, as a function of mean wellhead temperature:

$$\Delta t = 0.6 \cdot (t_{WH} - 25°C) \qquad (4)$$

From this, mean values for beneficial heat are calculated as:

$$\overline{q_B} = (\rho c)_f \cdot \left(\overline{ka/a}\right)_w \cdot M \cdot 0.6 \cdot (\overline{t_{WH}} - 25°C) \qquad (5)$$

Note that for values of $\overline{t_{WH}} \leq 25°C$ in equations 4 and 5 the useful Δt and the beneficial heat are zero. This limit is obtained both from defining low-temperature resources as being at least 10°C above the mean annual air temperature, which averages 15°C across the United States, and from consideration of heat-pump applications for which ground-water temperatures above 25°C significantly improve coefficients of performace.

Estimates of Resource Base, Resource, and Beneficial Heat

Preliminary results of our assessment of low-temperature resources in the United States indicate that the total recoverable thermal energy at temperatures less than 90°C (based on our well-spacing calculations) is of similar magnitude to corresponding estimates from previous assessments for identified intermediate-temperature (90° to 150°C) and high-temperature (above 150°C) hydrothermal convection systems. These totals are each on the order of 200 x 10^{18}J (about 200 Quads).

The major portion of the identified low-temperature resource occurs within the sedimentary basins east of the Rocky Mountains. Among these are portions of the Powder River and Williston Basins in Wyoming, Montana, North Dakota, and South Dakota where regional aquifers with resources at temperatures of 40" to 90°C exist in Paleozoic rocks of the Madison Group (limestone) and Cretaceous rocks of the Dakota Group (sandstone). Although the reservoir areas involved in these basins are large, the methods used in this assessment to estimate recoverable thermal energy appear to yield realistic results. For example, our preliminary estimate of recoverable energy for the Madison limestone in the Powder River and Williston Basins in Montana is 20 x 10^{18}J. This estimate involves 1800 production wells spread over an area of about 180,000 km^2. An alternative calculation, involving smaller-scale developments at each of about 60 population centers within this region, yields the same resource total for individual well fields with 30 wells per town.

In terms of total numbers of identified low-temperature areas, most areas occur in the western United States and are associated with hydrothermal convection systems of various kinds. We have identified approximately 1,900 individual areas in the United States; roughly 1,850 of these occur west of the Rocky Mountains. In most of these areas, evidence for the existence of a geothermal reservoir consists mainly of the presence of a single thermal spring or spring group, commonly along one or more active normal faults. In such cases a most likely reservoir volume of 1 km^3 and a thermal energy recovery factor of 25 percent were assigned. The resource estimate for such a system, with a reservoir temperature of 70°C, is 4 x 10^{16}J.

There are, however, numerous areas involving hydrothermal convection systems where sufficient information exists to delineate a larger reservoir size. Most notably, in portions of Idaho's Snake River Plain, thermal water moves upward along marginal faults and leaks laterally through permeable strata at relatively shallow depths towards the center of the Plain. Our preliminary estimate of the total recoverable energy for 24 low-temperature areas within the Snake River Plain is approximately 2 x 10^{18}J.

Low-temperature areas identified within the Eastern United States include the warm spring areas in the Appalachian Mountains of Virginia, West Virginia, and North Carolina in the south and of New York and Massachusetts in the north. Other warm spring areas in Arkansas and Georgia were identifed as containing resources, and portions of the Atlantic Coastal Plain in Delaware, Maryland, Virginia, and North Carolina were also included as low-temperature

areas. The western side of the Allegheny Basin in Pennsylvania contains a thick section of Devonian shale having low thermal conductivity, but it is not known if aquifers exist below the shale to form a geothermal reservoir. Outside these areas, however, the generally low crustal heat flow and low thermal gradients appear to restrict the occurrence of significant low-temperature resources.

Limited geohydrologic data requires us to treat many areas which appear favorable for the existence of low-temperature reservoirs as containing undiscovered, rather than identified resources. Undiscovered resources were assumed to be associated with 1) aquifers in sedimentary basins and coastal embayments where existing data could not support a quantitative assessment, 2) halos around identified intermediate and high-temperature systems, and 3) thermal energy in systems whose locations are as yet unknown. Estimates of the total undiscovered resource base, resource, and beneficial heat for various geologic provinces will be included in the final report along with estimates for identified areas.

References

Hantush, M. S., 1960, Modification of the theory of leaky aquifers: Journal of Geophysical Research, v. 65, n. 11, p. 3713-3725.

Muffler, L. J. P., ed., 1979, Assessment of geothermal resources of the United States--1978: U.S. Geological Survey Circular 790, 163 p.

Nathenson, Manuel, 1975, Physical factors determining the fraction of stored energy recoverable from hydrothermal convection systems and conduction-dominated areas: U.S. Geological Survey Open-file Report 75-525, 35 p.

Samnel, E. A., 1979, Occurrence of low-temperature geothermal waters in the United States, in Muffler, L. J. P., ed., Assessment of geothermal resources of the United States--1978: U.S. Geological Survey Circular 790, p. 86-131.

White, D. E., and Williams, D. L., eds., 1975, Assessment of geothermal resources of the United States--1975: U.S. Geological Survey Circular 726, 155 p.

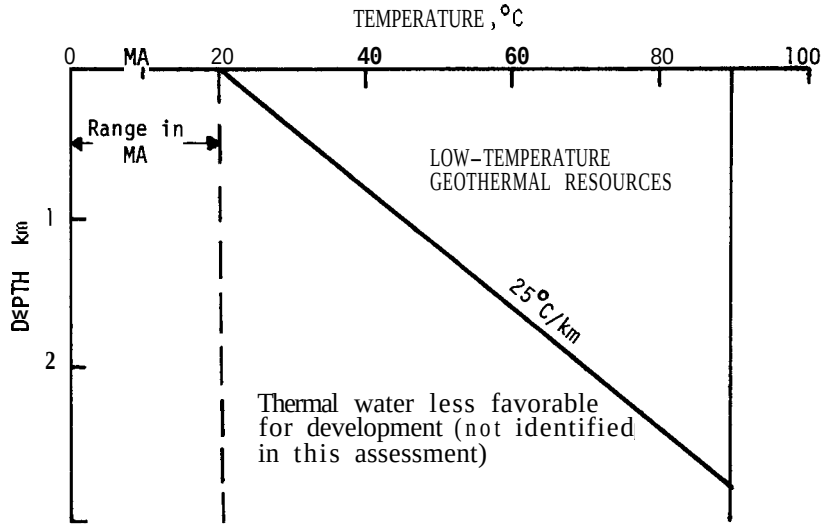

Figure 1. Diagram of temperature-depth criteria used to identify low-temperature geothermal resources. MA = mean annual air temperature. Maximum temperature limit = 90°C. Minimum temperature limit given by line with slope of 25°C/km and intercept of MA+10°C. Heavy solid line shows minimum temperature limit for example case MA = 10°C.

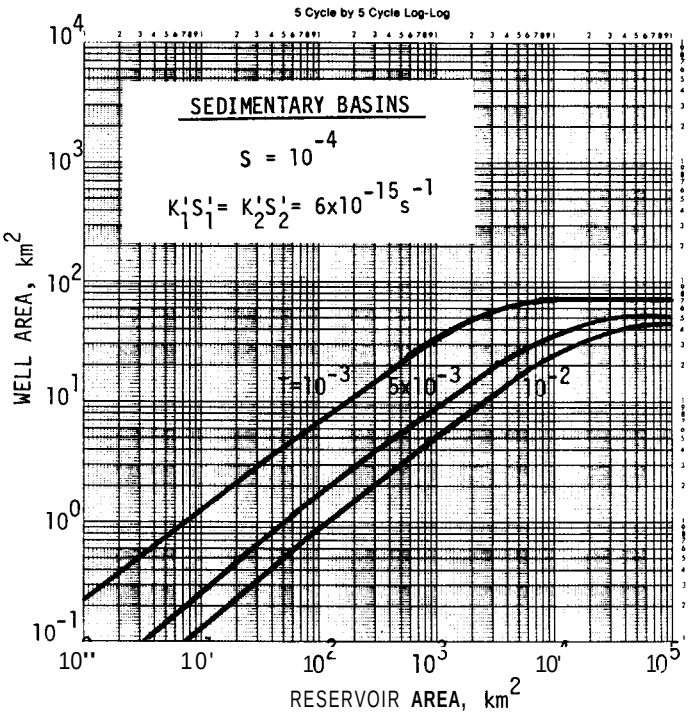

Figure 2. Curves of well area (well spacing squared) versus reservoir area developed for a production plan involving evenly spaced wells discharging for 30 years at 0.0315 m^3/s (500 gpm) with a maximum drawdown of 152 m (500 ft). T = reservoir transmissivity (m^2/s), S = reservoir storage coefficient, K' = hydraulic conductivity of confining beds (m/s), and S' = specific storage of confining beds (m^{-1}).

Proceedings Seventh Workshop Geothermal Reservoir Engineering
Stanford, December 1981. SGP-TR-55.

GEOTHERMAL WELL LOGGING AND ITS INTERPRETATION

Seiichi Hirakawa and Shinji Yamaguchi

The University of Tokyo,
Faculty of Engineering

ABSTRACT For Japanese geothermal developers of private companies, some conventional logs, such as temperature log, SP log and resistivity log, are available in geothermal fields. On the other hand, improvement is being made in well logging techniques on geothermal wells in the "National Sunshine Project." The purpose of this paper is (1) to explain the high temperature well logging developed on the Sunshine Project, and (2) to present algorithm which can estimate porosity distributions and detect fractured zones from conventional geothermal well logging.

HIGH TEMPERATURE LOGGING TOOL High temperature logging tools must be developed for geothermal reservoir potential evaluation. The plan for developing logging tools for geothermal wells started in 1974 as a part of the "National Sunshine Project". Eight basic logging tools had been developed by 1979. They are 1) Multi-Spacing Electrical Log 2) P-S Acoustic Log/Caliper Log 3) Micro-Spherically Focused Log/Caliper Log 4) Temperature Log 5) Pressure Log 6) Flowmeter 7) Bottom Hole Sampler 8) Borehole Televiewer. Table 1 shows the logging tools included in the project and their endurance ability. These logging tools were chosen after wide researches on the necessity of new tools. The developing plan in the Sunshine Project is divided into two steps according to the maximum temperature which logging tools can endure. The maximum temperature limits of the logging tools were 275°C in the first step (1976-1979). The logging tools developed were tested in geothermal reservoirs and good results were obtained. Now many data are being gathered. In the second step (1980~), the goals of the maximum temperature were fixed at 350°C.

INTERPRETATION TECHNIQUES Some conventional logs, such as temperature log, SP log and resistivity log, are available in Japanese geothermal fields. Algorithm is shown with which porosity distributions in a fractured geothermal reservoir can be estimated from conventional geothermal well loggings. In the idealized model of a fractured geothermal reservoir considered in this study, it is assumed that the spacing between parallelepipeds represents the fractures. This model considers both fractured porosity and matrix porosity. This algorithm consists of the basic equations in formation evaluation, empirical equations often used in oil reservoir evaluation and equations derived from double-porosity model theory. To show the validity of this algorithm, one example was chosen from well loggings. The total porosity distributions and the distributions of the fraction of total pore volume made up of fractures to the total pore volume of the system were obtained. The fractured zones estimated from these results agreed approximately with the fractured zones estimated from drilling charts. This algorithm may be one of effective methods for the estimation of porosity distributions in a fractured geothermal reservoir.

Theory The idealized model considered in this study is presented in Figure 1. In this model it is assumed that the spacing between parallelepipeds represents the fractures. It is similar to the one presented by Warren and Root to analyze pressure behavior in fractured reservoirs and to the one presented by Towle to study the relationship between formation resistivity factor and porosity. It is also similar to the one presented by Aguilera to analyze naturally fractured oil reservoirs from well logs. The difference between Aguilera's model and this model is that the former considers only fracture porosity and the latter considers both fracture porosity and matrix porosity. For the basis of this study, the following basic relationships in formation evaluation are assumed to be applicable to both the system and the matrix.

$$I_f = \frac{R_{ft}}{F_f R_w} = \frac{R_{ft}}{R_{fo}} \qquad (1)$$

$$F_f = \frac{a}{\phi^m} \qquad (2)$$

$$F = \frac{a_b}{\phi_b^{m_b}} \qquad (3)$$

where

I_f = resistivity index for the system
R_{ft} = true resistivity for the system
R_{fo} = resistivity for the system at 100-percent formation water saturation
F_f = formation factor for the system
ϕ = total porosity, fraction
m = double-porosity system exponent
F = matrix formation factor
ϕ_b = matrix porosity, fraction
m_b = matrix porosity exponent
R_w = connate water resistivity

The following equations can be derived on the basis of the double-porosity model.

$$\phi = 1 - X^3 + X^3\phi_b \qquad (4)$$

$$f_r = \frac{1-X^3}{1-X^3+X^3\phi_b} \qquad (5)$$

$$F_f = \frac{\frac{1-X}{X} + \frac{F(1-X+X\phi_b)(X^2-X+1)}{X^2\phi_b}}{\frac{X^2-X+1}{X} + \frac{F(1-X+X\phi_b)(1-X)(X^2+1)}{X^2\phi_b}} \qquad (6)$$

where

X = length of the block, fraction
f_r = the fraction of total pore volume made up of fractures to the pore volume of the system

On the basis of the fractured reservoir model and equations 1-6, the algorithm shown in Figure 2 has been developed. In step 4, R_w is calculated by the following method. The static spontaneous potential value, E_{ssp}, is related to R_w by:

$$E_{ssp} = -K_c \log \frac{R_{mf}}{R_w} \qquad (7)$$

$$K_c = 61 + 0.133(1.8T + 32) \qquad (8)$$

where

E_{ssp} = static spontaneous potential, mV
K_c = electrochemical SP coefficient
R_{mf} = resistivity of the flushed zone at reservoir temperature, ohm-m
R_w = connate water resistivity at reservoir temperature, ohm-m
T = reservoir temperature, °C

R_{mf} can be found from the log heading or calculated by the following equation.

$$R_{mf} = K_m(R_m)^{1.07} \qquad (9)$$

where

R_{mf} = resistivity of flushed zone at 24°C, ohm-m
R_m = resistivity of drilling muds at 24°C, ohm-m
K_m = coefficient

R_{mf} at *any* temperature can be calculated using Arp's equation.

$$R_{mf_2} = R_{mf_1}\left(\frac{1.8T_1 + 38.77}{1.8T_2 + 38.77}\right) \qquad (10)$$

where

R_{mf_2} = resistivity of the flushed zone at T_2, ohm-m
R_{mf_1} = resistivity of the flurhed zone at T_1, ohm-m
T_1 = temperature, °C
T_2 = temperature, °C

Temperature in above equations can be obtained by a temperature log.
R_w can be calculated as:

$$R_w = R_{mf}10^{(E_{ssp}/K_c)} \qquad (11)$$

In step 6, laboratory experimental data are required to determine matrix properties. In the case where laboratory experimental data cannot be obtained, conventional formula (e.g. Humble's formula) may be used. Total porosity distributions and fraction of total pore volume made up of fractures to the total pore volume of the system can be estimated with this algorithm.

Example And Discussion To show the validity of this algorithm, one example is presented here with the well data. A geothermal well was chosen among the wells, because it provided the best suite of logs. This example uses a temperature log, spontaneous potential log and an electrical log. The electrical log contains a long normal (electrode spacing = 100cm) and a short normal (electrode spacing = 25cm). The logs were run in 1975. Four hundred meters were examined, beginning at a depth of 1200m. From a temperature log, the temperature around the depth of interest is 130°C. This temperature is lower than 175°C, which is the maximum temperature limit of conventional logging tools used in oil fields. So, conventional logging was possible in this well in 1975. In step 4, R_w is calculated to be 1.5 ohm-m. From geological section of this well, the lithology

is determined to be rhyolite tuff around the depth of interest. In step 6, laboratory experiments with core samples are required to determine matrix properties. In the case where laboratory experimental data connot be obtained, conventional formula may be used. In this case, Humble's formula is assumed. Matrix formation factor F is determined to be 41 from electrical log and matrix porosity ϕ_b is calculated to be 0.14 using the Humble's formula. These values are substituted for F and ϕ_b in equation 6 and the relation between F_f and X is obtained. Figure 3 shows the plot of F_f versus X derived from equation 6. If F_f is obtained from electrical log in each zone, X can be obtained from this relation and porosity can be calculated using equation 4 in each zone. The total porosity distributions and the distributions of the fraction of total pore volume made up of fractures to the total pore volume of the system, which were obtained with this algorithm are presented in Figure 4 and in Figure 5 respectively. These figures show that depths of 1300m, 1360m and 1440m are highly fractured zones. The fact that much fluid loss is observed around the depth of 1400m on the drilling chart supports the above-mentioned results. This algorithm may be one of effective methods for the estimation of porosity distributions in a fractured geothermal reservoir.

CONCLUDING REMARKS Various logging tools for Japanese geothermal fields are being developed as a part of the "National Sunshine Project". On the other hand, some conventional logs, such as temperature log, SP log and resistivity log, are available for Japanese geothermal developers of private companies. Interpretation techniques of logging results obtained with these tools have not yet been put into practice in Japan. In this paper, one of the algorithms for a geothermal field is presented. With this algorithm porosity distributions in a fractured geothermal reservoir can be estimated. The validity of this algorithm has been shown with field data.

ACKNOWLEDGMENT This work has been carried out by a grant-in-aid for developmental scientific research of the Ministry of Education, to which the authors are very grateful.

REFERENCES

1. Aguilera, R. (1974), "Analysis of Naturally Fractured Reservoirs From Sonic and Resistivity Logs," J. Pet. Tech., vol.26, Nov., 1233-1238
2. Aguilera, R. (1976), "Analysis of Naturally Fractured Reservoirs From Conventional Well Logs," J. Pet. Tech., vol.28, July, 764-772
3. Arps, J. J. (1953), "The Effect of Temperature on the Density and Electrical Resistivity of Sodium Chloride Solutions," Petroleum Transactions, AIME, vol.198, 327-330
4. Pirson, S. J. (1957), "Log Interpretation in Rocks With Multiple Porosity Types-Water or Oil Wet," World Oil, vol.144, June, 196-198
5. Schlumberger, (1977), "Log Interpretation Charts"
6. Towle, G. (1962), "An Analysis of the Formation Resistivity Factor Porosity Relationship of Some Assumed Pore Geometries," paper presented at Third Annual Meeting of SPWLA, Houston

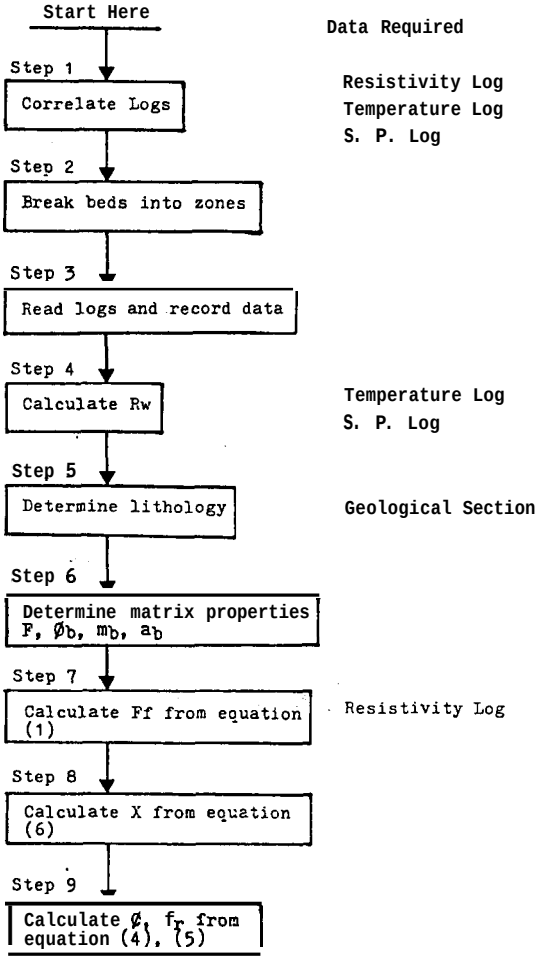

Fig. 2 Algorithm

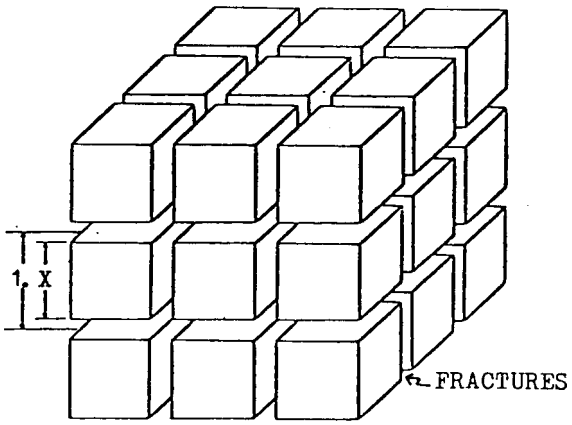

Fig. 1 Idealized Model

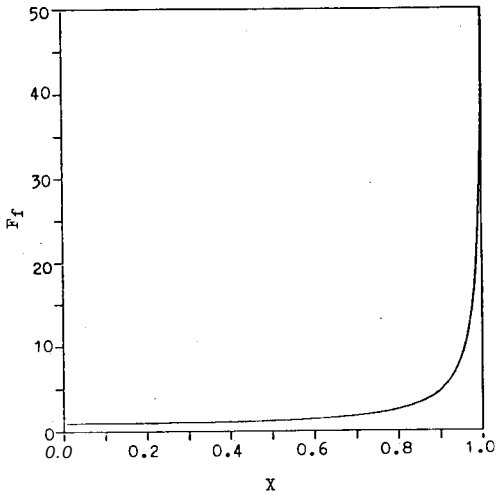

Fig. 3 F_f vs X

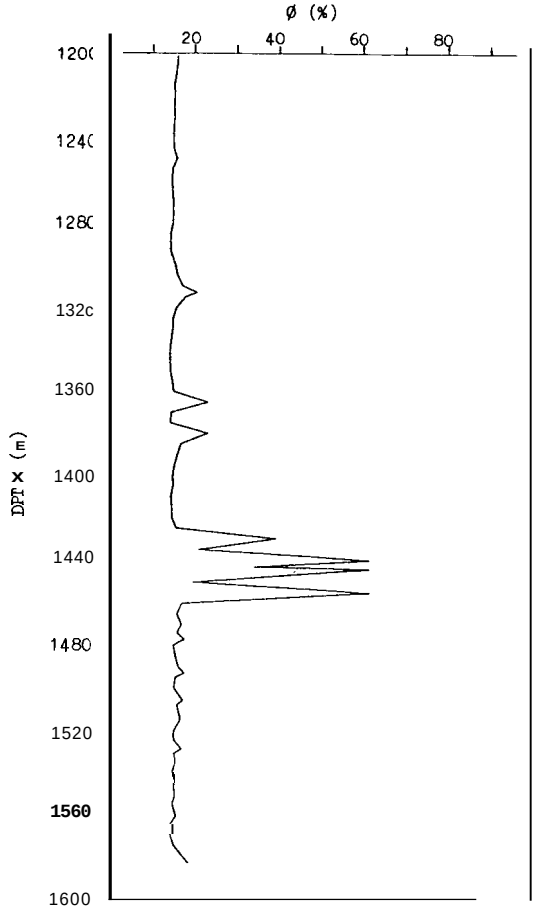

Fig. 4 ø vs Depth

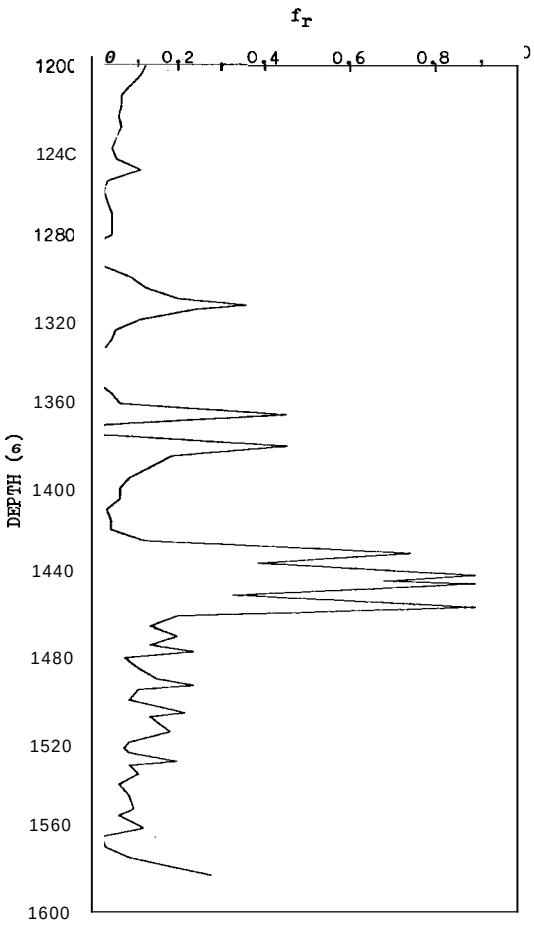

Fig. 5 f_r vs Depth

Table 1 Logging tools included in the "National Sunshine Project"

Log Type	Tool Diameter cm (in)	Min. Hole Size cm (in)	1st Step (1976-1979) Max. Temperature °C	Max. Pressure kp/cm²	Max. Time hours	2nd Step (1980-) Max. Temperature °C	Max. Pressure kp/cm²	Max. Time hours
Multi-Spacing Electrical Log	7.3 (2 7/8)	7.6 (3)	275	750	20	350	1000	20
P-S Acoustic Log/ Caliper Log	10.2 (4)	19.4 (7 5/8)	275	500	4	350	600	6
Micro-Spherically Focused Log/ Caliper Log	10.2 (4)	19.4 (7 5/8)	275	500	4	350	600	6
Temperature Log	4.3 (1 11/16)	5.1 (2)	275	500	20	350	700	20
Pressure Log	4.3 (1 11/16)	5.1 (2)	275	500	20	350	700	20
Flowmeter	4.3 (1 11/16) 4.3 (1 11/16)	5.1 (2) 5.1 (2)	275 275	500 500	20 20	--- 350	--- 700	-- 20
Bottom Hole Sampler	10.2 (4) 7.3 (2 7/8)	19.4 (7 5/8)	275 ---	500 ---	4 --	--- 350	--- 700	-- 6
Borehole Televiewer	9.8 (3 7/8) 9.8 (3 7/8)	12.7 (5) 12.7 (5)	200 ---	300 ---	4 --	--- 250	--- 500	-- 6
Neutron Log/ Density Log/ Caliper Log/ Natural Gamma Ray	10.2 (4)	19.4 (7 5/8)	---	---	--	275	500	4
Logging Cable	13 mm Ø 13 mm Ø	-- --	275 ---	500 ---	20 --	--- 350	--- 1000	-- 20
Logging Truck	weight 60 t, capacity 5000 m, Cable 2000 m							

Proceedings Seventh Workshop Geothermal Reservoir Engineering
Stanford, December 1981. SGP-TR-55.

MEASURING SALT WATER PERMEABILITIES

BRIAN D. GOBRAN

ARCO OIL AND GAS COMPANY

Abstract This study investigates flow of saline solutions through sandpacks at elevated temperatures and pressures in the laboratory. The purposes of this work are two-fold. First the experimental apparatus necessary to measure permeability with salt water flow at elevated temperatures must be designed and built. Then, the effect of temperature on absolute permeability to salt water will be compared to the effect with distilled water as the flowing fluid under similar conditions.

Introduction The absolute permeability of a formation occurs as a variable in all fluid flow equations. Since permeability is measured in the laboratory, experimenters have been trying for the last 40 years to simulate reservoir conditions (or at least those conditions thought important) in the laboratory. The first steps in this direction were to subject cores to confining pressures similar to those in the reservoir. This ranged from hydrostatic (Fatt and Davis) to radial (Wyble) to triaxial at a Poisson ratio of 0.33 (Gray, et al). The results of these studies showed that absolute permeability was a function of confining pressure while relative permeability (Fatt) was not.

The next approximation to reservoir conditions was to investigate the effect of temperature on the measured values of absolute and relative permeabilities. The initial studies (Poston, et al., Weinbrandt) found a reduction in absolute permeability and a shifting of the relative permeability curves when the temperature was increased. Further studies (Casse, Aruna) were initiated with distilled water flow through sandstones and sandpacks to better define the effect of temperature on absolute permeability. These researchers found a reduction in permeability with temperature increase when water (and only water, not mineral oil, gas or 2-octanol) flowed through sandstone (consolidated sandstone or unconsolidated sand but not limestone). This reduction was found to be reversible when this was investigated.

Once these results were obtained, explanations were sought from the literature.

Chemical engineering literature was a good source for explaining the observed permeability reductions with temperature increase. During this period (the early 1970's), chemical engineers all over the world were investigating anomalous water (Derjaguin and Churaev). Anomalous water was water condensed in very fine quartz capillaries having properties significantly different (such as fifteen times the viscosity) from normal or bulk water. So, the idea of some unexplained boundary layer phenomenon between quartz and water was used to explain the observed permeability reductions with water flowing through sand.

Although later investigations found no effect of temperature on absolute permeability with distilled water flow (Gobran, Sageev), there were still nagging questions about the quartz/water interface. Perhaps the addition of salt to the water would cause some interfacial forces that would yield a reduction in permeability with temperature increase. To answer these questions and to further simulate actual reservoir conditions in the laboratory, salt water permeabilities were measured in this study.

A similar work presented at this meeting last year (Potter, et al.) and the discussion that followed will be used as a basis of comparison for these results.

Experimental Apparatus and Procedure The experimental apparatus and procedure have been fully described elsewhere (Gobran), however, a brief description is appropriate here for the discussion that follows. A schematic diagram of the apparatus is shown in Figure 1. The fluid flow system begins with a Ruska constant rate pump (with two 403 stainless steel cylinders rated to 4000 psi). The tubing, core holder, differential pressure transducers and other components of the fluid flow system are made of 316 stainless steel.

The procedure for taking permeability measurements is the same as with distilled water (Gobran). At each temperature four different flow rates are used: three high (about one liter per hour) and one low (about 200 milliliters per hour). The value of permeability at each of the high flow rates is the average of the values after five and then ten incremental pore volumes. These values are then averaged to get the permeability at a given temperature. The low flow rate is maintained for only one pore volume and this value is used as a check to be sure there is no flowrate effect.

This system was designed for distilled water flow. It was used to measure the absolute permeability of sandpacks and consolidated sandstone cores as a function of temperature from 100 to 300°F, confining pressure from 2000 to 10,000 psi and pore pressure from 200 to 4000 psi. During the studies with distilled water, no effect of contamination was found on the inlet face of the porous media. Also, except for a settling or rearrangement of grains, there was no reduction in permeability caused exclusively by flow.

Results As stated previously, one of the goals of this study was to investigate the effect of temperature on absolute permeability of unconsolidated sandpacks with a 1%NaCl solution as the flowing fluid. The sandpacks were either 100–120 or 120–200 mesh Ottawa sand. The confining pressure and the pore pressure were 2000 and 200 psi, respectively, for all experiments.

During the distilled water experiments and the initial salt water experiment, a 15 micron filter was used in the flow line outside the air bath. During the first salt water experiment this filter plugged badly and there was a 20% reduction in permeability during the first 95 pore volumes of throughput (this is far higher than would be expected merely due to settling as will be seen later). At this point the core was at 150°F and the experiment was stopped. The 15 micron filter outside the air bath was replaced with a 2 micron filter and a second 2 micron filter was installed in the air bath immediately prior to the core holder.

The results of the second experiment are shown in Figure 2. Here permeability is graphed versus temperature. There was a loose wire to one of the air bath heating elements and the maximum attainable temperature was 284°F. These results show no significant reduction in absolute permeability during the heating portion of the experiment. There was, however, a large loss in permeability during the cooling cycle. The experiment was stopped before the usual four flowrate measurements could be made at 100°F.

Figure 3 shows permeability graphed versus throughput for this experiment. The results of this experiment with salt water can be compared with the results for distilled water flow shown in Figures 4 and 5. Figure 4 shows permeability as a function of throughput at 100°F. This shows the reduction in permeability that can be expected merely due to flow. Clearly, the reduction in permeability (20% in 95 pore volumes) in the first salt water experiment was excessive as was the reduction during the cooling cycle of the second experiment.

Figure 5 shows permeability as a function of temperature for distilled water flow. This compares very well with the heating cycle in the second salt water experiment with both showing no temperature dependence. Examination of the core and the *two* filters at the conclusion of the second salt water experiment showed that the filters were plugged with a brown particulate and that this same material coated the inlet face of the core.

The results of this experiment indicated that permeability was not dependent on temperature with salt water as the flowing fluid. It also showed that both the flow lines inside the air bath and the pump itself were corroding with the salt water flow. The progress of the corrosion-produced particulate cold be delayed by use of filters but there would still be permanent damage to the pump and flow lines.

At this point a solution (instead of a delaying approach) was sought. After phone calls to numerous major oil company research laboratories, it was determined that 100 parts per million of sodium sulfite (Na_2SO_3) would remove the dissolved oxygen from the salt water. Alternate materials such as titanium and mnel were considered as replacements for the 316 stainless steel tubing, but, due to time and cost limitations, were not used.

A system of check valves and cylinders which allowed flow of mercury in the pump and water in the system was implemented. This design is shown schematically in Figure 6. After several abortive experiments in which mercury leaked into the flow system, this design seemed to work successfully.

During the final experiment there was a continued decrease in permeability with

throughput (although not of the magnitude that would be caused by mercury in the core). The low flowrate measurements yielded permeability values significantly lower than the high rate values. This experiment was stopped while heating to 250°F when the differential pressure across the core kept increasing. This is indicative of flow of the confining oil into the core.

Discussion In his work, Mr. Potter found corrosion of his system (316 and 304 stainless steel) with distilled water flow at elevated temperatures. This was due to oxidation which produced Fe^{+3} ions. When the system was changed to titanium, no more corrosion problems were encountered. During the discussion following his presentation, it was suggested that the 304 stainless steel components caused the problems and that the 316 stainless would have no problems. This has been borne out by two recent studies (Gobran, Sageev). However, systems constructed of 316 stainless steel cannot be used with salt water flow at elevated temperatures. Baaed on the results of this work and other studies on stainless steel (Gordon), stainless steel and salt water are not compatible above 170°F. Therefore materials such as inconel, titanium or mnel are needed for such systems.

Conclusions Two conclusions can be made from this study: 1) Absolute permeability of sandpacks to salt water is not a function of temperature. 2) Materials other than 316 stainless steel must be used for salt water systems at elevated temperatures.

Acknowledgement I would like to acknowledge the financial support of the United States Department of Energy who funded this work through contract DE-C03-76ET12056 at the Stanford University Petroleum Research Institute. I would also like to thank ARCO Oil and Gas Company for all their assistance in the preparation of this paper and for allowing me to present it.

References

Aruna, M. (1976), "The Effects of Temperature and Pressure on Absolute Permeability of Sandstones," Ph.D. Dissertation, Stanford University.

Casse, F.J. (1974), "The Effect of Temperature and Confining Pressure on Fluid Flow Properties of Consolidated Rocks," Ph.D. Dissertation, Stanford University,

Derjaguin, B.V. and Churaev, N.V. (1973), "Nature of 'Anomalous Water'," Nature, Aug. 17, 1973, 430–431.

Fatt, I. (1953), "The Effect of Overburden Pressure on Relative Permeability," Trans., AIME, 198, 325–326.

Fatt, I. and Davis, D.H. (1952), "Reduction in Permeability with Overburden Pressure," Trans., AIME, 195, 329.

Gobran, B.D. (1981), "The Effects of Confining Pressure, Pore Pressure and Temperature on Absolute Permeability," Ph. D. Dissertation, Stanford University.

Gordon, B.M. (1980), "The Effect of Chloride and Oxygen on the Stress Corrosion Cracking of Stainless Steels: Review of Literature," Materials Performance, 19, April, 1980, 29–38.

Gray, D.H., Fatt, I. and Bergamini, G. (1963), "The Effect of Stress on Permeability of Sandstone Cores," Soc. Pet. Eng. J., June, 1963, 95–100.

Poston, S.W., Ysrael, S., Hossain, A.K.M.S., Montgomery, E.F., III, and Ramey, H.J., Jr. (1970), "The Effect of Temperature on Irreducible Water Saturation and Relative Permeability of Unconsolidated Sands," Soc. Pet. Eng. J., June, 1970, 171–180.

Potter, J.M., Nur, A. and Dibble, W.E., Jr. (1980), "Effect of Temperature and Solution Composition on the Permeability of St. Peters Sandstone: Role of Iron (III)," Proceedings: Sixth Workshop on Geothermal Reservoir Engineering, 316–321.

Sageev, A. (1980), "The Design and Construction of an Absolute Permeameter to Measure the Effect of Elevated Temperature on the Absolute Permeability to Distilled Water of Unconsolidated Sand Cores," M.S. Report, Stanford University.

Weinbrandt, R.M. (1972), "The Effect of Temperature on Relative Permeability," Ph.D. Dissertation, Stanford University.

Wyble, D.O. (1958), "Effect of Applied Pressure on the Conductivity, Porosity and Permeability of Sandstones," Trans., AIME, 213, 430–432.

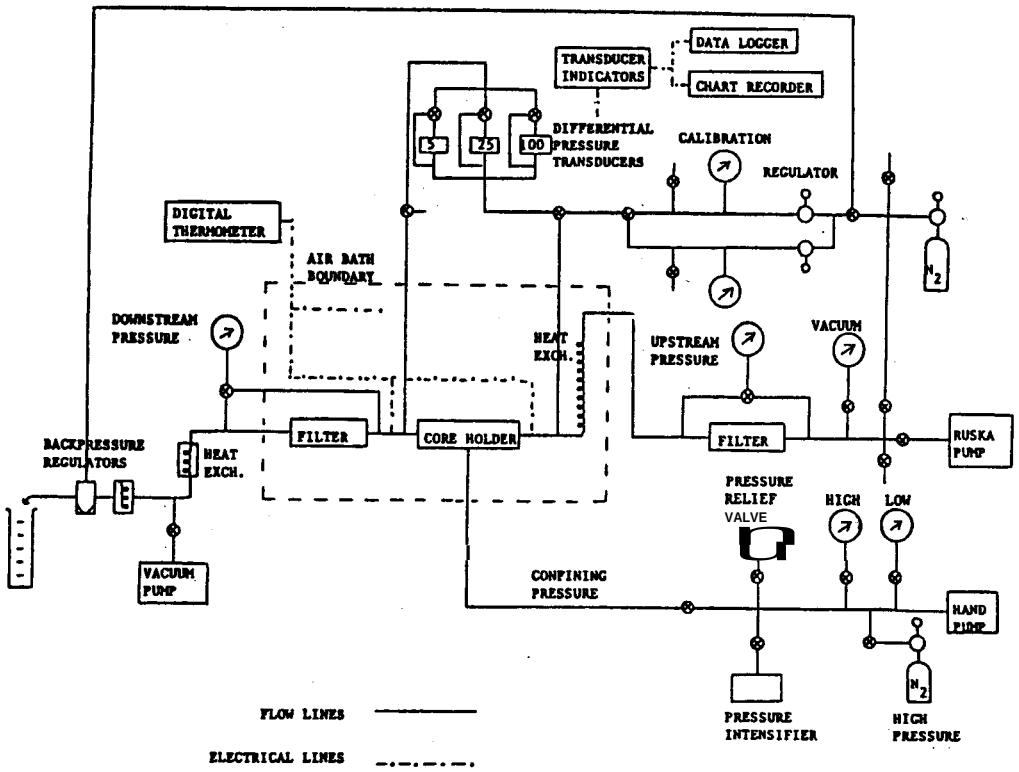

Figure 1. Schematic diagram of the experimental apparatus.

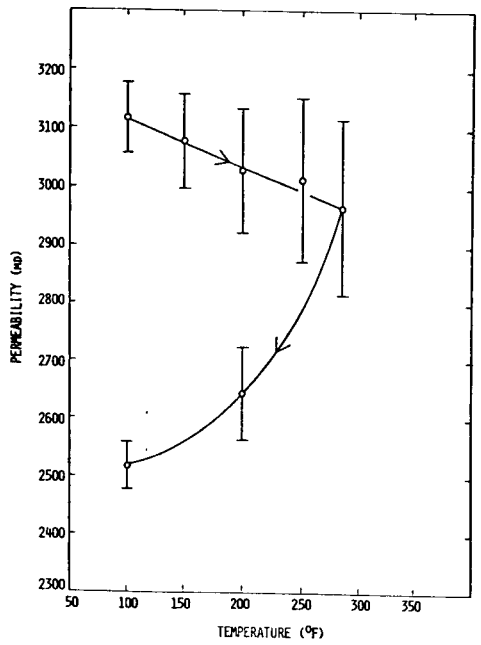

Figure 2. Salt water permeability versus temperature.

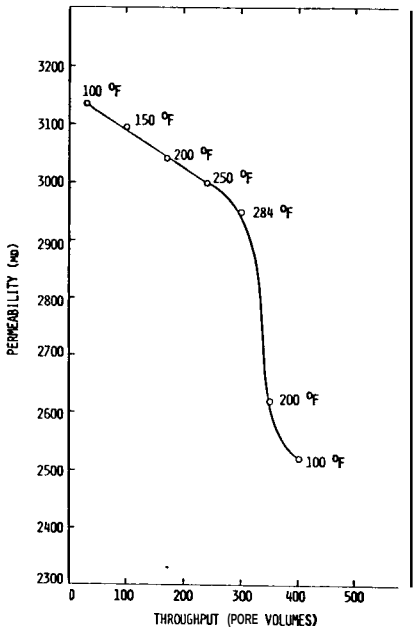

Figure 3. Salt water permeability versus throughput.

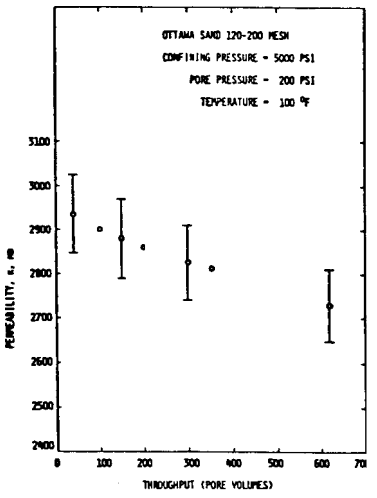

Figure 4. Distilled water permeability versus throughput.

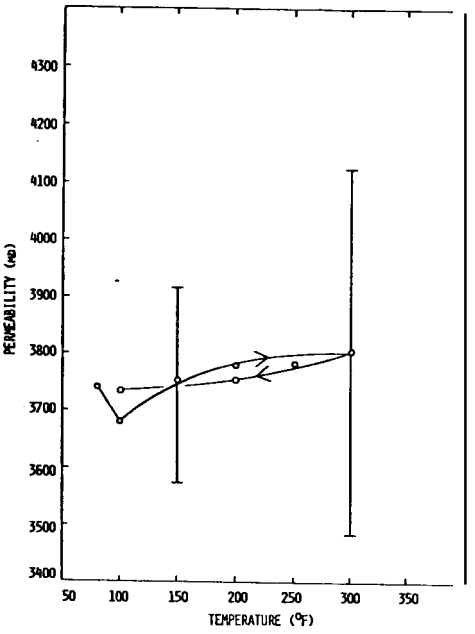

Figure 5. Distilled water permeability versus temperature.

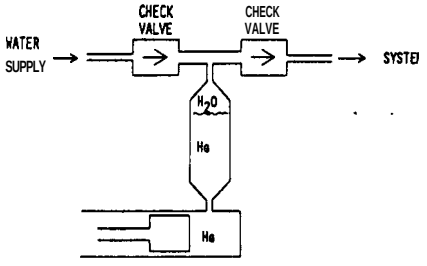

Figure 6. Mercury flow modifications.

Proceedings Seventh Workshop Geothermal Reservoir Engineering
Stanford, December 1981. SGP-TR-55.

SiO_2 PRECIPITATION ACCOMPANYING FLUID FLOW THROUGH GRANITE HELD IN A TEMPERATURE GRADIENT

D. E. Moore, C. A. Morrow, and J. D. Byerlee

U.S. Geological Survey, Menlo Park, California 94025

Abstract In experiments simulating the rise of hydrothermal fluids from a geothermal reservoir, water was flowed at a low rate down a temperature gradient through fractured and intact cylinders of Barre and Westerly Granite. Temperatures ranged from 80 to 105°C at the outer edges of the cylinders to 250 to 300°C along a central borehole which housed the heating coil. As a result of mineral deposition, particularly SiO_2, at low temperatures in the granite samples, permeabilities were reduced 10- to 100-fold in periods of 1 to 3 weeks. Chemical analyses were made of the low-temperature fluids discharged from the cylinders. Early-sampled fluids were supersaturated with respect to several minerals at low temperatures in the granites. Of the oversaturated species, SiO_2 showed the most rapid decrease with time, and in an experiment with low initial flow rate, the solution reached equilibrium with quartz at the low-temperature edge of the cylinder within about 6 days. Increasing the maximum temperature of the gradient at constant confining pressure led to higher SiO_2 concentrations in the discharged fluids. However, increasing confining pressure along with maximum temperature resulted in lower dissolved SiO_2 contents, because of enhanced reaction at the reduced flow rates accompanying the pressure increase. The behavior of SiO_2 contrasted with most other dissolved species, which were affected by changes in temperature but not flow rate in the time of the experiments.

Introduction A series of permeability experiments was conducted to model the flow of fluids from high to low temperatures across granitic rocks. As a result of several days of slow flow, the permeability of each granite specimen was reduced to 1 to 10% of its value prior to heating (Morrow and others, 1981). As an aid in determining the causes of the permeability reductions, the fluids discharged from the granite specimens were collected for chemical analysis (Moore and others, in press). An unexpected finding of the fluid analyses was that the variations in dissolved silica concentrations with changing experimental conditions differed from those of the other species in solution. The distinctive behavior of silica and its effect on the permeability of the granites form the subject of this summary paper.

Experiments The experimental design is shown in Figure 1. Cylindrical samples of granite 3" in diameter and 3-1/2" long contained a 1/2"-diameter borehole in which a coiled resistance heater produced a temperature gradient between the center and outer edge. Distilled water was flowed radially through the granite from high to low temperatures. Gold shims were placed

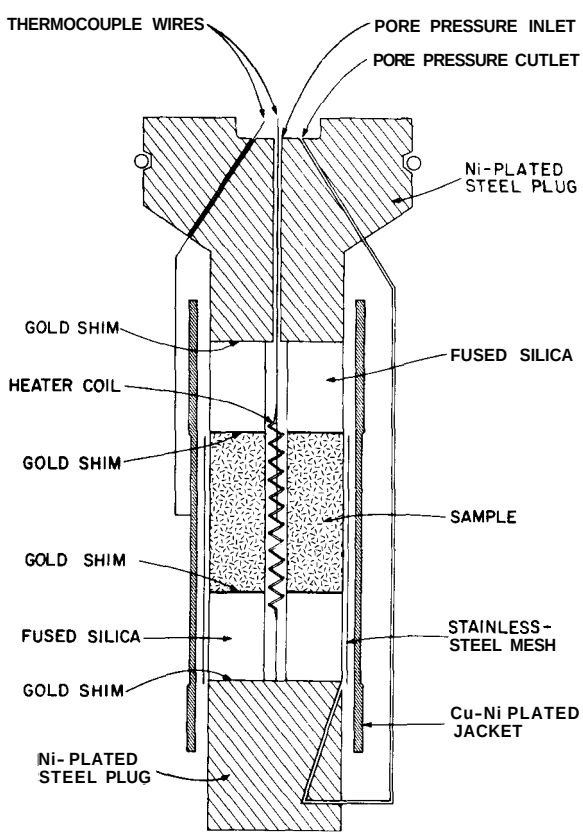

Figure 1 Schematic sample assembly.

at the ends of the granite samples to seal them from the adjoining fused silica cylinders that served as thermal insulators. Other exposed metal around the borehole was gold-plated to prevent contamination of the fluids. The sample assembly was separated from the containing jacket by a stainless steel mesh that allowed drainage of the discharged, low-temperature fluids away from the rock cylinder.

The experiments conducted are sumnarized in Table 1. Cylinders of Barre and Westerly Granite, both biotite-muscovite grariodiorites, were used in different experiments. Temperatures within the boreholes ranged from 250 to 300°C, and those at the outer edges were 80 to 105°C. Conlining pressures of 300 bars were coupled with pore pressures of 100 bars, corresponding to 1.2 km thickness of overburden with f1uid pressure resulting from the hydrostatic head. Confining pressures of 600 bars and pore pressures of 200 bars were also used. A 5 to 10 bar pore pressure differential produced a low rate of fluid flow. Distilled water was the starting fluid in the experiments listed in Table 1. An additional experiment using a $NaHCO_3$-$CaCl_2$ solution rather than distilled water resulted in similar permeability reductions.

Nine dissolved species were analyzed from 1.5 ml fluid samples, collected as separate 1.25 and 0.25 ml samples. Details of the analytical techniques and many fluid compositions are contained in Moore and others (in press). The 0.25 ml sample was analyzed for SiO_2 using the molybdate-blue method of spectrophotometric analysis (ASTM, 1974; p. 401-402). From the larger fluid sample, the cations Ca, Na, K, and Mg were determined using atomic absorption techniques. The bicarbonate content was determined from measurements of total inorganic carbon, made with a carbon analyzer. The anions Cl, F, and sulfate were determined using an ion chromatograph with integrator attachment.

Some of the fluid compositions were analyzed with the SOLMNEQ computer program of Kharaka and Barnes (1973), which determines the states of reaction (ΔG_R) of the solutions at a given temperature with respect to up to 158 mineral species. In order to determine the differences in reactivity of a given fluid across the sample, most of the solution compositions analyzed by SOLMNEQ were run at both the high- and low-temperature extremes of the granite cylinders.

Permeability Changes The variation in permeability with time was determined from measured changes in mass flow rate over the constant pore pressure differential, using the radial flow model of Darcy's Law. As an example of the trend of permeability decrease, the normalized permeabi1ity changes with time for NWD22 and 24 are shown in Figure 2. The granite cylinders in each experiment showed a rapid initial permeability drop followed by lower rates of decrease. At constant confining presures, an increase in borehole temperature resulted in a more rapid rate of permeability reduction. In addition, the larger the volume of fluid flowed through the cylinders, the greater the permeabi1ity drop.

Textural Evidence of Reaction Thin-section and SEM examinations yielded some evidence of mineral reaction and precipitation in the granite cylinders during the experiments. Observations of high-temperature mineral reaction were confined to narrow concentric zones around the boreholes. There, calcite showed pronounced etching along cleavage

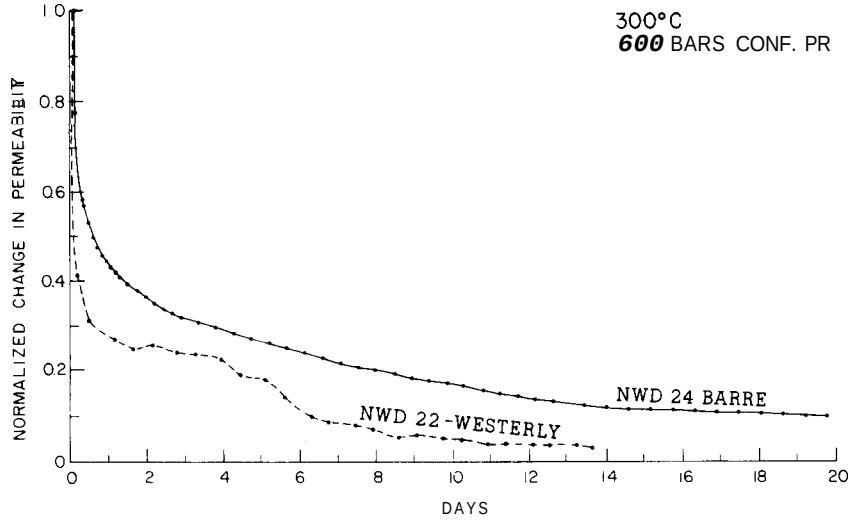

Figure 2 Normalized changes in permeabi1ity with time

Table 1. Experimental Conditions

Experiment	Rock Type	Temp. Gradient (°C)	Confining Pressure (bars)	Pore Pressure (bars)	Pore Pres. Differential (bars)	Duration of exp. (days)	Vol. Fluid Flow (mL)	Permeability initial k(da)	Permeability final k(da)
NWD10	Barre	80-250	300	100	5	18.0	41.8	7.9(10^{-7})	1.6(10^{-7})
NWD20	Barre	104-280	300	100	5	12.9	32.3	4.9(10^{-8})	1.7(10^{-8})
NWD21	Westerly	84-250	300	100	5	11.9	134.2	7.4(10^{-7})	4.7(10^{-8})
NWD22	Westerly	92-300	600	200	10	12.9	34.0	2.4(10^{-7})	9.3(10^{-9})
NWD23	Barre	103-250	300	100	5	9.0	114.0	2.0(10^{-6})	3.0(10^{-8})
NWD24	Barre	94-300	600	200	10	19.9	23.7	7.4(10^{-8})	7.6(10^{-9})

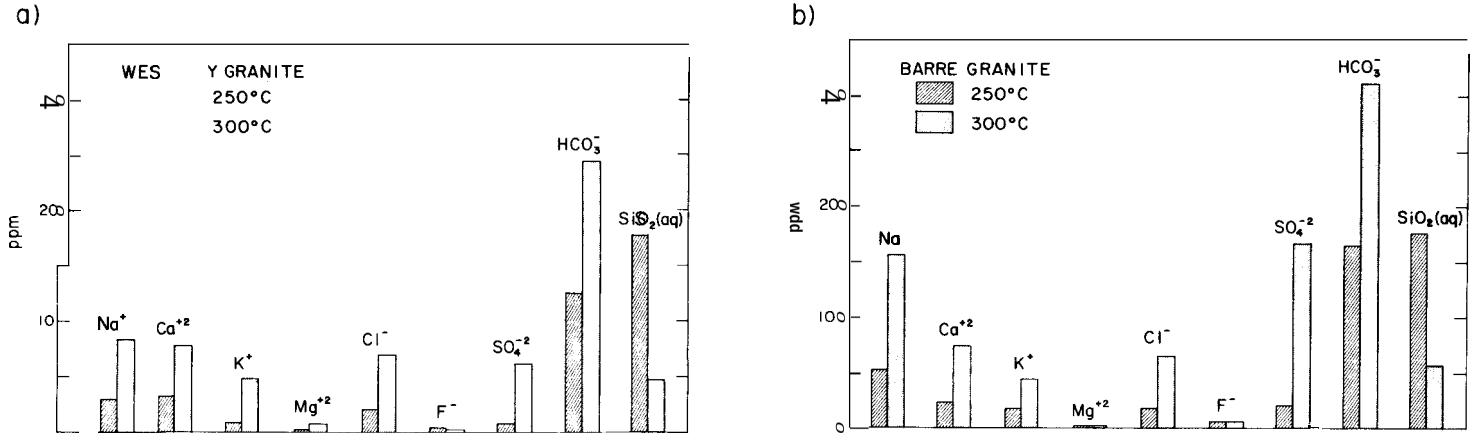

Figure 4 Effect of temperature on the composition of fluids discharged from a given granite type at similar times during an experiment: (a) Westerly Granite, fluid samples collected at 10.0 days. (b) Barre Granite 6.0 days.

and fracture traces and phyllosilicate alteration minerals in plagioclase had changed color from green to yellowish-brown. A few early experiments were conducted using samples containing a through-going fracture (Morrow and others, 1981). After the experiments, the fracture surfaces showed traces of mineral deposition near the low-temperature sides. Most of the deposits consisted of patchy masses and fibers of silica which formed on exposed quartz grains (Fig. 3). In addition, some Ca-rich fibers grew on plagioclase crystals.

Chloride and Sulfate Neither Cl nor S are major constituents of any mineral in Westerly or Barre; instead, they are concentrated in intergranular fluids and adsorbed onto grain surfaces (Ellis and Mahon, 1964). Considerable amounts of both ions were removed by flushing cold water through the rock cylinders for 3–5 days prior to heating. Nevertheless, the concentrations of both species in solution rose again upon initial heating with the higher-temperature water the more effective leaching agent (Fig. 4). Subsequently, both ions dropped rapidly to low values.

Na, Ca, K, Mg, F, and HCO_3 Unlike Cl and sulfate the concentrations of these 6 species are related to mineral solubilities, with temperature the major control on solution concentrations. The higher Na contents an Na/Ca ratios in Fluids derived from Barre Granite (Fig. 4) are consistent with the occurrence of a more Na-rich plagioclase and a separate albitic alteration phase in Barre. In the same way, the slightly Mg-enriched solutions from Westerly are related to the higher Mg contents of minerals in that granodiorite. The amounts of Na, K, and Ca in solution doubled or tripled with a 50°C temperature increase (Fig. 4). The

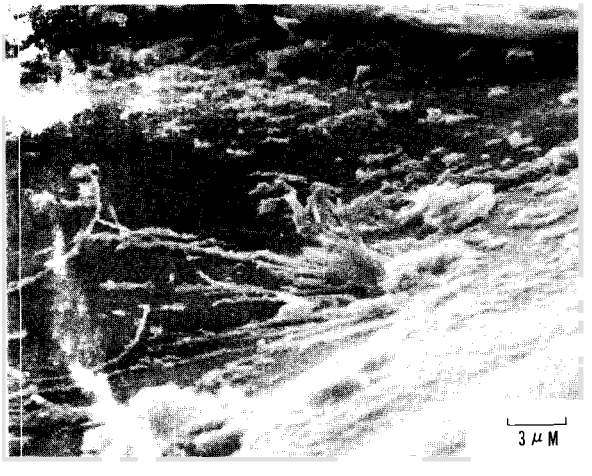

Figure 3 Low-temperature deposition of silica fibers on a quartz grain exposed along a fracture surface. SEM photomicrograph, 30,000 x magnification.

Table 2. Temperatures at which the SiO2 contents and Na, K, and Ca concentrations for selected fluid samples would be equilibrium values.

Sample	Quartz	Na-K-Ca
NWD20		
20	170	198
28	167	171
NWD21		
34	182	218
53	172	208
NWD22		
63	104	250
69	99	263
70	72	225
NWD23		
77	186	265
83	171	229
84	154	221
NWD24		
93	119	237
99	142	217
100	130	208

bicarbonate concentration also doubled, which contrasts with the negative temperature dependence of calcite solubility but which can be explained by differences in solution pH. The Mg and F contents were controlled by the solubility of mafic minerals and of accessory fluorite, respectively. The concentrations of these 2 ions did not increase with temperature, because minerals such as chlorite and fluorite show slightly negative solubility relationships in that temperature range (Ellis, 1971; Mahon, 1964). In the same way, the slightly Mg-enriched solutions from Westerly are related to the higher Mg contents of minerals in that granodiorite.

Changes in the ionic concentrations with time may reflect partial reaction of the solutions at lower temperatures in the granites. Equilibrium temperatures of selected fluid compositions calculated using the Na-K-Ca geothermometer of Fournier and Truesdell (1973) are listed in Table 2, along with quartz temperatures. Nearly all of the initial Na-K-Ca temperatures were below the borehole temperatures and they also decreased with time. The gradual decreases in temperature indicate increasing reaction of the solutions at low temperatures as flow rates decreased.

Throughout most of the 250°C experiments the solutions were undersaturated with respect to calcite at the lowest temperatures in the cylinders, and bicarbonate concentrations increased with

time. In contrast, the solutions were oversaturated wih calcite at the low-temperature edge for most of the 300°C experiments, and the bicarbonate concentrations decreased with time in an apparent attempt to reach equilibrium concentrations.

Ca concentrations decreased steadily during the experiments, particularly those at 300°C. The ratio Ca/HCO_3 also decreased with time. The lowered Ca contents relative to HCO_3 suggests that some limiting mineral solubility other than calcite, such as the precipitation of a Ca-zeolite or Ca-montmorillonite, may have caused Ca concentrations to decrease.

Silica The presence of silica in the fluids is controlled most strongly by the dissolution of quartz, which shows marked increases in solubility with increasing temperature (for example, Kennedy, 1950) and is by far the most reactive mineral in granodiorite subjected to flow of hydrothermal fluids (Charles, 1978). For experiments run at the same confining pressure with the same rock type (NWD20 and 23), a 30°C increase in temperature led to somewhat higher dissolved silica Concentrations. However, increasing confining pressure as well as temperature resulted in much lower silica contents (Fig. 4) and correspondingly lower equilibrium temperatures (Table 2). The lower concentrations at higher temperatures and confining pressures contrast markedly with the behavior of the other dissolved species that show positive temperature-dependent solubilities (Fig. 4).

None of the discharged fluids was saturated with respect to quartz at the borehole temperatures of the granite cylinders. However, silica phases such as quartz, chalcedony and a-cristobalite were oversaturated in at least some fluids at the low-temperature side. The values of ΔG_R for silica species decreased with time in an experiment, consistent with silica deposition from the low-temperature, oversaturated solutions. Quartz rather than some other silica species may be the crystallized phase, because the silica contents of the solutions continued to decrease to values below the solubilities of chalcedony and a-cristobalite. In addition, the final fluid samples of the 300°C Westerly Granite experiment (NWD22) were in equilibrium with quartz at the low-temperature, outer edge of the cylinder (Table 2).

The reduced dissolved silica concentrations in higher temperature and pressure experiments (Fig. 4) may be a function of the competing effects of temperature and flow rate on silica solution and redeposition. Rimstidt and Barnes (1980) have demonstrated the importance to quartz precipitation of the fluid volume and the relative interfacial area between solid and aqueous phases. With the very small channel size, large crystal surface areas, and low and progressively declining flow rates, the conditions of these experiments were highly favorable for quartz precipitation.

Thus, although the higher-T fluids will acquire greater amounts of dissolved silica near the borehole, the correspondingly decreased flow rates at the higher confining pressures will enhance reprecipitation of the silica at low temperatures in the granites.

Concluding Remarks As indicated by fluid chemistry and petrographic examination of fracture surfaces, quartz precipitation along grain boundaries and microfractures may have been the principal source of the observed permeability decreases in the granodiorites. The silica content of the discharged fluids is particularly sensitive to reductions in flow rate, in contrast to the other dissolved species. Other minerals, such as calcite and probably some aluminosilicates were also supersaturated in some of the fluids. These materials may have been deposited as well, but at low rates compared to quartz.

The effects of temperature and fluid volume on the rate of permeability decrease are explicable in terms of the amount of material transported from high to low temperatures across the granites. Increasing temperature raised the concentrations of the solutions around the borehole, thus increasing the amount of material that was transported and redeposited at low temperatures in the cylinders. However, decreasing flow rate reduced the amount of mass transfer in a given time; and if the fluid volume was sufficiently low, permeability decreases occurred at a lower rate despite increasing temperature.

REFERENCES

American Society For Testing and Materials (1974), "Annual Book of ASTM, part 31 [water]," Philadelphia, Pa., 902 pp.

Charles, R. W. (1978), "Experimental geothermal loop: 1, 295°C study," Los Alamos Scientific Laboratory Informal Rept. LA-7334-MS, 44pp.

Ellis, A. J. (1971), "Magnesium ion concentrations in the presence of magnesium chlorite, calcite, carbon dioxide, quartz," Am. J. Sci. 271, 481-489.

Ellis, A. J. and Mahon, W. A. J. (1964), "Natural hydrothermal systems and

experimental hot-waterhock interactions," Geochim. Cosmochim. Acta 28, 1323-1357.

Fournier, R. O. and Truesdell, A. H. (19731, "An empirical Na-K-Ca geothermometer for natural waters," Geochim. Cosmochim. Acta 37, 1255-1275.

Kennedy, G. C. (19501, "A portion of the system silica-water," Econ. Geol. 45, 629-653.

Kharaka, Y. K. and Barnes, I. (19731, "SOLMNEQ: Solution-mineral equilibrium computations," NTIS, U.S. Oept. Commerce, PB-215 899, 81 pp.

Mahon, W. A. J. (1964), "Flourine in the natural thermal waters of New Zealand," N. Z. J. Sci. 7, 3-28.

Moore, D. E., Morrow C., and Byerlee, J. D., "Chemical reactions accompanying fluid flow through granite held in a Temperature gradient," Geochim. Cosmochim. Acta, in press.

Morrow, C., Lockner, D., Moore, D., and Byerlee, J. (19811, "Permeability of granite in a temperature gradient," J. Geophys. Res. 86, 3002-3008.

Rimstidt, J. D. and Barnes, H. L. (1980), "The kinetics of silica-water reactions," Geochim. Gosmochim. Acta 44, 1683-1699.

Proceedings Seventh Workshop Geothermal Reservoir Engineering
Stanford, December 1981. SGP-TR-55.

STRESS INDUCED RELEASE OF Rn^{222} AND CH_4 TO PERCOLATING WATER IN GRANITIC ROCK

C. G. Sammis, M. Banerdt, and D. E. Hammond

Department of Geological Sciences
University of Southern California
Los Angeles, California 90007

Abstract The radon, methane, and carbon dioxide concentrations have been measured in water which has percolated through granitic rock under triaxial stresses ranging from 0.1 to 0.95 of the fracture stress. We simultaneously measured the permeability and porosity (hence hydraulic radius) of each sample. The first series of experiments were on seventeen initially dry rock samples. The radon concentration in the first 3 gm of water collected varied by a factor of 10, but was not correlated with stress. A good correlation was found between radon and permeability; rocks having high permeabilities tend to release less radon. In a second series of experiments, rock samples were saturated under stress, equilibrated for one month, then restressed and measured. These samples produced between 2 and 10 times more radon than initially dry rocks having the same permeability. In a third series of experiments, multiple successive water fractions were sampled. We found that most of the radon is removed with the first pore volume collected, while methane extraction requires several pore volumes. An experiment in which the stress was changed during a run produced an increase in CH_4 but no increase in Rn^{222}. These results are interpreted in terms of a numerical model for flow and gas extraction from a microcrack network.

Introduction The physical properties of radon gas (Rn^{222}) make it an ideal natural tracer for detecting changes in the fracture networks which permeate natural rock masses. As an intermediate daughter in the U^{238} decay series, Rn^{222} is constantly being generated in uranium bearing rocks. Formed by alpha-decay of the radium (Ra^{226}) parent, the radon atom has a recoil energy of about 100 KeV; sufficient energy to travel hundreds of lattice spacings upon formation. While most of these atoms lodge within the interior of a grain, some end up in the network of microcracks (and macrocracks) which permeate a rock mass, and may thereby enter the groundwater. The amount of radon dissolved in groundwater is thus primarily a function of the concentration and spatial distribution of radium within the rock, and the porosity and permeability of the fracture network. Changes in the fracture network may change the ground water radon concentrations observed at a sampling site in two ways; (1) directly, by changing the number of radon atoms which enter the groundwater, and (2) indirectly by changing the transport of radon from the site at which it is created to the sampling site.

The relatively short half-life of Rn^{222} ($T_{\frac{1}{2}}$ = 3.825 days) assures a short term causal refationship between changes in the fracture-network morphology and the resultant variation in groundwater radon. Because radon is an inert gas, it does not readily enter into chemical combination and its high solubility in water (22.4 cm^3 per 100 cm^3 H_2O at 25°C and one atmosphere) means that, in the presence of groundwater, most radon will be dissolved rather than adsorbed to the walls of the fracture network. The physical mechanisms by which radon is generated and transported are discussed in more detail by Tanner (1980).

Two applications in which groundwater radon has been monitored are earthquake prediction and geothermal reservoir engineering. The build-up of tectonic stress preceding an earthquake might be expected to change the morphology of a fracture network by creating and opening cracks parallel to the maximum principal stress while closing orthogonal cracks. In the laboratory, the crack opening process dominates when the differential stress, $\sigma_1-\sigma_3$ is greater than approximately one-half of the fracture stress and the rock actually increases in volume. Laboratory studies of this "dilatancy" phenomenon are reviewed by Brace (1978) and Byerlee (1978). Field observations of groundwater radon variations associated with earthquakes are summarized by Hauksson (1981) and Teng (1980). The withdrawal of water and heat from a geothermal reservoir might also be expected to change the morphology of the fracture network through the combined effects of thermal contraction and variations in pore pressure. The associated change in radon concentration could serve as a useful tool for nonitoring reservoir development. Radon measurements in geothermal systems are discussed by Stoker and Kruger (1975).

Interpretation of field anomalies requires three basic sets of information: (1) a thorough understanding of the subsurface hydrology (reservoirs, permeabilities, and pressures), (2) a detailed knowledge of the subsurface geology (rock types and uranium concentrations), and (3) empirical relationships between changes in stress, the resulting changes in fracture permeability, and the associated release of radon (and other gases) into the groundwater (as a function of rock-type). The laboratory measurements reported below were designed to explore relationships required in step (3) above. We have focused on the relationships between differential stress, permeability, and the release of radon and methane to water percolating through the natural fracture network in granitic rock.

Previous Laboratory Studies of Radon Emanation and Transport There have been several laboratory studies of radon emanation from rock surfaces. Chiang et al. (1978) demonstrated that radon emanation is proportional to surface area by measuring the radon emanated from a number of rock samples having the same volume but different surface areas. The relation between stress and radon emanation has been studied by the Group of Hydrochemistry of the Peking Seismological Brigade (1977), Holub and Brady (1981), and Jiang and Li (1981). In each of these experiments, air was circulated around the rock sample (or through holes bored in the sample in the 1977 study? al; uniaxial stress was applied. Radon levels in this circulating air were continuously monitored. In the two Chinese experiments only small increases in radon were observed during the uniaxial loading. Holub and Brady (1981) observed a 1arge (50%) temporary increase in radon at about half the breaking strength of the sample, presumably due to the opening of axial microfractures at the onset of dilatancy. In all three experiments, the radon level increased by a factor between two and ten upon failure, probably reflecting the large increase in surface area directly accessible to the circulating gas.

The fundamental difference between these studies and our experimental work described below is that the above studies measured radon emanation from the surface of rock samples while we measured the radon released to water percolating through the microfracture system. We are thus able to look for quantitative correlations between radon release and stress, permeability, porosity, hydraulic radius, and crack surface area.

Experimental Apparatus The experimental apparatus is shown schematically in Figure 1 below. The triaxial pressure vessel is standard except for an outlet at the base to allow sampling of the pore water.

fig. 1

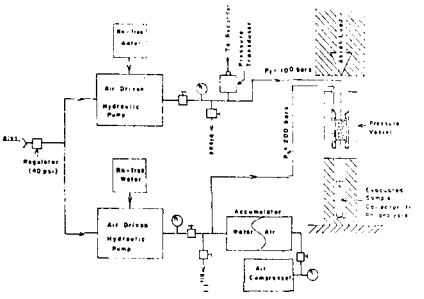

A cylindrical granite sample (two inches in diameter by four inches long) is loaded in the triaxial cell which is placed between the anvils of a 160,000 pound hydraulic press. This uniaxial stress is sufficient to cause failure of the samples under our nominal 200 bar confining pressure.

Confining pressure, σ_3, and flow pressure, p_f, are generated by air-driven hydraulic pumps with special stainless steel valve isolation chambers to maintain water purity. Radon free distilled water is flowed through the sample at constant flow pressure p_f of 100 bars. A one millimeter thick layer of 200 mesh ZrC powder spreads the water at p_f over the entire top surface area, A, of the sample. The lower surface of the sample is maintained at p=o since we are sampling into a vacuum. The base-plate has a pattern of radial and circumferential grooves which channel the flow water into the collection outlet hole. By measuring the amount of water as a function of time, the flow rate, $q(cm^3/sec)$, is determined. Darcy's law may then be used to calculate the sample permeability, k (cm^2), according to

$$k=-q\mu l/Ap_f \qquad (1)$$

where 1 is the sample length in cm and μ is the water viscosity in dynes sec/cm^2. We have been working at low values of the confining pressure (σ_3 nominally 200 bars). The functions of the confining pressure are (1) to seal the rubber sample jacket thus confining the fracture fluid within the sample, and (2) to maintain sample integrity at high values of uniaxial stress.

Granite Samples Approximately twenty feet of granite core was supplied by the U.S.G.S. The core is from the depth range 425-445 feet in the Sierra Nevada batholith, is very fresh, and appears both compositionally and mechanically uniform over its entire length. Radiogenic analysis of six samples (chosen as representing extremes in observed radon production as discussed below) showed U^{238} concentrations between 2.50 and 3.10 ppm. Uranium concentration was uncorrelated with Rn^{222} concentrations observed in the percolating water.

Rn^{222} Measurement Techniques Water samples were collected in evacuated pyrex test-tubes sketched below. Typical water samples were between 2 and 10 ml.

fig. 2

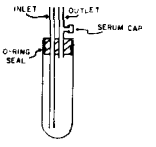

Radon was extracted from the water using recirculating helium as a carrier (e.g. Key et al., 1979). Radon was separated from the He carrier by two stages of liquid nitrogen cold-trapping. A drying column ($CaSO_4$+Ascarite) was used to separate CO_2 and H_2O from Rn^{222} which was subsequently transferred to a scintillation cell. Radon gas levels were measured by counting scintillations associated with its α decay. The overall detection efficiency is about 80% as established by analyzing Ra^{226} standard solutions. The background level is 0.7 cpm (counts per minute)*; our experimental measurements are always at least a factor of four above this limit. Note that radon dpm (disintegrations per minute) reported below are less than the total observed cpm since the two alpha emitting daughters of Rn^{222} (Po^{218} and Po^{214}) are detected with the same efficiency as their parent.

CH_4 and CO_2 Measurement Techniques Before radon was extracted from some water samples, small (~ 1 cc) aliquots of the gas phase in the sample container were drawn into glass syringes through a rubber septum. These samples were injected into a gas chromatagraph equipped with flame ionization and thermal conductivity detectors. CH_4 was isolated from other gases on a molecular sieve #5A column and CO_2 was isolated on a silica gel column. This sampling technique resulted in contamination of the sample with air, and typically 50-70% of the CH_4 and CO_2 peaks observed were due to this contamination. However, clearly detectable amounts of these two gases were released in most experiments. Analytical precision for duplicate analyses was about 8%. Blanks were run on the water before it passed through the rock to ensure that this was not a significant source of contamination. The total quantity of gas released from each sample was calculated by assuming equilibrium exists between liquid and gas in the sample container, knowing the volume of the gas and liquid phases in the container, and correcting for contamination from air (which was estimated from the O_2 content).

Experimental Procedures and Results Two series of experiments were run: experiments on initially dry rocks where a single water sample was collected, and experiments on dry and initially saturated rocks where sequential water samples were collected. In this second series the concentration of CH_4 and CO_2 were measured in addition to Rn^{222}.

In the initial series of experiments, a dry rock was jacketed and stressed axially to σ_1, under a confining pressure of σ_3. An evacuated sample collection vessel was then attached to the collection port in the baseplate, and a flow pressure, p_f, was established at the upper end of the sample at time t=o. The time at which the first drop of water appeared at the baseplate, t_f, was recorded, as was the time, t_s, when the sample bottle was sealed and removed. As discussed above, $\Delta t = t_s - t_f$ and the total volume were used to find the sample permeability. We show below that t_f may be used to find the sample porosity once the permeability is known.

The sealed sample vessel was then attached directly to the radon extraction apparatus and the radon concentration determined as discussed above. Following the radon extraction, σ_1 was increased slowly (40 bars/min) and the fracture stress, σ_f, was recorded.

The results of this first series of experiments are plotted as open circles in Figures 3-5.

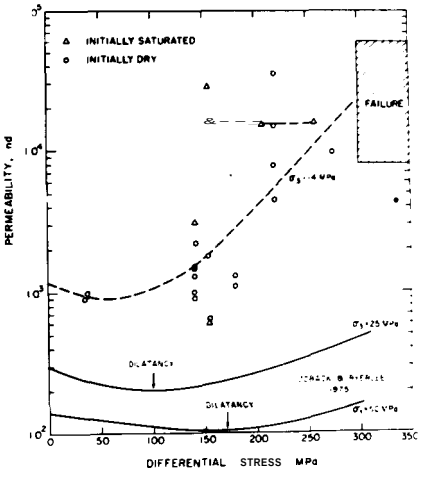

fig. 3

Figure 3 shows sample permeability, k, as a function of stress. Although the data scatter, they are consistent with a slight decrease in k with increasing σ_1 to approximately $\sigma_1 = \sigma_f/2$, followed by a more rapid increase in k as σ_1 approaches σ_f (as documented by Zoback and Byerlee (1975) at higher confining pressures). Our scatter is due to the fact that each data point represents a different rock, whereas Zoback and Byerlee measured k as a function of σ_1 on one sample. Figure 4 shows radon concentration in the first three grams of water collected as a function of the differential stress, $\sigma_1 - \sigma_3$. Note that there is no obvious relation between stress and radon. If the radon concentration is plotted as a function of the differential stress normalized to the fracture stress, $(\sigma_1 - \sigma_3)/\sigma_f$, there is still no obvious correlation.

*1 Curie = 2.2×10^{12} cpm

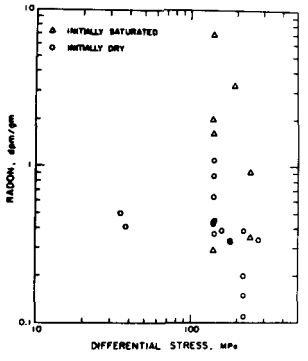

fig. 4

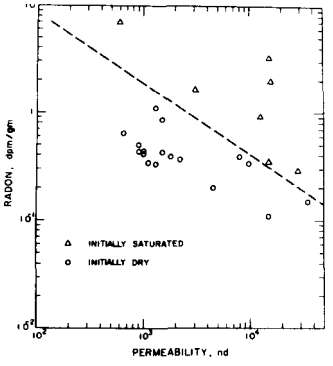

fig. 5

Figure 5 shows that radon concentration tends to decrease with increasing permeability.

The second set of experiments were designed to see if saturated rocks yield more radon than those which are initially dry. Several rock samples were stressed and saturated as above until the first drop of water was observed. They were then removed from the apparatus and stored under water for approximately one month to allow radon to establish an equilibrium concentration. They were then restressed and several successive water samples were collected. Sequential sampling experiments were also performed on two initially dry rocks for comparison.

The radon concentrations measured in the first three grams of water collected during these runs are plotted as open triangles in Figures 3-5. In Figure 5 it is apparent that, at a given permeability, the presence of water in the fracture network increases the radon release by a factor between two and ten.

fig. 6

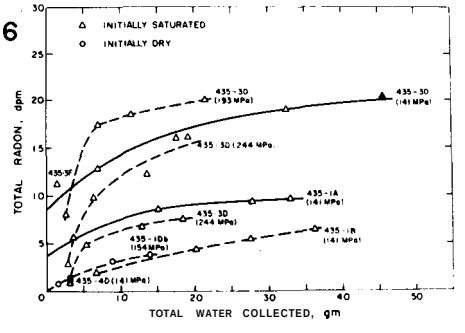

The results of the sequential sampling experiments are given in Figures 6 and 7 for radon and Figure 8 for nethane.

In Figure 6, the total radon is plotted as a function of the total water collected. The solid curves are calculated from a crack model discussed below. The dashed curves are sketched through data sets which could not be fit to the model.

fig. 7

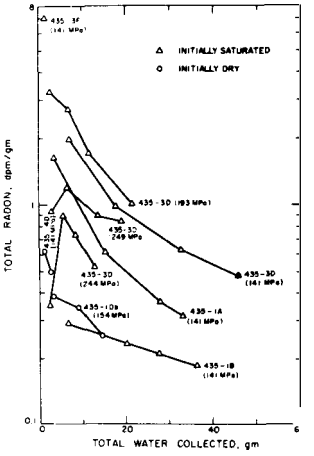

Figure 7 shows the radon concentration which would be measured if the experiment were stopped after the total amount of water shown on the abscissa had been collected.

Note that four of these multiple sample runs were on the same rock (435-3D). This rock was initially saturated, equilibrated, and then restressed to a differential stress of 141 MPa. Three successive water samples were collected. The stress was then increased to 193 MPa and a fourth sample was collected. This fourth point, the solid triangle in Figures 6 and 7, is on trend with the previous three points and shows no significant increase in radon following the stress change. The rock was then removed from the apparatus, re-equilibrated under water, and restressed to 193 MPa. The four, sequential, water samples collected at this stress contained slightly more radon (much less than a factor of two) than the 141 MPa run. The rock was removed, re-equilibrated, and then stressed to 244 MPa. Four samples were again taken, but this time an unusually low radon concentration was measured. The sample was observed to have developed a through-going, extensive fracture zone. Because the low radon level for this run is due almost entirely to the low concentration in the first sample collected, the rock was re-equilibrated and rerun at 244 MPa as a check. Again, the radon concentration in the first sample was anomalously low when compared with the other multiple sample runs.

In Figure 8, the total methane released is plotted as a function of the total water collected.

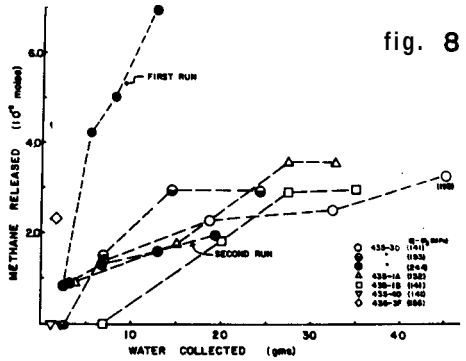

fig. 8

Note that the general shape of these curves is similar to the radon curves in Figure 6, but there are significant differences. More total water flow was required to extract all the available CH_4; in fact, some rocks released almost no methane to the first few grams of flow water. Also, the rock which was run at three different stresses (435-3D) released more methane at higher stresses. Even the stress change from 141 MPa to 193 MPa during the first run produced an increase in CH_4 concentration, while the Rn^{222} concentration was unaffected.

Carbon dioxide was more erratic than methane or radon when plotted as a function of total water collected. There was no apparent correlation between CH_4, CO_2, and Rn^{222}. Our interpretation of these results is that each of these gases must occupy different positions in the rock.

Sample Porosity and Hydraulic Radius The porosity of the sample under stress may be calculated from t_f, the time it takes to fill the initially dry rock with water. Following Brace et al. (1968) we approximate the flow law as $d^2p/dx^2 = 0$. Hence $dp/dx = f(t)$, i.e. the pressure gradient is approximated by a linear gradient which changes with time. Brace et al. (1968) have shown that transients due to %e— neglected terms are on the order of 10-30 sec. Since it takes at least an hour for our samples to fill, the linear gradient should be a good first approximation.

As water is pumped into the rock at a constant back-pressure, p_f, the water front will advance in the axial z direction at a rate

$$dz/dt = q/\eta A \qquad (2)$$

where η is the porosity. Using Darcy's law (1) for q gives

$$dz/dt = - kp_f/\mu\eta z \qquad (3)$$

which may be integrated to yield

$$\eta = 2kp_f t_f/\mu l^2 \qquad (4)$$

Once the porosity and permeability are known, the hydraulic radius, m, may be found (m is defined as the volume of the cracks divided by their surface area). For intact rock, Brace (1978) gives

$$k = m^2\eta^3/k_o \qquad (5)$$

where k, is a geometrical factor between 2 and 3, while for dilatant microcracks in low porosity rock, permeability in the direction of the microcracks has the form

$$k = m^2\eta/k_o \qquad (6)$$

For our samples the above analysis yielded porosities in the range 0.2% to 10%. Plotting porosity as a function of permeability yields k proportional to η^2, between the η^3 dependence of (5) and the linear dependence of (6). The implication is that the microcrack orientations are somewhere between random and vertical. The observed radon release did not correlate with pore volume, hydraulic radius, or crack surface area.

Models for Radon Release We consider two extreme-case models for the radon extraction process: (1) a well-mixed reservoir model, and (2) a pipe-flow model.

In the reservoir model, we assume that

$$dn_r/dt = - qn_r/V_c \qquad (7)$$

where n_r is the number of accessible radon atoms in the rock and V_c is the crack volume. Using $q \equiv dV/dt$ and $n_r + n_w = N_o$ where N_o is the total accessible radon and n_w is the number of accessible radon atoms in the flow water, (2) may be rewritten and solved to give

$$n_w = N_o[1-\exp(-V/V_c)] \qquad (8)$$

In terms of radon activity $a=\lambda n$ ($\lambda=1.26 \times 10^{-4}$ min^{-1})

$$a_w = A_o[1-\exp(1-V/V_c)] \qquad (9)$$

Only our dry samples, 435-4D and 435-1Db could be fit to this model (solid lines in Figure 6). They both lie on the same curve which is defined by the parameters A_o = 4.6 dpm and V_c = 9.0 cm^3. The total radon activity in these rocks should be 1.2 x 10^3 dpm (based on 3 ppm uranium). Hence we are removing about 0.4% of the available radon. A crack volume of 9 cm^3 corresponds to porosity (under stress) of about 4.5%, which seems a bit high.

None of the wet rocks could be fit to this model because the total radon curves in Figure 6 have too sharp a "knee" for the exponential form in (9). Such behavior is more typical of a pipe model which assumes all the radon is in solution and is simply pushed out by the advancing flow water with no mixing. In this case, Figures 6 and 7 should appear as sketched

below.

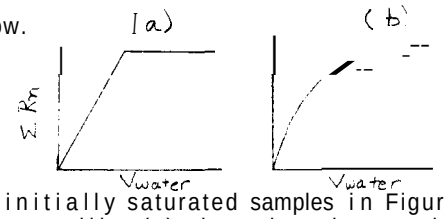

The initially saturated samples in Figure 6 look more like (a) above than the smooth curve predicted by (9). The true situation probably lies between these two extreme models, i.e. the water moves through as in a pipe model, but is continually being fed by side channels in the crack network thus rounding the sharp corners in (a) and (b) above.

Summary of Results We can briefly summarize our interpretation of the results presented in the previous section.

a. There was no correlation between radon released and stress applied to the initially dry samples. Among several possible explanations of this observation are: (1) the new microfractures opened by the higher stresses do not connect with the network of fractures which are carrying the water, and/or they do not carry a significant fraction of the water or (2) these new microfractures carry a significant fraction of the percolating water but they do not contain significant radon. They might not contain radon either because only pre-existing cracks have had time to concentrate and trap significant radon, or because radium is preferentially located as secondary surface coatings on existing cracks and this radium is responsible for virtually all of the observed Rn emanation (Tanner, 1980).

Explanation (1) is consistent with microscopic observations (Brace, 1977), but not with the results of the stress change experiment on sample 435-3D. The observation that Rn did not change while methane increased in response to a stress change during the first run on this sample implies that the flow water "saw" the new microcracks and removed the methane, but that there was no radon to be removed.

b. Samples which were saturated with water released more radon than those which were initially dry. These observations are not surprising in light of Tanner's (1980) discussion of the role of water as an absorber of the radon's recoil energy. Thus, the amount of water and the distribution of this water in the rock are critical factors controlling radon release.

c. Permeability and radon release are inversely correlated. This may be interpreted in two ways. Either water flows through the rock so quickly that radon does not have time to diffuse from side channels, or most of the water flows through a few, large, main channels (rather than many small channels) and thus removes a smaller fraction of the accessible radon atoms produced in the rock.

The hypothesis which is consistent with all our observations is that most of the observed radon is derived from radium which has been deposited on the walls of old microcracks. We are currently performing a series of experiments to test this hypothesis.

References

Brace, W. F., J. B. Walsh, and W. T. Frangos, "Permeability of granite under high pressure," J. Geophys. Res., 73, 2225-2236.

Brace, W. F. (1977), "Permeability from resistivity and pore shape," J. Geophys. Res., 82, 334313349.'

Brace, W. F. (1978), "A note on permeability changes in geological material due to stress," Pageoph,, 116, 627-633.

Chiang, J. H., W. S. Moore, and P. Talwani (1977), "Laboratory studies of the relationship between surface area and radon release in Henderson gneiss," Trans. Am. Geophys., 58, 434.

Hauksson, E. (1981), "Radon content of groundwater as an earthquake precursor: evaluation of worldwide data and physical basis," J. Geophys. Res., 86, 9397-9410.

Holub, R. F., and B. T. Brady (1981), "The effect of stress on radon emanation from rock," J. Geophys. Res., 86, 1776-1784.

Jiang, F., and G. Li (1981a), "The application of geochemical methods in earthquake prediction in China," Geophys. Res. Letters, 8, 469-472.

Key, R. M., R. L. Brewer, J. H. Stockwell, N. L. Guinasso Jr., and D. R. Schink (1979), "Some improved techniques for measuring radon and radium in marine sediments and in seawater," Marine Chemistry, 7, 251-264.

Stoker, A. K., and P. Kruger (1975), "Radon measurements in geothermal systems," Stanford Geothermal Program, Technical Report #4.

Tanner, A. B. (1980), "Radon migration in the ground: a supplementary review," Natural Radiation Environment, vol. 3, 5.

Teng, T. L. (1980), "Some recent studies on groundwater radon content as an earthquake precursor," J. Geophys. Res., 85, 3089-3099.

The Group of Hydro-Chemistry, The Seismological Brigade of Peking (1977), "An experimental study of the relation between rock rupture and variation of radon content," Acta Geophysica Sinica, 20, No. 4, 277-282.

Zoback, M. D., and J. D. Byerlee (1975), "The effect of microcrack dilatancy on the permeability of westerly granite," J. Geophys. Res., 80, 752.

Proceedings Seventh Workshop Geothermal Reservoir Engineering
Stanford, December 1981. SGP-TR-55.

INTERSTITIAL FLUID PRESSURE SIGNAL PROPAGATION ALONG FRACTURE LADDERS

Gunnar Bodvarsson

School of Oceanography
Oregon State University
Corvallis, Oregon 97331

Abstract Arrays of interconnected permeable fracture spaces that form fracture ladders propagate small amplitude fluid pressure signals in much the same way as slabs of porous formations. Data from geothermal fields in Iceland indicate that the fracture width there is of the order of 1 to 2 mm and the signal diffusivity 20 to 100 m^2/s. Well interference tests are not likely to furnish data to distinguish between fracture ladders and equivalent porous slabs.

Introduction The majority of medium to high-temperature geothermal systems are embedded in formations of igneous origin that generally are characterized by a fracture dominated fluid conductivity. The fractures are of elastomechanical/tectonic and/or thermoelastic or possibly chemoelastic origin. The fracture conductivity is invariably highly heterogeneous, anisotropic and is quite often confined to flat sheet-like structures such as fault zones and volcanic dikes. Quantitative relations relevant to axisymmetric Darcy type flow in homogeneous/isotropic porous media generally do not apply to such situations and an uncritical standard type interpretation of well test data from fractured reservoirs is therefore likely to lead to faulty conclusions. Unfortunately, since little is known about the dimensions and distribution of fractures in the various types of natural settings, it is difficult or even impossible to derive relevant quantitative relations. It is, nevertheless, of considerable interest to obtain some measure of the discrepancy that would result from an application of the standard interpretational procedures. The purpose of this short note is to discuss a few very simple concepts and relations that are useful in the present context.

The Fracture Ladder For the present purpose, we will consider a specific case of a composite fracture conductor consisting of a linear array of interconnected individual fracture spaces of similar dimensions as displayed in Fig. 1. We will refer to this system as a fracture ladder. The individual fractures or ladder-elements are assumed to have a quasi-rectangular shape with a characteristic edge length L. The two surfaces are welded together at the edges. The width of the open fracture space may vary over the L x L element area, and there may even be some asperities where the opposite surfaces meet, but we assume that they touch without a solid weld. From the elastomechanical point of view, the fracture element acts as an open space of an edge length L. Moreover, we assume that with regard to fluid flow, the fracture element has a well defined average flow width h. No specific assumptions have to be made as to the type of interconnection except that the fluid can flow freely between adjacent ladder elements and that the specific flow conductance can be taken to be approximately uniform over the length of the ladder. Obviously, it is possible to generalize this model by envisioning a system of parallel ladders that are interconnected along their entire length and form a fracture sheet.

The principal physical parameters of the linear ladder consisting of one strand of elements are easily defined. At steady-state laminar flow conditions, the vertically integrated fluid conductivity of a fracture space of width h between two parallel planes that would be referred to as the transmissivity c_F is obtained on the basis of the well known cubic law (Lamb, 1932)

$$c_F = h^3/12\nu \qquad (1)$$

where ν is the kinematic viscosity of the fluid. At these conditions, the mass flow through a unit length of the fracture is $q = c_F \nabla p$ where ∇p is the pressure gradient, and hence the local flow over the ladder is $Q = Lc_F \nabla p$.

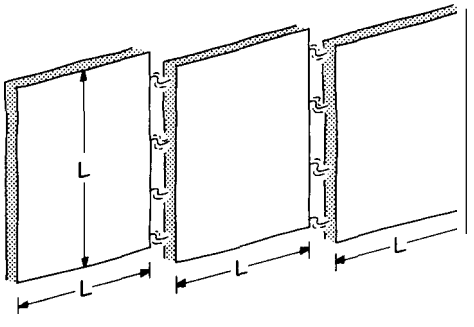

Figure 1 The Fracture Ladder

lo obtain the hydraulic capacitivity or storage coefficient of the ladder, we assume that the element walls are elastic Hookean with a rigidity μ. Moreover, let the volume elastance of a fracture space of volume V be defined by $e = dV/dp$ where p is the internal pressure that is assumed to be uniform, Since no analytical expression is available for the elastance of a rectangular fracture element, we will resort to approximating the element by a circular or penny-shaped element of equal area such that the diameter is 1.12L. The elastance of the penny-shaped cavity of diameter d has been obtained by Sneddon (1346) as $e = d^3/4\mu$ where Poisson's relation of equal Lame parameters has been assumed. Based on this result the elastance of a fracture element would approximately be $e = (1.12L)^3/4\mu$ or about $L^3/3\mu$. Hence, the elastance per unit area, that is, the capacitivity is

$$s_F = (L/3\mu) + h\kappa \qquad (2)$$

where κ is the compressibility of the fluid. We can usually take that μ is of the order of 10^{10} to 2×10^{10} Pa and assuming that the fluid is liquid water with $\kappa = 5 \times 10^{-10}$ Pa^{-1}, the product $\kappa\mu = 5$ to 10. The second term on the right of *(2)* can then be neglected when $L >> 30h$. In general, this condition holds and we will therefore simplify the expression for s_F by neglecting the fluid compressibility term. It is to be noted that the above expression for s_F neglects the possible presence of' satellite fracture that may contribute to the capacitivity.

On the basis of (1) and the simplified version of *(2)* follows the laminar flow diffusivity of the ladder

$$a_F = c_F/\rho s_F = h^3\mu/4L\eta \qquad (3)$$

where η is the absolute viscosity of the fluid. Moreover, there may be leakage from the fracture ladder into the adjacent formation. On a linear laminar flow model, the fluid loss per unit area of the ladder would be characterized by a coefficient b such that the leakage is bp where p is the fluid pressure in the ladder. We have no way of arriving at any expressions for this coefficient that has to be treated as a purely experimental parameter.

The Ladder and the Porous Slab It is interesting to compare the parameters of the fracture ladder to those of a homogeneous/isotropic porous slab with Darcy type flow of the thickness H, permeability k and hydraulic capacitivity (storage coefficient) s. The thickness of the slab of equal transmissivity is obtained by

$$kH/\nu = h^3/12\nu \qquad (4)$$

such that

$$H = h^3/12k \qquad (5)$$

Moreover, assuming equal transmissivity, the ratio of the diffusivities is

$$a_S/a_F = L/3\mu sH \qquad (6)$$

Finally assuming equal diffusivities, the ratio of the transmissivities is

$$c_S/c_F = 3\mu sH/L \qquad (7)$$

Borehole/Fracture Contacts It is quite evident that because of the small cross sections available, the local flow-velocities from fracture spaces into boreholes may be quite high and the flow regime therefore highly turbulent. The above relation for the laminar type transmissivity is then invalid and has to be revised. The resulting relatively large fracture/borehole contact resistance can be derived as follows.

Consider a borehole of diameter D which cuts a horizontal fracture of width h as shown in Fig. 2. Let the fluid be incompressible, of density ρ and the mass flow out of the fracture be M Moreover, let the fluid pressure at a distance r from the center of the hole be p(r) and the fluid velocity there be v(r).

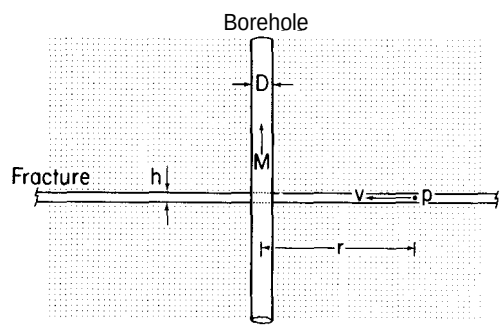

Figure 2 Borehole/Fracture Contact

We have then

$$M = 2\pi rh\rho v \quad \text{or} \quad v = M/2\pi rh\rho \qquad (8)$$

The pressure loss over the distance dr is due to the conversion of potential energy into kinetic energy and friction heat, viz.

$$dp = -\rho v dv + (f\rho v^2 dr/2h) \qquad (9)$$

the wall friction is represented by the second term on the right of this equation that is derived in the same manner as for the case of pipes and where f is the friction coefficient of the fracture. Assuming that the formation pressure at a large distance from the borehole is p_o this equation is easily integrated for p and we obtain

$$p = p_o - (M^2/8\pi^2h^2\rho)[(1/r^2) + (f/hr)] \qquad (10)$$

If the pressure in the borehole is p_b, the following expression is obtained for the mass flow into the hole

$$M = \pi\sqrt{2}\, hD\, [\rho(p_o - p_b)/(1+(fD/2h))]^{1/2} \qquad (11)$$

Abbreviating $(p_o - p_b) = \Delta p$ and $(1/\pi\sqrt{2}) = 0.23$, we define the contact resistance of the borehole

$$R = \Delta p/M = (0.23/hD)[(\Delta p/\rho)(1+(fD/2h))]^{1/2} \qquad (12)$$

Clearly, these results hold only for the turbulent region around the borehole. Little data is available on the values of the friction coefficient **f** for natural fractures, but based on experimental data for pipes with rough walls, we can expect that $f \sim 0.05$ to 0.10 (see, for example Moody, 1947). It should be pointed out that because of the quadratic terms in (9), the mass flow M is not a linear function of Δp and R therefore depends on Δp. The principal application of equation (11) is for the estimating of the fracture width h in field cases where M and Ap are known.

Field Data Little information is available on the dimensions of fractures in nature. Perhaps the most accessible extensive data is on some of the geothermal reservoirs in Iceland (Thorsteinsson, 1976, Bjornsson, 1979). It is well known that the hydrological systems of Iceland are embedded in fracture dominated flood-basalts of late Tertiary to Pleistocene age. This material enables us to make attempts at estimating fracture widths in some of the Iceland reservoirs. Very briefly, we can proceed as follows.

(1) Borehole production data in various geothermal fields in Iceland indicate that major fracture conductors can produce mass flows from a few up to a few tens of kg/s at pressure differentials of a few 10^5 Pa. A figure of M = 10 kg/s at $\Delta p = 4 \times 10^5$ Pa is quite representative of the performance of a productive individual fracture in a borehole of D = 0.22 m. Assuming that the conditions set forth in the previous section hold, equation (11) with **f** = 0.06 gives then an estimate of h = 1.3 mm.

(2) Well interference testing in 4 geothermal fields in Southwestern Iceland have yielded transmissivities of $c_F = 2.6 \times 10^{-4}$ to 25×10^{-4} ms. Reinterpreting these results in terms of single fracture systems flowing water at 100°C with $\nu = 3 \times 10^{-7}$ m²/s, we obtain with the help of equation (1) above the estimate of h = 1 to 2 mm. Moreover, during the same tests, unit area capacitivities (storage coefficients) of $s_F = 1 \times 10^{-8}$ to 4×10^{-8} m/Pa were obtained. Equation (2) then yields estimates of L = 400 to 1600 m and the resulting diffusivities are $a_F = 20$ to 100 m²/s.

(3) It is of interest to note that fracture widths can also be estimated on the basis of the overall flow resistance in individual geothermal systems. Knowing the distance of recharge, the available pressure differential and other parameters, it is possible to arrive at estimates of an average h. The present writer has obtained along these lines results that compare well with the above estimates. Unfortunately, space does not permit a discussion of this method.

Signal Propagation On the above premises, we now arrive at the basic equation for the propagation of pressure signals along a fracture ladder. Assuming a homogeneous/isotropic flat ladder and neglecting inertia forces, the basic equation is the diffusion equation in two spatial dimensions for the fluid pressure **p**, viz. ,

$$\rho s_F \partial_t p + bp + c_F \Pi_2 p = m \qquad (13)$$

where ρ is the density of the fluid, $\Pi_2 = -\nabla_2$ is the Laplacian in two dimensions and m is a source density. The leakage term on the left can be eliminated by a transformation $p = u \cdot \exp(-bt)$ where u is a new dependent variable. The principal small amplitude propagation parameters, the penetration depth and the skin depth (assuming b = 0)

$$d_p = (a_F t)^{1/2} \quad \text{and} \quad d_s = (2a_F/\omega)^{1/2} \qquad (14)$$

where **t** is time and ω the angular frequency, follow then in the usual way.

The pressure signal diffusivities indicated by the Iceland data are quite high and signal propagation therefore rapid. For example, at $a_F = 50$ m²/s the penetration depth for a period of 10^4 s is about 700 m. It is interesting to note that the fracture structures simulate porous slabs of H = 20 to 60 m and permeabilities of the order of $k = 10^{-11} = 10$ darcy. The global permeabilities of the host systems appear, nevertheless, to be orders of magnitude smaller (Bodvarsson and Zais, 1978).

Under the circumstances assumed here, an interference test would not provide data to distinguish between the two models, the ladder and the slab, and an interpretation on the basis of slabs only can therefore lead *to* erroneous conclusions.

References

Bjornsson, A. , 1979, (editor), "The Akureyri District Heating System," Report OS JHD 7827 by the National Energy Authority, Reykjavik.

Bodvarsson, G. and E. Zais, 1978, "A Field Example of Free Surface Testing," Workshop on Geothermal Reservoir Engineering, December, 1978, Stanford University, Stanford, CA.

Lamb, H., 1932, "Hydrodynamics," 6th ed. , Dover Publications, New York, N.Y., 738 pp.

Moody, L. F., "An approximate formula for Pipe Friction Factors," Mech. Eng. 69 (1947) 1005.

Sneddon, I. N., 1946, "The Distribution of Stress in the Neighbourhood of a Crack in an Elastic Solid," Proc. Roy. Soc., 187, 229.

Thorsteinsson, T. , 1976, 'Redevelopment of the Reykir Hydrothermal System in Southwestern Iceland," Second U.N. Symposium on the Development and Use of Geothermal Resources, San Francisco, 1975.

Proceedings Seventh Workshop Geothermal Reservoir Engineering
Stanford, December 1981. SGP-TR-55.

MEASURED ENTHALPY COMBINED WITH CHEMICAL CONCENTRATION DATA TO DIAGNOSE RESERVOIR BEHAVIOUR

M. SALTUKLAROGLU

ELC - ELECTROCONSULT (ITALY)

ABSTRACT: Concentrations of chemicals such as Cl and Na in a geothermal water separated at atmospheric pressure (at a silencer), or any other pressure, when related to the measured enthalpy of the produced steam/water mixture are indicative of reservoir production conditions. Achieving this relation by means of a mathematically meaningful graphical method, conditions in the reservoir such as boiling, steam gain or loss, heating or cooling (by conduction or mixing) can be inferred, and the fluids of different wells can be related. The method is illustrated with data obtained from Los Azufres Geothermal Field in Mexico.

INTRODUCTION: The relation between the enthalpy of a geothermal fluid and the concentrations of chemicals within the separated water has been long recognised and made use of. As early as 1967 Wilson et al.(1) used the changes in chloride concentrations of waters from Wairakei wells to calculate the underground changes in enthalpy, and by comparing their figures with the actually measured values they could comment on the production conditions within the reservoir. Later on Wilson (2) again dealt with the idea and published a graphical method by wich dilution of reservoir water or heat gain or loss by the reservoir fluid by means of conduction could be inferred.

The idea has been also applied by Truesdell and Fournier (3,4) and others (5) to relating boiling spring waters of an area and to calculation of their temperatures at depth, by making use of a graphical method, in wich enthalpy is plotted against chloride concentrations in spring waters with cartesian coordinates. The enthalpy is considered as that of water at an underground temperature indicated by geothermometers (silica or Na-K-Ca).

The method presented here and applied to Los Azufres wells has a similar graphical form to that used by Truesdell and Fournier, but with small modifications that make the form of the graph mathematically meaningful, and the enthalpy used is that of the steam/water mixture, as measured at the surface.

METHOD : When a geothermal fluid with an enthalpy of ho and Cl or Na concentrations of Co is produced and separated at atmospheric conditions (at silencer), the concentration of the water fraction would be (See Appendix for derivation and see nomenclature at the end):

$$Cwa = \left(\frac{hsa - hwa}{hsa - ho}\right) Co \qquad \ldots\ldots\ldots\ldots\ldots (1)$$

This mathematical expression can be represented in graphical form as shown in Fig. 1. If the fluid is water at reservoir conditions, Co would be the concentration in the reservoir water. Starting from this initial condition defined as So in Fig. 1, we can examine what would happen to the enthalpy concentration relationship in different cases of reservoir behaviour:

CASE 1. Evaporation in Reservoir (Gain of heat from reservoir rocks). This normally happens when the pressure in the reservoir decreases sufficiently, due to drawdown, for the water to boil. Say the enthalpy of the produced fluid increases to h_1. If all the fraction of the steam formed as a result of this is produced with the associated fraction of water, the state of the fluid would be represented by point S_1 immediately above So, as the concentration of the fluid in the reservoir (steam/water mixture) would stay the same. However, now, because of the increased enthalpy the concentration in the water separated at atmospheric conditions (Cwal) would be higher (Cwal > Cwa). Also due to the decrease in pressure, the temperature would decrease (assuming boiling in the formation), and the water fraction would have an enthalpy hwrl and a concentration Cwrl (where hwrl < ho and Cwrl > Co).

However,

$$Co=(1-Xrl)\ Cwrl=(1-Xal)\ Cwal \qquad \ldots\ldots\ldots\ldots (2)$$

$$\text{or } Co=\left(\frac{hsrl - hl}{hsrl - hwrl}\right) Cwrl=\left(\frac{hsa - hl}{hsa - hwa}\right) Cwal \ldots (3)$$

Therefore, evolution of a well with the points plotted on a diagram like in Fig. 2, and moving along line SoS1 would be indicative of this particular case.

However, because of the relative permeability effects steam and water may not enter into the flow in the same fractions as they may exist in the reservoir around the wellbottom. In other words, although due to evaporation in the reservoir an average steam fraction of Xrl can exist

arcund the wellbottom, corresponding to the enthalpy hl, the fluid which enters the well may have a different steam qualite (Xrl') Then:

Xrl' > Xrl, if there is steam gain (relatively more steam enters the flow)

Xrl" < Xrl, if there is steam loss, (relatively more water enters the flow, that is some steam is lost to the formations above before it *can* enter into the flow).

CASE 1.1. Steam Gain (Xrl' > Xrl) (See Fig.2) In this case the entalpy of the production would be hl', with the state being defined by the point Sl'. Then,

hl' > hl > ho, and it can be shown that (See **Appendix**) :

$$Cwal' = Cwrl \left(\frac{hsa - hwa}{hsrl - hwrl}\right)\left(\frac{hsrl - hl'}{hsa - hl'}\right) \quad \ldots\ldots\ldots(4)$$

But, from equation (3):

$$Cwal = Cwrl \left(\frac{hsa - hwa}{hsrl - hwrl}\right)\left(\frac{hsrl - hl}{hsa - hl}\right)$$

However, $\frac{hsrl - hl'}{hsa - hl'} \simeq \frac{hsrl - hl}{hsa - hl}$

Then $Cwal' = Cwal$ .....(5)

Also $\frac{Cl'}{Cwal'} = \frac{hsa - hl'}{hsa - hwa} \simeq \frac{Cl'}{Cwal}$ .....(6)

Therefore, it can be seen that Sl' is approximately on the hsa - Cwal line and movement of plctted points from Sl to Sl' along this line muld indicate steam gain.

This condition is similar to the case where steam enters the production from another level and yet no boiling may take place in the formatiCn, which is considered below as case 2.

~~CASE 1.2.~~ Steam Loss (Xrl" < Xrl) Similary it *can* be shown in this case that the pints would move down the hsa - Cwal line, like the point Sl". The enthalpy hl" would be smaller than hl.

~~W E 2.~~ Steam Gain or Loss without Boiling in the Reservoir As pointed out above this is very similar to Case 1.1. If the production enthalpy is h2 (h2 > ho) it can be shown that (assuming the temperature difference between the steam and water flows is negligible):

$$Cwa_2 = Co \left(\frac{hsa - hwa}{hsa - h2}\right)\left(\frac{hsr2 - h2}{hsr2 - ho}\right) \quad \ldots\ldots\ldots(7)$$

(See **Appendix** for derivation)

But, $Cwa = Co \left(\frac{hsa - hwa}{hsa - ho}\right)$ (equation 1)

and $\left(\frac{hsa - ho}{hsa - h2}\right)\left(\frac{hsr2 - h2}{hsr2 - ho}\right) \simeq 1$, ...(8)

Therefore, $Cwa2 \simeq Cwa$ .....(9)

This would mean that, the new condition point S2 is moving from So upwards along aproximately the hsa - Cwa line (See Fig. 3).

Therefore evolution of a well from the initial condition (So) along aproximately the initial condition line hsa - Cwa would mean steam gain from a different level with negligible or no additional steam forming in the formation from which the main water production comes. However, steam gain from evaporation in the formation would result in a path either like SoSlSI' or more likely move along SoSl' as the resultant of two componentprocesses. It is nevertheless obvious that it may be difficult to diferentiate between this case and the case 1.1, if the initial conditions of the well are not known.

In the case of steam loss the condition points would move downwards along the hsa - Cwa line.

CASE 3. Conductive Heating or Cooling Evaporation in the reservoir is reallv a special form of the conductive heating case. However, if the conditions do not permit evaporation and if there is conductive heating the condition of the well would evolve along So Sl, with an enthalpy hl, where:

N = hwrl > ho

and Cwrl = Co = Cl, Cwal > Cwa

As the relative permeability effects are normally present, a pure case of evaporation in the reservoir with condition points moving along So Sl muld be unlikely. If, however, this behaviour exists it is more likely to pint out to a conductive heating case without boiling taking place in the reservoir (However, this should also be checked by the enthalpy value).
The movement of the condition points in the opposite direction (with decreasing enthalpy) would indicate conductive cooling which may happen if a fluid has to travel across a cooler terrain to get to the well, as a result of the evolution of the field conditions. (See pint S3 in Fig. 4).

CASE 4. Heating or Cooling by Mixing Depending on the enthalpy of the mixing fluids, heating or cooling may result. If the initial conditions of the mixing (contaminating), fluid are defined by a point M, the points defining the condition of the mixture would move along the line SoM, their exact positions depending on the mixing ratio. Here again evolution of the condition points (enthalpy - concentration relationship) would be diagnostic of what is happening in the reservoir (See pint S4 in Fig. 4).
It is abvious that presence of other information would help to corroborate the deduction or inferences obtained by this method. Where possible this should be looked for in order to have more confidence in the results.

Also, it will be noted that when the initial

conditions of different wells are plotted on the *same* diagram, the conditions of production existing around the bottom of different wells *can* be identified with respect to the wells which seem to **be** producing the originally existing hot water.
In this way, wells within the *same* field, but producing with apparently different enthalpy - concentration relationships may be related.

EXAMPLES: The figures 5 through 9 show data plotted, as explained above, of several wells of Los Azufres Geothermal Field which is located in the state of Michoacan in Central Western Mexico. The geothermal reservoir is formed by volcanic rocks (mainly andesites) and seems to have a steam cap which at some locations is thick and results in *dry* steam production. The maximun temperature encountered is in the order of 300°C.

Figure 5 illustrates the relation between the initial production conditions at different wells. It appears that different wells display different degrees of steam gain or loss. The wells 2, 3, 4 and 18 indicate condition near to that of the hot water.
However, the wells **1**, 8, 13 and 19 show definite steam gain and the wells 7 and 15 indicate steam loss after boiling in the formation. Depending on the actual condition taken as representative of the undiluted hot water, possible conductive heating (4,18,5) or cooling (2,3) can also be inferred, but the data are not accurate enough to say anything definitly at this stage.
In figure 6 the behaviour of well 3 can be seen. Itwill be noted that the well produced a water which most probably was diluted with a water of similar temperature, but of low chemical concentration, possibly condensed steam. Over a period of two months the dilution gradually decreased and the well started producing the undiluted water with a small gain of steam.

Figure 7 shows the behaviour ***of*** well 5. It *can* **be** said that as the production rate increases the behaviour of this well is dominated by steam gain due to evaporation in the formation and probably also from a steam cap. This is confirmed by the production characteristics of the well presented in Fig. 10.

The behaviour of well 13 presented in Fig. 8 is similar, but indicates that the major part of the steam gain is coming from a steam level. The relatively high enthalpy also reflects this. Its production curves are shown in Fig. 11 and confirm these observations.
Finally, Fig. 9 show the behaviour of well 15 which originally produced a fluid which had lost steam. It seems that as the production time increased the well was producing a fluid which was gradually nearing to original reservoir water conditions (less steam loss).

CONCLUSIONS: It has been shown that concentrations of chemicals such as Cl **or** Na in a geothermal water separated at atmospheric conditions (at a silencer), **or** any other pressure, when related to the measured enthalpy of steam/water mixtures are indicative of reservoir conditions Basis of this relationship at different reservoir conditions, a methodology for interpretation and examples of it from a geothermal field in Central Mexico have also been presented.

ACKNOWLEDGEMENTS The author expresses his gratidue to C.F.E. (Comisión Federal de Electricidad) of Mexico for permitting the use of the data.

The author also states that the opinions expressed are his own and not necessarily those of his company **or** of the C.F.E.

REFERENCES 1.-WILSON, S.H.; MAHON, W.A.J., - and ALDOUS K.J. "The Calculation of Underground Changes in Enthalpy from Changes in Chloride Concentration of Waters from Wairakei Drillhole Discharges During 1965" New Zealand Journal of Science Vol. 10, No. 3. Sept. 1967.

2.- WILSON, S.H.; "Statistical Interpretation of Chemical Results from Drillholes as an Aid to Geothermal Prospecting and Exploration" Geothermics, Special Issue 2, 1970. (U.N.Symposium on the Development and Utilization of Geothermal Resources Pisa 1970, Vol. 2 Part. 2).

3.- TRUESDELL, A.H, and FOURNIER, R.O. "Calculation of Deep Temperatures in Geothermal Systems from the Chemistry of Boiling Spring Waters of Mixed Origin" U.N. Symposium San Francisco 1975, Vol. 1.

4.- _ _ _ _ _ _ -"Convective Heat Flow in Yellowstone National Park" U.N. Symposium, San Francisco, 1975, Vol. 1.

5.- CUSICANQUI, H.; MAHON, W.A.J. and ELLIS,A. J. "The Geochemistry of the El Tatio Geothermal Field, Northern Chile" U.N. Symposium, San Francisco 1975. Vol. **1.**

NOMENCLATURE

C Concentration (ppm) of a chemical like Cl or Na.
h Enthalpy
X Steam fraction

Subscripts:

s Steam
w Water
ws Evaporation
o Initial
a At atmospheric conditions
r At reservoir conditions
1, 2, 3, 4 cases considered

APPENDIX

Water fraction at atmospheric conditions: 1-Xa

$$Xa = \frac{ho - hwa}{hwsa} \quad \ldots\ldots\ldots (A.1)$$

$$1\text{-}Xa = \frac{hsa - ho}{hwsa} = \frac{hsa - ho}{hsa - hwa} \quad \ldots (A.2)$$

As all the Cl concentration intially in **a** unit mass of **fluid** muld now be concentred within this water fraction:

$$(1\text{-}Xa)\ Cwa = Co \quad \ldots\ldots\ldots (A.3)$$

$$Cwa = \frac{Co}{1\text{-}Xa} = \left(\frac{hsa - hwa}{hsa - ho}\right) Co \quad \ldots (A.4)$$

CASE 1.1. If the concentration around the well bottom within the reservoir is now Cl', with the same reasoning:

$$Cl' = Cwrl'\left(\frac{hsrl - hl'}{hsrl - hwrl}\right) = Cwal'\left(\frac{hsa - hl'}{hsa - hwa}\right)$$

$$\ldots\ldots (A.5)$$

The concentration within the water fraction does not change.

Therefore Cwrl' = Cwrl.

$$Cwal' = Cwrl\left(\frac{hsa - hwa}{hsrl - hwrl}\right)\left(\frac{hsrl - hl'}{hsa - hl'}\right). \quad (A.6)$$

CASE 2

$$C_2 = Cwa_2\ (1\text{-}Xa2) = Cwr_2\ (1\text{-}Xr_2) \quad \ldots (A.7)$$

However if no boiling or negligible boiling in the formation, then

$$Cwr_2 = Co \quad \ldots\ldots\ldots (A.8)$$

Then:

$$= Cwa2\left(\frac{hsa - h2}{hsa - hwa}\right) = Co\left(\frac{hsr2 - h2}{hsr2 - ho}\right)$$

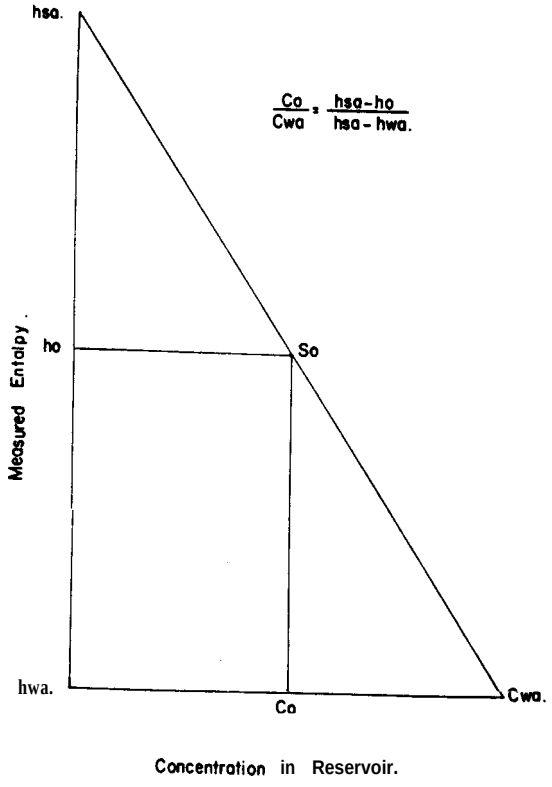

Fig: 1 Graphical Representation of the Method.

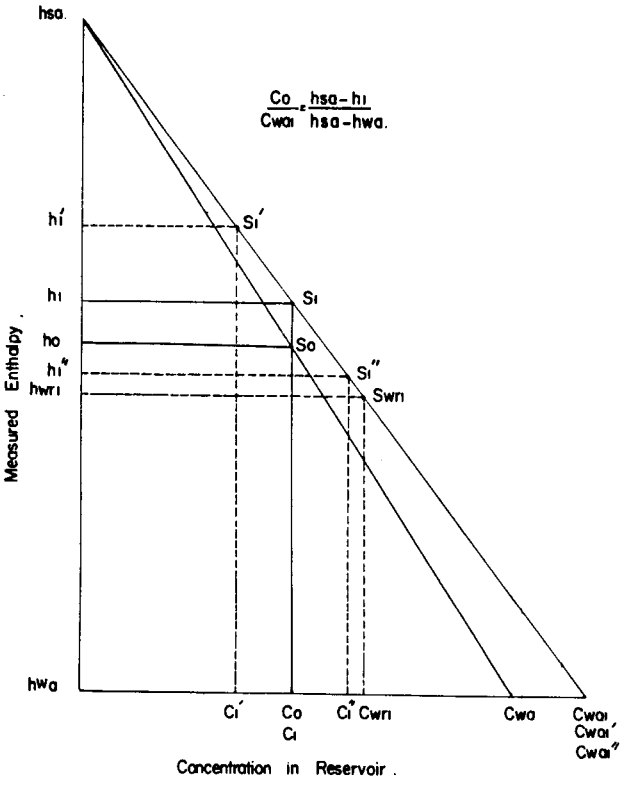

Fig. 2 Evaporation in Reservoir

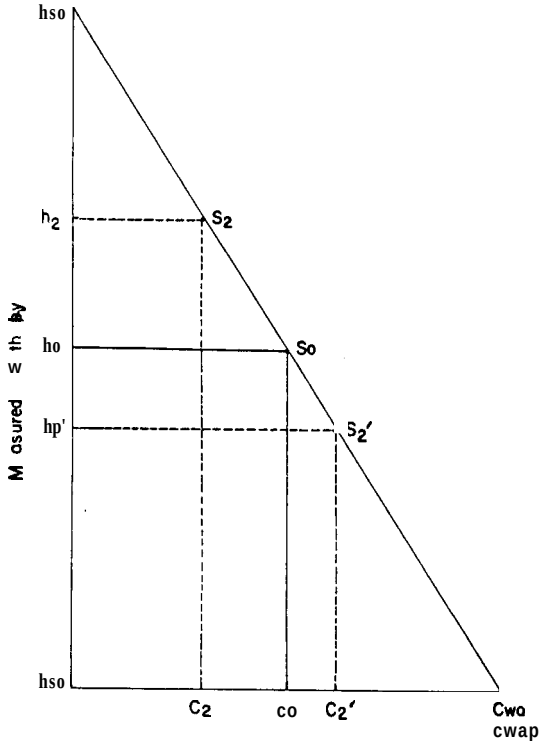

Fig. 3 Steam gain or loss without boiling in the reservoir

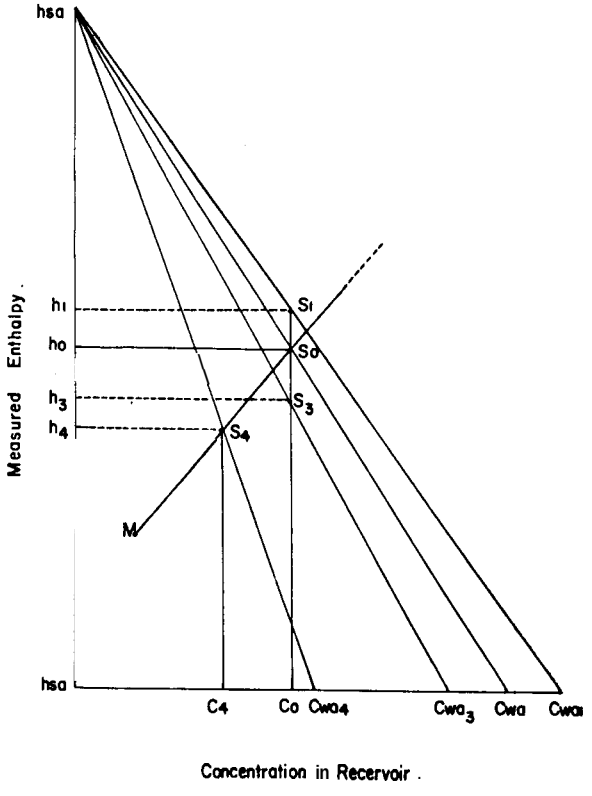

Fig: 4 Heating and cooling by conduction and mixing.

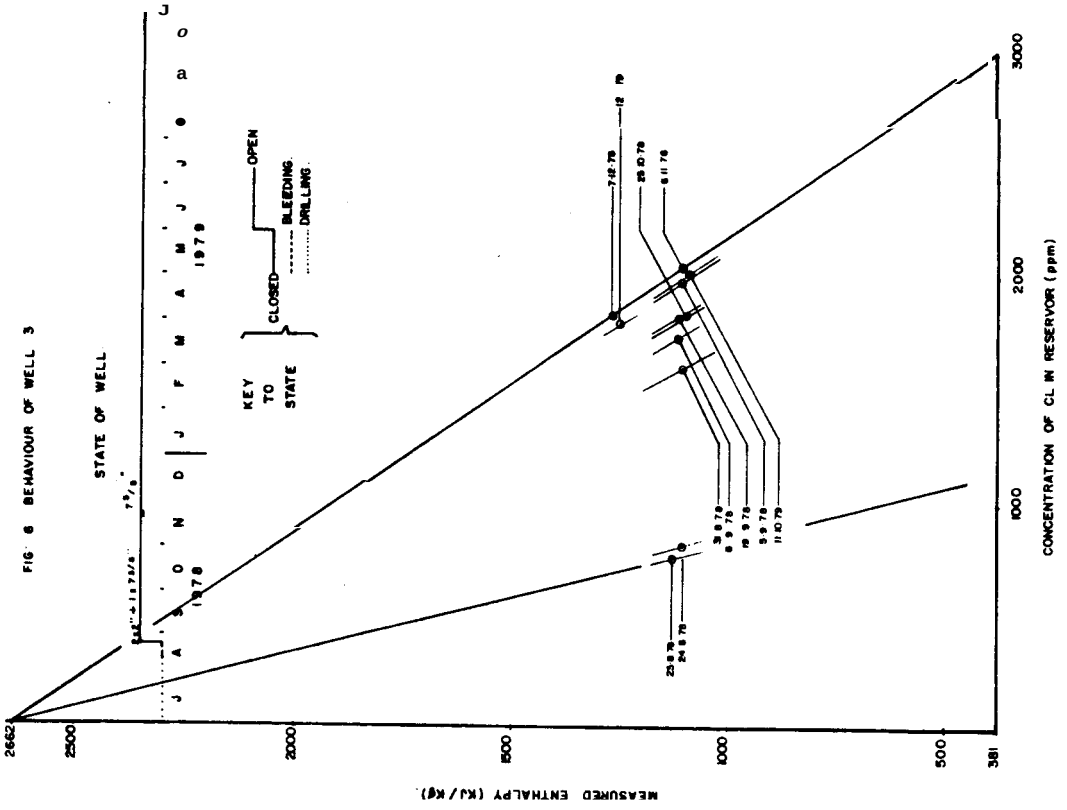
FIG 6 BEHAVIOUR OF WELL 3
STATE OF WELL
KEY TO STATE
OPEN
BLEEDING
DRILLING
CLOSED
1978
1979
MEASURED ENTHALPY (KJ/KG)
CONCENTRATION OF CL IN RESERVOIR (ppm)
2662
2500
2000
1500
1000
500
381
3000
2000
1000

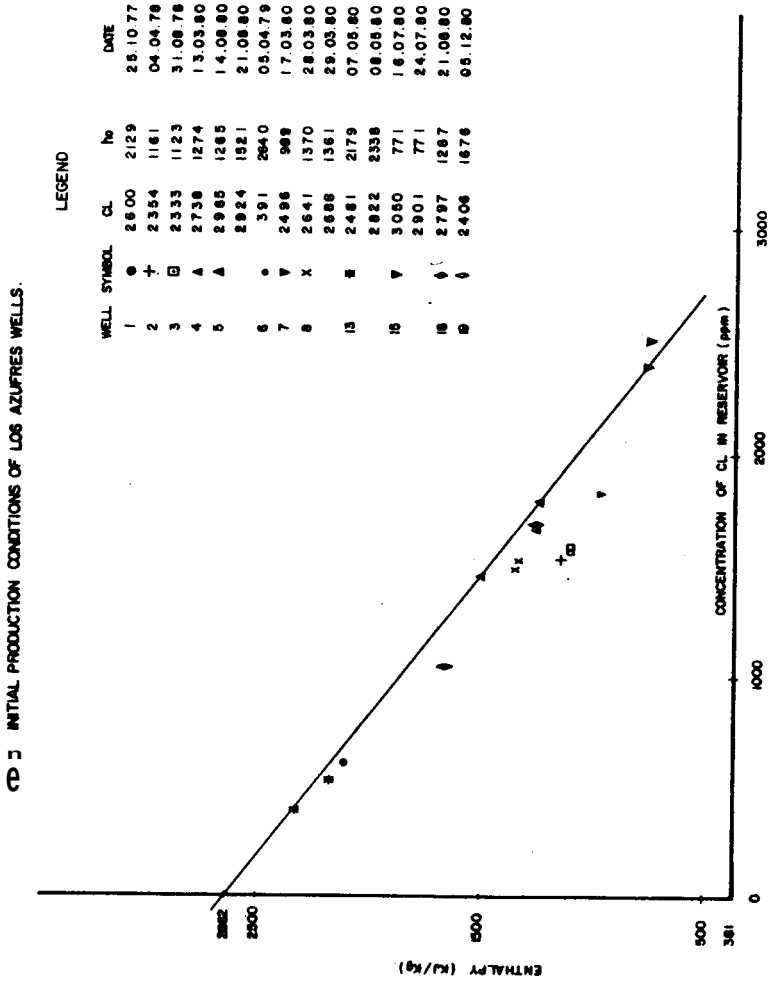
FIG 5 INITIAL PRODUCTION CONDITIONS OF LOS AZUFRES WELLS.
LEGEND
WELL SYMBOL CL hs DATE
1 ● 2600 2129 25.10.77
2 + 2354 1161 04.04.78
3 ⊡ 2333 1123 31.08.78
4 ▲ 2738 1274 13.03.80
5 ▲ 2985 1285 14.08.80
2824 1521 21.08.80
6 • 391 2840 05.04.79
7 ▼ 2496 988 17.03.80
8 X 2641 1370 28.03.80
2688 1361 29.03.80
13 ■ 2481 2179 07.08.80
2822 2338 08.08.80
15 ▼ 3050 771 16.07.80
2901 771 24.07.80
16 ◆ 2797 1287 21.08.80
9 ◊ 2406 1676 05.12.80
ENTHALPY (KJ/KG)
CONCENTRATION OF CL IN RESERVOIR (ppm)
2662
2500
1500
500
381
0
1000
2000
3000

FIG. 7. BEHAVIOUR OF WELL 5.

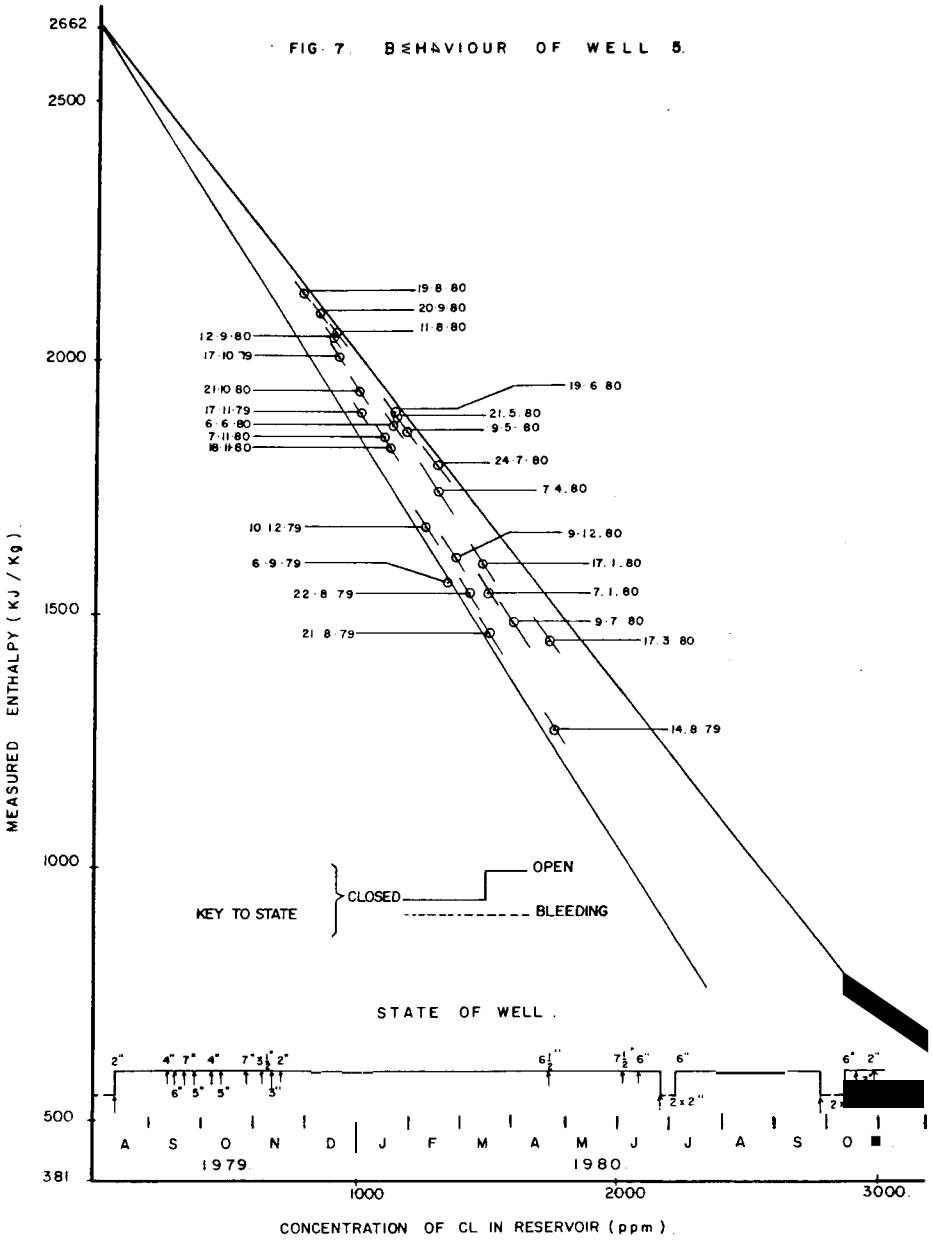

< 8 BEHAVIOUR OF WELL 13

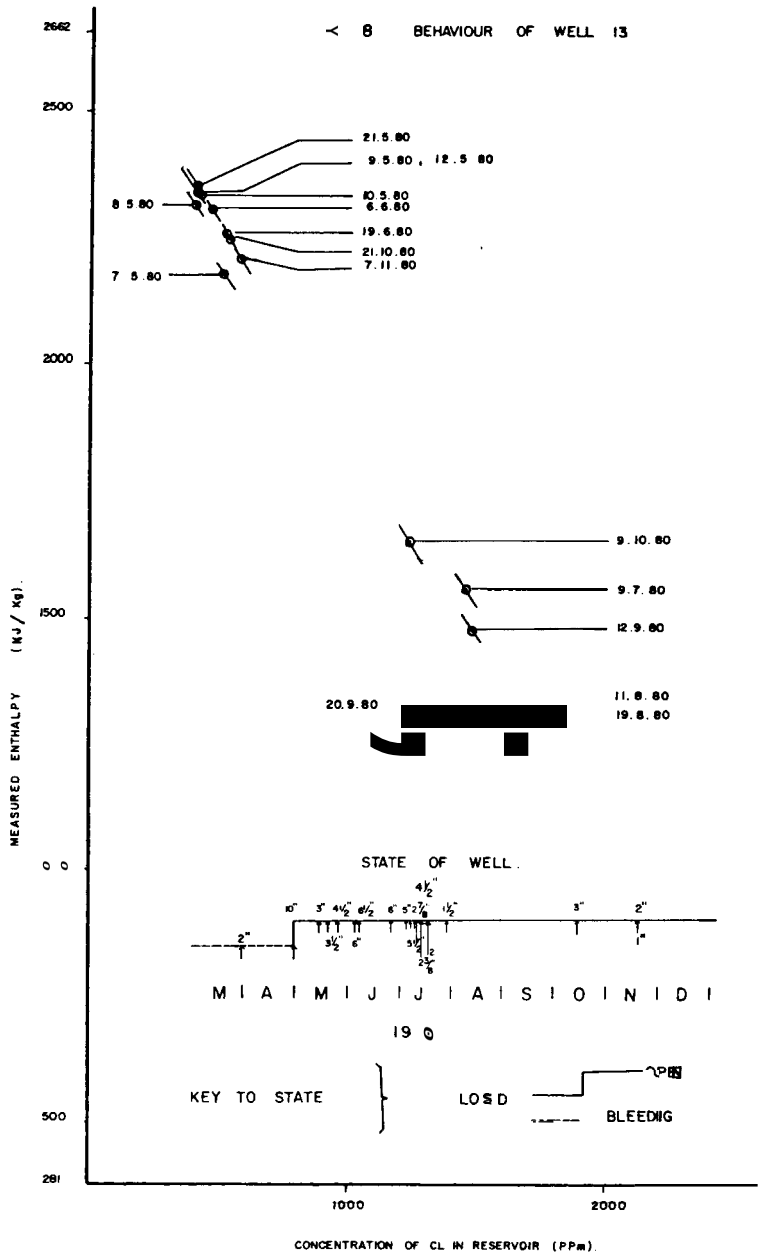

FIG. 9 BEHAVIOUR OF WELL 15.

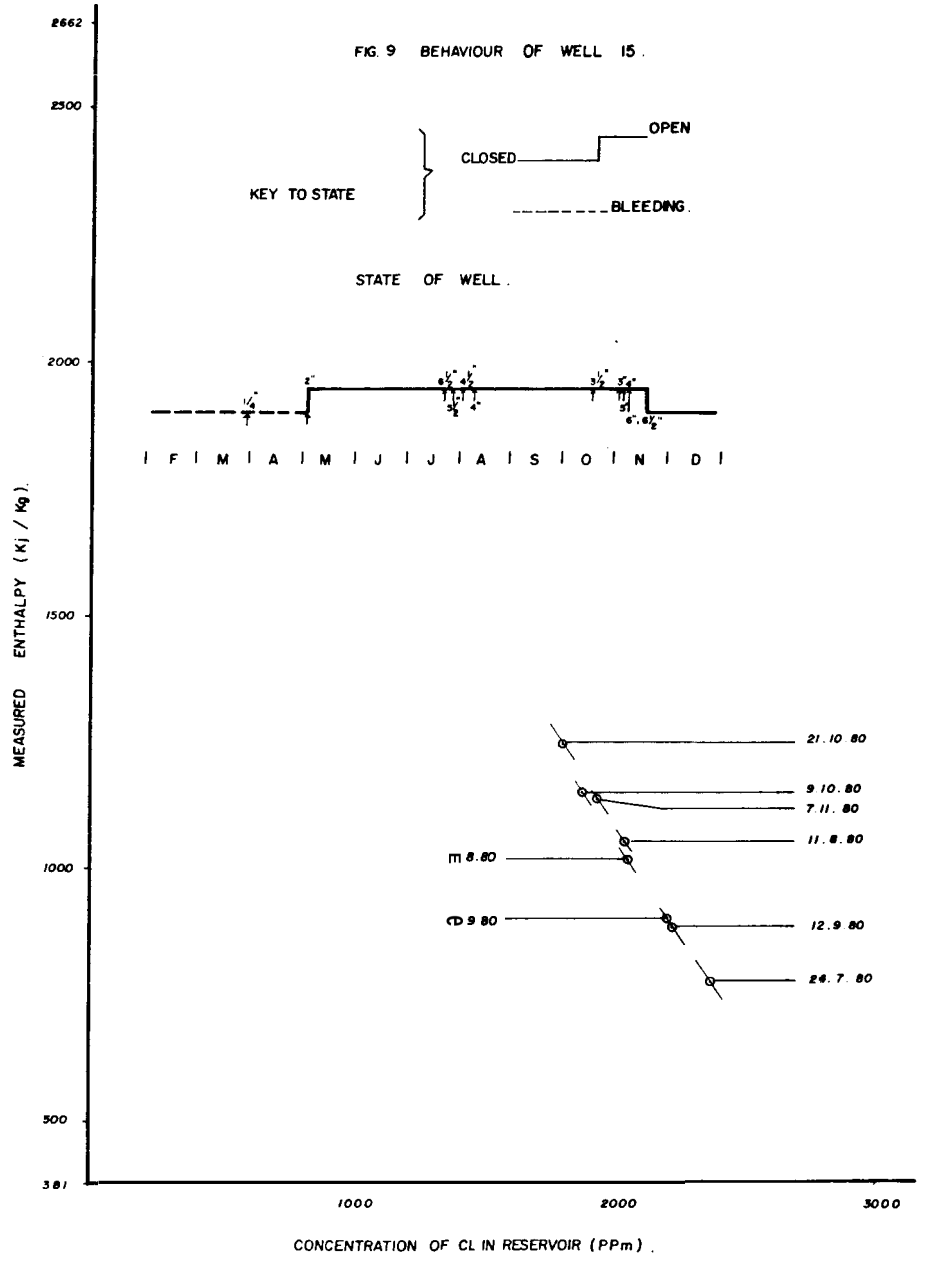

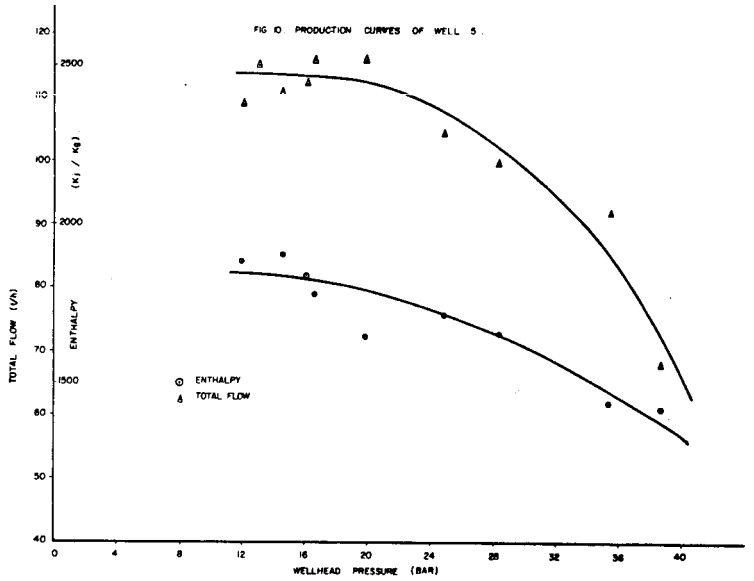

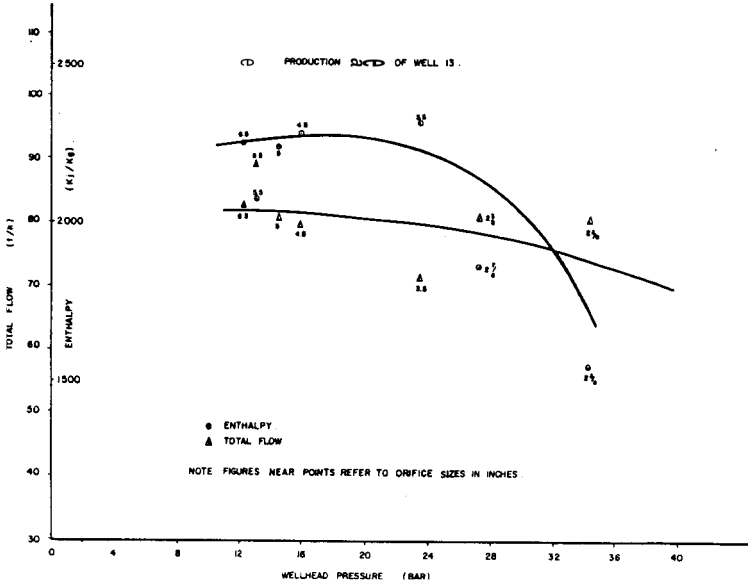

Proceedings Seventh Workshop Geothermal Reservoir Engineering
Stanford, December 1981. SGP-TR-55.

HEAT TRANSFER IN FRACTURED GEOTHERMAL RESERVOIRS WITH BOILING

Karsten Pruess

Earth Sciences Division
Lawrence Berkeley Laboratory
Berkeley, California **94720**

Introduction Most high-temperature geothermal reservoirs are highly fractured systems. The fractures provide conduits through which fluid (and heat) can flow at sufficiently large rates to attract commercial interest. The rock matrix has a low flow capacity, but it stores most of the heat and fluid reserves. The fractures represent a very small fraction of the void volume, and probably contain less than **1%** of total fluid and heat reserves in realistic cases. Sustained production from a fractured reservoir is only possible if the depletion of the fractures can be replenished by leakage from the matrix. The rate at which heat and fluid can be transferred from the matrix to the fractures is therefore of crucial importance for an assessment of reservoir longevity and energy recovery. Yet most work in the area of geothermal reservoir evaluation and analysis has employed a "porous medium"-approximation, which amounts to assuming instantaneous (thermal and hydrologic) equilibration between fractures and matrix. Effects of matrix/fracture interaction have been investigated by Bodvarsson and Tsang **(1981)** for single-phase reservoirs, and by Moench and coworkers **(1978, 1980)** for boiling reservoirs. Moench's work addresses the question of pressure transients during drawdown and build-up tests in fractured reservoirs. The present paper focuses on a complementary aspect, namely, enthalpy transients. We use simple analytical expressions to analyze fluid and heat transfer between rock matrix and fractures. It is shown that heat conduction in a matrix with low permeability can substantially increase flowing enthalpy in the fractures. This affects fluid mobility, and has important consequences for energy recovery and reservoir longevity. We present results of numerical simulations which illustrate these effects and show their dependence upon matrix permeability and fracture spacing.

Conductive Enhancement of Flowing Enthalpy Production from the fractures causes pressures to decline, and initiates fluid flow from the matrix into the fractures. Assuming Darcy's law to hold in the matrix, and neglecting gravity effects for the moment, the mass flux being discharged into the fracture system can be written:

$$\underset{\sim}{F} = \sum_{\substack{\beta=\text{liquid,}\\ \text{vapor}}} \underset{\sim}{F}_\beta = -k_m \sum_\beta \frac{k_\beta \rho_\beta}{\mu_\beta} (\nabla p)_n \qquad (1)$$

Here $(\nabla p)_n$ is the normal component of pressure gradient at the matrix/fracture interface. In a boiling reservoir, pressure gradients are accompanied by temperature gradients. Idealizing the reservoir fluid as pure water substance, the temperature gradient is given by the Clapeyron equation:

$$\nabla T = \frac{(v_v - v_\ell)(T + 273.15)}{h_v - h_\ell} \nabla p \qquad (2)$$

Therefore, there is a one-to-one correspondence between mass flux and the conductive heat flux which is given by

$$\underset{\sim}{q} = -K \nabla T \qquad (3)$$

The total heat flux discharged into the fracture system is

$$\underset{\sim}{G} = \sum_\beta h_\beta \underset{\sim}{F}_\beta - K(\nabla T)_n \qquad (4)$$

In the matrix, heat is stored in rocks and fluids. In the fractures, heat resides solely in the fluid filling the void space. The heat flux given by **(4)** has to be carried, therefore, by the mass flux given by **(2)**. Upon entering the fracture system, the fluid heat content is enhanced by the absorption of the conductive heat flux. From $\underset{\sim}{G} = h\underset{\sim}{F}$ we obtain the effective flowing enthalpy of the fluid entering the fractures:

$$h = \frac{\frac{k_\ell}{\mu_\ell}\rho_\ell \left[h_\ell + \frac{k_{lim}}{k_m k_\ell}(h_v - h_\ell)\right] + \frac{k_v}{\mu_v}\rho_v h_v}{\frac{k_\ell}{\mu_\ell}\rho_\ell + \frac{k_v}{\mu_v}\rho_v} \qquad (5$$

Here we have defined a limiting effective permeability, dependent upon heat conductivity and temperature, as:

$$k_{lim}(K,T) = \nu_g K \frac{\mu_a v_a (v_v - v_a)(T + 273.15)}{(h_v - h_\ell)^2} \quad (6)$$

In the absence of gravity effects, we have $\nu_g = 1$. The enhancement of flowing enthalpy occurs because the conductive heat flux vaporizes part (or all) of the liquid which is discharged into the fractures. The effect depends upon the ratio of heat conductivity K to effective permeability for the liquid phase, $k_m k_\ell$. The smaller the permeability of the matrix, the smaller is the mass flux which has to absorb the conductive heat flux, resulting in a stronger enhancement of flowing enthalpy. From (5) it can be seen that for $k_m k_\ell = k_{lim}$ all liquid is vaporized, giving rise to discharge of saturated steam from the matrix ($h = h_v$). Larger permeability ($k_m k_\ell > k_{lim}$) results in discharge of two-phase fluid, while for $k_m k_\ell < k_{lim}$ superheated steam is produced even if a mobile liquid phase is present in the matrix.

Gravity effects diminish the limiting effective permeability, hence the conductive enhancement of flowing enthalpy. This is easily understood by noting that gravity-driven flow does not require non-zero pressure gradients, and therefore need not be accompanied by conductive heat transfer. Pruoss and Narasimhan (1981) have shown that inclusion of gravity reduces the limiting effective permeability by a factor

$$\nu_g = \frac{\left(\frac{\partial p}{\partial r}\right)^2 + \frac{k_z}{k_r}\left[\frac{\partial p}{\partial z} + \rho_\ell g\right]\frac{\partial p}{\partial z}}{\left(\frac{\partial p}{\partial r}\right)^2 + \left(\frac{k_z}{k_r}\right)^2\left[\frac{\partial p}{\partial z} + \rho_\ell g\right]^2} \quad (7)$$

Gravity effects will be small if (i) vertical pressure gradients are close to hydrostatic ($\partial p/\partial z \approx -\rho_\ell g$), (ii) if vertical permeability is small ($k_z << k_r$), or (iii) if pressure gradients at the matrix/fracture interface are significantly larger than hydrostatic.

k_{lim} is plotted as a function of temperature in Figure 1 for the no-gravity case ($\nu_g = 1$). Figure 2 shows the effective flowing enthalpy of fluid discharged into the fractures as a function of matrix permeability calculated from (5). Curves are given for different values of vapor saturation; in these calculations the relative permeabilities were assumed to be given by Corey's equation with $S_{\ell r} = 0.3$, $S_{sr} = 0.05$. It is seen that conductive enhancement of flowing enthalpy becomes significant for $k < 10^{-15}$ m^2, and becomes very large for smaller permeability.

Numerical Simulations of Fractured Reservoir Behavior The above considerations are borne out by numerical simulations. We employ an idealized model of a fractured reservoir, with three perpendicular sets of infinite, plane, parallel fractures of equal aperture δ and spacing D (see Figure 3). Modeling of transient fluid and heat flow is accomplished with the "multiple interacting continua" method (MINC). This method is conceptually similar to, and is a generalization of, the well-known double-porosity approach (Barenblatt et al., 1960; Warren and Root, 1963). A detailed discussion of the MINC-method is given in Pruess and Narasimhan (1982). This method can be easily implemented with any simulator whose formulation is based on the "integral finite difference" method. The calculations presented below were made with LBL's geothermal simulators SHAFT79 and MULKOM, with parameters given in Table 1.

(i) Radial Flow The radial flow problem uses parameters applicable to a typical well at The Geysers, and assumes a mobile liquid phase ($k_\ell = .143$ at $S_\ell = .70$). The calculations show that for $k_m k_\ell < k_{lim}$, the produced enthalpy rises to above 2.8 MJ/kg (superheated steam) within minutes, whereas for $k_m k_\ell > k_{lim}$, a two-phase steam/water mixture is produced (Pruess and Narasimhan, 1981).

(ii) Areal Depletion Problem We have studied the depletion of an areal 7 km x 3 km reservoir, with parameters similar to those used by Bodvarsson et al. (1980) in their assessment of the geothermal reservoir at Baca, New Mexico. Results for enthalpies and pressures are given in Figures 4 and 5. Two basic depletion patterns are observed, depending upon whether matrix permeability is (relatively) "high" or "low". For low $k_m = 10^{-17}$ m^2, the boiling process is localized in the vicinity of the fractures, with vapor saturations in the matrix decreasing as a function of distance from the fractures. The opposite pattern is observed for "high" $k_m = 9\times10^{-17}$ m^2, 10^{-15} m^2, where the depletion process causes a boiling front to rapidly move into the matrix, giving rise to largest vapor saturations in the interior of the matrix, away from the fractures.

It is apparent from Figure 4 that produced enthalpy depends much more strongly upon matrix permeability than upon fracture spacing. Enthalpy increases with decreasing matrix permeability, in agreement with the discussion given above. From Figure 5 it can be noted that pressure decline is more rapid in case of higher enthalpy, due to the fact that the mobility of two-phase fluid generally decreases with increasing enthalpy. The crucial importance of matrix permeability is particularly evident in the case of $k_m = 10^{-17}$ m^2, where fracture spacings of 5 m and 50 m, respectively, result in virtually

identical enthalpy and pressure response, even though the matrix/fracture contact areas differ by a factor of 10. It might appear from Figures 4 and 5 that porous-medium type reservoirs will have greater longevity than equivalent fractured reservoirs. This is not generally true, however, and is caused by discretization effects in this case. Below we present calculations with better spatial resolution, which show that fractured reservoirs may in some cases have greater longevity than equivalent porous medium reservoirs.

It should be pointed out that the reservoir longevities predicted from this study are probably too pessimistic, due to the use of Corey-type relative permeability functions. The well test analysis from which the (permeability) x (thickness) product is derived uses Grant's relative permeabilities, which, for the sake of consistency, should also be employed in the analysis of reservoir depletion (Grant, 1977). Substantially greater .reservoir longevities would then be expected (Garg, 1981).

(iii) Five Spot For a more realistic assessment of the depletion of a naturally fractured boiling reservoir, we investigated a five-spot production/injection strategy for the reservoir discussed in the previous example. The basic mesh as given in Figure 6 takes advantage of flow symmetry. The production/injection rate was fixed at 30 kg/s, which corresponds to the more productive wells in the Baca reservoir.

Our results show that without injection, pressures will decline rapidly in all cases. The times after which production-well pressure declines below 0.5 MPa are: 1.49 yrs for a porous medium, 2.70 yrs for a fractured reservoir with D = 150 m, $k_m = 9 \times 10^{-17}$ m^2, and 0.44 yrs for D = 50 m, $k_m = 1 \times 10^{-17}$ m^2. Note that the fractured reservoir with large k_m (9×10^{-17} m^2) has a greater longevity than a porous reservoir. The reason for this is that the large matrix permeability provides good fluid supply to the fractures, while conductive heat supply is limited. Therefore, vapor saturation in the fractures remains relatively low, giving good mobility and a more rapid expansion of the drained volume.

The results obtained with 100% injection demonstrate the great importance of injection for pressure maintenance in fractured reservoirs with low permeability. Simulation of 90 years for the porous medium case, and 42 and 103 years, respectively, for fractured reservoirs with D = 50 m and D = 250 m ($k_m = 10^{-17}$ m^2), showed no catastrophic thermal depletion or pressure decline in either case. These times are significantly in excess of the 30.5 years needed to inject one pore volume of fluid. Figure 7 shows temperature and pressure profiles along the line connecting production and injection wells for the three cases studied after 36.5 years of simulated time. The temperatures of the porous-medium case and the fractured reservoir with D = 50 m agree remarkably well, indicating an excellent thermal sweep for the latter (see also Bodvarsson and Tsang, 1981). The temperature differences $\Delta T = T_m - T_f$ between matrix and fractures are very small: after 36.5 years, we have $\Delta T = .2$ °C near the production well, .001 °C near the injection well, and less than 5 °C in between. In the D = 50 m case, produced enthalpy remains essentially constant at h = 1.345 MJ/kg. It is interesting to note that this value is equal to the enthalpy of single-phase water at original reservoir temperature T = 300 °C. Thus, there is an approximately quasi-steady heat flow between the hydrodynamic front at T = 300 °C and the production well, with most of the produced heat being supplied by the thermally depleting zone around the injector.

At the larger fracture spacing of D = 250 m, the contact area between matrix and fractures is reduced, and portions of the matrix are at larger distance from the fractures. This slows thermal and hydrologic communication between matrix and fractures, causing the reservoir to respond quite differently to injection. After 36.5 years, thermal sweep is much less complete, with temperature differences between matrix and fractures amounting to 16 °C, 118 °C, and 60 °C, respectively, near producer, near injector, and in between. For the particular production and injection rates employed in this study, thermal depletion is slow enough that even at a large fracture spacing of D = 250 m, most of the heat reserves in the matrix can be produced. We are presently investigating energy recovery in the presence of a prominent short-circuiting fault or fracture between production and injection wells, under which conditions less favorable thermal sweeps are expected.

Acknowledgement The author expresses his gratitude to T.N. Narasimhan for many stimulating discussions throughout the course of this study. Thanks are due T.N. Narasimhan and J. Wang for a critical review of the manuscript. This work was supported by the Assistant Secretary for Conservation and Renewable Energy, Office of Renewable Technology, Division of Geothermal and Hydropower Technologies of the U.S. Department of Energy under Contract no. W-7405-ENG-48.

References

Barenblatt, G.E., Zheltov, I.P., and Kochina, I.N. (19601, "Basic Concepts in the Theory of Homogeneous Liquids in Fissured Rocks," Journal of Applied Mathematics (USSR), v. 24, n. 5, p. 1286-1303.

Bodvarsson, G.S., and Tsang, C.F. (1981), "Injection and Thermal Breakthrough in Fractured Geothermal Reservoirs," LBL-12698, Lawrence Berkeley Laboratory, Berkeley, California (May)(to be published in the Journal of Geophysical Research).

Bodvarsson, G.S., Vonder Haar. S., Wilt, M., and Tsang, C.F. (1980), "Preliminary Estimation of the Reservoir Capacity and the Longevity of the Baca Geothermal Field, New Mexico," SPE-9273, presented at the 55th Annual Fall Technical conference and Exhibition of the SPE, Dallas, Texas (September).

Garg, S.K. (1981), personal communication.

Grant, M.A. (1977), "Permeability Reduction Factors at Wairakei," Paper 77-HT-52, presented at AICHE-ASME Heat Transfer Conference, Salt Lake City, Utah (August).

Moench, A.F. (1978), "The Effect of Thermal Conduction upon Pressure Drawdown and Build-up in Fissured, Vapor-Dominated Reservoirs," Proceedings, Fourth Workshop on Geothermal Reservoir Engineering, Stanford University, Stanford, California.

Moench, A.F., and Denlinger, R. (19801, "Fissure-Block Model for Transient Pressure Analysis in Geothermal Steam Reservoirs," Proceedings, Sixth Workshop on Reservoir Engineering, Stanford University, Stanford, California (December).

Pruess, K., and Narasimhan, T.N. (1981), "On Fluid Reserves and the Production of Superheated Steam from Fractured, Vapor-Dominated Geothermal Reservoirs," LBL-12921, Lawrence Berkeley Laboratory, Berkeley, California (July)(submitted to Journal of Geophysical Research).

Pruess, K., and Narasimhan, T.N. (1982), "A Practical Method for Modeling Fluid and Heat Flow in Fractured Porous Media", SPE-10509, to be presented at the Sixth SPE Symposium on Reservoir Simulation, New Orleans, Louisiana (January).

Warren, J.E., and Root, P.J. (1963), "The Behavior of Naturally Fractured Reservoirs," Society of Petroleum Engineers Journal (September), p. 245-255.

Nomenclature

- D: Fracture spacing (m)
- $\tilde{F}$: Mass flux ($kg/m^2 \cdot s$)
- g: Gravitational acceleration (9.81 m/s^2)
- $\tilde{G}$: Heat flux (W/m^2)
- h: Specific enthalpy (J/kg)
- k: Absolute permeability (m^2)
- K: Heat conductivity ($W/m^{\circ}C$)
- k_{lim}: Limiting effective permeability (m^2)
- k_β: Relative permeability for phase β, dimensionless
- p: Pressure (Pa)
- $\tilde{q}$: Conductive heat flux (W/m^2)
- $\tilde{r}$: Radial coordinate (m)
- S: Saturation (void fraction), dimensionless
- $S_{\ell r}$: Irreducible liquid saturation, dimensionless
- S_{sr}: Irreducible vapor saturation, dimensionless
- T: Temperature ($^{\circ}C$)
- v: Specific volume (m^3/kg)
- z: Vertical coordinate (m)
- ν_g: Gravity reduction factor for k_{lim}, dimensionless
- μ_β: Viscosity of phase β (Pa·s)
- ρ_β: Density of phase β (kg/m^3)

Subscripts

- f: Fracture
- ℓ: Liquid
- m: Matrix
- n: Normal component
- v: vapor
- β: Phase (β = liquid, vapor)

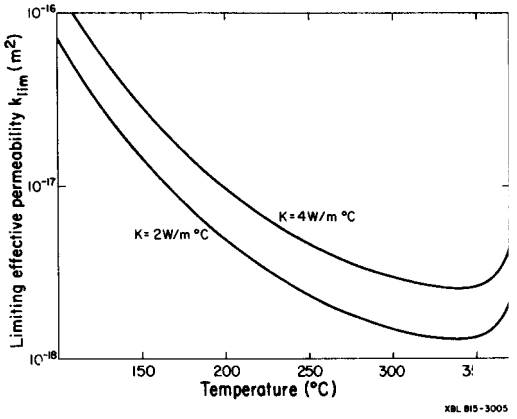

Figure 1: Limiting effective permeability.

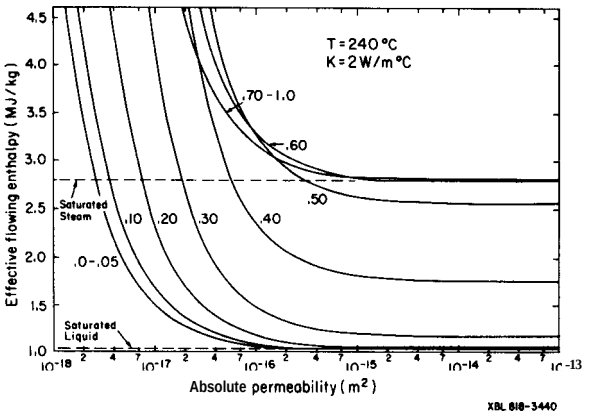

Figure 2: Effective flowing enthalpy.

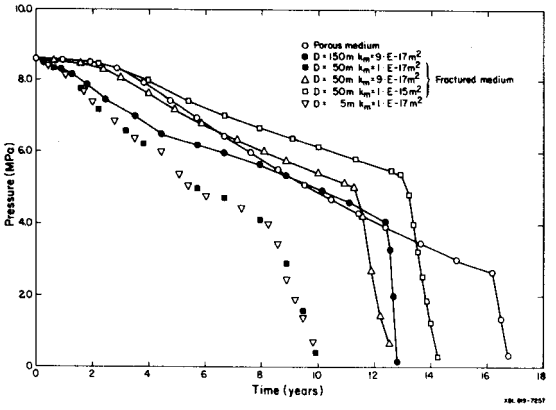

Figure 5: Pressure decline for areal depletion problem.

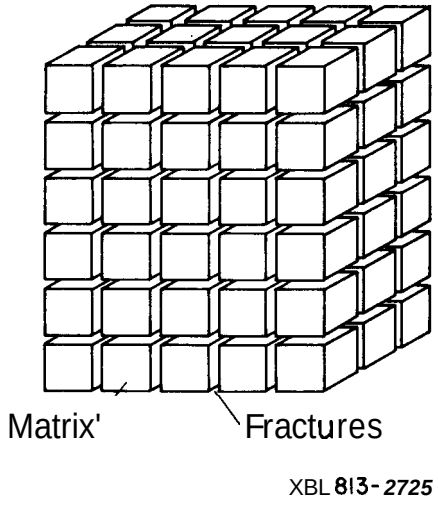

Figure 3: Idealized model of fractured reservoir.

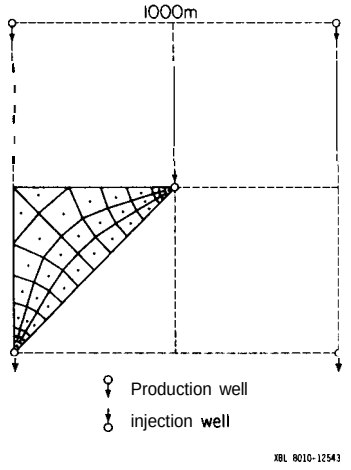

Figure 6: Five-spot computational mesh.

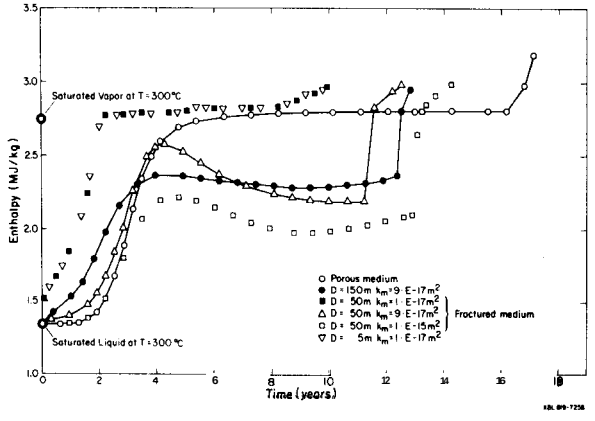

Figure 4: Produced enthalpy for areal depletion problem.

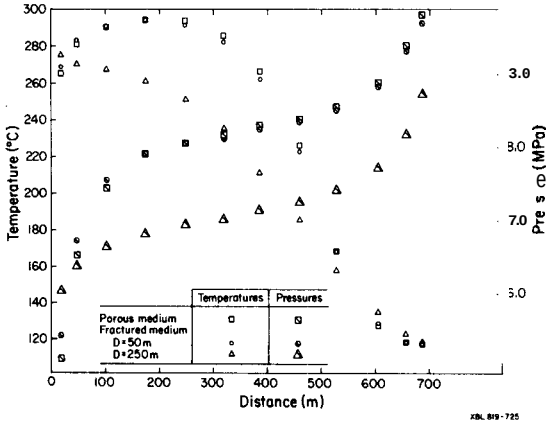

Figure 7: Temperature and pressure profiles for five-spot after 36.5 years.

TABLE I: Parameters Used in Simulations

	Radial Flow Problem	Depletion Problem
Formation		
rock grain density	ρ_R = 2400 kg/m^3	2600 kg/m^3
rock specific heat	C_R = 960 J/kg^oC	950 J/kg ^oC
rock heat conductivity	K = 4 W/m^oC	2.22 W/m ^oC
porosity	Φ = .08	.10
permeability x thickness	kh = 13.4x10^{-12} m^3	1.83x10^{-12} m^3
reservoir thickness	h = 500 m	305 m
matrix permeability	k_1 = 10^{-15} m^2, 10^{-16} m^2, 10^{-17} m^2	10^{-15} m^2, 9x10^{-17} m^2, 10^{-17} m^2
Fractures		
three orthogonal sets		
aperture	δ = 2x10^{-4} m	(a)
spacing	D = 50 m	5 m, 50 m, 150 m
permeability per fracture	k_f = 62/12 = 3.3x10^{-9} m^2	(a)
equivalent continuum permeability	$k_2 \approx 2k_f\delta/D$ = 26.8x10^{-15} m^2	6x10^{-15} m^2
equivalent continuum porosity	$\Phi_2 \approx 3\delta/D$ = 1.2x10^{-5}	.10
Relative Permeability		
Corey-curves	$S_{\ell r}$ = .30, S_{sr} = .05	$S_{\ell r}$ = .30, S_{sr} = .05
Initial Conditions		
temperature	T = 243 ^oC	300 ^oC
liquid saturation	S_ℓ = 70%	99%
Production		
wellbore radius	r_w = .112 m	
skin	s = –5.18	
effective wellbore radius	$r_w' = r_w e^{-s}$ = 20.0 m	
wellbore storage volume	V_w = 27.24 m^3	
production rate	q = 20 kg/s	82.5 kg/s[b]; 30 kg/s[c]
Injection		
rate	---	30 kg/s[c]
enthalpy	---	5x10^5 J/kg

(a) fractures modeled as extended regions of high permeability, with a widty of $\approx$ .2 m
(b) rectangular reservoir
(c) five-spot

Proceedings Seventh Workshop Geothermal Reservoir Engineering
Stanford, December 1981. SGP-TR-55.

SIMULATION OF FLOW IN FRACTURED POROUS MEDIA

A. M. Shapiro* and G. F. Pinder

Department of Civil Engineering
Princeton University
Princeton, New Jersey 08544

Introduction While flow in fractured porous media is a phenomenon often encountered in reservoir simulation, there exists no generally accepted simulation methodology. One can catalogue existing approaches as either discrete fracture or continuum. As the name implies the *discrete* ***fracture*** *model* considers each fracture as a geometrically well-defined ,entity wherein the fluid behavior is described using some variant of classical fluid mechanics. The geometry of the porous blocks is also assumed known and the pore fluid behavior is determined via the equations describing the physics of flow through porous media. The two systems are coupled through conservation constraints along the fracture-porous block interface. Discrete fracture models have been popular for some time. Early work was conducted by Berman (1953) and Crawford and Collins (1954); recently Grisak and Pickens (1980) used this approach to examine mass transport.

The ***continuum*** *model*, sometimes referred to as the double porosity model, does not attempt to describe the behavior in each porous block or fracture explicitly. Rather one abandons this detailed level of observation and alternatively examines the physical phenomenon from a more distant perspective. At this higher level of observation, one considers only the average properties of the pores and fractures. These properties are in turn represented by functions which are assumed to satisfy certain smoothness conditions consistent with the fundamental postulates of continuum mechanics. This approach relies more heavily on constitutive theory to establish meaningful experiments to determine these property functions. The concept of the continuum model, as applied to fractured reservoirs, is generally attributed to Barenblatt and Zheltov (1960). Only recently however have the mathematical-physical underpinnings of this approach been carefully examined. Duguid and Lee (1977) were the first to recognize the necessity of adhering to continuum principles in equation formulation A recent summary of work in this area can be found in Shapiro (1981).

The Model Problem Although both modelling approaches have received considerable attention, little effort has been expended in studying the relationship between them. The outstanding question is whether the continuum model can adequately represent the mathematical-physical behavior of the discrete system. To address this problem, we have constructed a discrete fracture model and a corresponding continuum model. The discrete fracture model is shown in figure 1. It consists of a set of infinitely long prisms with square cross-sections.

The equations describing fluid flow in the fractures are, for the x coordinate direction

$$(1)\quad D_t\rho + D_x(\rho\bar{v}_x) = \frac{2}{\ell}\,\rho v_y\Big|_{y=0}$$

(mass conservation)

and

$$(2)\quad (D_t\bar{v}_x + \bar{v}_x D_x\bar{v}_x) + D_x P - \left(\tfrac{4}{3}\mu + \lambda\right)D_x^2\bar{v}_x + \frac{12\bar{v}_x}{\ell^2}\mu + \bar{v}_x\left(\frac{2}{\ell}\,\rho v_y\Big|_{y=0}\right) = 0$$

(momentum conserv tion)

where ρ is fluid density,

P is fluid pressure,

$\bar{v}_x$ is the average fluid velocity,

μ is the shear fluid viscosity,

λ is the bulk fluid viscosity,

ℓ is the fracture thickness, and

$D_t(\cdot)$ and $D_x(\cdot)$ are partial derivatives in time and the x coordinate direction respectively.

A similar set of equations can be written for the y direction.

*Now at Wenner Gren Center, Stockholm, Sweden.

The equation describing flow in the porous blocks is

$$(3)\quad (c_f\phi + \rho\beta)D_t P - \rho \frac{k}{\mu} \nabla^2 P = 0$$

where c_f is medium compressibility,

β is fluid compressibility,

k is matrix permeability, and

$ is porosity.

The continuum equations for the porous medium and fractures are given by (Shapiro, 1981).

$$(4)\quad D_t(\rho^k \phi^k) - \frac{\rho^p k^p}{\mu^p} \nabla^2 p^p = -\rho^f \phi^f \sum_{\beta=f,p} (\alpha^\beta c_f p^\beta - \Lambda^\beta \frac{k^\beta}{\mu^\beta \phi^\beta} \nabla^2 p^\beta)$$

(porous medium)

$$(5)\quad \phi^f \frac{D}{Dt}(\rho^f) - \frac{\rho^f k^f}{\mu^f} \nabla^2 p^f = -\rho^f \phi^f \sum_{\beta=f,p} (\alpha^\beta c_f p^\beta - \Lambda^\beta \frac{k^\beta}{\mu^\beta \phi^\beta} \nabla^2 p^\beta)$$

(fractured medium)

where α^β and Λ^β are coefficients in the mass exchange function.
The terms on the right hand side of (4) and (5) represent the interaction between the blocks and the fractures.

Parameter Estimation and Analysis The immediate objective is to determine theability of equations (4) and (5) to describe the physical response of the fractured porous medium system represented by equations (1), (2) and (3). To examine this hypothesis, we determine the unknown parameters α^β and A^β using the solution to (1), (2) and (3). In other words we use the discrete fracture model and equations (1), (2) and (3) as our experimental observations and solve for the unknown parameters. TO establish the robustness of the continuum model we subsequently compare the solutions obtained using the two approaches. The parameters used in this mathematical experiment are listed in table 1. The two solutions are presented in figure 2.

It is apparent from figure 2 that the continuum model generated a solution qualitatively similar to that generated by the discrete fracture model. Experiments conducted using REVs of different sizes indicate that the continuum model solution is relatively unaffected by this parameter and that the continuum parameters are temporally stable.

Comparison with the earlier continuum representation of Barenblatt indicates that his formulation generates a solution somewhat different than either the discrete fracture or continuum formulations presented herein.

References

Barenblatt, G.I. and Yu. P. Zheltov (1960), "Fundamental Equations of Filtration of Homogeneous Liquids in Fissured Rocks", Soviet Physics-Doklady, 5, 1960, pp. 522-525.

Berman, A.S. (1953), "Laminar Flow in Channels with Porous Walls", Journal of Applied Physics, 24, 1953, pp. 1232-1235.

Crawford, P.B. and R.E. Collins (1954), "Estimated Effect of Vertical Fractures on Secondary Recovery", Trans. AIME, 201, 1954, pp. 192-196.

Duguid, J.O. and P.C.Y. Lee (1977), "Flow in Fractured Porous Media", Water Resour. Res., 13, 1977, pp. 558-566.

Grisak, G.E. and J.F. Pickens (1980), "Solute Transport through Fractured Media: 1. The Effect of Matrix Diffusion", Water Resour. Res., 16, 1980, pp. 719-730.

Shapiro, A.M. (1981), "Fractured Porous Media: Equation Development and Parameter Identification", Ph.D. dissertation, Princeton University, 1981, p. 373.

Table 1

Experimental Properties

	Property	Symbol	Value
1)	Porous medium properties		
	Porosity	ϕ	0.20
	Permeability	k	1.0E-08cm^2
	Matrix and Fluid Compressibility	$(\phi c_f + \rho\beta)$	1.0E-11gm/dyne-cm
2)	Fracture properties		
	Thickness	ℓ	0.01 cm
	Fracture spacing	L	8.0 E01cm
	Fluid velocity at inlet	v_0	1.0 cm/sec
3)	Fluid properties		
	Compressibility	c_f	0.48E-10cm^2/dyne
	Viscosity	μ	1.3E-02 dyne/cm^2-sec
	Reference density	ρ_0	1.0 gm/cm^3
	Reference pressure	P_0	0.0 dyne/cm^2

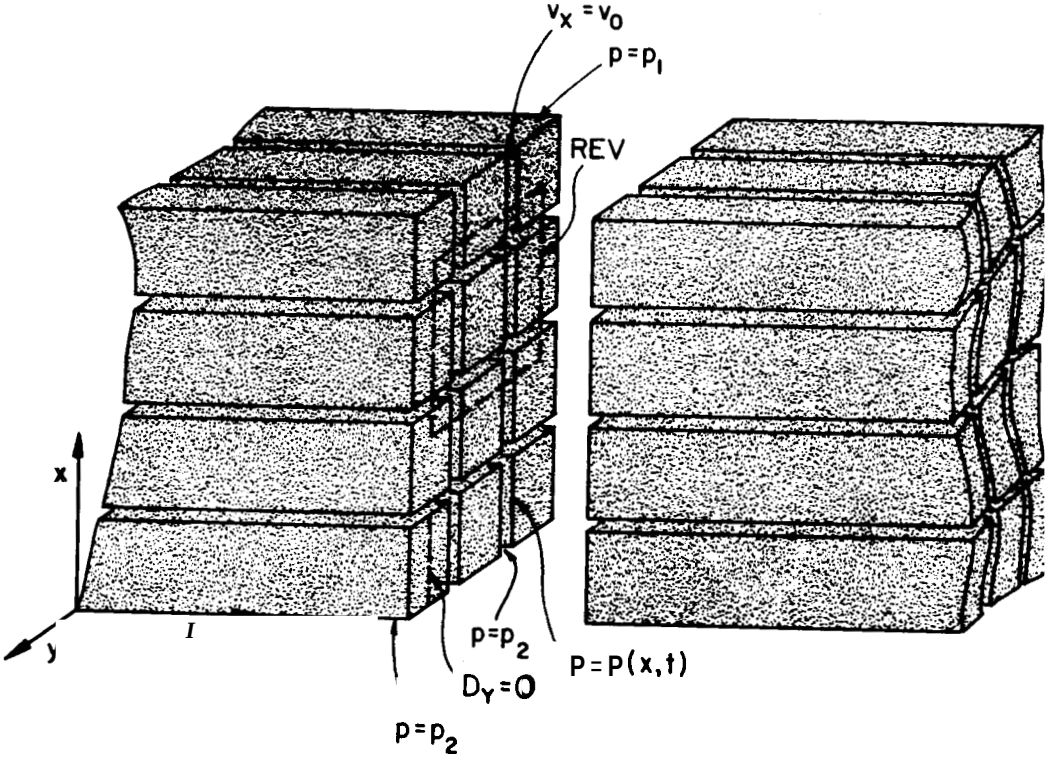

Figure 1: Diagrammatic representation of a discrete fracture system.

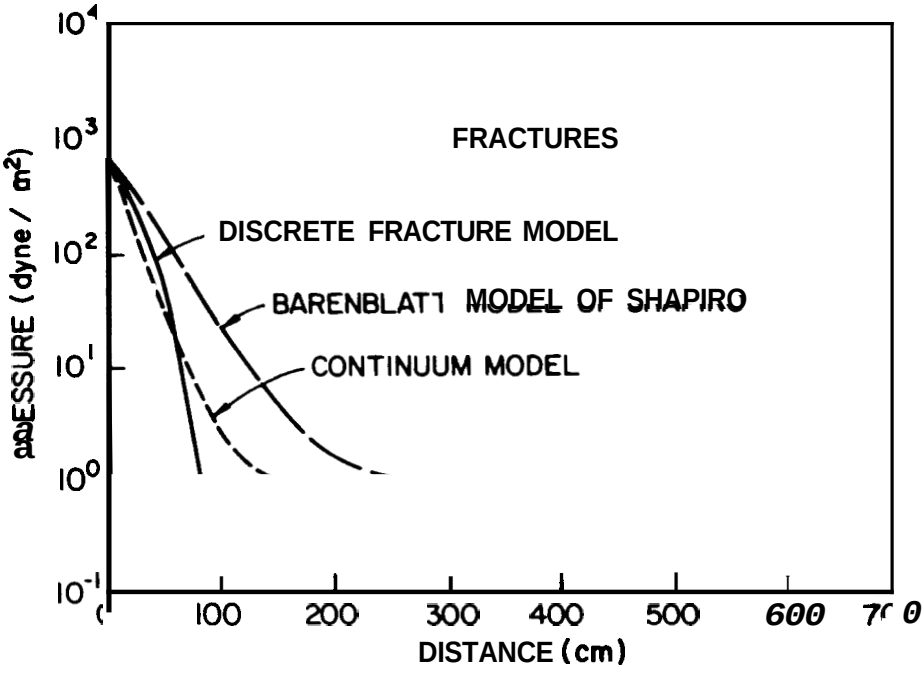

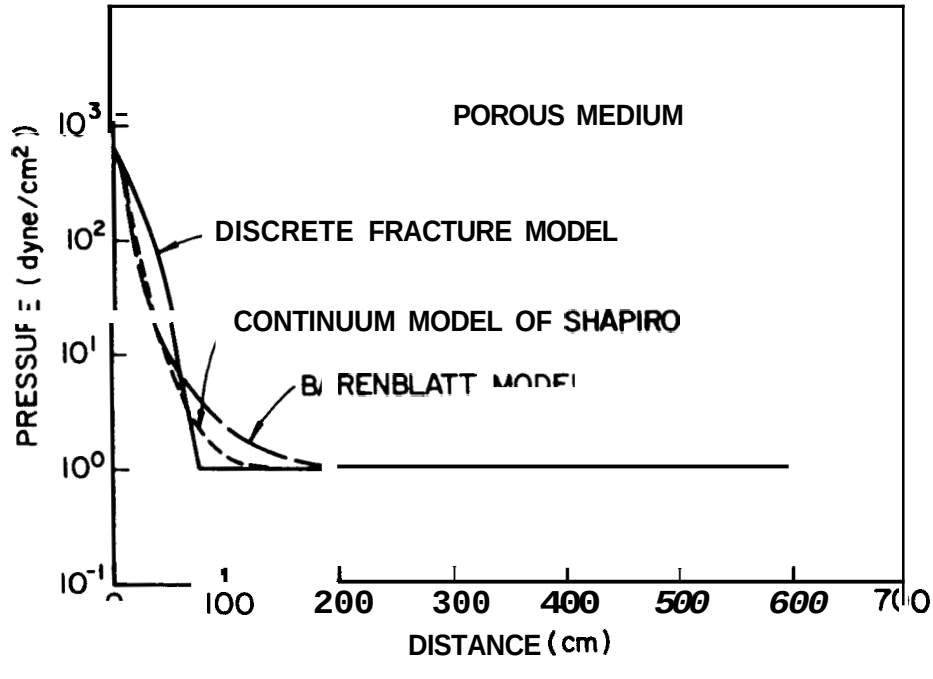

Figure 2: Pressure response calculated using discrete fracture and continuum models by Shapiro and Barenblatt.

Proceedings Seventh Workshop Geothermal Reservoir Engineering
Stanford, December 1981. SGP-TR-55.

RESERVOIR ENGINEERING OF SHALLOW FAULT-CHARGED HYDROTHERMAL SYSTEMS

S.M. Benson, G.S. Bodvarsson, and D.C. Mangold

Earth Sciences Division
Lawrence Berkeley Laboratory
Berkeley, California 94720

Introduction Many of the low-to-moderate temperature (< 150°C) hydrothermal resources being developed in the United States occur in near-surface aquifers. These shallow thermal anomalies, typical of the Basin and Range and Cascades are attributed to hydrothermal circulation. The aquifers are often associated with faults, fractures, and highly complex geological settings; they are often very limited in size and display anomalous temperature reversals with depth. Because of the shallow depth and often very warm temperatures of these resources, they are attractive for development of direct-use hydrothermal energy projects. However, development of the resources is hindered by their complexity, the often limited manifestation of the resource, and lack of established reservoir engineering and assessment methodology.

In this paper a conceptual model of these systems is postulated, a computational model is developed, and reservoir engineering methods (including reservoir longevity, pressure transient analysis, and well siting) are reevaluated to include the reservoir dynamics necessary to explain such systems. Finally, the techniques are applied to the Susanville, California hydrothermal anomally.

Thermal Model Figure 1 shows a schematic of the conceptual model developed to explain the occurrence of near-surface hot water aquifers.

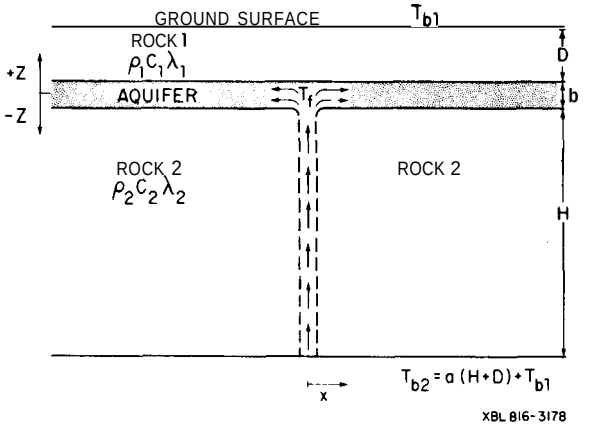

Figure 1 Schematic of a conceptual model for a fault-charged hydrothermal system.

Heated fluids rise along a fault until a highly permeable aquifer is intersected. Fluid then enters the aquifer and with time, replaces the existing fluid with hot water. As the water moves away from the fault it is cooled by equilibration with surrounding rock and conductive heat transfer to the overlying and underlying rock units. The model discussed in this paper is most applicable to thin aquifers as vertical temperature variations in the aquifer are not considered.

A semi-analytic model has been developed to calculate the temperature distribution of the system as a function of the flowrate into the aquifer, the temperature of the water entering the aquifer, initial linear temperature profile, system geometry, rock properties, and time (Bodvarsson et al., 1981). The primary assumptions are listed below:

(1) The mass flow is steady in the aquifer, horizontal conduction is neglected, and temperature is uniform in the vertical direction (thin aquifer). Thermal equilibrium between the fluid and the solids is instantaneous.

(2) The rock matrix above and below the aquifer is impermeable. Horizontal conduction in the rock matrix is neglected.

(3) The energy resistance at the contact between the aquifer and the rock matrix is negligible (infinite heat transfer coefficient).

(4) The thermal properties of the formations above and below the aquifer may be different, but all thermal parameters of the liquid and the rocks are constant.

The differential equation governing the temperature in the aquifer at any time (t) can be readily derived by performing an energy balance on a control volume in the aquifer:

$$z = 0: \quad \frac{\lambda_1}{b}\frac{\partial T_1}{\partial z}\bigg|_{z=0} - \frac{\lambda_2}{b}\frac{\partial T_2}{\partial z}\bigg|_{z=0} - \frac{\rho_w c_w q}{b}\frac{\partial T_a}{\partial x} - \rho_a c_a \frac{\partial T_a}{\partial t} = 0 \qquad (1)$$

The symbols are defined in the nomenclature. In the caprock and the bedrock the one-dimensional heat-conduction equation controls the temperature:

$$z > 0: \quad A_1 \frac{\partial^2 T_1}{\partial z^2} = \rho_1 c_1 \frac{\partial T_1}{\partial t} \tag{2}$$

$$z < 0: \quad \lambda_2 \frac{\partial^2 T_2}{\partial z^2} = \rho_2 c_2 \frac{\partial T_2}{\partial t} . \tag{3}$$

The initial conditions are:

$$T_a(x,0) = T_1(x,z,0) = T_2(x,z,0) = T_{b1} - a(z - D) \tag{4}$$

The boundary conditions are:

$$T_a(0,t) = T_f, \; t > 0 \tag{5a}$$

$$T_a(x,t) = T_1(x,0,t) = T_2(x,0,t) \tag{5b}$$

$$T_1(x,D,t) = T_{b1} \tag{5c}$$

$$T_2(x,-H,t) = T_{b2} = T_{b1} + a(H + D) \tag{5d}$$

The following dimensionless parameters are introduced:

$$\xi = \frac{A_1 x}{\rho_w c_w q D} ; \qquad \tau = \frac{\lambda_1 t}{\rho_1 c_1 D^2} \tag{6a,b}$$

$$\theta = \frac{b}{D} \frac{\rho_a c_a}{\rho_1 c_1} ; \qquad \eta = \frac{z}{D} \tag{6c,d}$$

$$\gamma = \frac{\rho_2 c_2}{\rho_1 c_1} ; \qquad \omega = \frac{\lambda_2}{\lambda_1} \tag{6e,f}$$

$$T_D = \frac{T - T_{b1}}{T_f - T_{b1}} ; \qquad T_g = \frac{aD}{T_f - T_{b1}} \tag{6g,h}$$

$$\alpha = H/D \tag{6i}$$

The solution of equations (1)-(3) can be easily obtained in the Laplace domain (Bodvarsson, 1981).

$$\eta = 0: \quad \mu = \frac{1}{p} [1 - T_g] \exp - \left[\theta p + \frac{\sqrt{p}}{\tanh\sqrt{p}} + \frac{\omega\sqrt{q}}{\tanh\sqrt{q}}\right] + \frac{T_g}{p} . \tag{7}$$

$$\eta > 0: \quad v = \left[u - T_g/p\right] \eta \cosh\sqrt{p} - \frac{\left[u - T_g/p\right]}{\tanh\sqrt{p}} \eta \sinh\sqrt{p} - \frac{T_g}{p} (\eta - 1) \tag{8}$$

$$\eta < 0: \quad w = \left[u - T_g/p\right] \eta \cosh\sqrt{\frac{\gamma p}{\omega}} + \frac{\left[u - T_g/p\right]}{\tanh\sqrt{\frac{\gamma p}{\omega}}} \eta \sinh\sqrt{\frac{\gamma p}{\omega}} - \frac{T_g}{p} (\eta - 1) . \tag{9}$$

In equations (7)-(9), u, v, and w represent the temperature, in the Laplace domain of the aquifer, the rock above the aquifer, and the rock below the aquifer, respectively. As equations (7)-(9) cannot easily be inverted from the Laplace domain, a numerical inverter was used to evaluate the equations.

Using this model, the evolution of these systems can be studied. In Figure 3, the evolution of a hypothetical system is shown. The dimensionless coordinates used are defined in equations (6a-6i). In simple terms, the graph can be envisioned as the evolution of a single temperature profile, at a given location (ξ) away from the fault. Before the incidence of hydrothermal circulation, the temperature profile is linear (normal geothermal gradient). When water begins to flow up the fault and into the aquifer, the aquifer begins to heat up. The fluid flows laterally in the aquifer, losing heat by conduction to the caprock and basement. A distinctive temperature reversal forms below the aquifer. With increasing time, conductive heat losses to the caprock stabilize and a typical linear conductive gradient is established. At very large times, the temperature below the aquifer stabilizes and for the case considered, becomes nearly constant with depth.

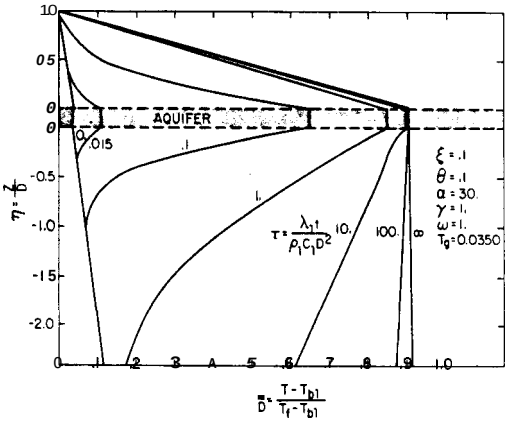

Figure 2 Evolution of a fault-charged hydrothermal system. This schematic represents the evolution of a single temperature profile over time.

Another application of this model is to calculate the rate of hot water recharge into an aquifer, given sufficient information about the areal and vertical temperature distribution in the aquifer. The model has been applied to the Susanville, California hydrothermal resource, a low-temperature system located in the foothills of the Sierra Nevada. Data from more than twenty shallow exploration and production wells have outlined a thermal anomaly which is elongated around a north-west trending axis (Benson et al., 1980). Temperature contours at a depth of approximately 125 m below the surface (elevation 1150 m) are shown in Figure 3. Temperature profiles from several of the wells are shown in Figure 4. In each well temperatures increase linearly with depth until approximately 125 m below the surface. Thereafter the temperatures remain isothermal or have a reversal. The shape of the thermal anomaly can be explained by a recharging fault, which is slightly to the east of Suzy 9 and aligned with the northwest trend of the anomaly. The match of calculated and observed temperatures shown in Figure 4 was obtained by assuming a hot water recharge rate (80°C) of 9 x 10^{-6} $m^3/sec/m$ (obtained by trial and error) along the length of the fault. The remaining parameters used to obtain this match are shown in Table 1. Temperature contours were also considered for the match of the calculated and observed temperature distribution. A match using the same recharge rate (9 x 10^{-6} $m^3/sec/m$) and recharge temperature (80°C) is shown in Figure 5. The match of observed and calculated values is very good close to the recharging fault. However, further from the fault the match is not very good. The discrepancy could be due to any number of factors: the regional flow of cold water from the north-west, complexity of the geologic setting, downflow of hot fluids at a distance from the fault, or the inaccuracy inherent in modeling a three-dimensional phenomenon in two dimensions.

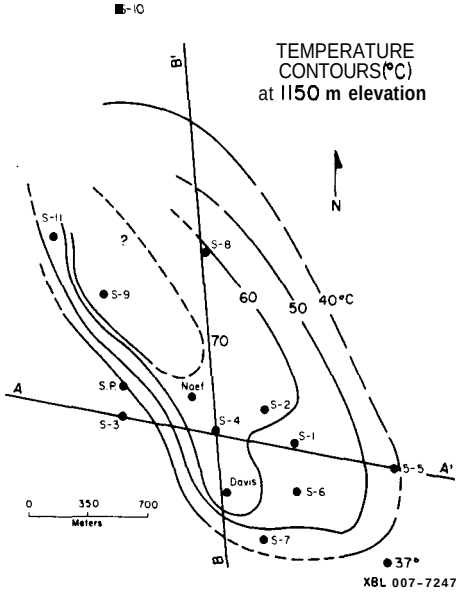

Figure 3 Temperature contours at a depth of 125 m below the surface at Susanville, California

Table 1 Parameters used for the Susanville model.

Parameter	
Aquifer thickness, b	35 m
Depth to aquifer, D	125 m
Aquifer porosity, ϕ	0.2
Thermal conductivity of rock, λ_1	1.5 J/m·s·°C
Rock heat capacity, c_1	1000 J/kg·°C
Rock density, ρ_1	2700 kg/m^3

The match shown in Figures 4 and 5 was obtained using two different sets of boundary conditions: 1) if the lower constant temperature boundary is placed very deep (H >> D), the parameters obtained indicate that the hydrothermal system has been evolving for approximately 2,000 years and that the fault charges the system at a rate of 9 x 10^{-6} $m^3/sec/m$; 2) placing a constant temperature boundary (22°C) at a depth of about 400 m results in a very similar match. In the second case, steady-state temperature conditions are reached (consequently the evolution time can be determined only as exceeding 10,000 years) but the calculated recharge rate is the same as in the first case (9 x 10^{-6} $m^3/sec/m$). If one considers the age of the subsurface formations at Susanville, the second case seems more likely.

Hydrothermal Simulation In order to predict the useful lifetime of a fault-charged system it is necessary to determine the effects of the hot water recharge on longevity, pressure transient behavior, and well siting strategy. A simple criterion for reservoir longevity was

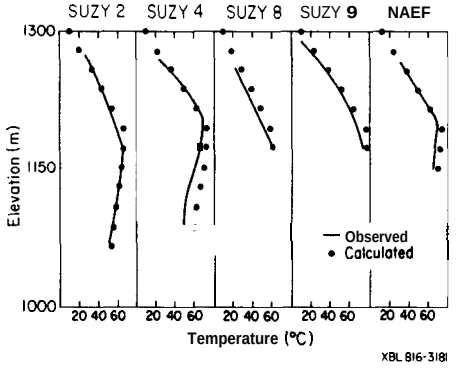

Figure 4 Temperature profiles for several of the Susanville wells demonstrating temperature reversals with depth. Also plotted are the temperature profiles calculated using the semi-analytic model.

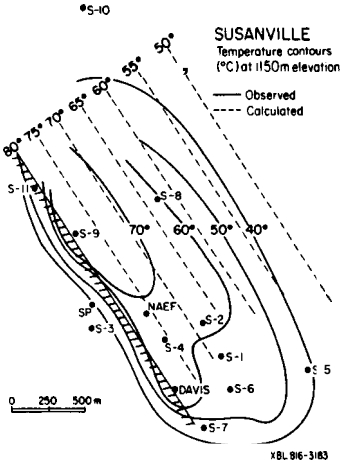

Figure 5 Match of calculated and observed temperature contours at Susanville.

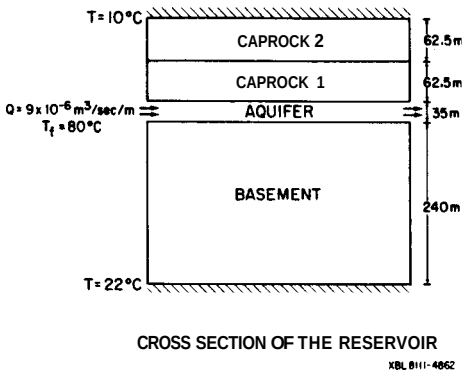

Figure 6 Cross section of the reservoir model used for numerical simulation of the Susanville hydrothermal system showing the four layers used in the mesh, the boundary conditions, and aquifer location.

used: maintenance of sufficiently high production temperature. Because the system is highly non-isothermal, and transient thermal phenomena are important, a numerical simulator was used to model the response of a fault-charged reservoir to pressure transient testing and sustained production from a well.

The recently developed numerical simulator PT (Pressure-Temperature) was used. The simulator solves the mass and energy transport equations for a liquid saturated heterogeneous porous and/or fractured media. The model includes the temperature dependence of fluid density, viscosity, and expansivity. It employs the integrated finite difference method for discretizing the medium and formulating the governing equations. The set of linear equations arising at each timestep are solved by direct means, using an efficient sparse solver. A detailed description of the simulator is given by Bodvarsson (1981).

To demonstrate the application of a numerical simulator to a fault-charged reservoir, the Susanville hydrothermal system was modeled. The geometry of the system was determined by correlation of well logs, drill cuttings and temperature profiles. Whereas the system is highly complex, we used a simplified model of the system which accounts for the major hydrothermal features. A cross section of the reservoir model and confining strata is shown in Figure 6. A 35 m-thick aquifer with a permeability of 2 Darcies is overlain by an impermeable caprock and underlain by a 240 m-thick impermeable bedrock. The ground surface temperature is a constant 10°C. The temperature at the bottom of the section (400 m depth) is a constant 22°C. To determine the temperature everywhere else in the system, the analytic solution discussed in the previous section was used, incorporating a recharge rate of 9×10^{-6} $m^3/sec/m$ (at 80°C). This temperature distribution is close to the measured temperature distribution.

The initial temperature and pressure distribution in the aquifer as a function of distance from the fault are shown in Figure 7. The pressure distribution in the aquifer was calculated so that the fault would sustain a rate of 9×10^{-6} m^3/sec per linear meter. As shown in Figure 7, the pressure gradient close to the fault is small compared to far from the fault, where it is approximately 17 psi/km. This is as expected because the fluid viscosity close to the fault is less than half the viscosity of the 20°C fluid far from the fault. Gravity was neglected in all of the simulations. A constant potential boundary condition was imposed at the downstream end of the system. At the fault, two different boundary conditions were imposed: constant potential and constant flow. The mesh used in the simulations is shown in Figure 8. Only one-half of the flow field is modeled, due to the symmetry in the problem.

Reservoir Longevity The first objective of this simulation was to determine the production temperature vs. time for a well located 600 m from the fault. The initial temperature at the production well was 60°C.

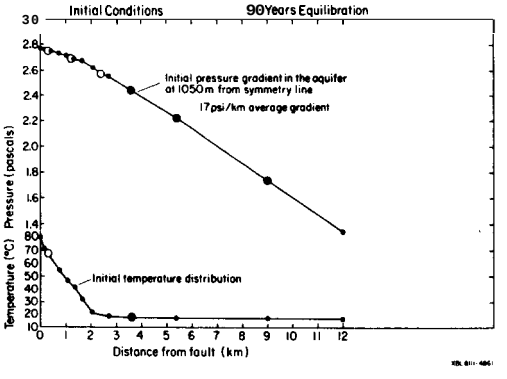

Figure 7 Initial pressure and temperature distribution in the aquifer.

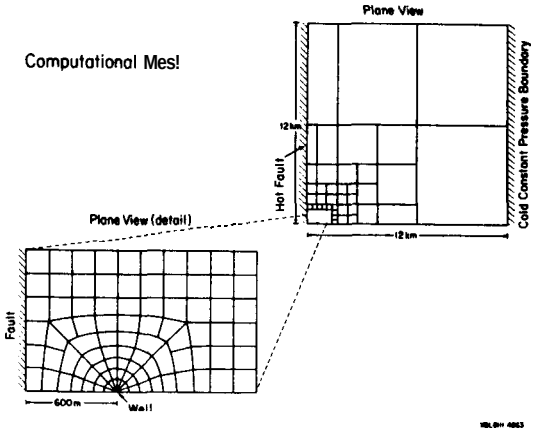

Figure 8 Plane view of the mesh used for the numerical simulations.

The well was then produced at a rate of 31 kg/sec (500 gpm). Figure 9 shows a plot of the production temperature over a 30-year lifetime for two cases: one with a constant 'potential fault and one in which the fault maintains a constant flow. As shown, the temperature in the constant flow rate case remained nearly constant during the 30-year lifetime. Only near the end of the period did the temperature begin to decline. Where the fault was at a constant potential, the temperature gradually increased with time and after the 30-year period the production temperature increased from 60°C to 67°C. This is readily explained by the increased rate of flow from the fault resulting from the production-induced drawdown near the fault. Figure 10 shows a plot of recharge rate vs. distance from the line of symmetry. Near the production well the recharge rate was nearly three times as great as the steady value which created the initial thermal anomaly. Temperature contours after 30 years of production are compared to the initial contours in Figure 11. As illustrated, the more mobile hot water moved quickly toward the production well causing the production temperature to increase. The cold water also moved toward the production well but at a slower rate.

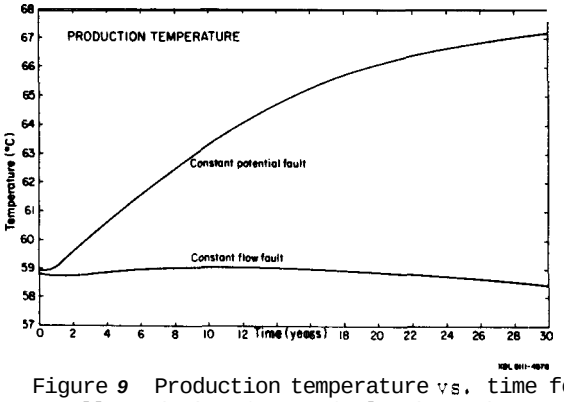

Figure 9 Production temperature vs. time for a well producing from a fault-charged reservoir for two cases: (1) a constant potential fault and (2) a constant flow fault.

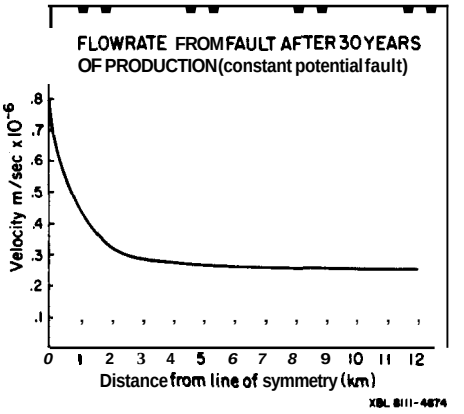

Figure 10 Flowrate from a constant potential fault near a well being produced at 31 kg/s (after 30 years of production).

This simulation demonstrates that for fault-charged hydrothermal systems, it is critical to include the recharge for an accurate reservoir assessment. If no recharge is considered then all of the hot water initially within the 60°C contour will be removed within ten years [at a rate of 31 kg/s (500 gpm)]. Both of the other cases (constant potential and constant flow) demonstrate that the resource will be adequate for a minimum of 30 years. The constant potential case suggests that the resource may be enhanced by exploitation. The nature of the recharging fault is clearly a key parameter to understanding and exploiting these systems.

Pressure Transient Analysis The same mesh and reservoir parameters were used to simulate a 30-day production/interference test in a fault charged reservoir. The production well was produced at a constant rate of 31 kg/s and pressure changes were observed in the production well and two interference wells. Analysis of the production well data gave a transmissivity of 4.8×10^5 md·ft/cp, the value used in the simulation (corresponding to

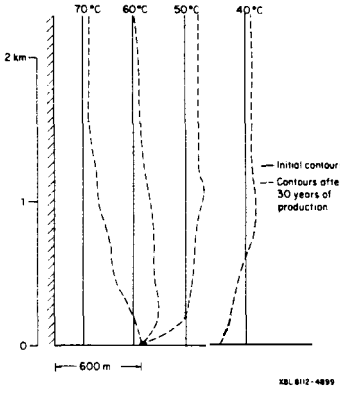

Figure 11 Comparison of temperature contours between their initial value and after 30 years of production from a well bounded by a constant potential fault.

the fluid viscosity at 60°C). Figure 12 shows a semi-log plot of the pressure transient data from the production well. As expected, the early time data falls on a straight line and later stabilizes, indicating a constant potential boundary. Figure 13 shows a schematic of the well locations, and the drawdowns at the observation wells for the constant potential fault case. At early times the drawdown at each well appears to follow the Theis curve, but later the drawdown falls below the Theis curve, indicating that the constant potential boundary is affecting the data. Type curve analyses were performed on both wells and transmissivities (kh/μ) of 1.1 x 10^6 md·ft/cp and 1.76 x 10^6 md·ft/cp were obtained. Because fluid viscosity changes by a factor of 2 1/2 in the temperature range considered, the highly non-isothermal temperature distribution and proximity to the "hot" fault obscure the normal pressure transient response. This effect of viscosity contrasts on non-isothermal well test analysis have been discussed previously (Mangold et al., 1981). This exercise seems to indicate that interference data may not provide data that can be accurately analyzed with standard methods. However, if sufficiently accurate early-time production data are available, a value for the reservoir transmissivity may be obtained and the nature of the fault may be determined. This type of pressure transient phenomena has been observed at the Susanville anomaly where analysis of production data gave a transmissivity value of 7.3 x 10^5 md·ft/cp and several observation wells yielded transmissivities ranging from 2.3 x 10^6 md·ft/cp to 3.6 x 10^6 md·ft/cp.

Production and Reinjection Well Siting
Location of the production well as close as possible to the fault will allow production of the hottest fluid; this will also optimize the stimulation of recharge from a fault. Proper reinjection well siting is critical in fault-charged systems because an inappropriately placed reinjection well can create premature cooling of the production well. Reinjection well siting criteria are as follows:

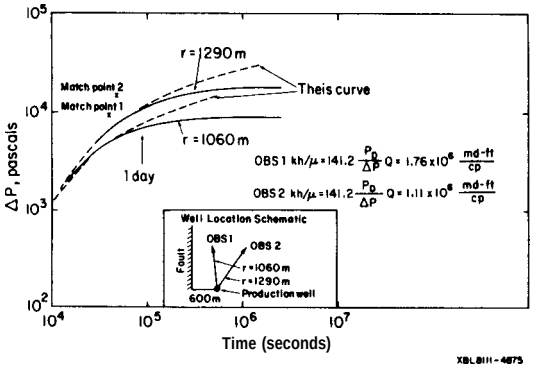

Figure 12 Drawdown and semi-log analysis of data from a production well in a reservoir bounded by a constant potential fault.

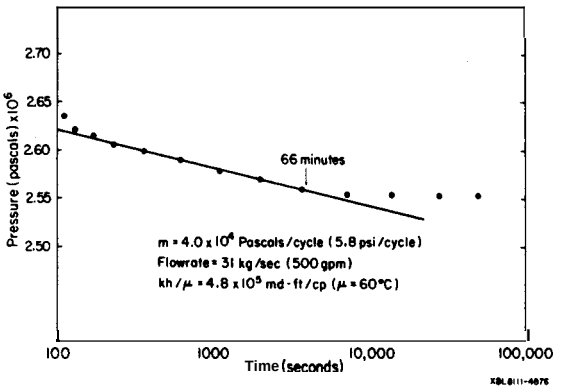

Figure 13 Drawdown and type curve analysis for the interference wells in an aquifer bounded by a constant potential fault.

(1) One should reinject downstream from the production well.

(2) If a constant potential fault is present, care should be taken to locate the reinjection well so that the pressure buildup due to reinjection does not negate the production-enhanced flow from the fault. If the aquifer is sufficiently permeable (pressure support not needed), and the produced fluids can be disposed of by some means other than reinjection, it may be desirable not to reinject or to reinject far from both the production well and the fault.

(3) The steady-state interflow between the production and injection well should be minimized. With proper siting, interflow between the wells may be negligible in an aquifer with regional flow (Dacosta and Bennett, 1960).

Conclusion By using a newly developed computational model for fault-charged reservoirs and a numerical simulator (PT), the effects of hot-water recharge into a near-surface hydrothermal aquifer have been included in reservoir engineering calculations. Key system parameters have been identified, the most important being the hydrologic characteristics of the fault itself. More simply, the ability of the fault to continue to provide hot water under production-induced reservoir conditions is critical to the longevity of the system. Two different boundary conditions for the fault have been investigated: a constant potential and a constant flow boundary. The constant flow case can be considered as a conservative case and the constant potential case as optimistic.

The methodology discussed in this paper has been applied to the Susanville, California hydrothermal resource. Predictions have been made of how the temperature will change with time, given a simple exploitation strategy.

Lifetime estimates and reservoir assessment using the methodology discussed herein are considerably more optimistic than those made if the hot water recharge into the system is ignored.

Nomenclature

a	=	Geothermal gradient (°C/m)
b	=	Aquifer thickness (m)
c	=	Heat capacity (J/kg·°C)
D	=	Thickness of caprock (m)
H	=	Thickness of bedrock (m)
k	=	Permeability (md, 10^{-15} m^2)
p	=	Laplace parameter
ϕ	=	Porosity
q	=	Fault recharge rate ($m^3/s \cdot m$)
Q	=	Well flow rate (kg/s)
t	=	Time (sec)
T	=	Temperature (°C)
T_{b1}	=	Temperature at ground surface (°C)
T_f	=	Temperatue of recharge water (°C)
u	=	Temperature in aquifer in Laplace domain
v	=	Temperature in rock matrix above aquifer in Laplace domain
w	=	Temperature in rock matrix below aquifer in Laplace domain
x	=	Lateral coordinate (m)
z	=	Vertical coordinate (m)
λ	=	Thermal conductivity (J/m·s·°C)
pc	=	Volumetric heat capacity ($J/m^3 \cdot °C$)
μ	=	Viscosity (cp, 10^{-3} Pa·s)

Subscripts

a	=	Aquifer
1	=	Rock matrix above aquifer
2	=	Rock matrix below aquifer
w	=	Liquid water

Acknowledgments This work was supported by the Assistant Secretary for Conservation and Renewable Energy, Office of Renewable Technology, Division of Geothermal and Hydropower Technologies of the U.S. Department of Energy under Contract No. W-7405-ENG-48.

References

Benson, S.M., Goranson, C.B., Noble, J., Schroeder, R.C., Corrigan, D., and Wollenberg, H. (1980), "Evaluation of the Susanville, California Geothermal Resource," Lawrence Berkeley Laboratory, Berkeley, California, LBL-11187.

Bodvarsson, G.S. (1981), "Mathematical Modeling of the Behavior of Geothermal Systems Under Exploitation," (Ph.D. dissertation) Lawrence Berkeley Laboratory, Berkeley, California.

Bodvarsson, G.S., Miller, C.W., and Benson, S.M. (1981), "A Simple Model for Fault-Charged Hydrothermal Systems," Lawrence Berkeley Laboratory, Berkeley, California, LBL-12869. Also presented at the Geothermal Resources Council Annual Meeting, 1981, Texas.

DaCosta, J.A., and Bennet, R.R. (1960). "The Pattern of Flow in the Vicinity of a Recharging and Discharging Pair of Wells in an Aquifer Having Areal Parallel Flow," Int. Ass. Sci. Hydrol. Publ. 52, Commission of Subterranean Waters, p. 524-536.

Mangold, D.C., Tsang, C.F., Lippmann, M.J., and Witherspoon, P.A. (1981), "A Study of Thermal Discontinuity in Well Test Analysis," Journal of Petroleum Technology, v. 33, n. 6 (June).

Proceedings Seventh Workshop Geothermal Reservoir Engineering
Stanford, December 1981. SGP-TR-55.

EXPERIMENTAL AND FINITE ELEMENT ANALYSIS OF THE STANFORD HYDROTHERMAL RESERVOIR MODEL

L.W. Swenson, Jr.
A. Hunsbedt

Stanford University
Stanford, CA 94305

Initial results are available from the first experiment to calibrate the heat extraction history of a physically simulated fractured hydrothermal reservoir using a rock loading of large, regular-shaped granite blocks. Thermocouples embedded in a set of the rock blocks and in water at various locations in the model provide heat extraction data. The data are also used to evaluate the effects of thermal stressing on heat transfer properties.

The results of the first experiment show a surprisingly uniform cross-sectional water temperature throughout the physical model indicating effective cross mixing between fracture channels. The temperature difference between rock centers and surrounding fluid reached 100°F during the cooling process, decreasing to smaller values by the end of the experiment, indicating that the rock energy extraction was relatively complete, with a high, constant temperature of the produced water.

For analysis of this and future experiments, a finite element method has been developed so that individual blocks can be represented as single elements. This approach allows less restraints on element shapes compared to finite difference models and provides possible application to full size reservoirs.

Introduction A major facet of the Stanford Geothermal Program since its inception in 1972 has been the realization that long-term commercial development of geothermal resources for electric power production will depend on optimum heat extraction from hydrothermal reservoirs. Optimum extraction is analogous to secondary and tertiary recovery of oil from petroleum reservoirs; in the geothermal case, the resource may be either heat-transfer limited or convecting-fluid limited. The effort in the Stanford Geothermal Program has been a combination of physical and mathematical modeling of heat extraction from fractured geothermal reservoirs. Experiments have included several rock loadings in the SGP physical model of a rechargeable hydrothermal reservoir, examination of thermal stressing on rock heat transfer properties, and development of mass transfer tracer methods for comparative analysis.

Although the present model predicts the overall energy extraction of the experimental reservoir quite well, it has several shortcomings with respect to modeling large scale systems. One of these was the uncertainty of axial heat conduction and heat transfer from the physical model itself.

This paper first discusses the results obtained from the Stanford Geothermal Program (SGP) physical model of a fractured hydrothermal reservoir using a rock matrix consisting of granite blocks with regular geometry. Following examination of these experimental data, concepts are introduced to extend standard finite element modeling procedures for regions experiencing steep temperature gradients and to provide a methodology for detailed investigations of extended thermal stressing on rock heat transfer properties.

Heat Extraction Experiments The SGP physical model has been described in several reports, e.g., Hunsbedt, Kruger and London (1977, 1978). The main component is a 5 ft high by 2 ft diameter insulated pressure vessel. The rock matrix used in these experiments consists of 30 granite rock blocks of 7.5" x 7.5" rectangular cross section and 24 triangular blocks as shown in Figure 1. The blocks are 10.4 inches high. The average pososity of the matrix is 17.5 percent.

Vertical channels between blocks are spaced at 0.25 inch and horizontal channels between layers are spaced at 0.17 inch. Significant vertical flow can also occur in the relatively large edge channel between the outer rock blocks and the pressure vessel.

Cold water is injected at the bottom of the vessel by a high pressure pump through a flow distribution baffle at the inlet to the rock matrix. System pressure is maintained above saturation by a flow control valve downstream of the vessel outlet. Most of the system pressure drop is in this valve while the rock matrix has essentially infinite permeability.

The water temperature is measured at the several locations shown in Figure 1: at the inlet to the vessel, the I-plane just below the baffle, the B-plane half-way up the first rock layer, the M-plane half-way up the third rock layer, the T-plane near the top of the

rock matrix, and at the vessel outlet. Temperatures were also measured at the center of four rock blocks and at two additional locations in the bottom central rock.

The rock-water-vessel system was heated to uniform initial temperature of 463±2°F, by electric strap heaters outside the vessel. The experiment was initiated by starting the injection pump and opening the flow control valve. The injection rate was constant during the experiment.

Experimental Run 5-1 has been completed with this rock matrix. Data for the experimental conditions and parameter values are summarized in Table 1.

Table 1
Experimental Data and Parameters for Run 5-1

Average Reservoir Pressure (psia)	545
Initial Reservoir Temperature (°F)	463
Final Top Temperature (°F)	312
Final Bottom Temperature (°F)	67
Injection Water Temperature (°F)	59
Initial Water Mass (lbm)	148
Injected Water Mass (lbm)	749
Water Injection Rate (lbm/hr)	150
Production Time (hr)	5

The results indicate that water temperature at the I-plane is initially slightly hotter near the surface wall due to heating by the steel. The injected water approached a uniform, constant temperature of 59°F, after about one hour. The data also show that the cross-sectional water temperatures were essentially uniform in each of the planes, with a maximum deviation of +4°F, well within the estimated uncertainty of thermocouple temperature difference of ±5°F.

Also given in Figure 2 are several representative rock center temperature transients. Comparison of these temperatures with the corresponding surrounding water temperatures showed that the maximum rock center to water temperature differences of about 100°F, developed during the cooling process decreasing to smaller values toward the end of the experiment. These data indicate that the rock energy extraction was relatively complete and the energy extracted from the rock resulted in a high, constant exit water temperature.

Data for the measured water and rock temperatures at the various thermocouple locations are given in Figure 2.

Finite Element Modeling In analyzing the heat extraction data from prior experiments in SGP physical reservoir as a one-dimensional lumped-parameter model, several problems have become evident: (1) the potential for axial heat conduction adding the need for a second-dimension in the analysis, (2) the large heat capacity of the physical model which distorts the heat transfer characteristics at the model boundaries, and (3) the need to accurately model thermal stressing effects. In order to extend the use of the lumped-parameter model to full-size geothermal reservoirs, it is desirable to remove these uncertainties in the physical model. For this purpose, a finite element heat transfer model of the present regular-shaped rock loading experiments has been developed. In this model, individual blocks can be represented as single elements. This approach allows less restraint on element shape compared to finite difference models.

The code as a general computational tool can evaluate a class of problems described by conduction or conduction-convection partial differential equations with boundary conditions consisting of specified temperature-time histories and/or specified heat flux-time histories controlled either by a direct source or by convection means. Specification of internal heat production (or loss) sources can also be included.

Some of the features of the finite-element code include: (1) free-field input of the model data; (2) automatic two- and three-dimensional block mesh generation; (3) automatic nodal renumbering to minimize the effective bandwidth; (4) line graphics presentation of the model mesh; and (5) printer and line graphics presentation of the results.

The model spatial discretization can be performed in two- or three-dimensional Cartesian coordinates or in axisymmetric cylindrical coordinates. An arbitrary number of general anisotropic material properties can be used to describe the particular reservoir being modeled. Results generated by the finite element code consist of temperature-time history curves and heat flux history curves. The data can be displayed in tables or graphically.

The development of the finite element discrete heat transfer equations begin with the governing partial differential equations given by:

$$c\frac{dT}{dt} = \nabla\cdot\underline{k}\cdot\nabla T + Q, \quad \underline{x}\in\Omega \qquad (1)$$

$$q_n = -\underline{n}\cdot\underline{k}\cdot\nabla T, \quad \underline{x}\in\Gamma_q \qquad (2)$$

$$T_s = T \qquad \underline{x}\in\Gamma_T \qquad (3)$$

where $c, T, t, \underline{k}, Q, q_n, \underline{n}$ and T_s are the material specific heat, temperature field, time, conductivity tensor, body heating source, specified normal component of heat flux, surface outward normal, and specified surface temperature, respectively. Equation (1) is the thermal equilibrium condition at each material point $\underline{x}$ in the domain Ω, while Equations (2) and (3) are the natural and essential boundary conditions, respectively.

The time derivative appearing in Equation (1) is the material time derivative,

$$\frac{d(\ )}{dt} = \frac{\partial(\ )}{\partial t} + \underline{v}\cdot\nabla(\ ) \qquad (4)$$

where, $\underline{v}$ is the velocity of the material point instantaneously positioned at the spatial point $\underline{x}$ and ∇ is the "del" vector operator with respect–to spatial coordinates. For a solid constituent $\underline{v}$ is taken to be zero while for a fluid domain $\underline{v}$ is generally non–zero. We consider the velocity field as given, being determined by previous analysis.

The discrete or weak form of Equations (1) - (3) are developed using the method of weighted residual approach. Approximating the temperature field in terms of a finite set of functions as

$$T \approx \tilde{T} = \sum_{a=1}^{q} g_a(\underline{x})\, \tau_a(t) \qquad (5)$$

and letting w_k be a generic element from a set of weighting or test functions, we use,

$$\int_{\Omega} w_k \left(c \frac{d\tilde{T}}{dt} - \underline{\nabla}\cdot\underline{k}\cdot\underline{\nabla}\tilde{T} - Q \right) d\Omega + \int_{\Gamma_q} w_k \left(q_m + \underline{n}\cdot\underline{k}\cdot\underline{\nabla}\tilde{T} \right) d\Gamma_q = 0 \qquad (6)$$

as the basis for the discretization process. Note that a constraint is placed on the approximation, Equation (5), and on the functions w_k such that $\tilde{T}(\underline{x},t) = T_s(\underline{x},t)$ and $w_k(\underline{x}) = 0$ for $\underline{x} \in \Gamma_T$.

Making use of the Green-Gauss theorem (and assuming appropriate continuity for the w_k), the second term in the domain integrand can be written as

$$-\int_{\Omega} w_k\, \underline{\nabla}\cdot\underline{k}\cdot\underline{\nabla}\tilde{T}\, d\Omega = -\int_{\Gamma_q} w_k\, \underline{n}\cdot\underline{k}\cdot\underline{\nabla}\tilde{T}\, d\Gamma_q + \int_{\Omega} \underline{\nabla} w_k \cdot \underline{k}\cdot\underline{\nabla}\tilde{T}\, d\Omega. \qquad (7)$$

Substituting (7) into (6) yields,

$$\int_{\Omega} w_k \left(c \frac{d\tilde{T}}{dt} \right) d\Omega + \int_{\Omega} \underline{\nabla} w_k \cdot \underline{k}\cdot\underline{\nabla}\tilde{T}\, d\Omega = \int_{\Omega} w_k\, Q\, d\Omega - \int_{\Gamma_q} w_k\, q_m\, d\Gamma_q. \qquad (8)$$

Finally, a choice remains to specifically identify the weighting functions w_k. We chose the Galerkin criterion and let the w_k be identified as those g_j basis functions in Equation (5) such that $g_j(\underline{x}) = 0$ for $\underline{x} \in \Gamma_T$. Substituting the approximation? and invoking the Galerkin criterion, the discretized set of heat transfer equations become,

$$[C]\{\dot{\tau}\} + [K]\{\tau\} = \{F\} \qquad (9.0)$$

where the matrix elements are given by,

$$C_{ab} = \int_{\Omega} c\, g_a\, g_b\, d\Omega \qquad (9.1)$$

$$K_{ab} = \int_{\Omega} \left(\underline{\nabla} g_a \cdot \underline{k}\cdot\underline{\nabla} g_b + c\, g_a \underline{v}\cdot\underline{\nabla} g_b \right) d\Omega \qquad (9.2)$$

$$F_a = \int_{\Omega} g_a Q\, d\Omega - \int_{\Gamma_q} g_a\, q_m\, d\Gamma_q. \qquad (9.3)$$

The convective part of K_{ab} is of course zero for solid constituents.

The evaluation of the matrix components appearing above are greatly simplified and readily computer automated by making use of finite element methodology. This approach takes the restrictions of the basis function g_k over sub-domain elements as relatively simple polynomials expressed in terms of local coordinates. Following this approach, thecomponent terms, relative to a generic element "e," can be written as

$$C^e_{ab} = \int_{\Omega^e} c\, g^e_a\, g^e_b\, d\Omega^e \qquad (10.1)$$

$$K^e_{ab} = \int_{\Omega^e} \left(\underline{\nabla} g^e_a \cdot \underline{k}\cdot\underline{\nabla} g^e_b + c\, g^e_a \underline{v}\cdot\underline{\nabla} g^e_b \right) \qquad (10.2)$$

$$F^e_a = \int_{\Omega^e} g^e_a\, Q\, d\Omega^e - \int_{\Gamma^e_q} g^e_a\, q_m\, d\Gamma^e_q \qquad (10.3)$$

where g^e_k is the restriction of g_k on the element domain Ω^e and element material boundary Γ^e_q. Global results are obtained by summing efement contributions.

Refined Element Analysis When cold water is first injected during the experiment start-up steep axial temperature gradients exist in the lower half of the physical model, see Figure 3. In addition, secondary heat extraction by cool-water reinjection will induce tensile thermal stresses in reservoir regions just below the fracture surfaces. Such stresses may result in important changes in reservoir energy extraction behavior, such as creation and growth of new cracks with additional heat transfer area and alterations in the mechanical and heat transfer properties of the rock itself. These conditions require that either a refined mesh of low order elements or a sparser mesh of high order elements be used to accurately represent the rapidly varying temperature field. Either of these modeling approaches will increase the number of problem degrees-of-freedom (DOF's), increase the analyst's modeling effort, produce longer computer runs, and lead to overall increased expenses. In an effort to achieve a balance between the requirement for high-order temperature approximation and the desire to reduce the overall number of DOF's, a condensed super-element methodology was used.

Consider a super-element, defined as an assembly of many simpler elements, as shown schematica11y below.

$$\{\tau\} = \begin{Bmatrix} \underline{\tau}^E \\ \underline{\tau}^I \end{Bmatrix} \qquad (11)$$

The temperature parameters $\underline{\tau}$ can be considered partitioned into two sets, one containing the "exterior" parameters $\underline{\tau}^E$ and the second containing the "interior" parameters $\underline{\tau}^I$. In like manner the super-element thermal equilibrium equations can be partitioned and written as

$$\begin{bmatrix} \underline{C}^{EE} & \underline{C}^{EI} \\ \underline{C}^{IE} & \underline{C}^{II} \end{bmatrix} \begin{Bmatrix} \dot{\underline{\tau}}^E \\ \dot{\underline{\tau}}^I \end{Bmatrix} + \begin{bmatrix} \underline{K}^{EE} & \underline{K}^{EI} \\ \underline{K}^{IE} & \underline{K}^{II} \end{bmatrix} \begin{Bmatrix} \underline{\tau}^E \\ \underline{\tau}^I \end{Bmatrix} = \begin{Bmatrix} \underline{F}^E \\ \underline{F}^I \end{Bmatrix} \qquad (12)$$

Reduction of the total number of DOF's is effected in two parts. Constraint conditions among the τ^E set can be written as

$$\tau^E = (G)\,\tau^{\hat{E}} \qquad (13)$$

where (G) is a matrix of constants relating the total exterior set τ^E in terms of a subset of τ^E, $\tau^{\hat{E}}$, which are to be retained in the analysis.

Secondly, constraint conditions among the τ^I set is taken to be of the form

$$\tau^I = (S)\,\eta \qquad (14$$

where (S) is a matrix of numbers and η is a vector of generalized time dependent coordinates. While the analyst is at liberty to select (S) in any manner deemed appropriate, a seemingly natural choice is to choose the columns of (S) as certain eigenvectors of the generalized eigenvalue problem

$$\left([K^{II}] - \alpha_k [C^{II}]\right) S_k = 0 . \qquad (15)$$

Here, α_k is the k^{th} eigenvalue associated with the k^{th} eigenvector S_k. Physically, S_k can be identified as an approximation to the k^{th} thermal eigenfunction associated with the continuum interior of the super-element domain while α_k is an approximation to the associated characteristic diffusivity.

Finally reduction of the super-element equations, Equation (12), is performed using the transformation

$$\begin{Bmatrix} \tau^E \\ \tau^I \end{Bmatrix} = \begin{pmatrix} G & 0 \\ 0 & S \end{pmatrix} \begin{Bmatrix} \tau^{\hat{E}} \\ \eta \end{Bmatrix} \qquad (16)$$

and congruent transformations, leading to

$$\begin{bmatrix} C^{\hat{E}\hat{E}} & C^{\hat{E}N} \\ C^{N\hat{E}} & C^{NN} \end{bmatrix} \begin{Bmatrix} \dot{\tau}^{\hat{E}} \\ \dot{\eta} \end{Bmatrix} + \begin{bmatrix} K^{\hat{E}\hat{E}} & K^{\hat{E}N} \\ K^{N\hat{E}} & K^{NN} \end{bmatrix} \begin{Bmatrix} \tau^{\hat{E}} \\ \eta \end{Bmatrix} = \begin{Bmatrix} F^{\hat{E}} \\ F^{N} \end{Bmatrix} \qquad (17$$

where the condensed super-element submatrices in this equation are given by

$$C^{\hat{E}\hat{E}} = G^T C^{EE} G , \quad K^{\hat{E}\hat{E}} = G^T K^{EE} G \qquad (18.1-.2)$$

$$C^{\hat{E}N} = G^T C^{EI} S , \quad K^{\hat{E}N} = G^T K^{EI} S \qquad (18.3-.4)$$

$$C^{N\hat{E}} = S^T C^{IE} G , \quad K^{N\hat{E}} = S^T K^{IE} G \qquad (18.5-.6)$$

$$C^{NN} = S^T C^{II} S , \quad K^{NN} = S^T K^{II} S \qquad (18.7-.8)$$

$$F^{\hat{E}} = G^T F^E \;\&\; F^N = S^T F^N . \qquad (18.9-.10)$$

It should be noted that with proper scaling of the eigenvectors S_k, the submatrices C^{nn} and K^{nn} are the identity matrix, I and the diagonal matrix of associated eigenvalues, respectively.

DISCUSSION The results of the first experiment using the large, regular-shaped granite blocks indicates that the attempt to calibrate the spatial time-temperature history of the loading will be successful. Several additional experiments are planned with larger injection flow rates to produce "heat transfer limited" reservoir conditions, in which substantial rock-water temperature differences exist throughout the transient. Such conditions should result in a much more rapid exit water temperature decrease.

In the completed experiment, the observed cross-sectional water temperatures were relatively uniform even with the relatively large flow area at the edge channels between the rock loading and the vessel. Possible explanations of this apparent uniform cross-sectional water temperature, inter-block channel area, include: (1) relative magnitudes of the heat available at the various channels; (2) relative pressure drops in each channel; and (3) cross mixing between channels.

Estimates of the heat transfer from around the edge channels (including heat from the steel vessel) compared to the inter-block channels were about 1.65, not quite as large as the flow area ratio of 2.07. Thus, the edge channels may be lower in temperature than the inter-block channels. The perforated flow distribution baffle at the bottom of the vessel has been shown to be sufficiently efficient in providing uniform flow entering the rock matrix below the lowest rock layer. Channel to channel pressure drop differences are not expected to be sufficiently large to affect the average channel flow velocities at the mean flow rate of only 5 ft/hr. The most likely reason for the observed uniform water temperatures appears to be the energy exchange between channels due to mass transfer. This aspect of the analysis warrants further observations in the future experiments and in the analysis.

Examination of the experimental data clearly indicate that steep axial temperature gradients exist in the lower half of the physical model. The maximum spatial axial temperature gradient varies with time, being largest at the start of the experiment and slowly decreasing as the experiment progresses. In addition, the physical location of the peak axial temperature gradient starts at the base of the rock pile and gradually moves upward. Significant temperature variations were also measured within the individual granite blocks; temperature differences between the center of the blocks and the surrounding fluid measured as much as 100°F.

Observation of these temperature gradients in the water and in the individual blocks has motivated the development of a refined finite element methodology. The approach developed for analysis of the physical chimney model uses a super-element technique with certain imposed constraints to reduce the overall degrees-of-freedom. Super-element DOF reduction was

generalized by separating the external constraints relations from the internal constraint relations. This separation of constraint equations permits the analyst considerable flexibility in approximating the super-element "surface" temperature field and the "internal" temperature field to a degree that is deemed appropriate for each. Initial experience has shown that refined super-elements perform well in regions where steep fluid and rock temperature gradients exist and hold promise for efficient hydro-thermal finite element analysis.

REFERENCES

Hunsbedt, A., P. Kruger, and A.L. London, "Recovery of Energy from Fracture-Stimulated Geothermal Reservoirs," Journal of Petroleum Technology, August 1977.

Hunsbedt, A., P. Kruger, and A.L. London, "Laboratory Studies of Fluid Production from Artificially Fractured Geothermal Reservoirs," Journal of Petroleum Technology, May 1978.

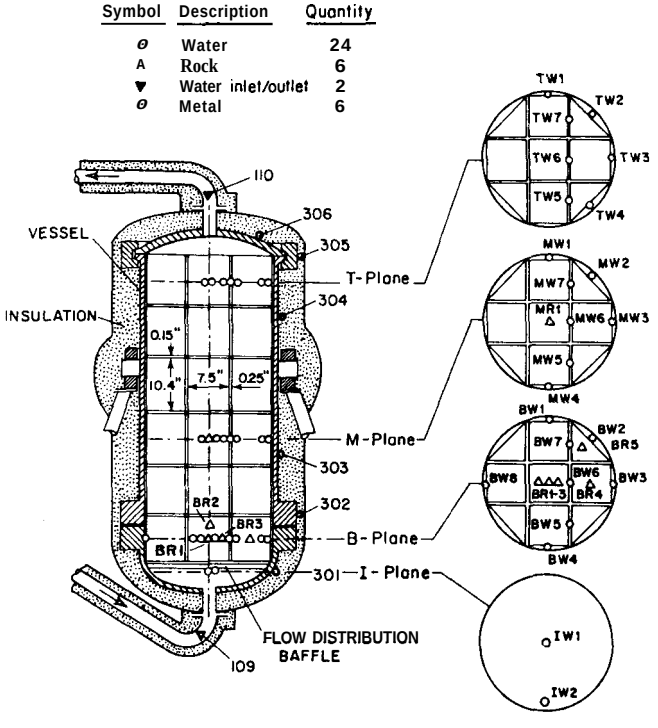

Figure 1. Experimental Rock Matrix Configuration and Thermocouple Locations.

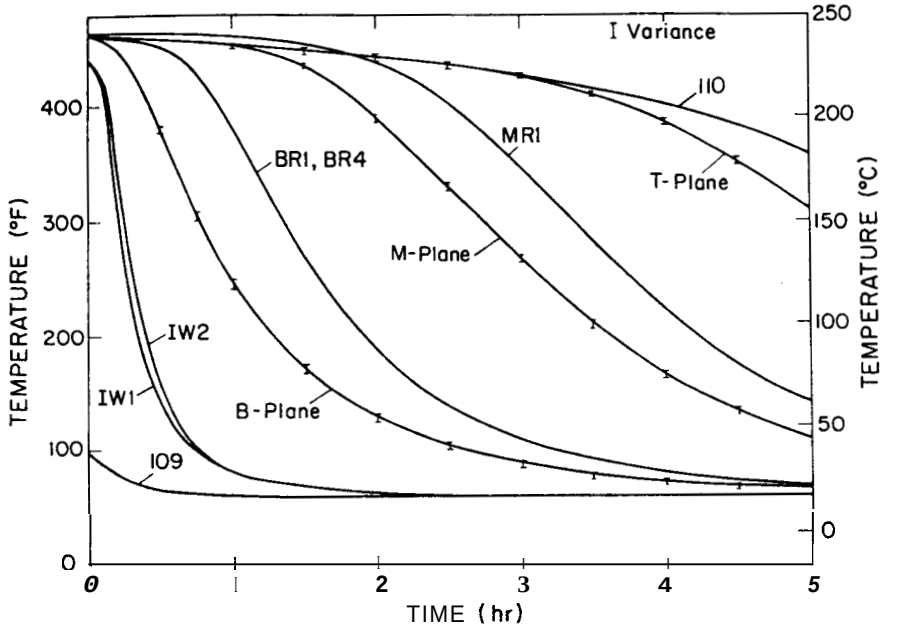

Figure 2. Water and Rock Temperatures as Functions of Time

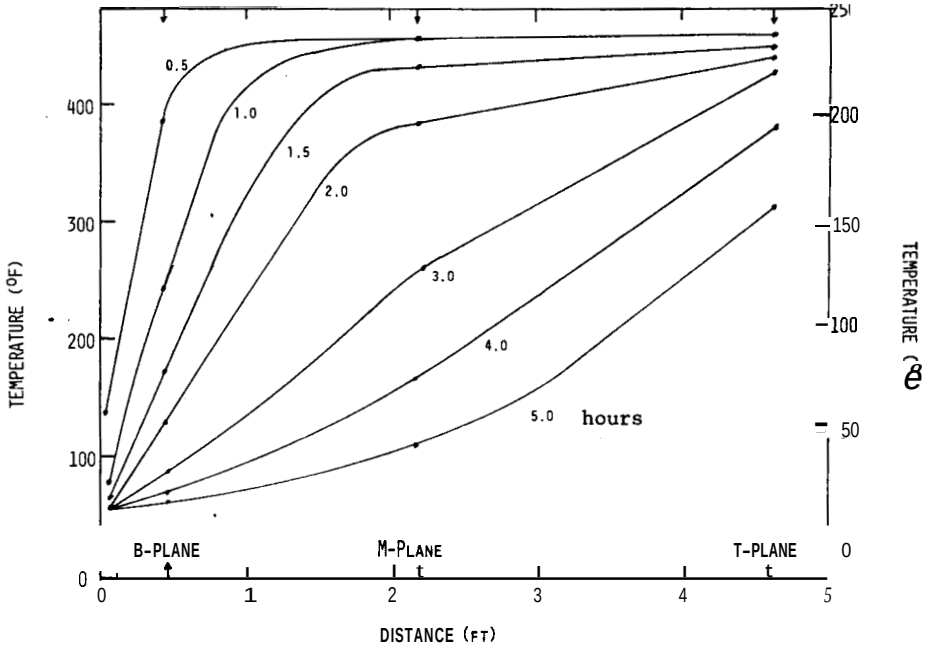

Figure 3. Isochronal Water Temperature Distributions

Proceedings Seventh Workshop Geothermal Reservoir Engineering
Stanford, December 1981. SGP-TR-55.

COLD WATER INJECTION INTO TWO-PHASE GEOTHERMAL RESERVOIRS

S. K. Garg and J. W. Pritchett

Systems, Science and Software (S^3)
P. O. Box 1620
La Jolla, California 92038

A geothermal reservoir simulator (CHARGR) is employed in its one-dimensional radial mode to examine the response of geothermal reservoirs to cold water injection from a single well. The numerical solutions are analyzed to generate interpretation techniques for pressure transient data during injection and subsequent well shutin. It is shown that the pressure buildup (i.e., injection) data may be analyzed in a straightforward manner to yield the absolute formation permeability; the pressure fall-off (i.e. shutin) data, on the other hand, appear to be of lesser utility.

Introduction Recently Garg [1980], Grant [1978], Moench and Atkinson [1977] and Sorey, et al. [1980] have examined the drawdown and buildup response of initially two-phase geothermal reservoirs. The plot of pressure drop versus logarithm of time (for drawdown test; for buildup Δp versus log $t+\Delta t/\Delta t$ should be plotted) asymptotes to a straight line after an initial non-linear period; the slope m of the straight line can be used to infer the kinematic mobility. For two-phase geothermal reservoirs, however, it is not possible to obtain the absolute formation permeability from conventional drawdown/buildup tests. If absolute formation permeability is desired, it is necessary to conduct an injection test.

At the present time, theoretical analyses of pressure injection/fall-off data are unavailable in the published literature. In the present paper, we employ a numerical reservoir simulator (CHARGR; Pritchett [1980]) to examine the response of two-phase geothermal reservoirs during cold water injection.

An examination of the numerical simulations shows that the pressure injection data may be analyzed in the conventional manner to yield absolute formation permeability. The pressure fall-off response, on the other hand, is very complex and is seen to be of limited utility in evaluating formation properties.

Numerical Examples To examine the response of a geothermal reservoir under cold water injection, the CHARGR reservoir simulator was exercised in its one-dimensional radial mode. The radially infinite reservoir was simulated using a 60-zone [Δr_1 = 0.11 m; Δr_2 = 1.2 Δr_1; Δr_3 = 1.2 Δr_2, ..., Δr_{60} = 1.2 Δr_{59}] radial grid. The outer radius of the grid is 25,825 m and is sufficiently large such that no signal reaches this boundary during the test period. The formation thickness is H = 250 m. The well is assumed to be coincident with Zone 1. (In the CHARGR code, a well can be represented as an integral part of the grid by assigning to the well-block sufficiently high permeability and porosity.) The reservoir rock is assumed to be a typical sandstone. The relevant rock properties are given in Table 1. The mixture (rock/fluid) thermal conductivity is approximated by Budiansky's formula (Pritchett [1980]). In this paper, considerations of skin effect and well storage have been ignored. These effects, while important in practical well testing, are not germane to the present discussion.

Table 1
ROCK PROPERTIES EMPLOYED IN NUMERICAL SIMULATIONS

	Rock Matrix ($2 \le i \le 60$)
Porosity, ϕ	0.1
Permeability, k(m^2)	5×10^{-14}
Uniaxial Formation Compressibility, C_m(MPa^{-1})	0
Rock Grain Density, ρ_r(kg/m^3)	2650
Grain Thermal Conductivity, K_r(W/m-°C)	5.25
Heat Capacity, c_r(kJ/kg°C)	1
Relative Permeability, ($k_{r\ell}$, k_{rg})	Corey*
Residual Liquid Saturation, $S_{\ell r}$	0.3
Residual Gas Saturation, S_{gr}	0.05

* $k_{r\ell} = (S^*_\ell)^4$, $k_{rg} = (1-S^{*2}_\ell)(1-S^*_\ell)^2$, $S^*_\ell = (S_\ell - S_{\ell r})/(1-S_{\ell r}-S_{gr})$, $S_\ell (S_g)$ = liquid (gas) volume fraction.

The initial fluid state for the two cases considered in the following is given in Table 2. The cold water is injected at a constant rate of 35 kg/s for $t = 5.868 \times 10^5$ s; the well is then shut in for $\Delta t = 1.3932 \times 10^6$ s.

Table 2
INITIAL FLUID STATE FOR COLD WATER INJECTION INTO TWO-PHASE RESERVOIRS

Case No.	Pressure MPa	Temperature °C	Steam Sat.
1	8.5917 MPa	300	0.28
2	8.5917 MPa	300	0.05

Pressure Injection Data The pressure build-up (injection) data (Figures 1 and 2) closely fit straight lines with identical slopes. The slope implies a flowing kinematic viscosity of 2.02×10^{-7} m^2/s which is in good agreement with the kinematic viscosity of the cold injected water

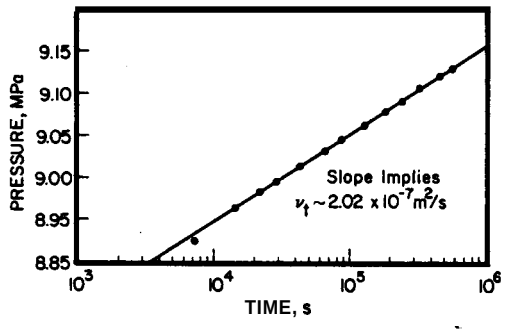

Figure 1 Pressure Injection Data for Case 1.

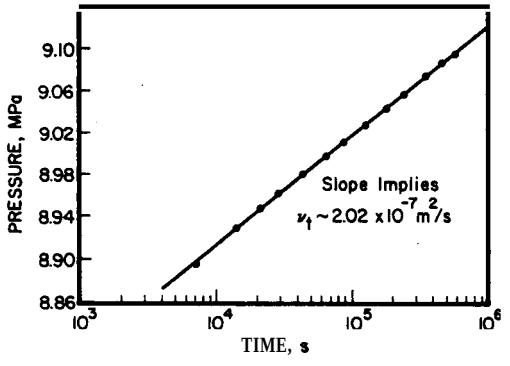

Figure 2 Pressure Injection Data for Case 2.

($\nu \sim 1.96 \times 10^{-7}$ m^2/s). Figures 3 and 4 show the radial distribution of steam saturation and temperature at the end of the injection period ($t = 5.868 \times 10^5$ s). The condensation front (especially in the low steam saturation case 2) is seen to have advanced further into the formation than the

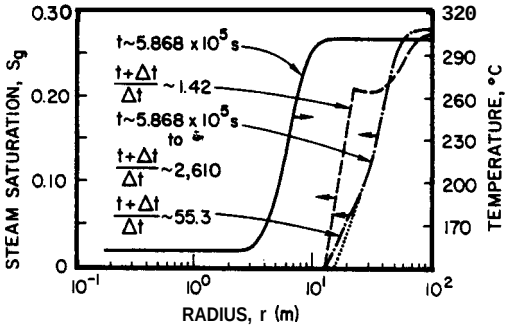

Figure 3 Radial Distribution of Temperature and Steam Saturation at Selected Times for Case 1.

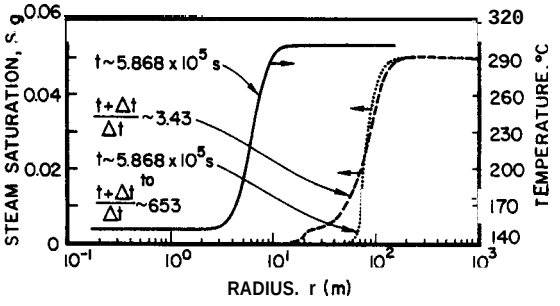

Figure 4 Radial Distribution of Temperature and Steam Saturation at Selected Times for Case 2.

edge of the thermal front. The latter effect is due to the fact that pressure changes are experienced over a much larger portion of tne reservoir than that which was cooled by the injected cold water.

Pressure Fall-Off Response Horner plots of pressure fall-off data are given in Fiqures 5 and 6. Tnree regions can be identified on these plots:

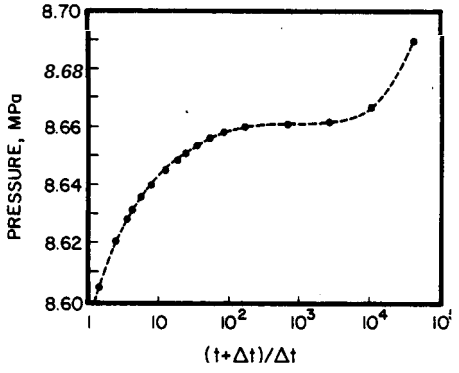

Figure 5 Pressure Fall-Off Data (Horner Plot) for Case 1.

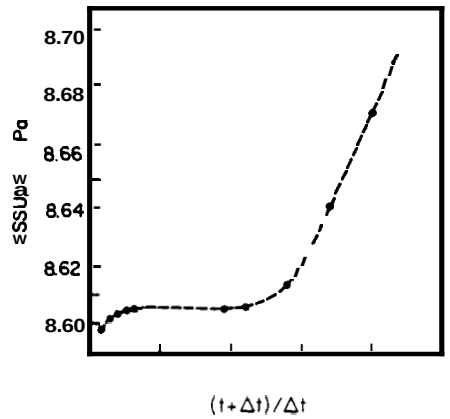

Figure 6 Pressure Fall-Off Data (Horner Plot) for Case 2.

(i) for large $(t + \Delta t)/\Delta t$ (i.e., small shutin times), pressure falls off relatively rapidly

(ii) for moderate values of $(t + \Delta t)/\Delta t$, pressure is essentially constant

(iii) for small values of $(t + \Delta t)/\Delta t$ (i.e., large buildup times), pressure again starts to fall rather rapidly.

The first region (i.e., $(t + \Delta t)/\Delta t$ large) of the fall-off curve is governed by the pressure response of the condensed fluid region. Due to the large contrast in single-phase and two-phase compressibilities, the two-phase region remains practically unaffected during this time period (see e.g., steam saturation profiles in Figures 3 and 4). The condensed fluid region behaves like a reservoir with a constant pressure (= pressure at the edge of the condensation front) boundary. These early pressure fall-off data are replotted in Figures 7 and 8; these figures clearly demonstrate that the early fall-off behavior in the present cases resembles that of a reservoir with a constant pressure boundary. The condensation front radius, r_e, can, therefore, be calculated from the formula (Earlougher [1977]):

$$r_e = \left(\frac{k \Delta t_s}{1.25 \phi \mu C_T} \right)^{0.5} \qquad (1)$$

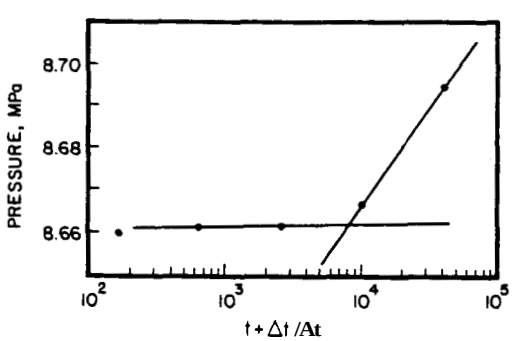

Figure 7 Early Pressure Fall-Off Data for Case 1.

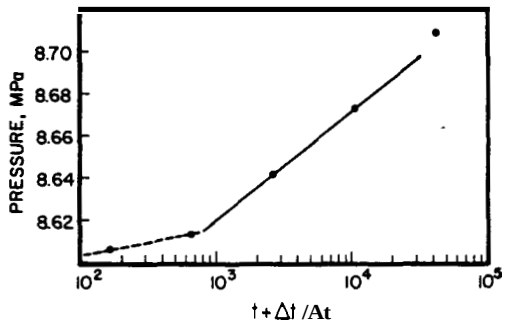

Figure 8 Early Pressure Fall-Off Data for Case 2.

where

k = formation permeability
Δt_s = time to startup of semi-steady reservoir behavior (time at which pressure curve bends over)
μ = viscosity of injected liquid water
C_T = Total formation compressibility in the condensed region.

The condensation front radii inferred from Equation (1) and the data of Figures 7 and 8 are compared with the actual values in Table 3.

Table 3
CONDENSATION FRONT RADII
($\mu = 1.8 \times 10^{-4}$ Pa-s; $C_T = 0.075 \times 10^{-8}$ Pa^{-1})

Case No	Δt_s	r_e (inferred)	r_e (actual)
1	72 s	14.6 m	(15.5 ± 1.5) m
2	753 s	47.2 m	(57.1 ± 5.2) m

Although the inferred values for r_e are in reasonable agreement with the actual values, a note of caution is in order here. In practical situations, the early fall-off data (such as that utilized in the above calculation for r_e) are liable to be dominated by wellbore storage, and it may well be impossible to identify the time at which the well starts exhibiting "semi-steady" response.

An examination of the numerical results snows that at the end of the first part of the fall-off curve, the pressure gradient in the single-phase (condensed) region is essentially zero whereas the pressure at the edge of the condensation front remains at its value at $\Delta t = 0$ (start of shutin period). Also, the edge of the condensation front is stationary throughout this initial period (Figures 3 and 4 - See steam saturation profiles for $t = 5.868 \times 10^5$ s to $(t + \Delta t)/\Delta t$ - (2610 in Figure 3, and 653 in Figure 4)).

During the intermediate fall-off period, the condensation front starts moving towards the wellbore. This part of the well response is cnaracterized by an essentially constant pressure. At the end of this period, the condensation front becomes coincident with the edge of the thermal front (see e.g., steam saturation curve labeled $(t + \Delta t)/\Delta t$ = 3.43 in Figure 4). The condensation front once again becomes stationary at this point.

For large fall-off times (i.e., for the third fall-off period), the well response is governed by the two-phase region. As can be seen from Figures 5 and 6, the pressure fall-off data do not, however, asymptote to a straight line. It is convenient to plot the fall-off data in a somewhat different manner. Figures 9 and 10 are plots of log Δp ($\Delta p = p_w(\Delta t) - p_f$ where p_f is the last flowing pressure) versus log Δt. Referring to Figure 10, it may be seen that the two-phase fall-off data lie on the unit slope line. A unit slope line can also be identified on Figure 9. It is well known that the presence of a unit slope line indicates that the well response is controlled by storage type effects; this part of the fall-off data is useless for analysis purposes in the absence of data regarding the location of tne condensation front (~ effective well-bore radius for two-phase fall-off regime). For single-phase flow, a rough rule of thumb is that the semi-log straight line starts at a time which is one and one-half log cycles removed from the time at which the pressure data begin to deviate from the unit slope straight line. Utilizing the latter criterion, it is seen from Figure 9 that only the last point or two may be expected to lie on the semi-log line. In view of the non-linear nature of two-phase flow in porous media, especially prior to the start of semi-log straight line, it would very likely be futile to try to analyze tne two-phase fall-off data of Figure 9 to derive kinematic mobility.

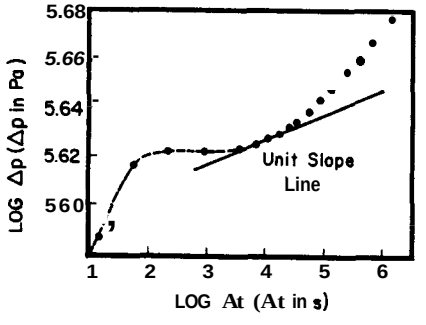

Figure 9 Plot of Log Δp Versus Log Δt for Case 1. ($\Delta p = p_w - p_f$; p_w is the well pressure at Δt and p_f is the last flowing pressure.) Note tnat the Vertical and Horizontal Scales are Different.

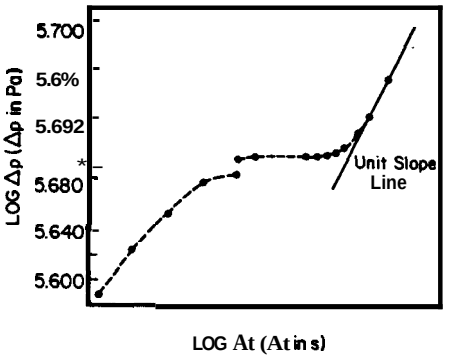

Figure 10 Plot of Log Δp Versus Log Δt for Case 2. ($\Delta p = p_w - p_f$; p_w is the well pressure at Δt and p_f is the last flowing pressure.) Note that (1) the Vertical and Horizontal Scales are Different, and (2) the Vertical Scale is Discontinuous.

Acknowledgment

Work performed under subcontract to WESTEC Services, Inc. with funding provided by the U. S. Department of Energy Under cooperative Agreement No. DE-FC03-78ET27163.

References

EARLOUGHER, R. C., Jr. [1977], Advances in Well Test Analysis, Monograph Series, Vol. 5, Society of Petroleum Engineers, Dallas, TX.

GARG, S. K. [1980], "Pressure Transient Analysis for Two-Phase (Water/Steam) Geothermal Reservoirs," SPEJ, pp. 206-214, June.

GRANT, M. A. [1978], "Two-Phase Linear Geothermal Pressure Transients: A Comparison With Single-phase Transients," New Zealand J. Sci., Vol. 21, pp. 355-364.

MOENCH, A. F. and P. G. Atkinson [1977], "Transient Pressure Analysis in Geothermal Steam Reservoirs With an Immobile Vaporizing Liquid Phase - Summary Report," Proc. Third Stanford Workshop on Geothermal Reservoir Engineering, Stanford, CA, pp. 64-69.

PRITCHETT, J.W. [1980], "Geothermal Reservoir Engineering Computer Code Comparison and Validation Calculations Using MSHM and CHARGR Geothermal Reservoir Simulators," Systems, Science and Software Report SSS-R-81-4749, November.

SOREY, M. L., M. A. Grant and E. Bradford [1980], "Nonlinear Effects in Two-Phase Flow to Wells in Geothermal Reservoirs," Water Resources Research, August.

Proceedings Seventh Workshop Geothermal Reservoir Engineering
Stanford, December 1981. SGP-TR-55.

ANALYTICAL APPROACH TO THE SIMULATION OF LABORATORY STEAM-FLOW EXPERIMENTS

Allen F. Moench and William N. Herkelrath

U.S. Geological Survey
345 Middlefield Road
Menlo Park, CA 94025

Abstract A partial differential equation with pressure as the dependent variable is derived for the flow of steam in porous materials under conditions of low liquid-water saturation. The equation includes effects of vapor-pressure lowering and latent heat of adsorption. An apparent steam diffusivity is obtained that includes these effects.

The equation is tested using pressure-transient experiments conducted in the laboratory at 100°C. The experiments, described in earlier Workshop summaries, were run by bringing a cylinder of porous material to a uniform pressure and then making a step increase in pressure at one end of the sample while monitoring the pressure response at the other end.

Because the apparent steam diffusivity was found to be nearly constant over the pressure range of the experiments, it was possible to use a simple analytical solution to simulate the experimental results.

Introduction Laboratory steam-flow experiments conducted on a cylinder of porous material have been described in a series of reports by Herkelrath and Moench (1978, 1980, 1981). In these experiments the sample was brought to a uniform pressure and then subjected to a step increase in pressure at one end while monitoring the pressure response at the other end. The experiments were run at pressures less than saturated vapor pressure and at various temperatures. Results showed that the pressure pulse propagated through the material 10 to 25 times slower than predicted by standard noncondensable gas-flow theory. Numerical simulation supported the hypothesis that the delay was due to adsorption of the steam by the porous matrix.

The purpose of this paper is to develop a linear equation for the simulation of experiments run at 100°C with initial pressures of 0.483 and 0.684 bars and final pressures of 0.951 and 0.963 bars, respectively.

Theory The analytical approach used in this report requires a linearized differential equation for one-dimensional, planar steam flow in a porous medium. The derivation of this equation makes use of equations given by Herkelrath and Moench (1981), reproduced below for convenience.

The governing equation for steam flow was

$$\frac{\partial}{\partial z}\left(\rho_v \frac{KK_{rv}}{\mu_v}\frac{\partial P}{\partial z}\right) = \phi \frac{\partial\left[\rho_v(1-S)\right]}{\partial t} + q' \quad . \qquad (1)$$

Symbols are defined in the nomenclature. A similar equation could be written for the flow of liquid; however, because adsorbed water was assumed immobile and incompressible, the equation reduced to

$$q' = \phi\rho_\ell \frac{\partial S}{\partial T} \quad . \qquad (2)$$

Temperature changes in the porous medium were assumed to occur only as a result of phase changes, hence the following simplified form of the energy equation was used:

$$L_v q' = H_c \frac{\partial T}{\partial t} \quad . \qquad (3)$$

In addition to the above, it was necessary to consider steam pressure as a function not only of temperature but also of the amount of adsorbed water:

$$P = P(T,S) = R(S)\, P_o(T) \quad . \qquad (4)$$

The functional relationship, R(S), was established experimentally for the sample material. It was described by the following empirical relationship:

$$R(S) = 10^{-(10^{(A-S)/B})} \quad . \qquad (5)$$

Using the chain rule of partial differentiation (4) is expanded as

$$\frac{\partial P}{\partial t} = \left(\frac{\partial P}{\partial S}\right)_T \frac{\partial S}{\partial t} + \left(\frac{\partial P}{\partial T}\right)_S \frac{\partial T}{\partial t} \quad . \qquad (6)$$

Combining (2) and (3), and substituting the results into (6) yields.

$$\frac{\partial P}{\partial t} = \left[\left(\frac{\partial P}{\partial S}\right)_T + \left(\frac{\partial P}{\partial T}\right)_S \phi\rho_\ell \frac{L_v}{H_c}\right] \frac{\partial S}{\partial t} \quad . \qquad (7)$$

Solving (7) for $\partial S/\partial t$ and substituting in (1) yields

$$\frac{\partial}{\partial z}\left(\rho_v \frac{KK_{rv}}{\mu_v}\frac{\partial P}{\partial z}\right) = \phi\frac{\partial[\rho_v(1-S)]}{\partial t} + \phi\rho_\ell\left[\left(\frac{\partial P}{\partial S}\right)_T + \left(\frac{\partial P}{\partial T}\right)_S \phi\rho_\ell \frac{L_v}{H_c}\right]^{-1}\frac{\partial P}{\partial t} \quad . \quad (8)$$

In the absence of vapor-pressure lowering (8) reduces to the equation derived by Moench and Atkinson (1978) for steam flow through porous materials. For the purposes of this paper the first term on the right-hand side of (8) can be neglected. Its omission in this study can be shown to decrease the numerical value of the right-hand side of (8) by at most 3%.

The left-hand side of (8) can be linearized by using pressure squared as the dependent variable. This yields an equation similar to that which describes the flow of noncondensable gas through a porous medium

$$\frac{\partial P^2}{\partial z^2} = \frac{1}{\alpha}\frac{\partial P^2}{\partial t} \quad (9)$$

where in this case the pressure-dependent diffusivity is defined as:

$$\alpha = \rho_v \frac{KK_{rv}}{\mu_v \phi\rho_\ell}\left[\left(\frac{\partial P}{\partial S}\right)_T + \phi\rho_\ell \frac{L_v}{H_c}\left(\frac{\partial P}{\partial T}\right)_S\right] \quad . \quad (10)$$

Permeability was found by Herkelrath and Moench (1981) to be a function of pressure as defined by Klinkenberg (1941):

$$K = K_o(1 + b/P) \quad . \quad (11)$$

The slope of the isothermal vapor-pressure lowering curve (illustrated by Herkelrath and Moench, 1980, fig. 2) obtained from (4) and (5) is

$$\left(\frac{\partial P}{\partial S}\right)_T = -\frac{P \ln P/P_o(T)}{0.4343\ B} \quad . \quad (12)$$

The change of pressure with temperature at constant saturation obtained from (4) is

$$\left(\frac{\partial P}{\partial T}\right)_S = R(S)\frac{\partial P_o(T)}{\partial T} + Po(T)\left(\frac{\partial R(S)}{\partial T}\right)_S \quad . \quad (13)$$

Preliminary data by Herkelrath and Moench (1980, fig. 2) show that the second term on the right-hand side of (13) is small compared with the first term. For purposes of this report it will be neglected. All parameters in (10) are obtained either by experimentation or from the steam tables (Keenan and others, 1969).

Evaluation of (10) shows that a is constant over a limited range of pressures. Thus a linear system is applicable and the governing differential equation can be written as:

$$\frac{\partial^2 P_D^2}{\partial z^2} = \frac{1}{a}\frac{\partial P_D^2}{\partial t} \quad , \quad 0 \le z \le L \quad (14)$$

where the initial condition is

$$P_D^2 = 0 \quad , t=0,\ 0 \le z \le L \quad (15)$$

and the boundary conditions are

$$P_D^2 = 1 \quad , \quad z=L \quad (16)$$

$$\frac{\partial P_D^2}{\partial Z} = 0 \quad . \quad z=0 \quad (17)$$

The dimensionless pressure is defined as

$$P_D^2 = \frac{P2 - P_i^2}{P_f^2 - P_i^2} \quad (18)$$

The solution to (14) subject to (15)-(17) evaluated at z=0 can be written down directly from the solution given by Carslaw and Jaeger (1959, p. 309):

$$P_D^2 = 2\sum_{n=0}^{\infty}(-1)^n \operatorname{erfc}\left[\frac{(2n+1)L}{2\sqrt{\alpha t}}\right] \quad . \quad (19)$$

Results The apparent pressure-dependent diffusivity defined by (10) was evaluated at 100°C for the sample material described by Herkelrath and Moench (1981). Table 1 shows the values of the measured parameters needed in the calculations. Values of the apparent diffusivity evaluated over the pressure range of 0.05 to 0.95 bars are shown in fig. 1. The apparent steam diffusivity is nearly constant over the pressure range of 0.5 to 0.95 bars.

Steam-flow experiments similar to those described in detail by Herkelrath and Moench (1980, 1981) were run on the same sample of unconsolidated porous material at 100°C using different starting pressures. The experimental results of two runs with starting pressures of 0.483 and 0.684 bars and final pressures of 0.951 and 0.963 bars, respectively, are presented in fig. 2.

Also shown in fig. 2 are the results of computations using (19) and an average diffusivity of 15 cm^2/sec. The reasonably close agreement between the experimental and analytical results tends to support the assumptions used in the development of the 1inearized governing differential equation.

Nomenclature

A & B	fitting factor in relative vapor-pressure function
b	Klinkenberg slip factor
H_c	heat capacity of porous medium

K	permeability
K_o	intrinsic permeability
K_{rv}	relative permeability to steam
L	sample 1ength
L_v	latent heat of vaporization
P	steam pressure
	saturated vapor-pressure function
P_i	initial steam pressure
P_f	final steam pressure
	dimensionless steam pressure
q'	rate of steam adsorption
R(S)	relative vapor-pressure function
S	liquid saturation
T	Temperature
t	time
z	distance along sample
α	apparent steam diffusivity
μ_v	viscosity of steam
ϕ	porosity
ρ_v	density of steam
ρ_ℓ	density of liquid

References

Carslaw, H.S., and Jaeger, J.C., 1959, Conduction of heat in solids, second edition, Oxford Univ. Press, Oxford, 510 pp.

Herkelrath, W.N., and Moench, A.F., 1978, Laboratory investigations of steam pressure-transient behavior in porous materials: Proc. of the 4th Workshop on Geothermal Reservoir Engineering, Stanford, CA, Dec 13-15, p. 54-59.

_____1980, Transient steam flow in porous media - theory and experiment. Proc. of the 6th Workshop on Geothermal Reservoir Engineering, Stanford, CA, Dec 16-18, p. 322-327.

_____1981, Laboratory investigations of the physics of steam flow in a porous medium: U.S.G.S. open-file report 82-95, 38 pp.

Keenan, J.H., Keyes, F.G., Hill, P.G., and Moore, J.G., 1969, Steam tables - thermodynamic properties of water including vapor, liquid, and solid phases: John Wiley & Sons, Inc., N.Y., 162 pp.

Klinkenberg, L.G., 1941, The permeability of porous media to liquid and gases: Drilling and Production Practice, American Petroleum Institute, p. 200-213.

Moench, A.F., and Atkinson, P.G., 1978, Transient-pressure analysis in geothermal steam reservoirs with an immobile vaporizing liquid phase: Geothermics, v. 7, p. 253-264.

Table 1. Values of parameters*

A	8.65 x 10^{-3}	
B	2.30 x 10^{-2}	
b	0.14	bars
H_c	0.32	cal/cm^3 °C
K_{rv}	1	
K_o	3.60 x 10^{-8}	cm^2
L	61	cm
T	100	°C
ϕ	0.42	

*remaining parameters are known properties of water at the prevailing temperature and pressure

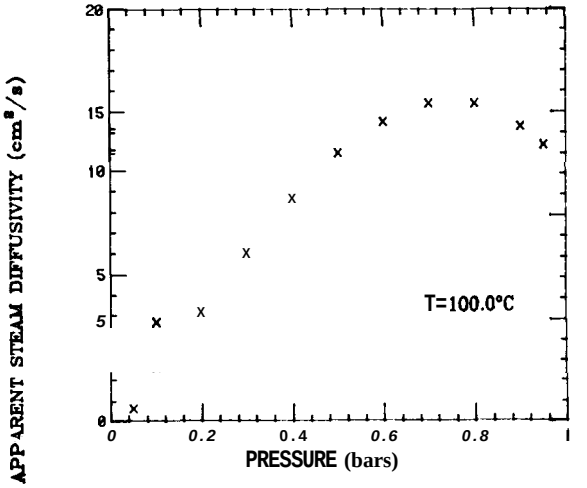

Figure 1. Calculated values of apparent steam diffusivity in the porous sample material versus pressure.

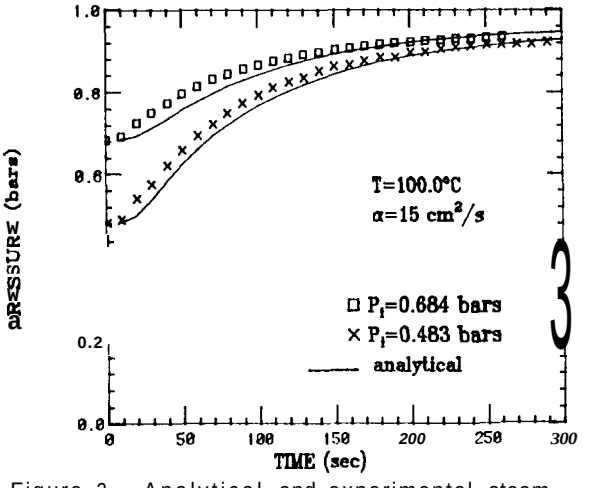

Figure 2. Analytical and experimental steam-pressure buildup at the closed end of the porous cylinder as a function of time since a step increase in pressure was impdsed at the other end.

SEVENTH STANFORD WORKSHOP ON GEOTHERMAL RESERVOIR ENGINEERING

Participants List

Usman Ahmed
Terra Tek, Inc.
420 Wakara Way
Salt Lake City, UT 84108

David N. Anderson
Geothermal Resources Council
P. O. Box 98
Davis, CA 95617

Paul Atkinson
Union Oil Company
P. O. Box 6854
Santa Rosa, CA 95406

Benjamin J. Barker
Union Oil Co., Geothermal Division
Box 6854
Santa Rosa, CA 95406

Phil Beilin
Geoexplor International
81 Buckeye Avenue
Oakland, CA 94618

Toro Beniamino
C. N. R.
c/o Instituto di geologia e paleontologia
dell'Uniersita di Roma
Piazzale A. Moro 5 Roma
ITALY

Sally Benson
Lawrence Berkeley Laboratory
P. O. Box 528
Berkeley, CA 94701

Lavonne Blucher-Nameny
NUS Corporation
2740 Sand Hill Road
Menlo Park, CA 94025

Gudmundur Bodvarsson
Lawrence Berkeley Laboratory
Building 90
Berkeley, CA 94720

Warren H. Bossert
Naval Facilities Engineering Command
P. O. Box 727
San Bruno, CA 94066

Winston F. Bott
Rogers Engineering Co., Inc.
111 Pine Street, Suite 600
San Francisco, CA 94111

William T. Box, Jr.
AMINOIL USA, Inc.
P. O. Box 11279
Santa Rosa, CA

William E. Brigham
SUPRI
Stanford University
Stanford, CA 94305

Dr. Charles G. Bufe
USGS and DOE
906 National Center
Reston, VA 22092

Mario Castaneda
Instituto Investigaciones Electricas
Mexicali, B. C. Mexico

Louis M. Castanier
SUPRI
Stanford University
Stanford, CA 94305

Romano Celati
CNR Italy
Instituto Internazionale per le
Richerche Geotermiche
via del Buongusto, 1
56100 PISA (Italy)

Kenneth Y. Chan
USGS-CD
Mail Stop 92
345 Middlefield Road
Menlo Park, CA 94025

Mitchell Che
GeothermEx
5221 Central Avenue
Richmond, CA 94804

Franco D'Amore
C.N.R. Italy
Instituto Internazionale per le
Richerche Geotermiche
via del Buongusto, 1
56100 PISA (Italy)

Zora Dash
Los Alamos National Laboratory
P. O. Box 1663, Mail Stop 981
Los Alamos, NM 87545

Bernardo Dominguez A.
C.F.E.
P. O. Box 248
Calexico, CA 92231

Dick Dondanville
Union Oil Company, Geothermal Division
P. O. Box 6854
Santa Rosa, CA 95406

Richard C. Dudley
Bank of America
Project Finance Group #5044
555 California Street
San Francisco, CA 94104

Herman Dykstra
Consultant
4180 Treat Blvd., Suite I
Concord. CA 94518

Steven L. Enedy
Union Oil Company
P. O. Box 6854
Santa Rosa, CA 95406

I. J. Epperson
Chevron Resources
P. O. Box 3722
San Francisco, CA 94119

Iraj Ershaghi
University of Southern California
University Park
Los Angeles, CA 90007

Giancarlo Facca
81 Buckeye Avenue
Oakland, CA 94618

Jim Fallon
Union Oil Company
2099 Range Avenue
P. O. Box 6854
Santa Rosa, CA 95406

Derek Freeston
University of Auckland
Geothermal Institute
Private Bag
Auckland, NEW ZEALAND

Sabodh K. Garg
Systems, Science and Software
P. O. Box 1620
La Jolla, CA 92038

Brian Gobran
ARCO Oil and Gas Company
3000 Plano Parkway
Room E116
Plano, TX 75075

Norman E. Goldstein
Lawrence Berkeley Laboratory
Building 90
Berkeley, CA 94720

Jon S. Gudmundsson
Dept. of Petroleum Engineering
Stanford University
Stanford, CA 94305

Colin Guranson
BGI
245 Gravatt Drive
Berkeley, CA 94705

Mohinder S. Gulati
Union Oil Company, Geothermal Division
2099 Range Avenue
P. O. Box 6854
Santa Rosa, CA 95406

Roger Harrison
KRTA (USA) Ltd.
332 Pine Street, Suite 506
San Francisco, CA 94104

Bruce Hellier
USGS - Conservation Division
345 Middlefield Road
Mail Stop 92
Menlo Park, CA 94025

Roland N. Horne
Dept. of Petroleum Engineering
Stanford University
Stanford, CA 94305

Anstein Hunsbedt
Dept. of Civil Engineering
Terman Engineering Center
Stanford University
Stanford, CA 94305

Trevor M. Hunt
Geothermal Research Center
D.S. I.R. (Wairakei)
Private Bag
Taupo, NEW ZEALAND

Dr. Eduardo Iglesias
Instituto de Investigaciones Electricas
Interior Internado Palmira
(Apartado Postal 475)
Cuernavaca, Morelos,
MEXICO

Pam Irvine
Union Oil Company, Geothermal Division
P. O. Box 6854
Santa Rosa, CA 95406

Tsutomu Kuichi
SAI Engineers Inc.
3030 Patrick Henry Drive
Santa Clara, CA 95050

Christopher W. Klein
GeothermEx, Inc.
5221 Central Avenue, 6201
Richmond, CA 94804

Paul Kruger
Dept. of Civil Engineering
Terman Engineering Center
Stanford University
Stanford, CA 94305

Mark K. Kumataka
Occidental Geothermal, Inc.
5000 Stockdale Highway
Bakersfield, CA 93309

Robert G. Lacy
San Diego Gas & Electric
P. O. Box 1831
San Diego, CA 92112

Gaylon K. Lee
California Energy Commission
1111 Howe Avenue
Sacramento, CA 95825

Paul Lienau
Oregon Institute of Technology
Geothermal Heat Center
Oretech Branch Post Office
Klamath Falls. OR 97601

Paolo Emilio Liguori
ELC-Electroconsult
Via Chiabrera 8
Milan 20151
ITALY

Donald R. Lindsay
Occidental Geothermal, Inc.
5000 Stockdale Highway
Bakersfield. CA 93309

Steve Lipman
Union Oil Company
2099 Range Street
Santa Rosa, CA 95406

Marcelo J. Lippmann
Lawrence Berkeley Laboratory
Building 90
Berkeley, CA 94720

Pablo Martinez
SAI Engineers, Inc.
3030 Patrick Henry Drive
Santa Clara, CA 95050

Kathleen L. McAnany
Aminoil USA
P. O. Box 11279
Santa Rosa, CA 95406

James R. McNitt
GeothermEx Inc.
5221 Central Avenue
Richmond, CA 94804

Robert L. Macy
Sunoco Energy Development Company
12700 Park Central Place
Suite 1500
Dallas, TX 75251

Robert J. Membreno
SAI Engineers, Inc.
3030 Patrick Henry Drive
Santa Clara, CA 95050

Philip H. Messer
Union Oil Company, Geothermal Division
P. O. Box 1805
Indio, CA 92201

Frank G. Miller
Dept. of Petroleum Engineering
Stanford University
Stanford, CA 94305

Allen Moench
USGS
345 Middlefield Road
Mail Stop 96
Menlo Park, CA 94025

Dr. Martin W. Molloy
U. S. Department of Energy
Geothermal Energy Division
1333 Broadway
Oakland, CA 94612

Diane Moore
USGS
345 Middlefield Road
Mail Stop 77
Menlo Park, CA 94025

Charles W. Morris
Republic Geothermal, Inc.
11823 E. Slauson Avenue
Santa Fe Springs, CA 90670

Shigetaka Nakanishi
Geothermal Project Office
Electric Power Development Co., Ltd.
8-9 Ginza 2-Chome
Chuo-ku, TOKYO, 104
JAPAN

Manuel Nathenson
USGS
345 Middlefield Road
Menlo Park, CA 94025

Guillermo Noffal
SAI Engineers, Inc.
3030 Patrick Henry Drive
Santa Clara, CA 95050

George F. Pinder
Princeton University
Dept. of Civil Engineering
Princeton, NJ 08540

Alfonso, S. Pingol, Jr.
Union Oil Company, Geothermal Division
2099 Range Avenue
P. O. Box 6854
Santa Rosa, CA 95401

Lyndon Pittinger
Union Oil Company, Geothermal Division
P. O. Box 6854
Santa Rosa, CA 95406

John W. Pritchett
Systems, Science and Software
P. O. Box 1620
La Jolla, CA 92038

Karsten Pruess
Lawrence Berkeley Laboratory
Building 90
Berkeley, CA 94720

Francesca F. Quercia
AGIP (Italy)
S. Donato Milanese (MI)
ITALY

Gregory Raasch
Union Oil Company
2099 Range Avenue
P. O. Box 6854
Santa Rosa, CA 95406

Marshall Reed
USGS
345 Middlefield Road
Menlo Park, CA 94025

T. David Riney
S-Cubed
P. O. Box 1620
La Jolla, CA 92037

Charles L. Ritz
Republic Geothermal, Inc.
11823 E. Slauson Avenue
Santa Fe Springs, CA 90670

Vasel Roberts
Electric Power Research Institute
P. O. Box 10412
Palo Alto, CA 94303

David Rohrs
Union Geothermal
2099 Range Avenue
Santa Rosa. CA 95404

Mehmet Saltuklaroglu
ELC-Electronsult
Apartado Postal 105-150
Mexico 5 D.F.
MEXICO

Charles G. Sammis
University of Southern California
Dept. of Geological Sciences
University Park
Los Angeles, CA 90007

Subir Sanyal
GeothermEx, Inc.
5221 Central Avenue, St. 201
Richmond, CA 94804

Alex Schriener
Union Oil Company, Geothermal Division
P. O. Box 6854
Santa Rosa, CA 95406

Ron Schroeder
BGI (Berkeley Group Inc.)
245 Gravatt Drive
Berkeley, CA 94705

Lewis Semprini
SGP
Dept. of Civil Engineering
Terman Engineering Center
Stanford University
Stanford, CA 94305

Rae Shikuma
PG&E
77 Beale Street
San Francisco, CA 94106

Christian Smith
Chevron Resources Company
P.O. Box 3722
San Francisco, CA 94119

Mike Sorey
USGS
345 Middlefield Road
Menlo Park, CA 94025

Valgardur Stefansson
Iceland Energy Authority
Grensasvegur 9
Reykjavik, ICELAND

Kenneth Stelling
State of California
2904 McBride Lane
Santa Rosa, CA 95401

Tsutomu Sugiura
JAPEX
1-6-1 Ohtemachi, Chiyoda-ku
Tokyo 100
JAPAN

Lyle W. Swenson, Jr.
Stanford Geothermal Program
Stanford University
Stanford, CA 94305

Shiro Tamanyu
Geological Survey of Japan
1918 Cooley Avenue, Apt. 3
Palo Alto, CA 94303

Maren A. Teilman
Int'l Engineering Company
180 Howard Street
San Francisco, CA

Richard Thomas
California Division of Oil and Gas
1416 9th Street, Room 1310
Sacramento, CA 95826

Alfred H. Truesdell
USGS
345 Middlefield Road
Menlo Park, CA 94025

James Wazlaw
SAI Engineers, Inc.
3030 Patrick Henry Drive
Santa Clara, CA 95050

John D. Westwood
Marathon Oil Company
P. O. Box 269
Littleton, CO 80120

A. J. Whittome
Chevron Resources Company
595 Market Street
Box 3722
San Francisco, CA 94119

Paul A. Witherspoon
University of California
Berkeley, CA 94720

Laraine J. Woitke
PG&E
77 Beale Street
San Francisco, CA 94106

Mr. S. Yamaguchi
Faculty of Engineering
University of Tokyo
Bunkyo-ku
Tokyo, JAPAN